Department of Molecular & Clinical Cancer Medicine

Investigation of molecular modulation of taxane response in respiratory tract cancers by differential expression of mitotic spindle associated genes

Thesis submitted in accordance with the requirements
of the University of Liverpool for the degree of Doctor in Philosophy by
Ahmed Salim Kadhim Al-Khafaji

August 2015

Supervisors: Dr. Triantafillos Liloglou, Dr. Janet Risk, Prof. Richard Shaw &Prof. John K Field

To my Wonderful family;
Wife – Asmaa, Daughter – Ucer and Sons – Hashim and Ali

To my Dearest Sisters and Brothers

To the Memory of my Beloved Father and Older Brothers

Most of all, all that I am or Hope to be I Owe to my Angel Mother

Acknowledgements:

I am heartily grateful to my supervisors, Dr. Triantafillos Liloglou, Dr. Janet M. Risk, Prof. Richard J. Shaw & Prof. John K Field, whose encouragement, guidance and support from the initial to the final step in this study, enabled me to develop my understanding on the subject and complete this thesis.

I am also grateful to the staff, colleagues and collaborators; Prof. Andrea Varro, Dr. Michael P.A. Davies, Dr. Michael W. Marcus, Dr. Russell Hyde, Dr. Joseph Slupsky, Dr. John Stanbury, Mr Ben Brown, Miss Paschalia Pantazi, Miss Lena Kovstiski, Mrs Israa Al-Humairi, Miss Syeda Ali, Dr. Julie Bryan, Mrs Stephanie Unsworth, Mr Nial Hodge, Mr Andy Birss and all other members of the Liverpool Lung Project for their help and support throughout these four years. Special thanks to Mrs Beverley Green for taking care of all the administrative issues involved. I also would acknowledge the International Support Team (IST) staff at the university of particular Mr Christopher Bennett, Christopher Fawn and Mrs Bev Sinclair.

Finally, I would like to acknowledge the University of Baghdad/IRAQ and Roy Castle Lung Cancer Foundation/UK for sponsoring this project.

Disclaimer:
All of the work presented in this thesis, unless otherwise stated, is the work of the author.

Table of Contents

Abstract 9

Abbreviation table 11

Glossary table 15

Chapter 1 - Introduction 19

1.1 Lung cancer 21

1.1.1 Histological description 22

1.1.2 Preneoplastic precursors 27

1.1.3 Epidemiology 28

1.1.4 Diagnosis 30

1.1.5 Therapy 33

1.1.6 Prognosis 35

1.2 Head and Neck Squamous Cell carcinoma (HNSCC) 37

1.2.1 Histological description 38

1.2.2 Epidemiology (risk factors) 42

1.2.3 Diagnosis 44

1.2.4 Therapy 45

1.2.5 Prognosis 47

1.3 Taxanes and mitotic spindle in cancer therapeutics 49

1.3.1 History of taxanes 49

1.3.2 Therapeutic schemes using taxanes in lung and HN cancers: 51

1.3.3 Molecular predictive biomarkers of taxanes: 52

1.3.4 Mechanism of taxane action: 55

1.3.5 Spindle assembly and cancer therapy 58

1.4 Hypothesis 80

1.5 Aims and Objectives 80

Chapter 2: Materials and methods 81

2.1 Primary NSCLC tumour samples: 81

2.1.1 Cryosectioning 81

2.2 Cell lines & Growth conditions: 82

2.2.1 Cell growth curves 82

2.3 Examination of cell growth 84

2.3.1 Cellular phenotypic characteristics 84

2.3.2 Exposure to therapeutic agents 84

2.3.2 MTT proliferation assay 84

2.4 mRNA expression analyses 85

2.4.1 RNA extraction 85

2.4.2 Agilent RNA 6000 Nano kit 86

2.4.3 Reverse transcription 87

2.4.4 Quantitative Real-Time PCR expression assays 87

2.5 DNA methylation analysis 91

2.5.1 DNA extraction 91

2.5.2 DNA methylation 92

2.5.3 Bisulphite treatment of DNA 93

2.5.4 Pyrosequencing Methylation Analysis (PMA). 94

2.5.5 Decitabine efficiency 98

2.6 Transfection 99

2.6.1 *AURKA, AURKB* and *TPX2* mRNA downregulation 99

2.6.2 *AURKB* overexpression by constructed pCMV6-XL4-*AURKB*/*Bsd* plasmid 104

2.7 Western blot 111

2.7.1 Protein extraction 111

2.7.2 The BicinChoninic Acid (BCA) assay for protein quantitation..... 112

2.8 Data interpretation and Statistical analysis..... 114

Chapter 3: AURKA involvement in docetaxel resistance in non-small cell lung cancer..... 116

Chapter 4: Aurora B expression as a potential predictive biomarker for paclitaxel response in NSCLC..... 143

Chapter 5: *AURKA* mRNA expression is an independent predictor of poor prognosis in patients with NSCLC..... 158

Chapter 6: Epigenetic sensitization of respiratory tract cancer cells to paclitaxel..... 187

Chapter 7: Discussion..... 198

7.1 Aurora kinase A involvement in docetaxel resistance in NSCLC..... 198

7.2 Aurora kinase B expression can predict response of NSCLC to paclitaxel..... 201

7.3 *AURKA* mRNA expression is an independent predictor of poor prognosis in patients with NSCLC..... 210

7.4 Epigenetic sensitization of respiratory tract cancer cells to paclitaxel..... 213

Appendices..... 239

Appendix 1: Publication/communication material out of this study..... 239

Appendix 2: Clinicopathological characteristics of the patients included in this study..... 240

Appendix 3: Representative data of cell line authentication determined by DNA fragmentation analysis using GenePrint 10 System..... 243

Appendix 4: Representative pyrosequencing assay design and its analysis report for detection methylation status of *KIF11* gene promoter. The forward biontinylated (Fb), reverse (R) and Sequencing (S) primers were designed using PyroMark assay design 2.0 software..... 244

Appendix 5 (A): The sequencing confirmation of *AURKB* cDNA sequence on pCMV6-XL4-*AURKB*/*Bsd* recombinant plasmid analysed on 3130 Genetic Analyzer..... 245

Appendix 5 (B): The map of genetically engineered plasmid pCMV6-XL4-*AURKB-Bsd* highlighting the insertion site of *BSD* gene..... 246

Appendix 6: *AURKB* mRNA expression of Calu-3 cell line and its derivative overexpressed clones (A) in relation to their response to both taxanes (B). 247

Appendix 7: mRNA expression of *AURKC*, *CKAP5* and *TUBB3* in lung cancer tissues. 248

Appendix 8(A): Kaplan-Meier analysis of overall survival (OS) of NSCLC cancer patients dichotomised by median *AURKB* mRNA expression. The p value was derived from Log Rank (Mantel-Cox) test. 249

Appendix 8(B): Kaplan-Meier analysis of overall survival (OS) of NSCLC cancer patients dichotomised by median *AURKC* mRNA expression. The p value was derived from Log Rank (Mantel-Cox) test. 250

Appendix 8(C): Kaplan-Meier analysis of overall survival (OS) of NSCLC cancer patients dichotomised by median *CKAP5* mRNA expression. The p value was derived from Log Rank (Mantel-Cox) test. 251

Appendix 8(D): Kaplan-Meier analysis of overall survival (OS) of NSCLC cancer patients dichotomised by median *DLGAP5* mRNA expression. The p value was derived from Log Rank (Mantel-Cox) test. 252

Appendix 8(E): Kaplan-Meier analysis of overall survival (OS) of NSCLC cancer patients dichotomised by median *KIF11* mRNA expression. The p value was derived from Log Rank (Mantel-Cox) test. 253

Appendix 8(F): Kaplan-Meier analysis of overall survival (OS) of NSCLC cancer patients dichotomised by median *TTK* mRNA expression. The p value was derived from Log Rank (Mantel-Cox) test. 254

Appendix 8(G): Kaplan-Meier analysis of overall survival (OS) of NSCLC cancer patients dichotomised by median *TUBB* mRNA expression. The p value was derived from Log Rank (Mantel-Cox) test. 255

Appendix 8(H): Kaplan-Meier analysis of overall survival (OS) of NSCLC cancer patients dichotomised by median *TUBB3* mRNA expression. The p value was derived from Log Rank (Mantel-Cox) test. 256

Abstract

Respiratory (Lung and head and neck) cancers contribute highly to the burden of cancer-related deaths. Taxanes are microtubule-targeting agents used to treat a variety of human cancers. Paclitaxel and Docetaxel represent the most prominent members of the taxane family, demonstrating significant activity mainly as part of complex chemotherapeutic regimens. Mitotic spindle formation and spindle checkpoint are critical for the maintenance of cell division and chromosome segregation. Many of mitotic spindle associated members, including *AURKA*, *AURKB*, *AURKC*, *CKAP5*, *DLGAP5*, *KIF11*, *TPX2*, *TUBB*, *TUBB3*, and *TTK* are implicated in several malignancies including lung cancer due to their frequent deregulation and may be associated with response to taxanes based therapy in NSCLC.

The aims of this project were to

1) Explore the association between the expression profiles of ten genes listed above and clinicopathological characteristics in human non-small cell lung carcinoma and

2) Investigate the potential of some of these genes to predict response to taxane involving regimens in lung and head and neck cancerous cells.

qPCR-based RNA gene expression profiles of 132 non-small cell lung carcinomas (NSCLC) and 44 adjacent normal tissues were generated and Cox proportional hazard regression was used to examine associations. Associations between mitotic spindle gene expression and resistance to both taxanes were established in 23 cancer cell lines of respiratory tract

origin. *AURKA* mRNA expression (Hazard Ratio (HR)= 1.81; 95%CI 1.16-2.84, P= 0.009) was the only molecular independent predictor of poor prognosis in patients with NSCLC. Poor prognosis of those patients with high AURKA expression suggests they may benefit from combined therapy with AURKA inhibitors. Furthermore, in LUDLU1, SKLU1 and SK-MES1 cell lines, shRNA driven *AURKA* down-regulation sensitized cells to docetaxel. Inhibition of Aurora A kinase activity using the selective inhibitor alisertib augmented docetaxel efficiency in the above mentioned cell lines.

AURKB overexpression in NSCLC cell lines strongly correlated with resistance to both docetaxel (p=0.0016) and paclitaxel (p=0.0096). Conversely, AURKB knock down derivatives of two cell lines consistently showed a dose-dependent association between *AURKB* mRNA expression and resistance to paclitaxel. Inhibition of Aurora B activity by barasertib also demonstrated a strong dose-dependent efficiency in triggering paclitaxel resistance in all the cell lines tested.

This study clearly demonstrated that *AURKA* mRNA over-expression could prognosticate the clinical outcome in NSCLC patients suggesting that patients bearing tumours with high AURKA expression may benefit from combined use of AURKA inhibitors. The present study has also clearly uncovered a role for AURKB in the response of NSCLC cells to paclitaxel and provided unique evidence for a dose-dependent association. Given the large extent of AURKB deregulation in NSCLC, these findings suggest that assessing the levels of AURKB protein in surgical samples could become a determinant in the clinical decision tree for managing patients and have potential for development as a predictive biomarker.

Abbreviation table

AAH	Atypical Adenomatous Hyperplasias
ABC	ATP-Binding Cassette
AdC	Adenocarcinoma
AIS	Adenocarcinoma In Situ
APC	Anaphase-Promoting Complex
BAC	Bronchiolo-Alveolar Carcinoma
BCA	BicinChoninic Acid
Bcl-2	B-cell lymphoma2
BSA	Bovine Serum Albumin
cdc-2	Cell division control-2 kinase
ch- TOG	Colonic and hepatic Tumour Over-expressed Gene
CHART	Continuous Hyper fractionated Accelerated Radiotherapy
CHFR	Checkpoint with Forkhead and Ringfinger domains gene
ch-TOG	colonic and hepatic Tumour Over-expressed Gene
CIS	Carcinoma In Situ
CPC	Chromosomal Passenger Complex
CRT	Concurrent chemoradiotherapy
CSS	Cancer-Specific Survival
CT	Computed Tomography
ΔCt	Delta Cycle Threshold

CT $_{\text{Conversion}}$	Conversion of unmethylated Cytosine to Thymine
DLGAP5	Disks Large-Associated Protein 5
DNMT	DNA methyltransferase
DSS	Disease-Specific Survival
EBUS	Endobronchial Ultrasound
Eg5	Kinesin-related motor protein
EGFR	Epidermal Growth Factor Receptor
ESCC	Esophageal Squamous cell carcinoma
G1 phase	Gap one phase
G2 phase	Gap two phase
GWAS	genome-wide association studies
HBEC	Human Bronchial Epithelial Cells
HDAC	Histone Deacetylase
HNSCC	Head and Neck Squamous Cell Carcinoma
HPV	Human Papilloma Viruse
HURP	Hepatoma Up Regulated Protein
INCENP	Inner Centromere Protein
KRAS	Kirsten Rat Sarcoma viral gene
LCNEC	Large Cell Neuroendocrine cancer
LCT	Lung Carcinoid Tumours
LD-CT	Low-Dose Computed Tomography
M phase	Mitotic phase
mC	methylated Cytosine

MDR	Multi-Drug Resistance
MIA	Minimally Invasive Adenocarcinoma
MSC	Mitotic Spindle Checkpoint
MTR	Malignant Transformation Rate
MTT	3-(4,5-Dimethylthiazol-2-Yl)-2,5-Diphenyltetrazolium Bromide
NLST	National Lung Screening Trial
NSCLC	Non-Small Cell Lung Carcinoma
OED	Oral Epithelial Dysplasia
OPSCC	Oropharyngeal Squamous Cell Carcinoma
OS	Overall Survival
PFS	Progression-Free Survival
PPi	Pyrophosphate
PSQ	Pyrosequencing
qMSP	Quantitative Methylation Specific PCR
RCC	Renal Cell Carcinoma
RFS	Relapse-Free Survival
RQ	Relative Quantity
RTCs	Respiratory Tract Cancers
S phase	DNA synthesis phase
SABR	Stereotactic Ablative Body Radiotherapy
SAC	Spindle Assembly Checkpoint
SBRT	Stereotactic Body Radiation Therapy
shRNA	short hairpin RNA

SqCLC	Squamous Cell lung Carcinoma
TA overhang	Thymine and Adenine overhang
TACC3	Transforming Acidic Coiled-Coil-containing protein 3
TKIs	Tyrosine Kinase Inhibitors
TPF	docetaxel, cisplatin, and fluorouracil
TPX2	Targeting Protein for Xenopus kinesin-like protein 2
TUBB	Tubulin Beta class I
TUBB3	Tubulin Beta class III
VAST	Video Assisted Thoracoscopic Surgery
VPA	Valproic Acid

Glossary table

Aneuploidy	An abnormal number of chromosomes per cell, differing from the normal karyotype (somatic number 2n, or n in gametes) by loss or gain of pairs of chromosomes, whole chromosomes or chromosome fragments. Chromosome missegregation in mitosis or meiosis can produce aneuploid cells or organisms respectively (Extracted from www.nature.com).
Cancer incidence rate	The number of new cancers of a specific site/type occurring in a specified population during a year, usually expressed as the number of cancers per 100,000 population at risk. That is, Incidence rate = (New cancers / Population) × 100,000. (Extracted from surveillance.cancer.gov).
Cancer mortality rate	The number of deaths, with cancer as the underlying cause of death, occurring in a specified population during a year. Cancer mortality is usually expressed as the number of deaths due to cancer per 100,000 population. That is, Mortality Rate = (Cancer Deaths / Population) × 100,000. (Extracted from surveillance.cancer.gov).
Centrosome	The centrosome is the major microtubule-organising centre of the cell and consists of two centrioles surrounded by pericentriolar material. The centrosome is duplicated during the cell cycle and in mitosis the two centrosomes form the poles of the mitotic spindle, which segregates the chromosomes into two daughter cells (Extracted from www.nature.com).

DNA methylation	The covalent addition of methyl groups to DNA bases, typically the cytosine of CpG dinucleotides. It is catalyzed by methyltransferase enzymes using a S-adenosyl methionine donor and can lead to mitotic propagation of the modified sequence with consequences for the binding of regulatory proteins such as transcription factors (Extracted from www.nature.com).
Extra-capsular spread	Extension of the tumour through the capsule of the lymph node into the perinodal tissues (Extracted from (1)).
Hazard Ratio	A measure of how often a particular event happens in one group compared to how often it happens in another group, over time. In cancer research, hazard ratios are often used in clinical trials to measure survival at any point in time in a group of patients who have been given a specific treatment compared to a control group given another treatment or a placebo. A hazard ratio of one means that there is no difference in survival between the two groups. A hazard ratio of greater than one or less than one means that survival was better in one of the groups (Extracted from www.cancer.gov).
Kinetochore	Kinetochores are large protein complexes that assemble at the centromere of a chromosome, and function to connect the chromosome to microtubules in the mitotic spindle (Extracted from www.nature.com).
Microtubule	Microtubules are cylindrical polymers composed of alpha and beta tubulin. They are a major component of the cytoskeleton and mediate crucial cellular functions including formation of the mitotic spindle that segregates chromosomes during cell division and intracellular trafficking. (Extracted from www.nature.com).
Mitotic spindle	The mitotic spindle is the microtubule-based bipolar structure that

segregates the chromosomes in mitosis. The poles of the mitotic spindle are made up of centrosomes and the chromosomes are lined up at the spindle equator to ensure their correct bi-orientation and segregation (Extracted from www.nature.com).

Multivariate analysis Exploring the association between one outcome variable (referred to as the dependent variable) and one or more predictor variables (referred to as independent variables). Multivariate techniques concern the statistical analysis of relationships among a set of variables, particularly when at least three variables are involved. Regression analysis one example of a multivariable technique (Extracted from practice.sph.umich.edu).

Overall survival The percentage of people in a study or treatment group who are still alive for a certain period of time after they were diagnosed with or started treatment for a disease, such as cancer. The overall survival rate is often stated as a five-year survival rate, which is the percentage of people in a study or treatment group who are alive five years after their diagnosis or the start of treatment. Also called survival rate (Extracted from surveillance.cancer.gov).

Phase I trials Small dose-finding studies designed to rapidly identify the optimal dose of a new agent, which is administered on one or more dosing schedules that were shown to be effective in preclinical models of human cancer (Extracted from (2)).

Phase II trials The primary objective of phase II trials is to define the spectrum of antitumor activity for a new agent administered at the optimal dose and schedule from phase I trials (Extracted from (2)).

Phase III trials Designed to determine efficacy or clinical benefit. They are typically

large cooperative group trials that randomize patients to new regimens versus standard therapy (Extracted from (2)).

Polyploidy The presence of more than two homologous sets of chromosomes in a cell or organism. It occurs as a result of genome duplication due to nondisjunction during meiosis (Extracted from www.nature.com).

Pyrosequencing Pyrosequencing is a sequencing-by-synthesis method that quantitatively monitors the real-time incorporation of nucleotides through the enzymatic conversion of released pyrophosphate into a proportional light signal (Extracted from (3)).

Univariate analysis Exploring one variable at a time in a data set. It investigates each variable in a data set separately and looks at the range of values, as well as the central tendency of the values. For this type of analysis, researchers look at the range, mean, median and mode of each variable as well as describe any apparent patterns (Extracted from practice.sph.umich.edu).

Chapter 1 - Introduction

Respiratory Tract Cancers (RTCs), which include malignancies of lung, upper respiratory tract and head/neck affect almost 2.5 million people world-wide and represent the first cause of cancer-death (Figure 1) (4).

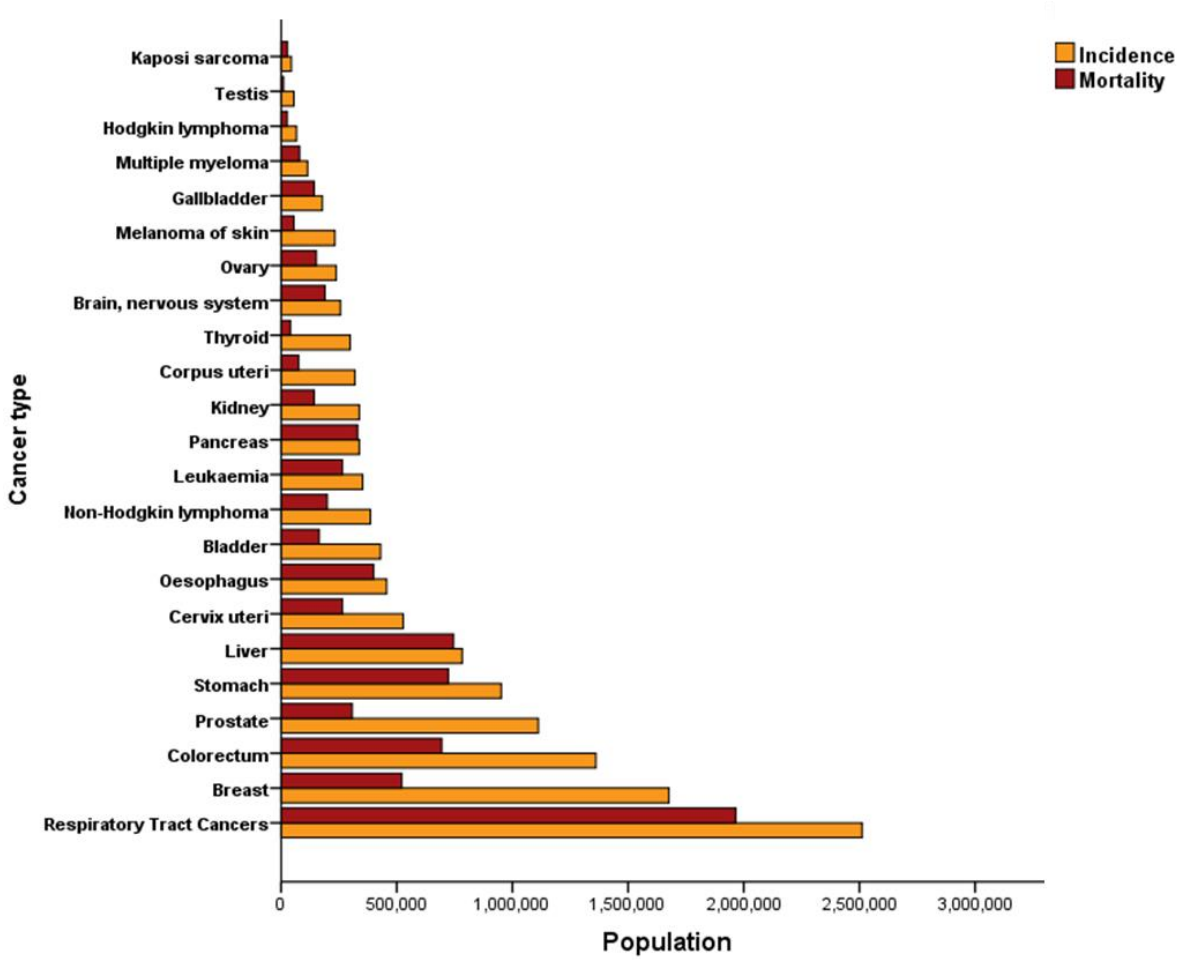

Figure 1: Incidence and mortality rates for the most frequently diagnosed malignancies for both sexes worldwide/ 2012. Respiratory Tract Cancers are the most frequent cancer types with 2,511,029 cases. This bar chart has been plotted based on the data obtained on 15th May 2015from the GLOBCAN 2012 website.

The proportion of all reported RTCs cases are approximately 18% worldwide and 15% within the UK among diagnosed cancer cases. Overall incidence of RTCs in men is two times higher than that in women, whereas the difference between the genders in the UK is less. The mortality due to RTCs represents quarter of all reported cancer deaths. The proportion of men who die from RTCs is twice as high as that of women across the world although this difference is smaller in both British genders (Table 1).

Table 1: (%) Estimated incidence & mortality of respiratory tract cancers in comparison of all cancers excluding non-melanoma skin cancer. The data obtained from GLOBCAN 2012 and NCRI 2013/4 data base.

	WORLDWIDE				UNITED KINGDOM			
Cancer	**Incidence**		**Mortality**		**Incidence**		**Mortality**	
	Number	(%)	Number	(%)	Number	(%)	Number	(%)
Both sexes								
Lip, oral cavity	300373	2.1	145353	1.8	4986	1.5	1296	0.8
Nasopharynx	86691	0.6	50831	0.6	309	0.1	117	0.1
Other pharynx	142387	1	96105	1.2	2200	0.7	846	0.5
Larynx	156877	1.1	83376	1	2201	0.7	765	0.5
Lung	1824701	13	1589925	19.4	40382	12.3	35581	22.5
Women								
Lip, oral cavity	101398	1.5	47413	1.3	1848	1.1	497	0.7
Nasopharynx	25795	0.4	15075	0.4	94	0.1	37	0
Other pharynx	27256	0.4	18507	0.5	553	0.3	229	0.3
Larynx	18775	0.3	10115	0.3	390	0.2	142	0.2
Lung	583100	8.8	491223	13.8	18537	11.4	16186	21.6
Men								
Lip, oral cavity	198975	2.7	97940	2.1	3138	1.9	799	1
Nasopharynx	60896	0.8	35756	0.8	215	0.1	80	0.1
Other pharynx	115131	1.6	77598	1.7	1647	1	617	0.7
Larynx	138102	1.9	73261	1.6	1811	1.1	623	0.8
Lung	1241601	16.7	1098702	23.6	21845	13.2	19395	23.4

1.1 Lung cancer

Lung malignancies represent a serious medical problem worldwide. According to the GLOBCAN 2012 database, Lung cancer, which is almost close to colorectum cancer incidence, ranks as the second most common malignant disease after breast cancer in females and prostate cancer in males in the UK (Figure 1.1).

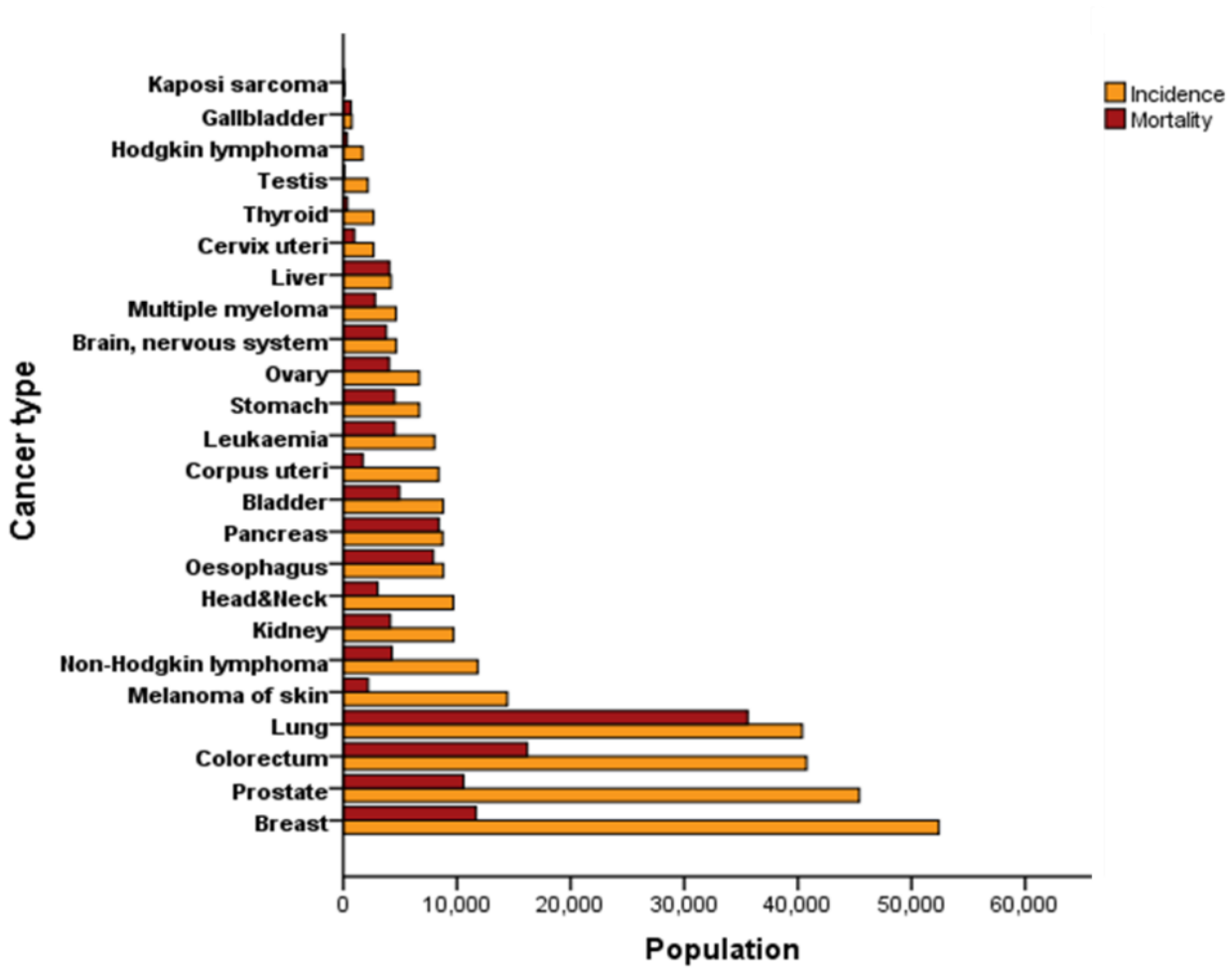

Figure 1.1: Bar chart demonstrating the estimated incidence and mortality rates for both sexes in the UK. This chart has been plotted using data obtained on 15th May 2015 from GLOBCAN 2012 website.

1.1.1 Histological description

Lung cancers include three main different histological types; Non-Small Cell Lung Carcinoma (NSCLC), accounting for over 85%, Small Cell Lung Carcinoma (SCLC), which accounts for less than 10-15%, and Lung Carcinoid Tumours (LCT) which represent fewer than 5% of lung cancers. NSCLC is subdivided into Squamous Cell lung Carcinoma (SqCLC), lung adenocarcinoma (LAdC) and large-cell lung carcinoma. LAdC is the most common histological subtype of NSCLC (~44%) followed by SqCLC (~20%) (csg.ncri.org.uk), (5).

The lung is a complex organ, which is anatomically sectioned into central and peripheral airway compartments. As these compartments have entirely different histological structures, each one develops distinct histologic subtypes of NSCLC. Whereas SqCLC and SCLC widely emerge from the central airways, most if not all of adenocarcinomas emerges from the peripheral ones. In general, SqCLC and LAdC are the most common histologic subtypes of NSCLC (6).

Recently, the formerly restricted term “bronchioloalveolar carcinoma (BAC)” has been reclassified into wider spectrum of subtypes e.g. adenocarcinoma in situ (AIS), minimally invasive adenocarcinoma (MIA), lepidic-predominant adenocarcinoma, major invasive adenocarcinoma with a lepidic component, and invasive mucinous adenocarcinoma (Figure 1.2) (7). According this new classification, Adenocarcinoma is developed from preinvasive lesions, through minimally invasive adenocarcinoma (MIA), to invasiveness stage which could be either invasive adenocarcinoma or mucinous adenocarcinoma. Preinvasive lesions include AIS and atypical adenomatous hyperplasia. AIS is described as a localised small (≤3 cm) adenocarcinoma which is mainly non-mucinous composing of pneumocytes and/or Clara cells but rarely to be mucinous AIS (6). MIA is known as a small, solitary adenocarcinoma (≤3 cm), with maximum dimension of invasion in any one focus measuring

≤5 mm expect lymphatics, blood vessels, or pleura. Similar to AIS, MIA is typically non-mucinous, but rare cases of mucinous MIA occur (8) ,(9). Instead of AIS or MIA, Lepidic-predominant adenocarcinoma diagnosis is made if the invasiveness includes lymphatics, blood vessels or pleura, or if the tumour contains necrosis. Invasive adenocarcinomas are suspected when the invasiveness is more than 3 cm and measuring higher than 5 mm dimension in at least one focus where the invasive predominant components/lesions are included. Invasive adenocarcinomas accounts for higher than 70% to 90% of surgically resected LAdC due to the rarity of AIS and MIA. It has been recently classified as predominant pattern and subtyped with lepidic, acinar, papillary, solid patterns, and newly added histologic subtype “micropapillary”. Variants of invasive adenocarcinoma include colloid, fetal, enteric and invasive mucinous adenocarcinoma, which previously categorised as mucinous BAC. Invasive mucinous adenocarcinoma shows a high level of KRAS mutation but lack of EGFR mutation (7).

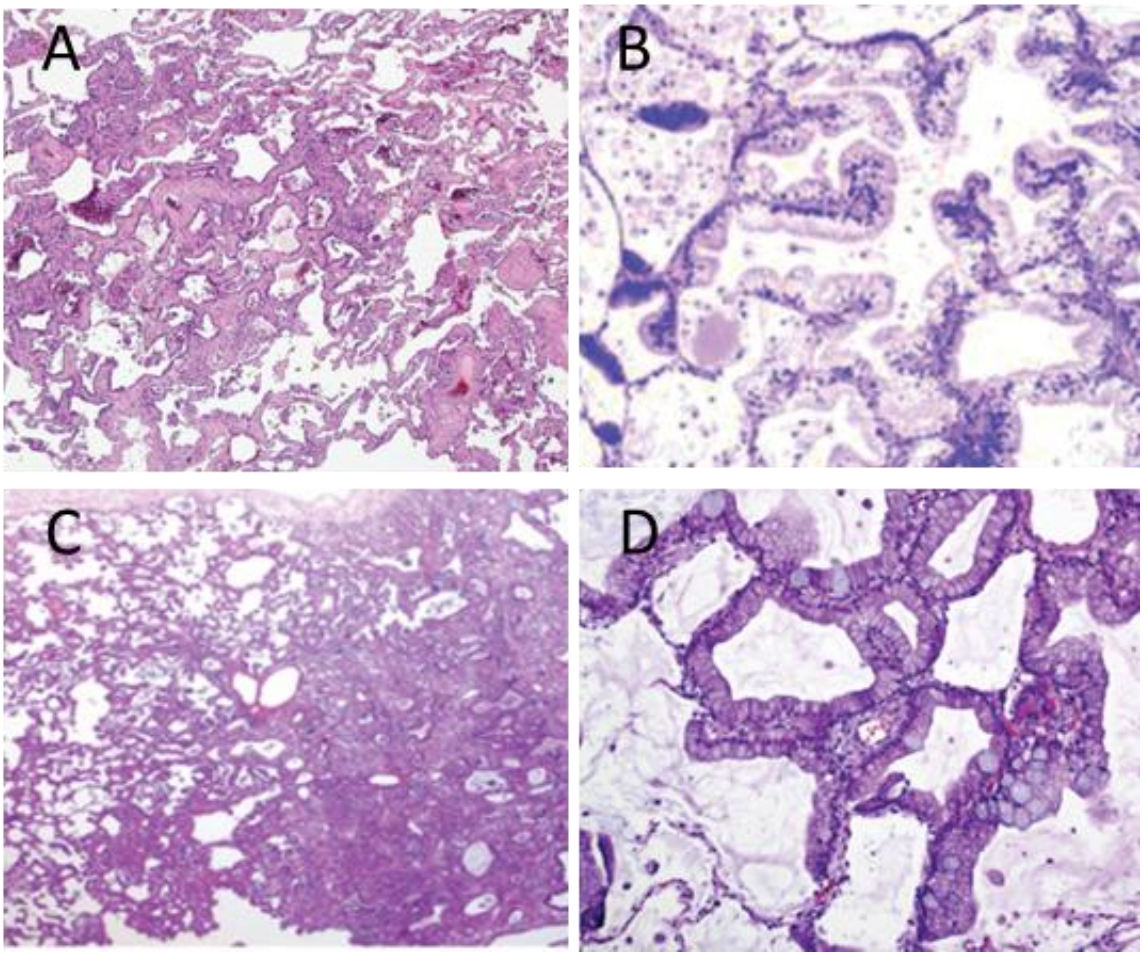

Figure 1.2: (A) Non-mucinous AIS (B) Mucinous AIS (C) Nonmucinous minimally invasive adenocarcinoma (D) Invasive mucinous adenocarcinoma. Adapted from (6), (7), (10).

Squamous cell carcinomas are thought to arise after a series of sequential events. Mucosal pathological changes in the central lung compartments, which may give rise to invasive squamous cell carcinoma, progress from normal to carcinoma in situ (CIS), through metaplasia for lung and dysplastic steps of increasing severity (Figure 1.3) (11). In the classification of preinvasive lesions, squamous dysplasia is the counterpart to AAH, which proliferate mildly to moderately, and squamous cell CIS the counterpart to AIS (Figure 1.4: A- C) (6).

SCLC is microscopically defined as small sized and round-to-fusiform shaped tumour cells. Despite of the small size of its cancerous cells, it is the most aggressive form of lung malignancies due high mitotic rate. The most prominent morphological diagnostic characteristic of SCLC is the presence of neuroendocrine morphology (Figure 1.4.A) (12) , (13).

Finally, the rest of lung carcinomas specified as neuroendocrine tumours are lung carcinoid tumours (Figure 1.4.B) large cell neuroendocrine cancer (LCNEC) (Figure 1.4.C). Lung carcinoid malignancies are ranged from the low-grade typical carcinoid to intermediate-grade atypical carcinoid, while LCNEC represents the high-grade large cell neuroendocrine cancer (14).

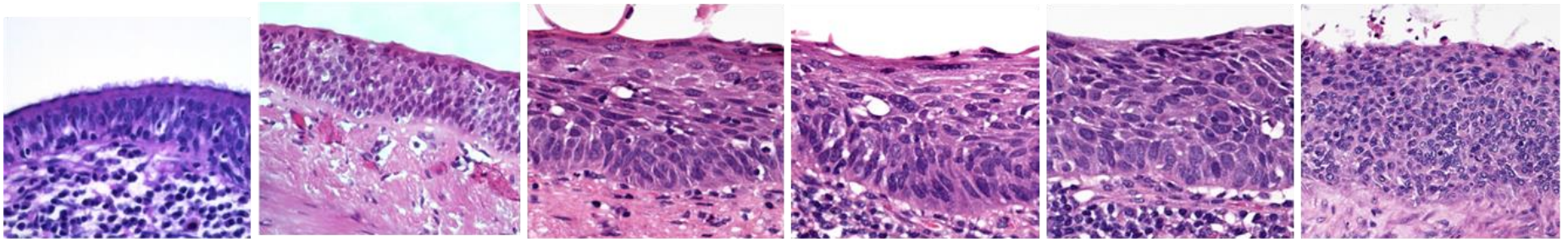

Figure 1.3: Histological changes through the pathogenesis of lung squamous cell carcinoma. Adapted from (13).

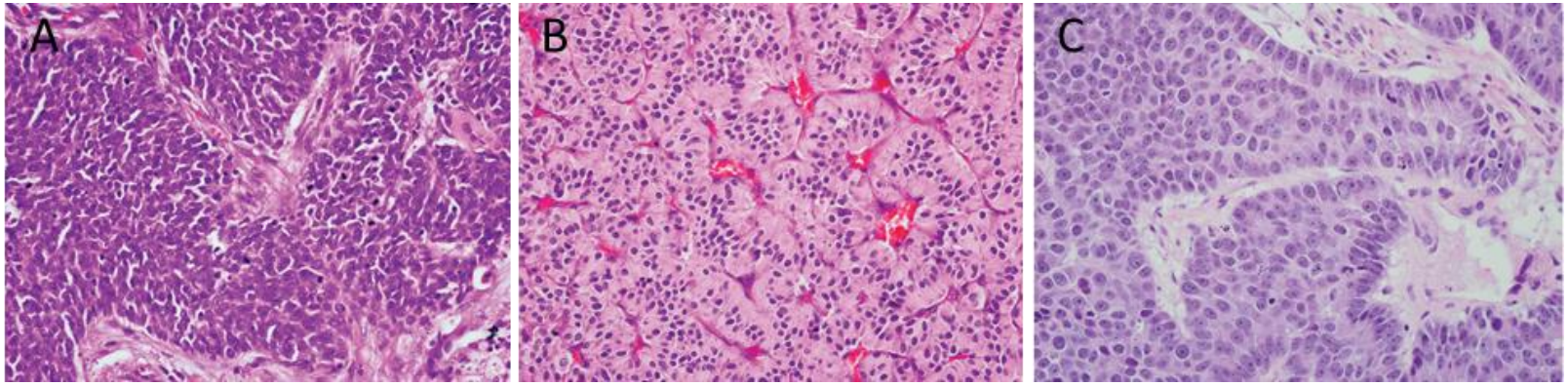

Figure 1.4: Histological preparations of representative examples of (A) Small-cell carcinoma, (B) Carcinoid tumour, (C) Large-cell neuroendocrine carcinoma. Adapted from (15).

1.1.2 Preneoplastic precursors

As with other malignancies, lung cancers arise through a series of preneoplastic changes constituting a multistage pathogenesis of these carcinomas. The accumulative precursors' lesions are crucial to develop respiratory tract malignancies including lung cancer. Long-term observations elucidate that not all lung tumours pursue a particular histological trend, and it is undoubtedly difficult to predict the clinical course particularly for early lesions. Such preinvasive lesions may offer opportunities for predicting risk of cancer progression (16).

1.1.2.1 Squamous preneoplasia:

Epithelial dysplastic squamous lesions of central lung airway vary in degree from mild to severe (17). Nonetheless, a continuous histologic irregular alteration is the feature of the dysplastic lesions that may result in some overlapping between stages. Less histological irregularity is shown in mild squamous dysplasia in comparison of that of moderate dysplasia or even for that of severe dysplasia (18). CIS demonstrate severe cytological aberrations which is disorganised histologically, it has, however, non-damaged basement membrane with free invasion stroma (11), (19). It is also of note that the molecular events involved in the squamous carcinogenesis present an accumulation of genetic & epigenetic changes such as loss of heterozygosity on the same hotspots (of the 3p, 9p & 17p chromosomes), p53 mutations, p16 methylation and many more (11).

1.1.2.2 Adenomatous preneoplasia

The atypical adenomatous hyperplasias (AAH) feature has been represented as the main precursor lesion of adenocarcinoma for long term beside Clara cells or type 2 pneumocytes (20). However, recent evidence has generated other categories being determine as

additional pre-invasive lesions (adenocarcinoma in situ/AIS, minimally invasive adenocarcinoma/MIA, lepidic predominant growth pat-tern, and invasive adenocarcinomas or predominant non-lepidic growth (6). However, the pathogenesis of many peripheral adenocarcinomas remains to be fully understood (21). The genetic abnormalities arising adenocarcinoma are categorised into two pathways depending on the smoking status of adenocarcinomas patients. While the main genetic aberration pathway in non-smokers is EGFR mutation and ⁄ or up-regulation, KRAS mutation, p16 methylation and p53 inactivation are the main abnormalities engaged in progressing the pre-invasive lesions in smoking NSCLC patients (20).

1.1.3 Epidemiology

Lung cancer is regarded as an age related disease. More than 50% of individuals diagnosed with lung cancer occur over the age of 65 years and about one third of all cases are diagnosed in those aged (70-79) (22), (23). By 2030, it is expected that two thirds of total lung cancer patients will be age 65 years and over (24). Moreover, there is a dramatic increase in mortality rates of lung cancer cases in elderly females in comparison of that in elderly men, which may lag behind improvement observed in younger NSCLC patients (25). Regarding the patient gender, global rates of Incidence and mortality are half in women in comparison of those in men. However, these rates of lung carcinoma for British women are only lower to those for British men respectively (Table 1).

1.1.3.1 Genetic predisposition

Lung cancer is a typical example of disease evolving through the interaction of environment on the human genetic background. Over the last decade there have been comprehensive genome-wide association studies (GWAS) in an effort to identify genetic polymorphisms

that are potentially associated with higher risk. GWAS on lung cancer were carried out utilising case-control designs that included thousands of recruits across Europe. Conclusive evidence was provided on the association of SNPs in a region at 15q25 to lung cancer. However, their contribution to the overall risk estimation was 14% of 2,513 lung cancer cases irrespective of smoking status (26), (27). Additional GWAS analyses have also confirmed the strong link between genetic variants at 15q and Respiratory Tract Cancers (RTCs) even when adjusted for smoking (28), (29). The five variants reported in the latter study have close proximity to genes previously shown to be related to lung cancer development (29). The most recent comprehensive GWAS has indicated etiological heterogeneity to lung malignancy development affected by genetic variation, in particular in squamous cell lung carcinoma (30). Despite the existing information originating from very high powered studies involving multinational cohorts, the identified polymorphisms have not been yet successfully incorporated into lung cancer risk models.

1.1.3.2 Lifestyle factors

The most important known risk factor that causes RTCs is tobacco. Although most lung malignancies are diagnosed in former or current smokers, patients diagnosed with NSCLC who are non-smokers account for 10%-25% of all cases. Among ethnic groups of patients, there is remarkable variation of non-smokers distribution, with higher proportion in women compared with men and in Asian patients as opposed to Caucasians (Samet 2009 , Scagliotti 2009). Approximately two third of Asian women diagnosed with lung malignancies are never-smokers (31). This variation may result from gender and geographic diversity in smoking environments [WHO Report on the Global Tobacco Epidemic, 2008]. Whilst smoking proportions in few developed countries decrease, the proportion of NSCLC patients who are non-smokers is probably to increase in such countries (32). The reason

why those non-smokers are diagnosed with NSCLC remains to be fully understood. However, the environmental factors such as passive smoking, genetic factors, and history of lung illness could be contributors (33).

In many respects, genetic instability features of NSCLC in never-smokers are different from those in smokers. For instance, mutations of epidermal growth factor receptor (EGFR) seem to be two fold higher in never-smokers than that in smokers In contrast, KRAS mutations are 4 fold more prevalent in smokers than in never-smoked NCLC patients (34). These findings are comparable with what has been proved in previous study (35). Regardless of their treatment setting or genetic variation, Never-smoked NSCLC patients have predominantly higher survival rates than smokers (36), (37). Taken together, these reported data may suggest that the smoking status could confer prognostic and predict values for NCLC treatment.

The differences in socio-economic status among lung patients groups during the period from diagnosis to therapy are important to determine systematically. The socio-economic inequalities, if existence could be useful to inform the development interventions to minimise the diagnostic-to- treatment time intervals, eventually reducing inequalities in survival rate (38). Malnutrition is an additional risk factor that significantly reduces survival among cancer patient after surgery (39), (40).

1.1.4 Diagnosis

The main reason behind the high mortality of lung cancer, (4) can be attributed to the fact that less than 25% of the lung malignancies are diagnosed at early stages (41). This appalling prognosis for lung malignancies warranted the improvement of lung cancer screening by under taking many clinical trials that would decrease the mortality rates of

lung cancer by diagnosing this malignancy at early stages, long before it would reach advance stage or become incurable. The early attempts of reducing lung cancer deaths employing chest radiographs were carried out since 1950s. This technique resulted in an augmented diagnosis of lung carcinoma at earlier stages in comparison of control cohorts. However, reducing the mortality of lung cancer was not reached the desired aim (42), (43). A higher sensitivity imaging for lung cancer diagnosis had become available with developing the volumetric computed tomography (CT) (Figure 1.5). CT allows measuring pulmonary nodules with diameter less than 3mm with high accuracy (44). Screening with low-dose CT (LD-CT) reduces lung cancer mortality by 20% in the national lung screening trial (NLST) study (41). Endobronchial ultrasound (EBUS) probes were initially developed to assess the invasion depth of malignancies in the bronchi and also for lymph node screening in lung cancer patients. New techniques of EBUS, EBUS-TBNA (Figure 1.5) and EUS-FNA, as well as video assisted thoracoscopic surgery (VAST) were introduced for staging NSCLC with higher than 84% sensitivity for malignancy (45) (46), (47).

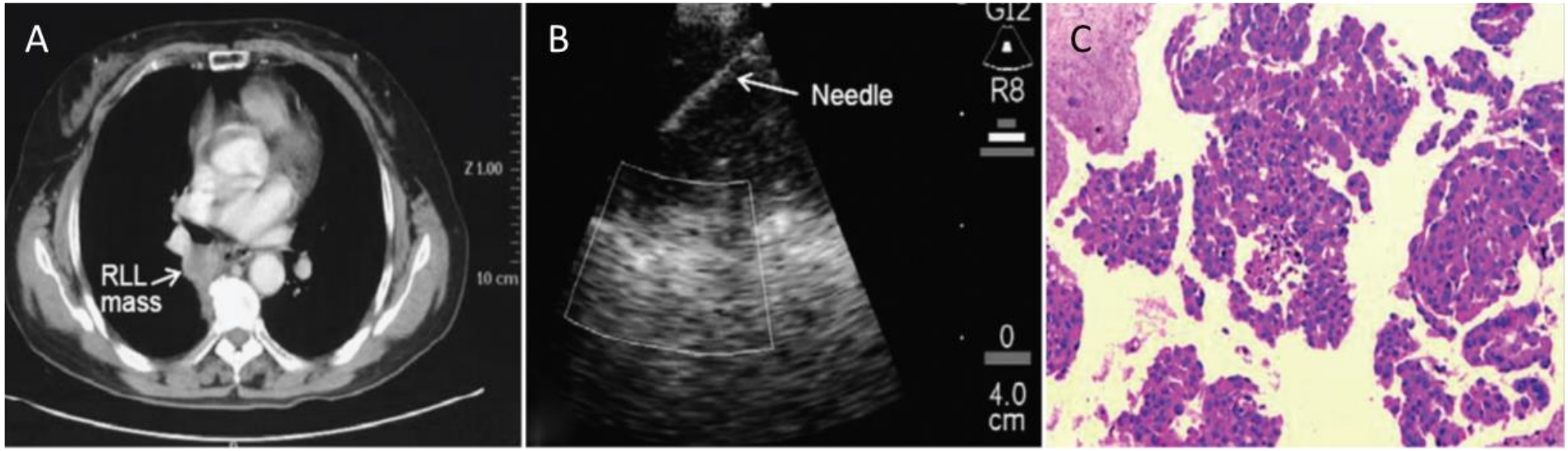

Figure 1.5: (A) Chest CT demonstrates Right middle lobe (RML) mass diagnosed as lung adenocarcinoma. (B) Representative case of EBUS-TBNA, (C) Histological diagnosis. The figures were adapted from (45).

1.1.5 Therapy

1.1.5.1 Surgery

The outcomes of surgical therapy applied on lung cancer patients have been improved by early diagnosis and accurate surgical procedures. However, patients with advanced lung cancer encounter recurrence, even postoperative treatment. Moreover, about 70% of patients diagnosed with NSCLC have unresectable advanced cancer (48), (49). Recently, it has been strongly approved that the same short term surgical outcome could be obtained by either thoracoscopic lobectomy or segmentectomy, therefore thoracoscopic segmentectomy is the choice to minimise the postoperative respiratory malfunction (50).

1.1.5.2 Chemotherapy

Many chemotherapeutic schemes are utilised in NSCLC treatment either as preoperative (neoadjuvant) or post-operative (adjuvant) regimens. Whether to apply neoadjuvant or adjuvant treatment in cancer therapeutic setting remains a debatable topic. However, postoperative chemotherapy is still the regimen of choice in NSCLC treatment. (51). Chemotherapy is also classified as first-line (initial) or second line (subsequent, if first line fails). If both these lines have not improved the outcome, the third line therapy would be the choice. The most commonly used chemotherapeutic agents in aforementioned NSCLC therapeutic regimes are organometalics, such as cisplatin, carboplatin and oxaliplatin (52), and anti-mitotics, for instance paclitaxel, docetaxel, and vinorelbine (53) as well as antimetabolites like pemetrexed (54) (Table 1.1).

Recent advances in targeted therapies for lung cancer have witnessed discovering new generations of drugs used for NSCLC treatment by targeting the epidermal growth factor

Table 1.1 : The most commonly used chemotherapeutic agents in NSCLC therapy

Agent	Target	Molecular mechanism	Reference
Organometalics			
Cisplatin, Carboplatin & Oxaliplatin	Target DNA producing intrastrand cross-links with the purine bases.	Interfering with DNA repair mechanisms, causing DNA damage, and inducing apoptosis.	(52)
Antimitotics			
Vinca alkaloids (Vinorelbine)	Binds to Beta-tubulin of microtubules disrupting their interactions resulting in microtubule depolymerisation.	Mitotic arrest and apoptosis induction by bcl-2 phosphorylation and the elevations of p53 and p21.	(55)
Taxanes (Paclitaxel & Docetaxel)	Stabilise the microtubules resulting in blockage of cell mitosis and induces apoptotic and non-apoptotic cell death.	Apoptosis induction by activating mitotic spindle checkpoint.	(56)
Antimetabolites			
Pemetrexed & Methotrixate	Deactivate folate-dependent enzymes required for nucleotide synthesis during DNA replication.	Cause DNA damage, arresting cell cycle at S-phase, and inducing caspase- dependent and independent apoptosis.	(57)
Gemcitabine	Targets of ribonucleotide reductase (RNR) blocking DNA replication and repair.	Induces apoptosis via replacing cytidine, during DNA replication and then arrests cancerous cell growth.	(58)

receptor (EGFR) pathways using small molecule tyrosine kinase inhibitors (EGFR-TKIs) and anti-EGFR monoclonal antibodies. They have evolved from single receptor 1st-generation inhibitors, such as Erlotinib (59)and Gefitinib (60), in random population of patients to biomarker-driven clinical trials of more powerful 2nd and 3rd- generation irreversible multi-targeted EGFR-TKIs, e.g. Afatinib (61) and AZ9291 respectively, as well as anti-EGFR monoclonal antibodies (62). There are about 11 clinical trials recruiting in the UK administrating taxanes either as a monotherapy or in combination with other chemotherapeutic agents [UK clinical trials].

1.1.5.3 Radiotherapy

Radiotherapy can be given with the aim of curing cancer or preventing recurrence post operation. Many approaches of having radiotherapy, such as conventional external radiotherapy, Continuous Hyper fractionated Accelerated Radiotherapy (CHART) and Stereotactic Body Radiation Therapy (SBRT), may vary from daily application to shorter interval. They can be used to treat NSCLC tumours as an alternative to surgery for patient who can't have surgery, or where the tumour is in a difficult area to operate on (63). For instance, accumulative evidence has proved that Stereotactic ablative body radiotherapy (SABR), which is ordinarily applied for shorter interval than conventional external radiotherapy, can accomplish superior therapeutic outcomes (64). Therefore, SABR has been accepted as the standard radiotherapy for treating patients diagnosed with early stage NSCLC in few nations for example the UK and Netherlands (65).

1.1.6 Prognosis

In the chemotherapeutic setting of NSCLC, the two main targets are to prolong survival duration and to reduce the symptoms related to the disease and therapy (66). As aforementioned, several therapeutic options are currently available for advanced NSCLC

including organometalics, antimitotics and antimetabolites (Table 1.1), in addition to molecular/targeted therapies (e.g. erlotinib and bevacizumab). However, the prognosis is still to be improved (67). Despite the advance in molecular medicine of lung cancer, survival in both early and advanced NSCLC stages is still low (68). Many areas of research, such as genetics , epigenetics (69), (70), proteomics (71), (72), circulating tumour cells (73), and others, have made significant progress in identifying genes, or their encoded proteins, as prognostic or predictive biomarkers for lung cancer therapy. However, the prognosis is still poor. Very recent phase III clinical study using pooled analysis of mature overall survival (OS) data, among 631 Asian patients with advanced NSCLC carried common EGFR mutations, has proved that including afatinib in chemotherapeutic regimen improved OS (median 27.3 months) compared with afatinib-free chemotherapy (median 24.3 months). This is the real benefit of survival was not observe in previous clinical study with erlotinib or gefitinib (61).

1.2 Head and Neck Squamous Cell carcinoma (HNSCC)

The majority of head and neck tumours, which constitute a heterogeneous group of malignancies, are squamous cell carcinomas. They include the malignancies of the lip, oral cavity, pharynx, and larynx which arise from the mucosal tissue of the upper aerodigestive tract. HNSCC develops over a long period of time, which may span 20 years or more (74), (4). Among all cancer types reported over the world, excluding non-melanoma skin cancer, head and neck cancers represent the seventh most commonly occurring malignancy (incidence of 686,328 in 2012) and ranks as the seventh most common cause of cancer-related death (375665 cases in 2012). While in the UK, it has rank eight of incidence with (9516 cases in 2013/14), and the fifteenth most common cause of cancer related death with (3033 cases in 2013/14) (NCRI HNSCC CSG Annual Repeport 2013/2014) (Table 1 and Figure 1.1). On the other hand, Amit et al 2013 data shows that during the last decades the disease-specific survival DSS associated with surgical therapy has improved significantly from 69%, during the period between 1990 and 2000, to 81% at the period between 2001 and 2011 in the UK (75). Although OS is usually around 55% at 5 years, the risk factors for HNSCC also predispose to lung cancer, COPD, heart disease, stroke etc. The mortality, therefore, in cured individuals remains high. In addition, the HNSCC cases were slightly higher in males than females, while worldwide, this difference in men is almost twice as high as in women which is related to risk factors such as smoking and the gender difference is reducing (Table 1). Taken together, these reported data may indicate the improvement in HNSCCs prognosis in the UK, of particular in women, in comparison of that around the globe.

1.2.1 Histological description

Squamous carcinogenesis has very similar histopathological stages in both lung and HNSCC Carcinomas. It progresses from normal to carcinoma, through hyperplasia (instead of metaplasia for lung) and dysplastic steps of increasing severity (76) (Figure 1.6).

1.2.1.1 Preneoplastic precursors

HNSCC may require many years to develop from pre-neoplastic cells, evolving through accumulation of genetic and epigenetic changes in epithelial cells that result in histological abnormalities (77). This frequently occurs in so called field cancerization (Figure 1.7). This concept was first referred to more than 60 years ago in an HNSCC clinical study in which a correlation was established between non-visible molecular or cellular abnormalities and HNSCC recurrence (78). Pre-neoplastic cells expand in a distinct cancer field owing to the early genetic events. Some clones of these cells undergo subsequent genetic alterations that transform them to cancerous phenotype. A meta-analysis of 14 non-randomized studies reporting a malignant transformation rate (MTR) included 992 oral dysplasia patients and found an overall MTR for surgical resected oral dysplastic lesions to be 5.4% (341 patients) in comparison to 14.6% of 651 patients who didn't undergo surgery ($p = 0.003$) (79). Overall, the population of pre-neoplastic daughter cells, with or without histological abnormalities, represent the field cancerization (77). Cancer-related genetic alterations are the main characteristics of pre-neoplastic cells, particularly loss of 17p (p53), 9p (CDKN2A) and 3p, leading to either up or down regulation of the indicated tumour suppressor genes or oncogens (80). While these alterations occur in dysplasia and may reflect early carcinogenesis, alterations at chromosomes 8, 4q and 11q may associate with late stage of carcinogenesis (81). These molecular markers, in addition to p53 inactivation, show that above one third of the HNSCC tumours are surrounded by

genetically altered mucosal epithelium, which has a macroscopically normal morphology, but histologically could be dysplastic fields (82). These fields are usually overlapped with the surgical margins during tumour resection and may remain in the patient causing the local recurrences or developing second primary tumours (80).

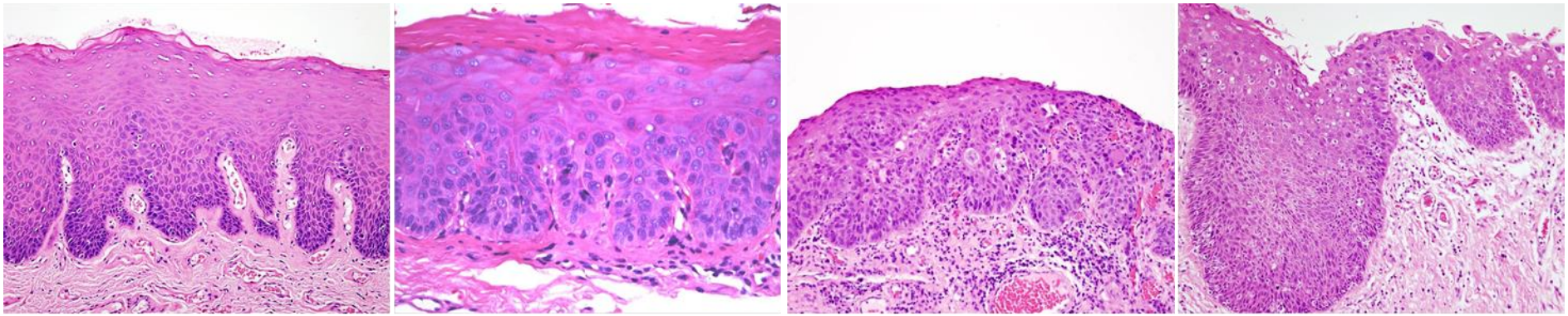

Figure 1.6: Histological changes through the pathogenesis of Head and Neck squamous cell carcinoma. The figures extracted from (76).

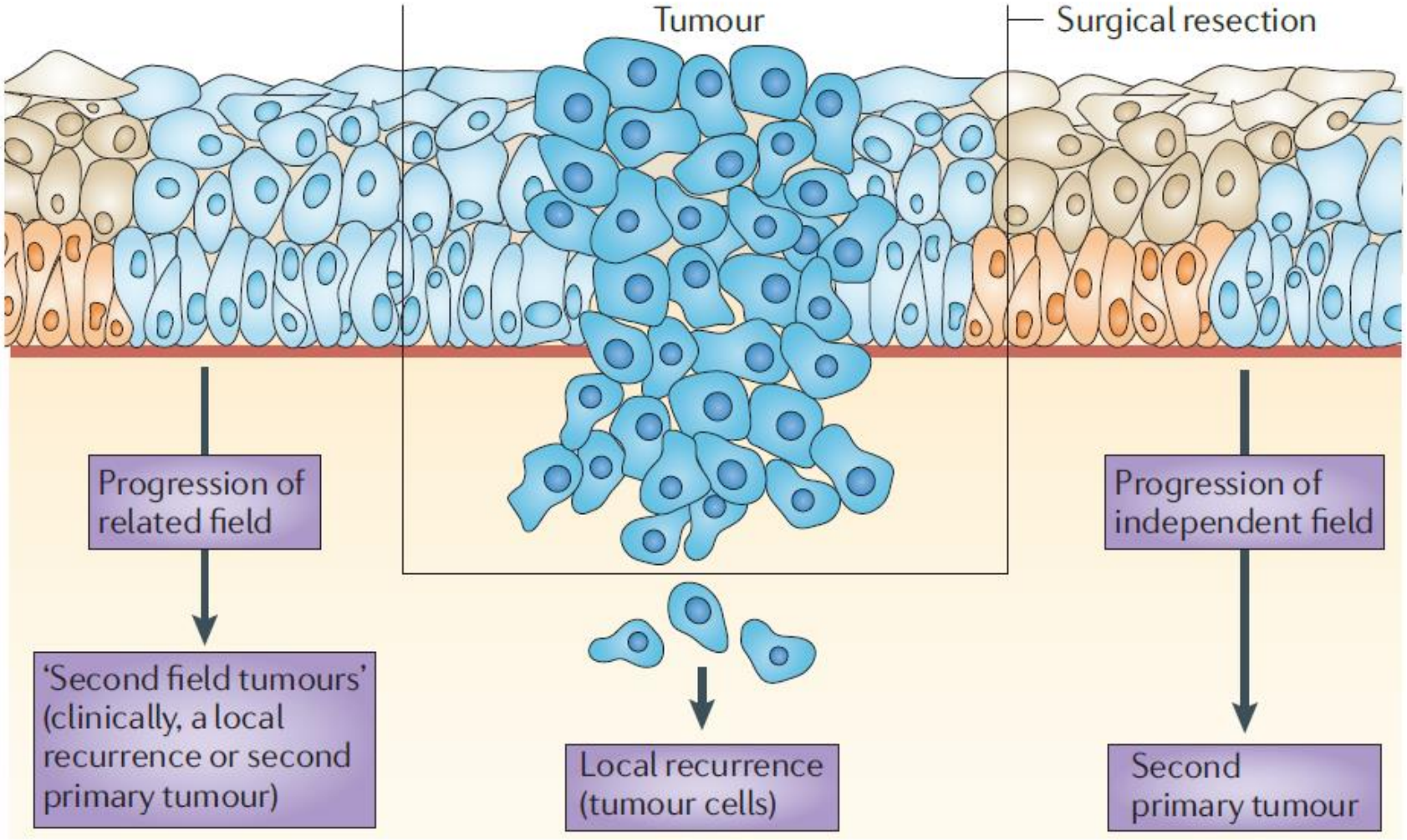

Figure 1.7: Field cancerization and local relapse. The figure was extracted from (80).

1.2.2 Epidemiology (risk factors)

The traditional risk factors for HNSCC are tobacco smoking and excessive alcohol consumption, while infection with high-risk human papillomaviruses (HPV) is mostly related to non-smoking HNSCC patients with cancers at the oropharyngeal subsite (83), (84).

1.2.2.1 Smoking and alcohol

It is well known that smoking and excessive consumption of alcohol are the most common risk factors for head and neck malignancies. These factors act independently and, when combined, they exhibit a synergistic effect (85). In a study of 1303 head and neck cancer patients, however, a marked number (172) had never smoked or drunk (i.e. 13%) (86). In addition, the role of tobacco smoking and alcohol as risk factors is implicated in oral epithelial dysplasia (OED), which is a preneoplastic lesion that gives rise to HNSCC at a rate of 12.1% (79). However, this perception of risk in OED remains to be fully understood. In a recent study, particular factors in non-smoking patients such as non-homogeneous appearance, large size and lesion position, specifically lateral tongue, may increase the rate of malignant transformation even in patients with mild or moderate dysplasia (87). In study on 291 Israeli patients with oral tongue squamous cell carcinoma, the outcome was similar regardless the risk factors (smoking and alcohol) (88). However, the oral cancer prognosis was worse in those younger patients under 40 and without risk factors.

1.2.2.2 Human Papilloma Viruses (HPV)

Human Papilloma Viruses (HPV) is an important risk factor in oropharyngeal squamous cell carcinoma (OPSCC). Decreasing in smoking has been related with decline in the incidence of all HNSCCs types (89) except HPV-positive oropharyngeal cancers (base of tongue and tonsils) which have risen in incidence (90). In contrast to tobacco smoking and alcohol

consumption, HPV infection is believed to be an etiologic factor in oropharyngeal cancers but not in oral, laryngeal or hypopharyngeal cancer (91), (84), (92). HPV-positive Head and Neck cancer, which has recently witnessed increasing incidence in many countries including the UK, seems to be linked with oral sexual behaviour and non-related with smoking (83).

1.2.2.3 Age

HNSCC cases are most frequently diagnosed in individuals who are older than 50 years. Nevertheless, oral squamous cell carcinoma among young generations is currently increasing around the globe (93). The role of age in HNSCC prognosis is not fully understood. However, it was demonstrated as criterion to prognosticate a therapeutic regime outcome since findings showed that disease-specific survival was significantly influenced by age in elderly patients (94). Cases that are above 70 are considered a preclusion to use of concomitant chemoradiotherapy (95). Recently, it has been reported that the younger non-smoker HNSCC patients, which are mainly HPV-positive HNSCCs, have a mean value of genetic aberrations 50% lower than that in those older smoker ones, where the age cut off was 40 years old. In particular, losses in 3p and 9p21 are not frequent molecular events in young patients, while they remain detectable in the entire older cases (96). Very recent studies reported an increased incidence of young patients with HPV positive Oropharyngeal Squamous Cell Carcinomas, who are overwhelmingly non-smoking (93).

1.2.3 Diagnosis

Early diagnosis of oral malignancies is essential for improving prognosis. There are a variety of diagnostic tools using in early detection of oral cancers that allow the delivery of timely treatment intervention to minimise the evolution of oral potentially malignant disorders to cancer. Two of these important approaches are the following:

1.2.3.1 Optical diagnosis

Auto-fluorescence based imaging system (VELscope™) has been suggested to visualise and manage oral malignancies (97). However, despite its high sensitivity in detection of oral mucosal disorders (84%), this technique has low specificity (15%) in discriminating high risk dysplasia from low risk or benign lesions. A combination of NIR optical imaging and real-time fluorescence imaging during surgery is one of recent successful strategies used during the surgery to target specific hallmarks of head and neck cancer to facilitate assessing tumour margins to optimise radical resection avoiding unwanted damage to the healthy tissues (98).

1.2.3.2 Molecular diagnosis

Diagnosis of oral malignancies at their earliest stages could markedly affect patient prognosis, therapeutic intervention, disease-specific survival, and recurrence. The discovery of body fluids-based molecular biomarkers delivers unique accessible tool to bypass painful invasive methods like biopsies that add excessive stress to an already disturbing experience. Utilizing plasma, serum, saliva and urine in detection of oral cancers including distant metastases is being evaluated. Determining promoter hypermethylation of tumour suppressor genes or LOH of 3p and 9p, and HPV and microRNA using these body fluids is an attractive target for early detection of OSCC (99), (100), (101). In a cohort of HNSCC patients collocated and evaluated at diagnosis, frequent hyper-methylation was identified in a panel

of 6 gene promoters (CDH1, CDKN2A/p16, DAPK, MGMT, RASSF1A and TIMP3) at very close levels of 82% and 78% in paired tumour and saliva samples respectively. The detection of promoter hyper-methylation in this small number of genes was sensitive enough to early diagnosis of neoplastic exfoliated cells in saliva months prior to clinical diagnosis of relapse (102). The problem, however, is that patients at risk from recurrence have usually received radiotherapy, therefore have xerostomia and cannot expectorate saliva. Frequent promoter hyper-methylation of KIF1A (103), EDNRB and DCC (104) has also recently been employed as molecular diagnostic tool of oral dysplasia/cancer in salivary rinses. Very recently, 40 pairs of oral cavity squamous cell carcinomas (OSCCs) and saliva samples collected from healthy individuals have been evaluated by Quantitative Methylation Specific PCR (qMSP) and identified a combination of 4 gene panel (CCNA1, DAPK, DCC and TIMP3) with high frequency of hypermethylation with sensitivity and specificity up to 92.5% (105). This panel of hyper-methylated genes may offer a feasible tool for diagnosing early stages of OSCC in clinical practice if pursued.

1.2.4 Therapy

Surgical resection and radiation therapy are the cornerstone of HNSCC treatment. However, recent years have witnessed increasing incorporation of systematic chemotherapy into therapeutic regimens of HNSCC patients either before surgery as an induction or neoadjuvant chemotherapy or during radiotherapy as a concomitant chemo-radiotherapy (106).

1.2.4.1 Surgery

Approximately, one-third of HNSCC patients are diagnosed at early stage cancer (stage I and II), and those patients are subjected to surgery or radiotherapy. The remaining patients, who

diagnosed with advanced stage cancer, are subjected to a combination of surgery, radiotherapy, chemotherapy or all. In order to prevent malignancy recurrence, postoperative chemo-radiotherapy is highly recommended, in particular, to high risk patients of recurrence, for instance cases with positive resection margin or extra-capsular metastatic invasion of cervical lymph nodes (107).

1.2.4.2 Concurrent chemoradiotherapy (CRT)

Up until 2000, radiotherapy was almost only the non-surgical therapy administrated to the HNCC patients. After several phase III clinical trials showed a survival benefit of combining chemotherapy with radiotherapy vs radiotherapy alone, concurrent chemoradiotherapy (CRT) was introduced to treat patients with advanced HNSCC (108), (109), (110). Eighty-seven clinical trials, reported by Pignon et al on 16485 HNSCC patients, demonstrated a range survival benefit for chemotherapeutic regimens of 4.5% at 5 years as well as for concurrent chemo-radiotherapy of 6.5% (95). However, no significant benefit was shown either for induction chemotherapeutic regimen in the total HNSCC patient cohort. This meta-analysis showed the superiority of concomitant chemotherapy over induction chemotherapy. Despite the prognostic improvement in locally advanced HNSCC patients treated with concurrent chemo-radio therapeutic regimen compared with radiotherapy alone, increasing toxicity remains the issue (108). However, induction chemotherapy with docetaxel, cisplatin, and fluorouracil (TPF) (111) is recommended for patients with N3 locally advanced HNSCC (112) prior to concurrent chemo-radiotherapy.

1.2.4.3 Targeted therapy

Although multiple EGFR tyrosine kinase inhibitors (TKIs) have been tested in HNSCCs clinical trials, the outcome in most cases was disappointing. Erlotinib has been used as a single agent in phase II clinical trials in recurrent or metastatic HNSCC patients. The response rate,

however, was 4.3% with a 38% stable disease rate (113). Although the response was slightly higher when used as combination with cisplatin, the prognosis of using this Erlotinib involving regimen remained disappointing (114). Gefitinib also has not shown a prognostic improvement in recurrent or metastatic head and neck cancer patients in phase III randomized trial when combined with docetaxel compared with using docetaxel alone (115). Recently, one encouraging phase II trial of using dacomitinib as first-line chemotherapy in recurrent/metastatic HNSCC has shown favourable disease control and improved overall survival (116). The presence of HPV DNA is not related with response to EGFR inhibitors in HNSCC patients with recurrence or metastatic spread (117). Regarding locally advanced HNSCC, although combining cetuximab to conventional chemo-radiotherapy with cisplatin has not been encouraging so far, outcome of the ongoing monotheraputic comparison of ceutaximab vs cisplatin given with radiotherapy may change the care standard of this disease in the future (118).

1.2.5 Prognosis

As with other head and neck cancers, good prognosis in HNSCC is associated with early detection of stage of disease (stage I or II) with favourable outcome of up to 90% after surgery or radiotherapy (119). In a retrospective cohort study performed in the North-West of England on oral cancer patients who were relatively elderly, the value of oral cancer-specific survival (CSS) has been emphasised as an indicator of a successful therapeutic regimen since the overall survival is influenced by age, poor socioeconomic circumstances and comorbidity. Extra-capsular spread and pathological node status are the main pathological characteristics of the tumour that were reported as the most powerful prognostic markers of oral cancer-specific survival in addition to the age, clinical appearance

of the oral tumour and its differentiation, pattern of invasion, pathological stage and perineural invasion (94), (120). HPV appears to have a prognostic value for both disease-specific survival (P = 0.005) and overall survival (P = 0.003); HPV negative status is significantly correlated with poor prognosis in OPSCC patients, while good prognosis is related with those who are HPV positive even if presenting with late stage disease. p16 association with both disease-specific survival and overall survival shows similar significant prognostic trend as that for HPV status either separately or collectively (121).

1.3 Taxanes and mitotic spindle in cancer therapeutics

1.3.1 History of taxanes

In 1962, Arthur Barclay, who was a botanist at U.S. Department of Agriculture (USDA), obtained crude extract of from of bark of Pacific yew tree, *Taxus brevifolia*, and found it to have cytotoxic activity. Taxol (paclitaxel) (Figure 1.8) was then isolated from the bark extract of Taxus brevifolia by Wani group 1970 [Wani 1970] and reported to possess anti-tumourgenic activity and was the first type of taxanes that had been isolated. In 1979, Schiff gruop investigated the depolymerising action of paclitaxel on mitotic spindle microtubules in cancerous HeLa cell line (122). This mitotic stabilising activity resulted in forming a paralyzed cytoskeleton that restrains the mitotic cell division. Eight years later paclitaxel was extensively utilised in a number of phase I clinical trials to treat patients with a variety of malignancies, including NSCLC, along with pharmacokinetic studies (123), (124), (125), (126), (127). Although these trials were run and encountered several difficulties such as weak response to paclitaxel therapy of most studied cancer cases, except few such as ovarian cancer (123), in addition to undesirable side effects, particularly hypersensitivity reactions and Neutropenia. These difficulties were about to threaten the prospects for administrating paclitaxel in further. The findings, however, led to further investigation of paclitaxel efficacy in treating cancer patients. In 1992, paclitaxel has been approved by the Food and Drug Administration for treating females with ovarian cancer as a marked response was already established as either a complete or a 50% partial response (128). In 1993, two different phase II clinical trials that administrated paclitaxel on patients with advanced NSCLC showed more efficacy and favourable outcome as single agent or in comparison of other therapies (Merbarone and piroxantrone) were used to

treat lung cancer (129), (130). In the same year, paclitaxel evaluation in phase II study administrated on untreated patients with metastatic head and neck squamous-cell carcinoma, also demonstrated promising results in favour of patient response to this agent (131).

Docetaxel (Figure 1.8), which is a paclitaxel analogue, was derived from the European Yew tree Taxus baccata by a semisynthetic process [Denis 1990]. Similar to paclitaxel, docetaxel acts as microtubule stabilising agent that disrupts microtubule dynamics leading to mitotic arrest of cell cycle (132). Docetaxel demonstrated a marked significant efficacy in treating different types of cancers including lung and head and lung cancers. In 1994, the outcomes of very early phase II clinical studies that had been conducted on advanced NSCLC cases using docetaxel based therapy showed a significant anti-tumour activity in those patients (133), (134). These finding led to involve docetaxel in chemotherapeutic setting of respiratory tract cancers in later clinical studies.

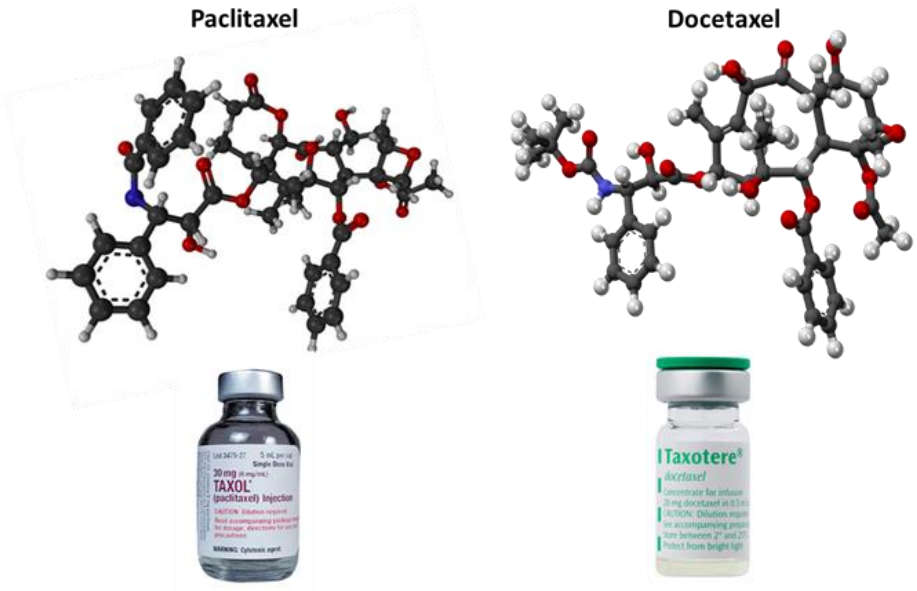

Figure 1.8: Three dimension chemical structures of taxanes (paclitaxel and docetaxel) and their common names (taxol and taxotere).

1.3.2 Therapeutic schemes using taxanes in lung and HN cancers:

Taxanes are used to treat a variety of human cancers (135), (136), (137) including carcinomas of lung (138) as well as head and neck (139). Paclitaxel and Docetaxel, which represent the most prominent members of the taxane family, have manifested significant activity in treating lung tumours used either as part of complex chemotherapeutic regimens (140), (141) or less frequently as monotherapy if the complex regimens have undesirable effects (142), (143). Regarding head and neck cancers treatment, Several randomized clinical trials have shown that including taxanes in induction regimens comprising of cis-platin and fluorouracil could be superior to that of excluding taxanes (144), (145), (146), (147), (111), (139). Most of these clinical trials have demonstrated a marked improvement in overall survival (OS) and progression-free survival (PFS) with less toxicity in the taxane containing regimens.

1.3.2.1 Taxane resistance in RTC cancers

There are many factors are implicated in cellular response to taxanes of respiratory tract cancers. ATP-binding cassette (ABC) transporter superfamily members are responsible for extruding substrates of a variety of chemotherapeutic agents including taxanes (148). This efflux mechanism accordingly results in augmentation of cellular resistance of NSCLC. In vitro studies reported that Overexpression of ABCC10 is correlated with resistance to paclitaxel ($r = 0.574$; $P < 0.05$) in 17 NSCLC cell lines (149). mRNA expression of *MRP5* and *MRP8* (the MDR-related pump members which also belong to ABC superfamily) in 49 NSCLC tissue specimens was correlated with docetaxel response (150). In ex vivo study, although the authors reported that ABCC3 overexpression is predictive of poor prognosis and resistance in NSCLC to chemotherapeutic setting of five drugs including paclitaxel and docetaxel, the data in their paper does not clearly demonstrate the degree of ABCC3-

induced chemoresistance in each individual drugs (151). Thus far, the range of relevant interactions is not clear and the mechanisms related to taxane resistance acquisition are still largely unexplored, in spite of their long clinical use in cancer therapeutics (152).

1.3.3 Molecular predictive biomarkers of taxanes:

A number of genes have been implicated in taxane resistance in NSCLC (Table 1.2). In vitro studies demonstrate that functional p53 induces sensitivity to docetaxel (153) and paclitaxel (154) in NSCLC cell lines. High expression levels of Bax and low expression levels of Cyclin E were reported to predict sensitivity paclitaxel in HNSCC cells (155). A phase-III randomized trial showed that KRAS mutations decrease NSCLC cells response to therapy involving paclitaxel, carboplatin and erlotinib (156) However, in vitro studies demonstrate KRAS independency when using docetaxel as a single agent or in combination with erlotinib (157) or gefitinib (158). Several studies attempted to investigate whether the expression of genes involved in mitotic spindle formation may be predictors of sensitivity to taxanes. Tubulin bIII mutations have been associated with resistance to docetaxel in NSCLC patients (159) as well as paclitaxel in cultured lung cancer cells (160). However, the inclusion of TUBB3 expression levels in the prediction model for docetaxel sensitivity shows no improvement (150). In fact, the latter study demonstrated a correlation between docetaxel activity mainly with the expression of certain drug pump genes (MRP5 and MVP) and genes involved in the detoxification process. In retrospective clinical study on locally advanced HNSCC, TUBB3 expression was suggested as a predictor of resistance to docetaxel involving induction chemotherapy (161). Another study pointed to the expression of the Checkpoint with Forkhead and Ringfinger domains (CHFR) gene as a potential predictor of response of NSCLC patients to first-line therapy with carboplatin and

paclitaxel (162). Nevertheless, the available information on taxane efficacy predictors does not provide conclusive evidence. Although an increasing number of targeted therapeutic agents have come into clinical use (163), it is estimated that taxanes will still be used in chemotherapy regimens for lung cancer treatment for the foreseeable future (164). Therefore, the identification of relevant response predictors will highly benefit clinical practice by stratifying patients into suitable currently available schemes (165).

Table 1.2: Potential molecular predictors of taxane-based thereby

Gene	Therapeutic type	RTC type	Study type	Reference
p53	Docetaxel & Paclitaxel	NSCLC	*In vitro* functional	(153), (154)
Bax	Paclitaxel	HNSCC	*In vitro* study	(155)
Cyclin E	Paclitaxel	HNSCC	*In vitro* study	(155)
KRAS	paclitaxel, carboplatin and erlotinib	NSCLC	phase-III trial	(156)
KRAS	docetaxel alone or in combination	NSCLC	*In vitro* study	(157), (158)
TUBB3	docetaxel	NSCLC	Clinical cohort	(159)
TUBB3	paclitaxel	NSCLC	*In vitro* study	(160)
TUBB3	Docetaxel-involving induction chemotherapy	HNSCC	Clinical retrospective	(161)
CHFR	Paclitaxel-based First Line Therapy	NSCLC	Clinical cohort	(162)

1.3.4 Mechanism of taxane action:

The classic cytotoxic action of these compounds is mediated mainly through their binding of β tubulin monomers, leading to microtubule stabilization (Figure 1.9), thus blocking their depolymerisation and subsequently triggering cell cycle arrest at the G2/M phase (166), (167). In addition, there are a number of other well-known molecular mechanisms of action. One mechanism is activation of kinase activity of cdc-2 (cell division control-2 kinase) (168), which leads to apoptosis due to cytosolic accumulation of cytochrome c and caspase 3 activation. Paclitaxel induces mitotic arrest due to activation of spindle assembly checkpoint in the presence of Aurora b activity which maintains a dynamic equilibrium between attached kinetochore with those unattached (169), (170). Therefore, a functional spindle assembly checkpoint is required for efficient paclitaxel-induced mitotic arrest and thus cell death. Taxanes also induced apoptosis due to B-cell lymphoma2 (Bcl-2) phosphorylation (171), (52). However, many other pathways may also be involved in modulating their therapeutic effect such as causing cancerous cell death due to affecting interphase cells or inducing multipolar divisions (172). However, no any of these notions has been clearly established.

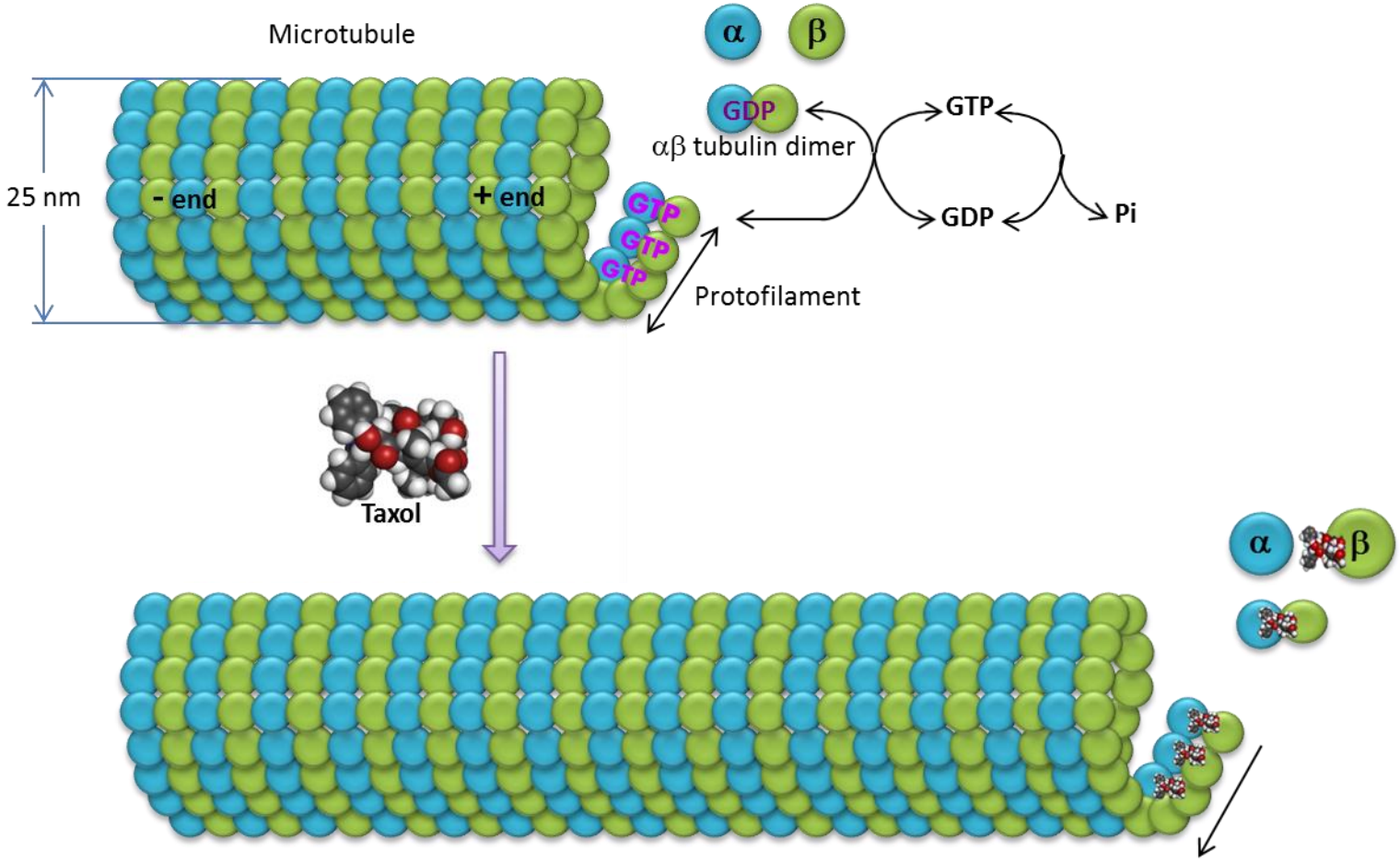

Figure 1.9: Figure depicting the classic mechanism of Taxol-β tubulin interaction promoting assembly of αβ-tubulin heterodimers that mimic that of GTP binding effect. However, Taxol binds β-tubulin while GTP binds the tubulin heterodimer forming a protofilament, which subsequently configures the microtubule. GTP hydrolysis allows microtubule depolymerisation, while tubulin dimerization promoting by paclitaxel is irreversible activation and thus results in microtubule stabilisation.

1.3.4.1 Molecular differentiation between response to Paclitaxel and Docetaxel

The two microtubule stabiliser taxanes, paclitaxel and docetaxel, are clinically approved to treat advanced Head and Neck Squamous Cell Carcinoma (HNSCC) (106), as well as Non-Small Cell Lung Cancer (NSCLC) (173), (174). However, the exact molecular action of these drugs is not fully understood, therefore they are still under comprehensive investigation to predict response of respiratory carcinomas to their chemotherapeutic action. Despite the fact that both taxanes are mainly implicated in apoptosis by causing microtubule catastrophe leading to cell arrest at the G2/M phase (175), they are not identical in their substantial clinical (176) and molecular (175) action. Therefore, cancer cells respond differently to these taxanes (177). This variance in cancerous cell response to paclitaxel and docetaxel was first described by Hanauske et al (1992) (178) and this led to the investigation of the unique mechanisms underlying differences in sensitivity to these taxanes in in vitro and in vivo experiments together with preclinical and clinical studies. It has been reported that docetaxel induces Bcl-2 and apoptosis at 100 fold lower concentrations than that of paclitaxel (179). Comparatively, docetaxel has almost twice as much affinity for β-tubulin as paclitaxel (180), with broader cell cycle effectiveness in three phases (S/G2/M) compared with two (G2/M) for paclitaxel. Furthermore, the retention time of docetaxel in tumour cells is longer than that of paclitaxel due to higher uptake and lower efflux (181). However, the efficacy of docetaxel and paclitaxel noted in preclinical and clinical studies cannot be explained merely based on molecular determination or even pharmacokinetics. Despite the evidence that docetaxel has superior activity in comparison of paclitaxel in terms of treating cancer cells (docetaxel IC50 is ten folds less than that of paclitaxel) (175), Paclitaxel, occasionally, exhibits more inhibitory effect against cancer cell lines than that of docetaxel (177). Although a phase III clinical study demonstrated that

docetaxel-based therapy was significantly associated with good prognosis in metastatic breast cancer patients (P< 0.0001) compared with paclitaxel, there was no significant difference in overall response rate in treating those patients (176). Docetaxel mainly targets centrosome organization leading to incomplete mitosis and cell damage in S phase with partial toxic effect during mitosis, whereas paclitaxel affects the mitotic spindle causing cell death (182). This difference in site of action may explain some difference in their efficacy in killing cancer cells.

1.3.5 Spindle assembly and cancer therapy

In order to understand the mechanism of therapeutic action of taxane, it is important to consider the role of mitotic spindle formation and spindle assembly checkpoint

1.3.5.1 Mitosis and Bipolar Spindle formation

Accurate sharing of genetic material during cell division is accomplished after assembling of a bipolar microtubule-based structure called the bipolar spindle. This spindle is a dynamic structure that drives the congregation and segregation of chromosomes during mitosis and is monitored by so called mitotic spindle checkpoint (MSC), it is also known as spindle assembly checkpoint (SAC), which is the important cell cycle surveillance mechanism that ensure faithful distribution of DNA content between the daughter cells (183), (184). The normal process of assembling the bipolar spindle is mediated within very well-known distinct subsequent mitotic stages (Figure 1.10). The first stage in mitosis (prophase) can begin once the DNA is duplicated and matured centrosomes are separated. At this stage, the cylindrical polymers “microtubules” are nucleated from these centrosomes utilising α/β-tubulin heterodimers. These mitotic filaments have a fast-polymerising plus end and a slow polymerising minus end that capped by a ring-like

microtubule nucleator called γ-tubulin ring complex (185). Next, pro-metaphase is begins once the nuclear membrane is decomposed. Some of polymerised microtubules attach to kinetochores (Kinetochores microtubules) at their plus-end. These attached kinetochores attach, in turn, to the centromeres of each sister chromatid forming what so called "Amphitelic attachment" which represents a proper dynamic form of attachment for bipolar spindle assembly that results in accurate chromosomal segregation (Figure 1.11) (186). Non-kinetochore microtubules represent another microtubule bundles that antiparallel overlapped at their plus ends without chromosomal attachment. The third array is called astral microtubules. They are polymerising apart of chromosomes and their plus ends anchor to the cell cortex mediating the position of the bipolar spindle (187). Metaphase is the next stage where the sister chromatids align along the central plate of the mitotic spindle enabling these chromatids to be separated at the next stage. The correct chromosomal alignment and their proper attachment to the microtubules are ensured by the spindle checkpoint prior chromosome segregation can progress (188) Through this stage, the kinetochore fibres are pulled towards the poles of the cell those in turn move farther apart. Anaphase is the penultimate stage where the sister chromatids are moved apart toward the cell poles resulted in accurate chromosomal segregation microtubule disassembly at this phase (189). During the final stage of mitosis (Telophase) the cellular compartments begin to appear and, simultaneously, the microtubules are depolymerising. At this point, a new nuclear membrane appears surrounding the uncoiled chromosomes that eventually return to uncondensed phase. The cell then divided into two daughter cells by cytokinesis.

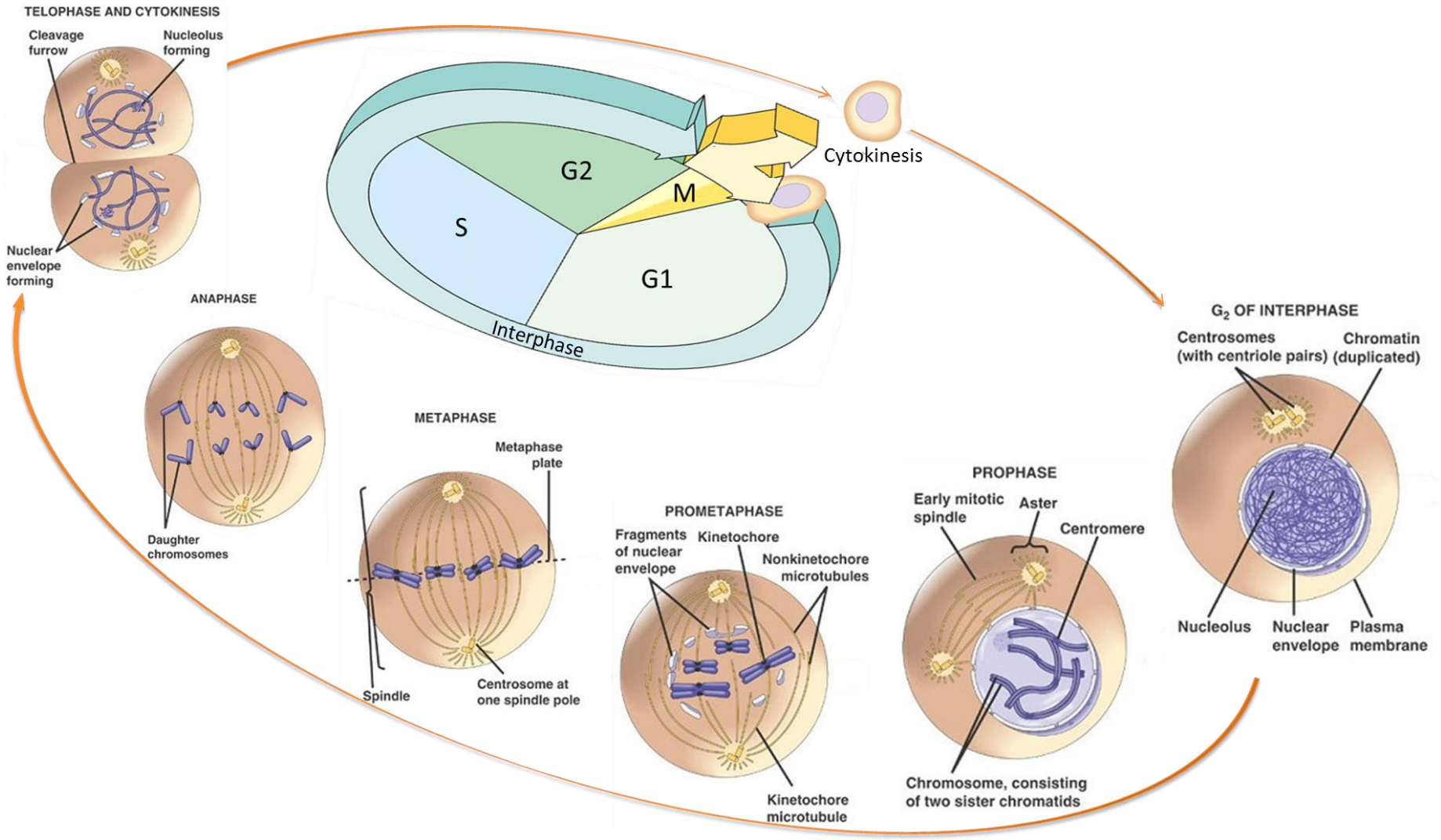

Figure 1.10: Mitotic stages of normal cells. The figure was adapted from figures extracted from websites (study.com) & (Cummings 2003)

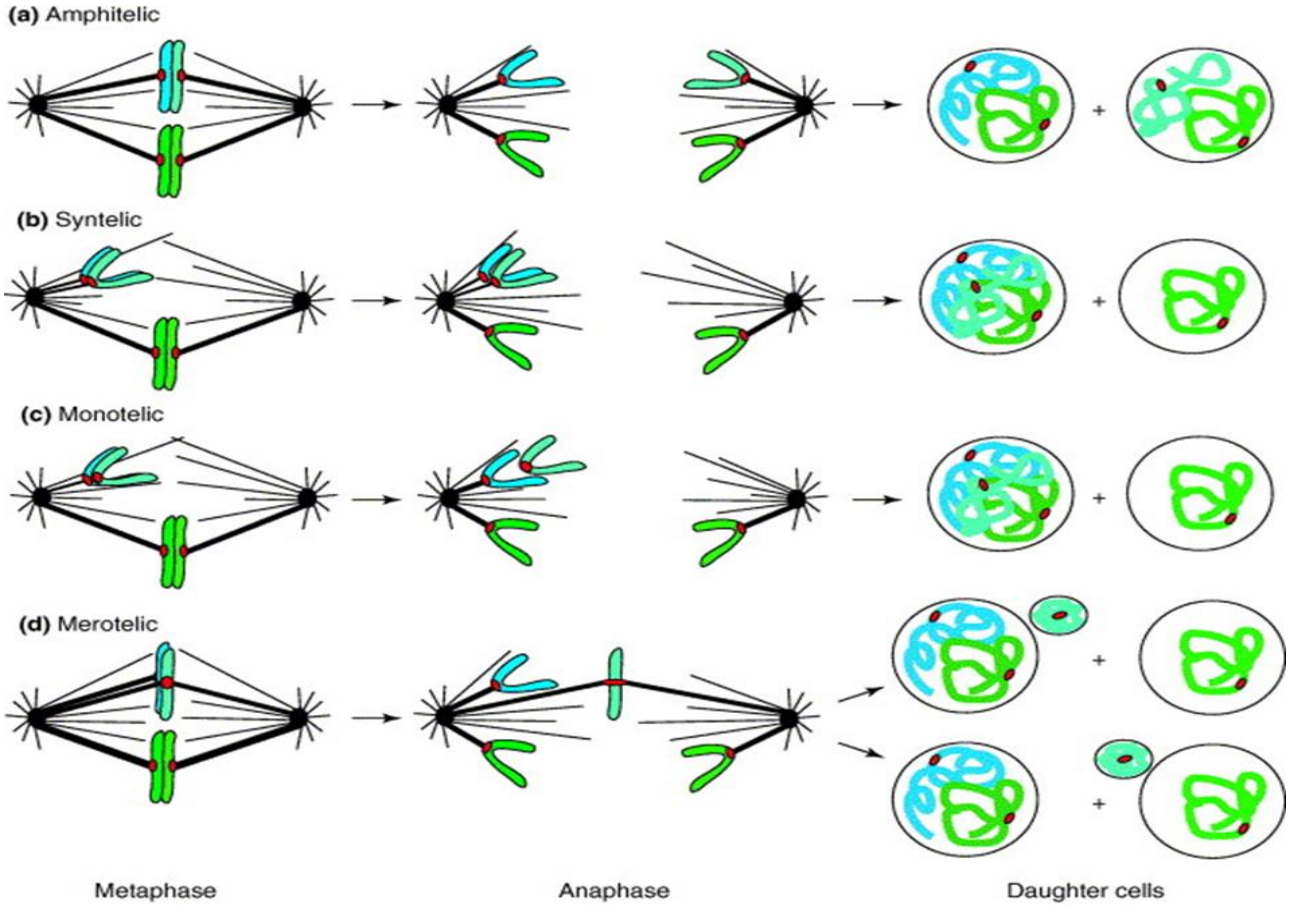

Figure 1.11: This figure shows the chromosome orientation at metaphase to the left column, chromosome segregation at anaphase in the middle and the divided daughter nuclei at telophase to the right. Four different types of kinetochore–microtubule attachments lead to chromosomal segregation; Amphitelic orientation (a) represents accurate segregation. Syntelic (b), monotelic (c) and merotelic (d) orientations which represent continuous kinetochore mis-orientation produce mis-segregated chromosomes at anaphase accordingly aneuploid daughter cells. The figure was reproduced from (190).

1.3.5.2 Mitotic Spindle Assembly and its checkpoint in cancer cells

Characterizing the molecular components involved in mitotic events during the cell cycle, and exploring differences in their expression signature between normal and malignant cells, could help to facilitate discovering and developing predictors for chemotherapeutic compounds that personalised cancer patient for treatment (188). Bipolarity of mitotic spindle, which is contributed by several molecular pathways, is the most obvious and preserved aspects. The chromosomal congregation and segregation during mitosis is firmly regulated either by a mechanism of correction of improper kinetochore-microtubule attachment or by the mitotic spindle checkpoint members (191). There are three types of improper attachments could accrue in the mitotic spindle. They happen when sister kinetochores are not be able of binding to microtubules accurately to form the proper amphitelic attachment (Figure 1.11). Sister kinetochores may be mono-oriented when they both attach to microtubules from the same pole forming what so called "syntelic attachments" but when only one of the them attaches they form monotelic. If multiple microtubules from both spindle poles attach with individual kinetochores they form merotelic attachment (190). This checkpoint ensures that the genetic contents pass properly to the daughter cells during mitosis until this process has correctly completed (192). Defects in the aforementioned mechanisms, that control the accurate chromosome segregation, predispose cells to death in most cases because of chromosome miss-segregation, chromosome instability or subsequently aneuploidy. In some cases, however, aneuploidy cell is triggered for cancerous transformation and transformed to a neoplastic cell (191), (188), (193). Therefore, activating the mitotic spindle checkpoint and targeting the progression of the oncogenic mitotic process are extremely successful strategies for cancer chemotherapy (54). Nevertheless, the greatest challenges of following these

strategies are the emergence of drug resistance and dose-related toxicity of anti-mitotic agents (194).

1.3.5.3 Spindle assembly associated members

Mitotic spindle formation and spindle checkpoint are critical for the maintenance of cell division and chromosome segregation (195). Many of the mitotic spindle associated members are implicated in several malignancies including lung and head and neck cancers (196), (197) due to their frequent overexpression. Overexpression and gene amplification have been reported to contribute to the development and progression of malignant tumours for a number of mitotic spindle associated genes. These genes include those involved in centrosome maturation (e.g. AURKA, TPX2, and KIF11) (198) , (199), microtubule formation (e.g. AURKA, CKAP5, TUBB and TUBB3) (200), (201), (202) and chromosomal alignment and segregation (e.g. AURKA, AURKB, AURKC, DLGAP and TTK) (203), (204), (205). Aurora A plays a central role in recruiting other mitotic spindle members (196). Several studies conducted to date have investigated the prognostic value of some of the aforementioned genes in lung cancer such as AURKA (206), AURKB (207) and TPX2 (208). However, the information relevant to lung cancer prognosis remains to be fully understood. No such information has been provided to date for DLGAP5, CKAP5 and TTK, while the prognostic value of AURKA (209), (210), (206) and AURKB (211), (207), (212), (213) in human NSCLC is still debated.

1.3.5.3.1 AURKA

Aurora kinase A, which is the gene product of *AURKA* (20q13.31) (Figure 1.12), is a member of the Aurora kinase subfamily of conserved Serine/Threonine kinases, which also includes Aurora B and Aurora C. Deregulation of Aurora kinases leads to impairment of mitotic spindle checkpoints causing abnormal spindle assembly (196). Overexpression of

AURKA is known to play an important role in cancer aggressiveness through a range of mechanisms. Elevated levels of AURKA perturb mitotic spindle formation and thus cytokinesis due to centrosome amplification, aneuploidy and chromosomal instability (214), (196). When overexpressed, AURKA also inactivates the activity of several tumour suppressor genes including p53 (215). The association between AURKA overexpression and p53 mutation with high tumour grade and high cancer stage was also reported in patients with hepatocellular carcinoma (216) and with clinically aggressive disease and reduced survival in ovarian cancer (217). The perturbation of spindle formation and inactivation of tumour suppressor genes by elevated AURKA may explain the association between up-regulated AURKA and poor outcome of aforementioned cancer patients. Nonetheless, the notion that up-regulated AURKA contributes to a poor outcome in lung cancer has been debated, presumably because NSCLC represents a set of heterogeneous malignancies (218), with differing outcomes, even amongst those with the same clinicopathological features.

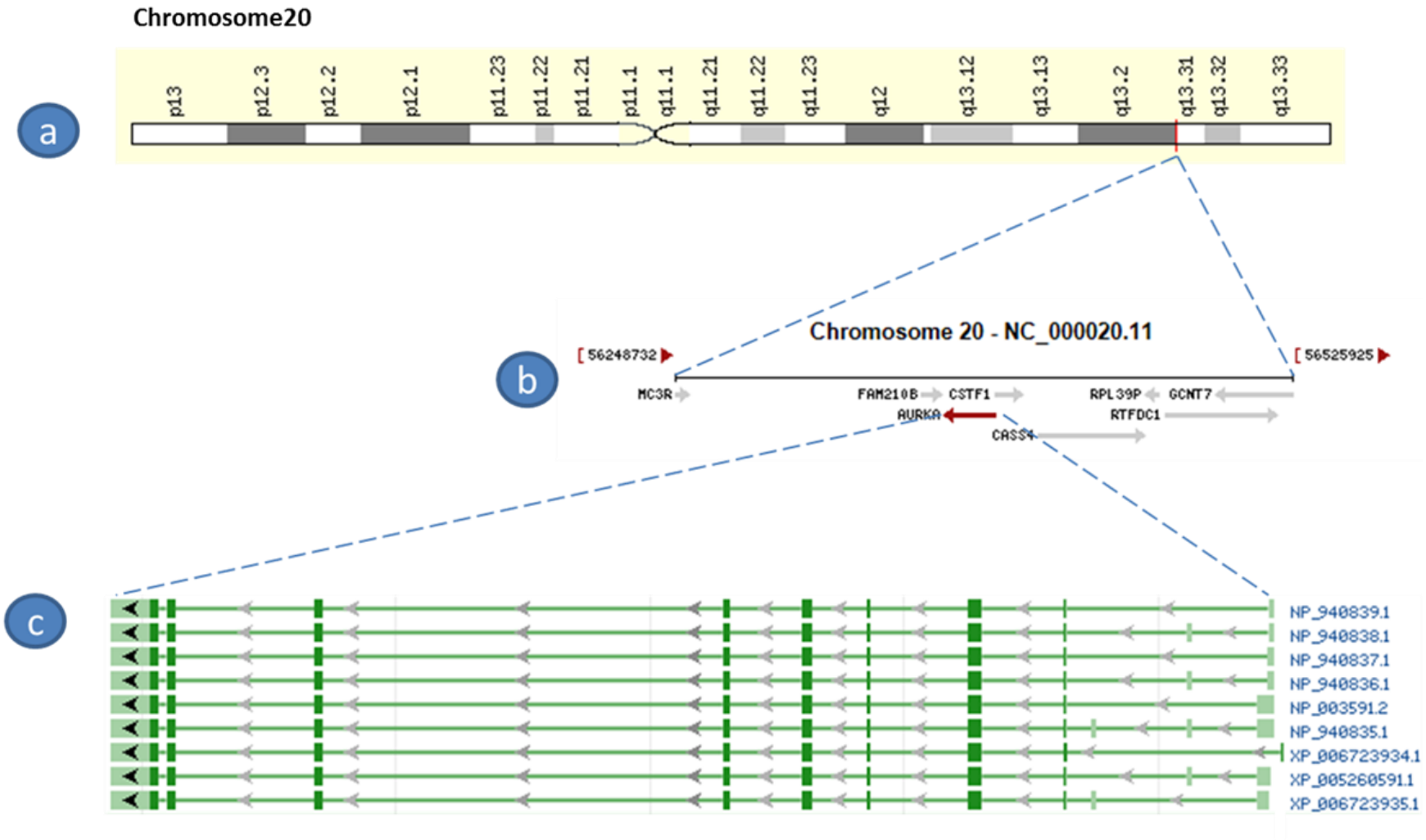

Figure 1.12: Genomic regions and transcripts of *AURKA*. The figure was adapted based on figures extracted from (genecards.org) & (ncbi.nlm.nih.gov)

1.3.5.3.2 AURKB

Aurora kinase B, which is encoded by the *AURKB* gene (17p13.1) (Figure 1.13), plays a key role during mitosis by regulating chromosomal alignment, segregation and cytokinesis, as the catalytic protein of the Chromosomal Passenger Complex (CPC). Activation of Aurora B by the inner centromere protein (INCENP) is required for promoting transfer of the CPC sub-complex (INCENP–Survivin–Borealin subcomplex) to the spindle midzone during mitotic exit (219). Here it is localised to centromere and is required for the kinetochore localization and chromosome attachment to the mitotic spindle (169), as well as establishing the SAC to correct anomalous chromosome-kinetochore microtubule attachment before the cell enters anaphase (220). AURKB is frequently overexpressed in NSCLC (211) and is associated with genetic instability (212), aneuploidy and poor patient prognosis (221), (207). However, high Aurora B kinase expression has been associated with improved relapse-free survival (RFS) in ovarian cancer patients on taxane-based therapy (222).

1.3.5.3.3 AURKC

Aurora kinase C, which is encoded by *AURKC* (19q13.43) (Figure 1.14), represents the third member identified in the Aurora kinase family. It is very similar to Aurora kinase B in both molecular structural and subcellular localization (223), (224). Aurora kinase C also conducts similar functions as Aurora kinase B supporting mitotic progression through cell cycle in the absence of Aurora kinase B (205). Although it was originally detected in reproductive organs testes (225), AURKC deregulation has been reported in numerous malignancies (226), (227). Upregulated Aurora kinase C has been associated with promoting oncogenic activity of cancerous cells (228).

1.3.5.3.4 CKAP5

Aurora kinase A recruits the interaction between the CKAP5 (11p11.2) (Figure 1.15) encoded protein, colonic and hepatic Tumour Over-expressed Gene (ch-TOG), and TACC3 to centrosomes and proximal spindle microtubules (229). ch-TOG up regulation in cancer was first demonstrated by Charrasse et al 1995 in liver and colon tumours compared with the corresponding normal tissues (230). However, up to now, there is no available data could show such association between CKAP5 expression and survival in cancer patients that could potentially prognosticate the disease outcome. This may need more exploration of CKAP5 role in predicting survival in cancer patient including lung cases.

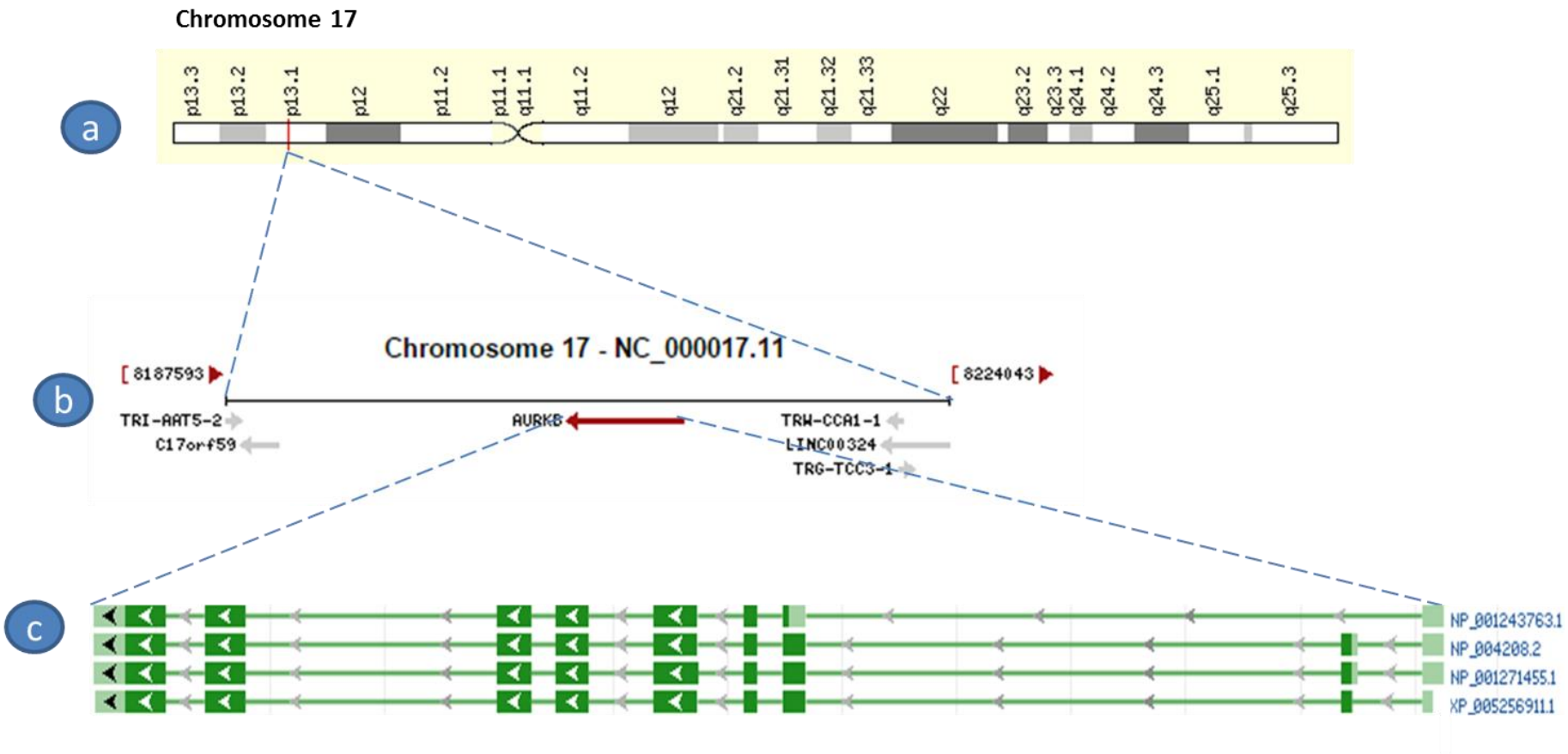

Figure 1.13: Genomic regions and transcripts of *AURKB*. The figure was adapted based on figures extracted from (genecards.org) & (ncbi.nlm.nih.gov)

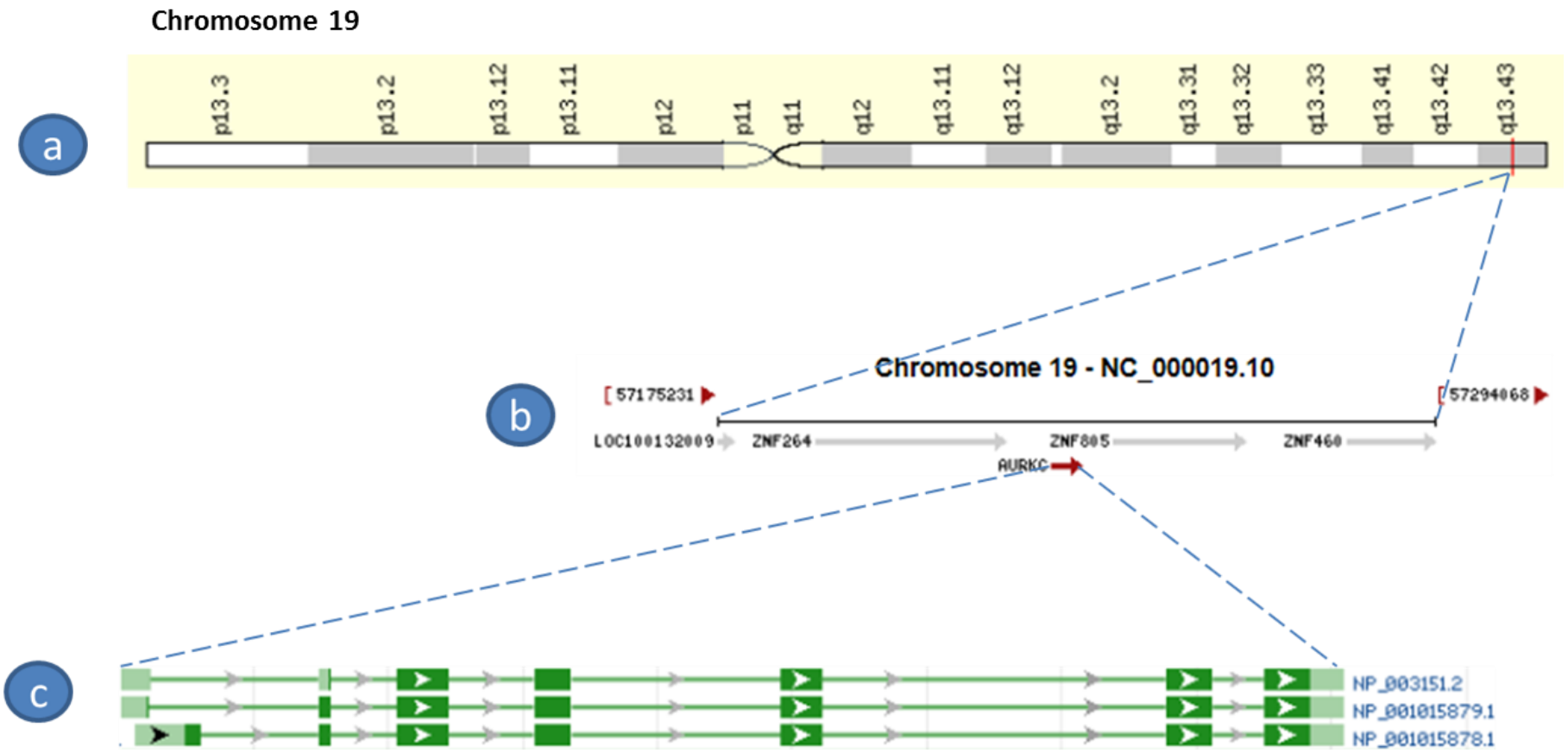

Figure 1.14: Genomic regions and transcripts of AURKC. The figure was adapted based on figures extracted from (genecards.org) & (ncbi.nlm.nih.gov)

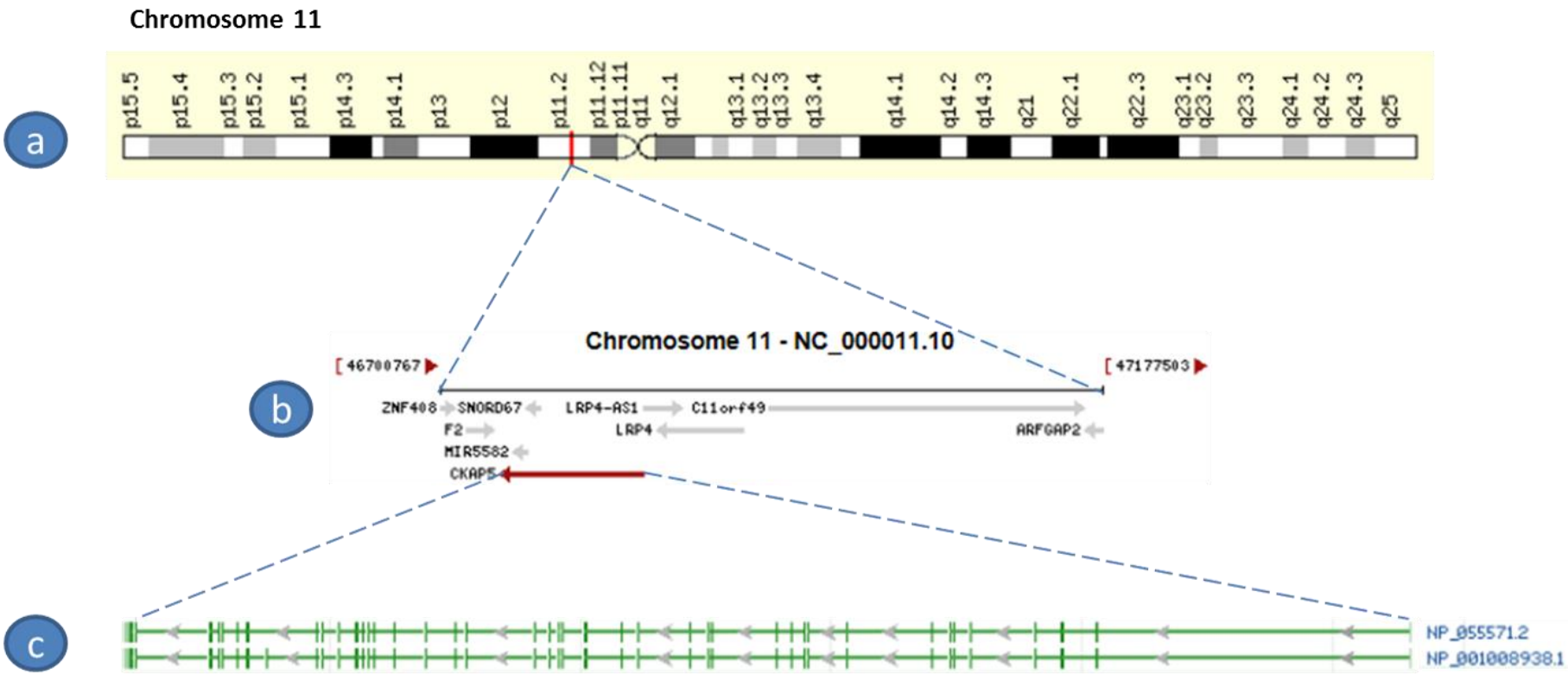

Figure 1.15: Genomic regions and transcripts of CKAP5. The figure was adapted based on figures extracted from (genecards.org) & (ncbi.nlm.nih.gov)

1.3.5.3.5 DLGAP5

DLGAP5 (14q22.3) (Figure 1.16), whose encoded protein is regulated by AURKA (231), was first described by Tsou et al as an up-regulated transcript in hepatocellular cancer called Hepatoma Up Regulated Protein (HURP) (232). HURP is a kinetochore microtubule-associated protein that mediates Ran-GTP-dependent mitotic spindle assembly, promoting microtubule polymerization and spindle formation, activating chromosome congregation and alignment during mitosis in normal and cancer cells (233). Increased expression levels of DLGAP5 are related to tumour aggressiveness in several cancers such as hepatocellular carcinoma (234), adrenocortical tumours (235), and meningioma (236). Up-regulation of DLGAP5 is correlated with bad prognosis in liver (237) and prostate (238) cancers.

1.3.5.3.6 KIF11

KIF11 (10q24.1) (Figure 1.17) encodes kinesin-5 motors Eg5, a microtubule motor, which localizes in centrosomes and asters of antiparallel microtubules moving them apart. Recently, it has been reported that defects in specific mitotic spindle members have been indicated to induce the aberrant spindles assembly with monopolar form or with poor centrosomes' separation. Monopolar spindles formation is induced by Eg5 suppression leading to mitotic arrest (239). This Induction could be employed as a feasible strategy for cancer treatment, where cell death often caused by aberrant mitotic machinery.

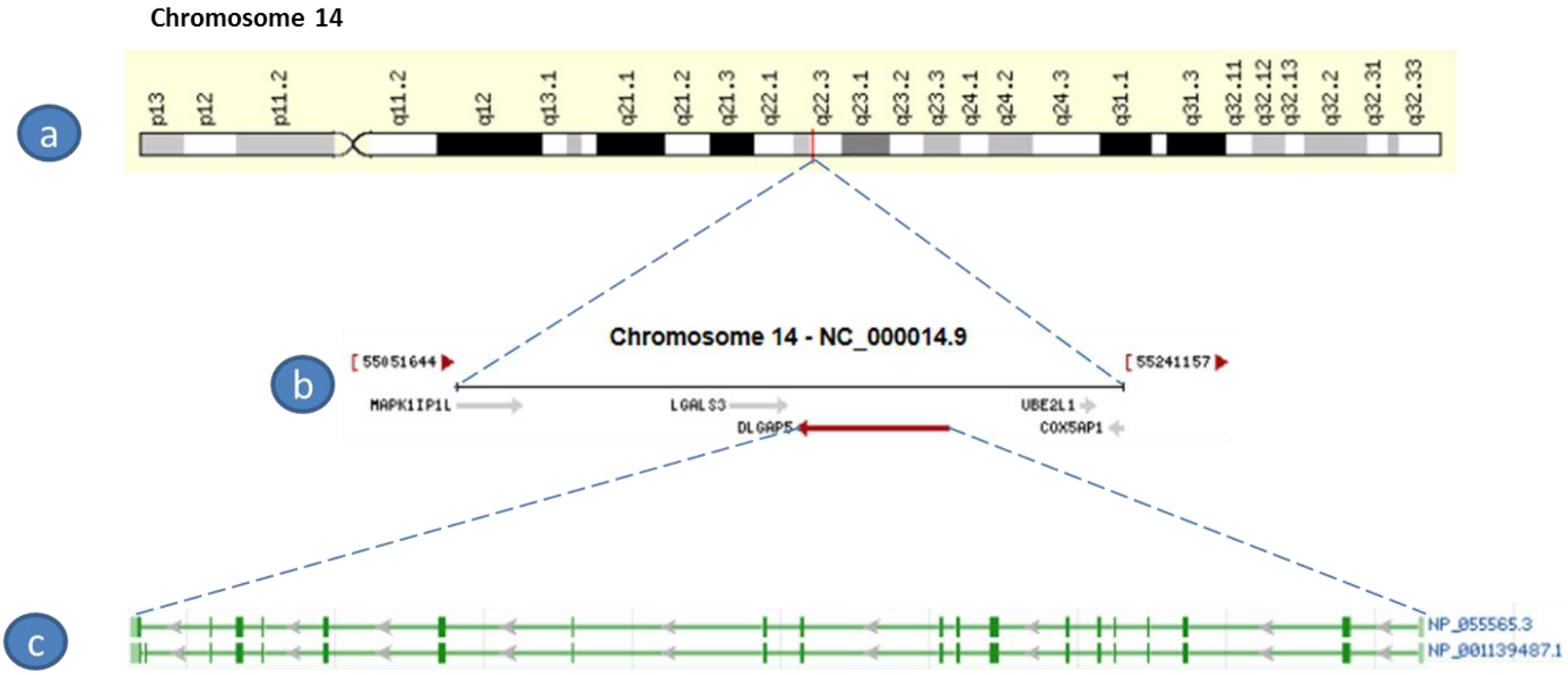

Figure 1.16: Genomic regions and transcripts of DLGAP5. The figure was adapted based on figures extracted from (genecards.org) & (ncbi.nlm.nih.gov)

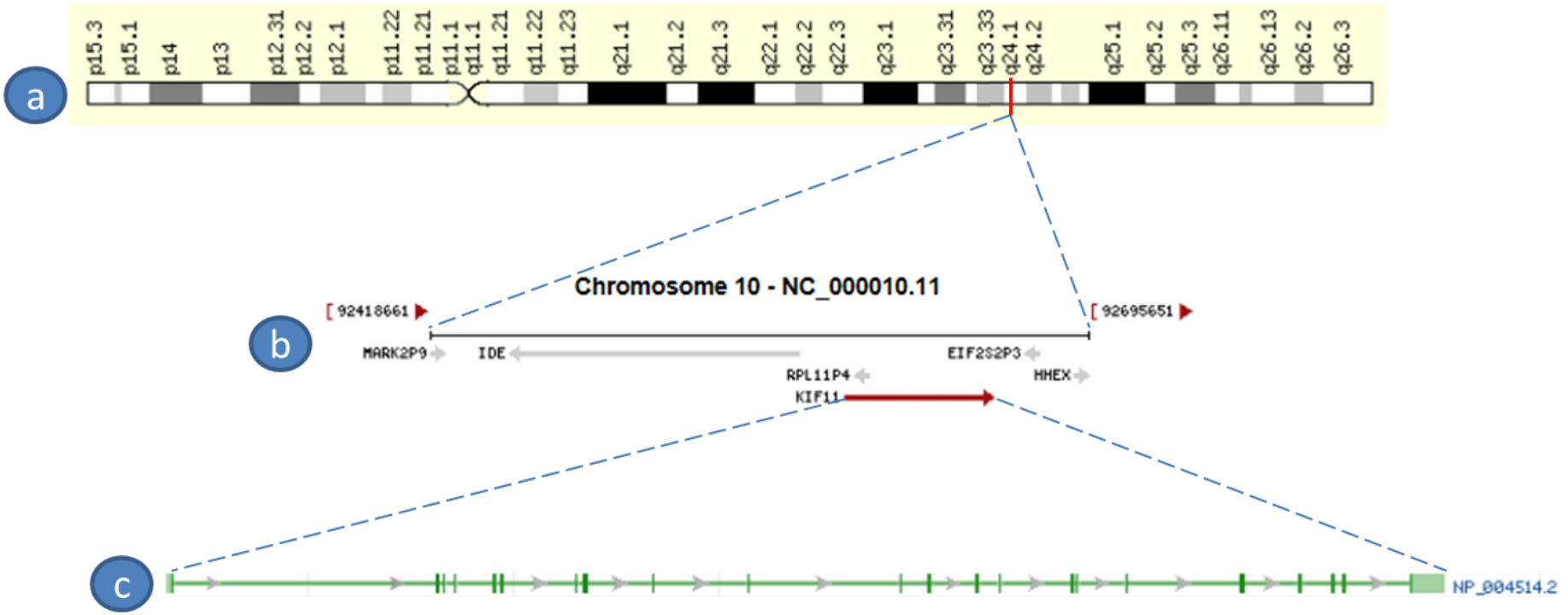

Figure 1.17: Genomic regions and transcripts of KIF11. The figure was adapted based on figures extracted from (genecards.org) & (ncbi.nlm.nih.gov)

1.3.5.3.7 TPX2

The kinase activity of Aurora kinase A is regulated by TPX2, Targeting Protein for Xenopus kinesin-like protein 2, (20q11.21) (Figure 1.18) through their interaction during mitosis (240). At the end of mitotic cell division, both Aurora A (241) and TPX2 (242) are degraded by the anaphase promoting cyclosome/complex E3 ubiquitin ligase. TPX2 expression was differentially detected in cancerous lung tissues and not in normal lung tissue (243). Investigation of the distinctively higher expression of TPX2 in mitotic phases of cell cycle led to the suggestion it may serve as a biomarker for cancer prognosis (244). several studies on TPX2 expression have demonstrated the potential prognostic value of this gene when overexpressed in lung cancer using different approaches either as independent marker by immunohistochemistry (245), or as a part of 5 gene cluster/ panel signature ($P < 0.001$, HR = 2.84) employing lung adenocarcinoma microarray data sets (69), (208). Nevertheless, *TPX2* mRNA involvement in NSCLC prognosis has not been previously investigated independently in lung cancer cases.

1.3.5.3.8 TTK

TTK (6q14.1) (Figure 1.19) encodes protein MPS1 which plays important role, as a substrate to Aurora B kinase, in recruitments the MSC entities particularly Mad2 to deactivate APC until all the chromosomes biorientated properly at the middle plate of mitotic spindle so the microtubules attached accurately to the kinetochores (246). Activating MSC by TTK in existence of unattached kinetochores is enhanced by AURKB, which is necessary for TTK to accomplish rapid activation once cells enter mitosis, and thus rescues mitotic checkpoint function (247). Breast cancer is the only malignancy that TTK has been reported to be deregulated and that is associated with high histologic grade (248).

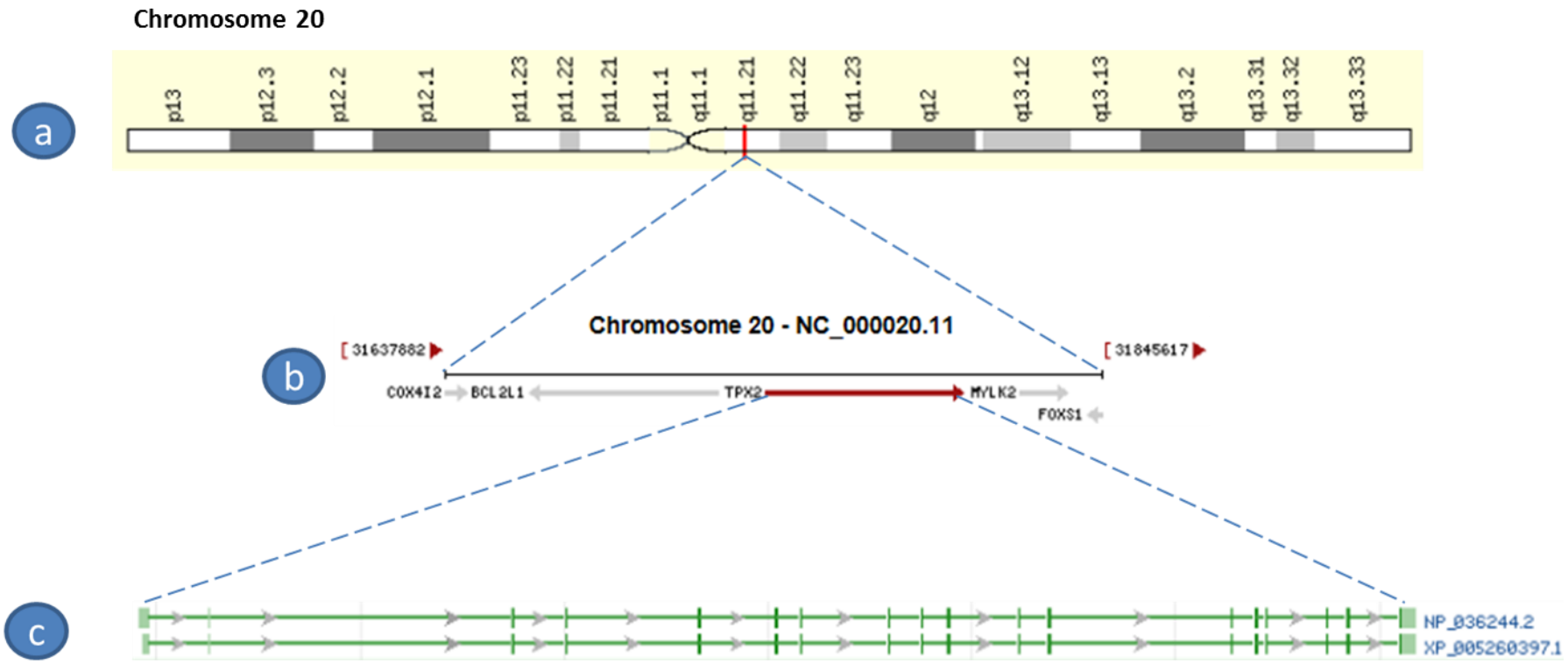

Figure 1.18: Genomic regions and transcripts of TPX2. The figure was adapted based on figures extracted from (genecards.org) & (ncbi.nlm.nih.gov)

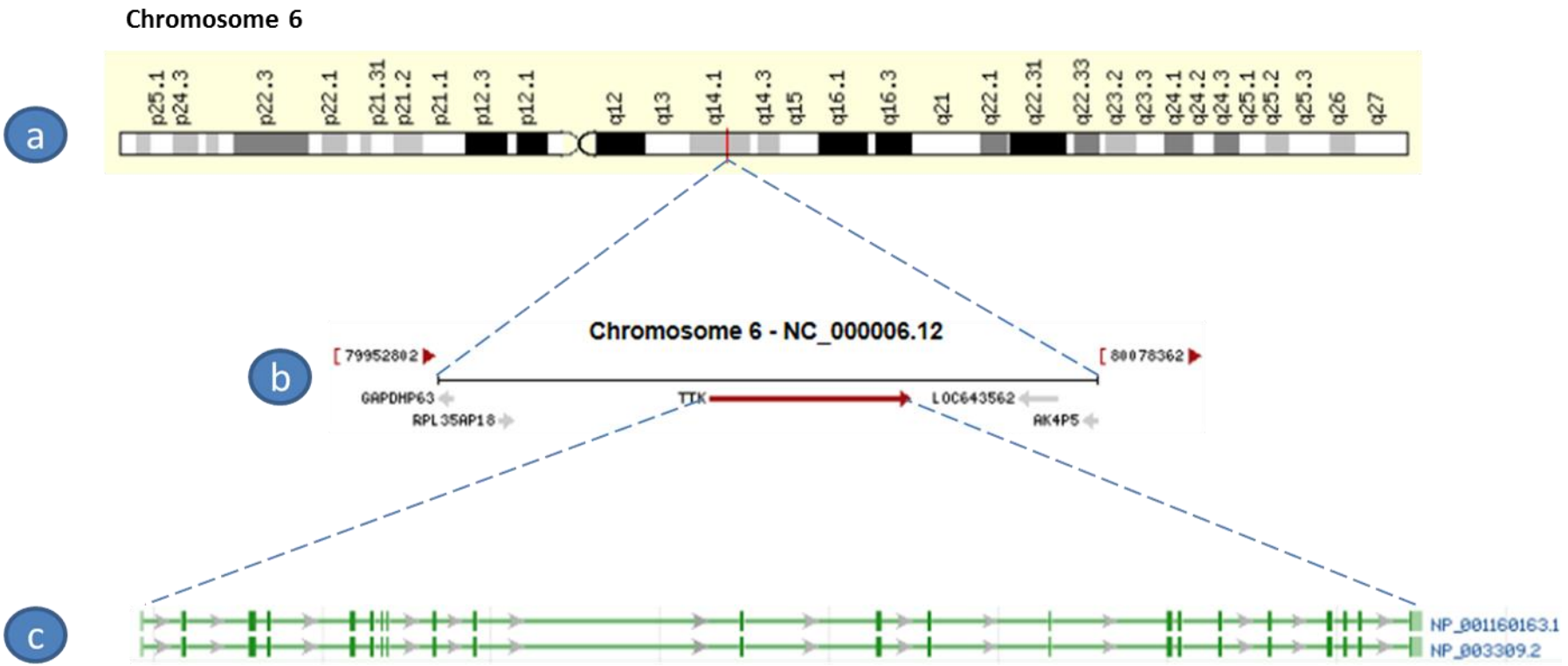

Figure 1.19: Genomic regions and transcripts of TTK. The figure was adapted based on figures extracted from (genecards.org) & (ncbi.nlm.nih.gov)

1.3.5.3.9 TUBB and TUBB3

TUBB (6p21.33) (Figure 1.20) and *TUBB3* (16q24.3) (Figure 1.21) encode class I β-tubulin and class III β-tubulin respectively. These tubulins are members of β-tubulin family that represents one of two core protein families along with β-tubulin family. The heterodimerised tubulin is the leading target for taxanes. β tubulins are heterodimerised with α tubulins to assemble the microtubules, the key components of the mitotic spindle as mentioned above (249). Tubulin bIII mutations has been reported to be associated with resistance to taxanes in NSCLC patients (159) also lung cancer cells (160). This is not confirmed in a study where the addition of TUBB3 expression in the prediction model for docetaxel sensitivity shows no improvement (150). The same study demonstrates correlation of docetaxel activity in NSCLC cells mainly with the expression of drug pump genes, MRP5 and MVP, and detoxification process.

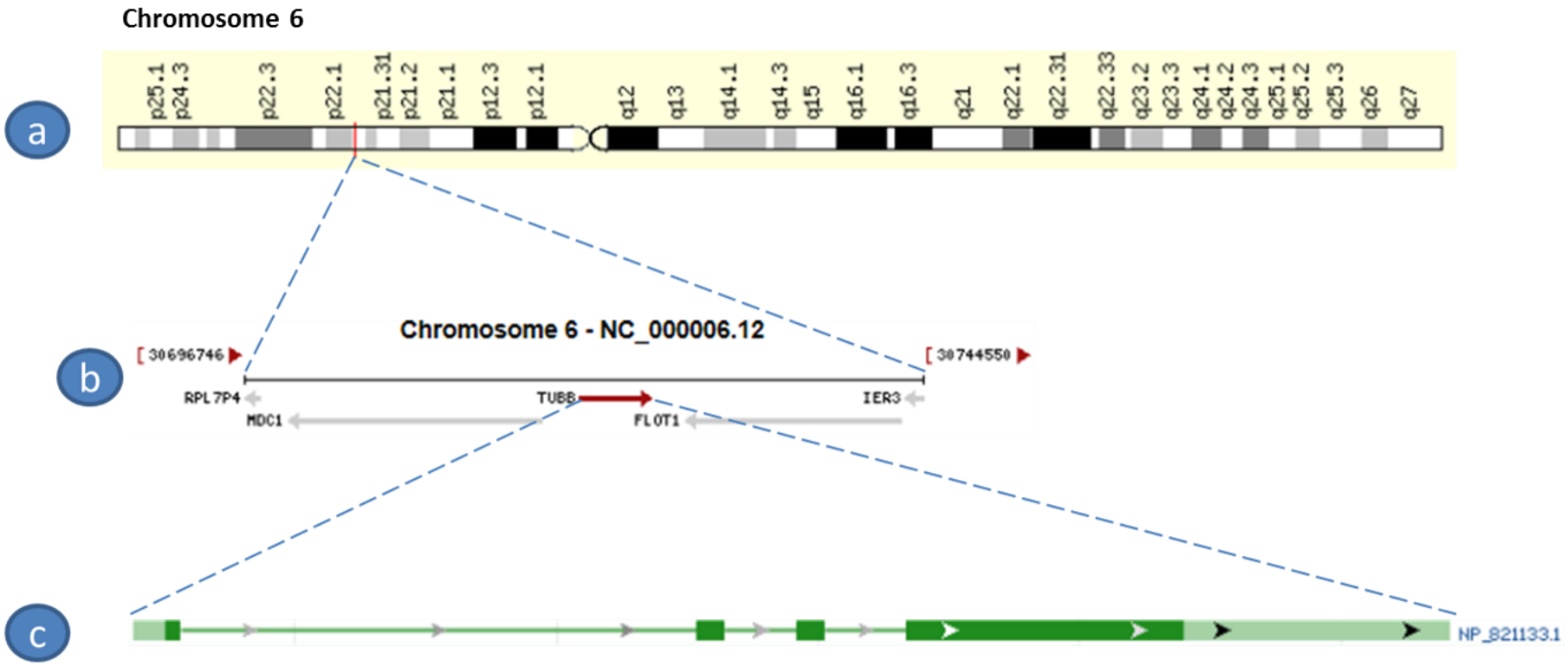

Figure 1.20: Genomic regions and transcripts of TUBB. The figure was adapted based on figures extracted from (genecards.org) & (ncbi.nlm.nih.gov)

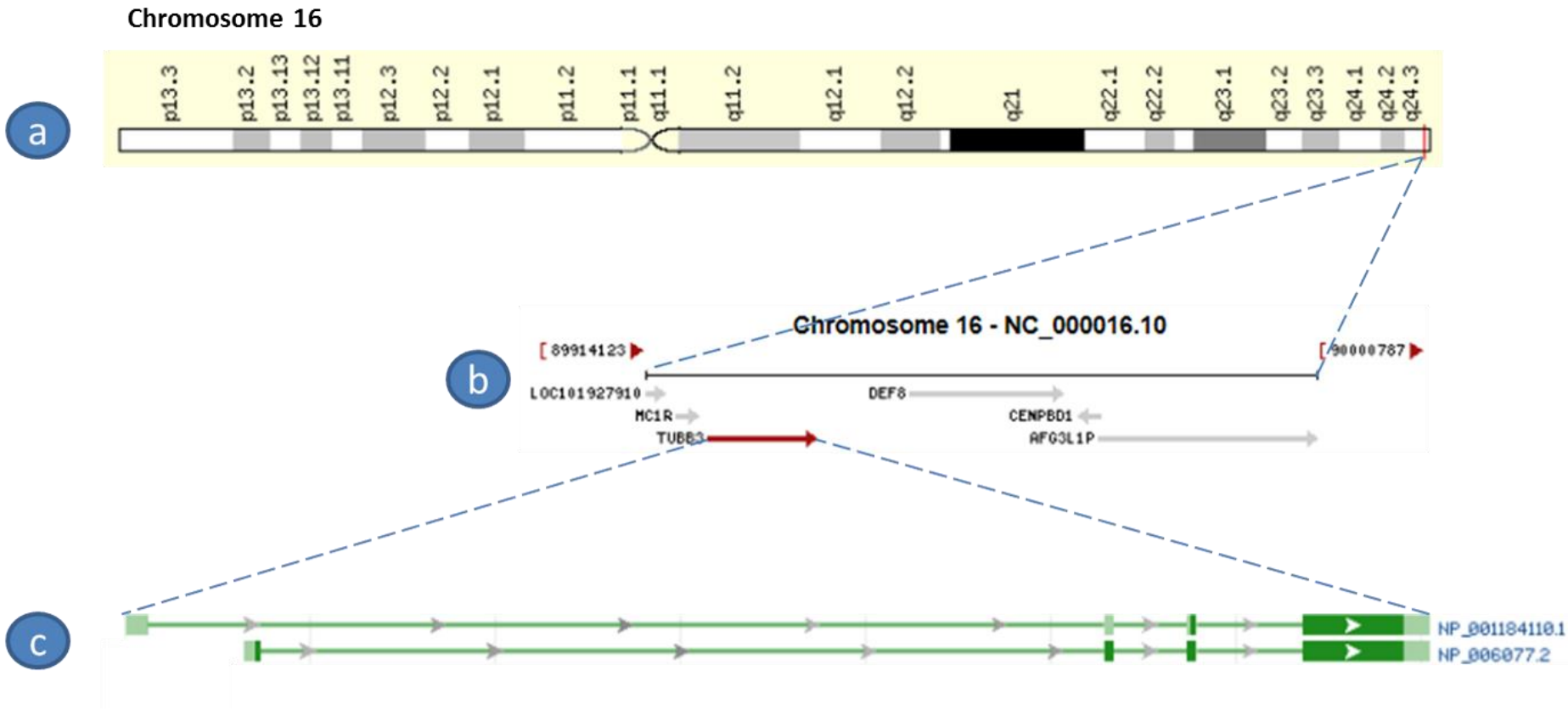

Figure 1.21: Genomic regions and transcripts of TUBB3. The figure was adapted based on figures extracted from (genecards.org) & (ncbi.nlm.nih.gov)

1.4 Hypothesis

Expression of mitotic spindle members may predict outcome and modifies the response to taxane-based therapy in respiratory tract carcinomas.

1.5 Aims and Objectives

This study aims to identify genes involved in the spindle assembly checkpoint process *(AURKA*, *AURKB*, *AURKC*, *CKAP5*, *DLGAP5*, *KIF11*, *TPX2*, *TTK*, *TUBB* and *TUBB3*) that may modulate taxane resistance in the human airways carcinomas.

Specific objectives include:

1. Explore the association between the expression profiles of these ten genes and clinico-pathological characteristics and survival in human non-small cell lung carcinoma.
2. Investigate the sensitization of cancer cells to taxanes by modifying the expression/activity of certain targets.
3. Examine the potential sensitisation of lung and oral cancer cells to paclitaxel by epigenetic modifiers.

Chapter 2: Materials and methods

2.1 Primary NSCLC tumour samples:

This study was undertaken in association with Liverpool Lung Project. Appropriate Ethical approval has been acquired from Liverpool Research Ethics Committee (Reference number 97/141) and all patients have provided written informed consent. One hundred and thirty three frozen surgical tumour samples were included in the study; fifty-six from adenocarcinomas (AdC) and seventy six from squamous cell carcinomas (SqCCL). In addition, 44 non-tumour adjacent paired surgical tissues (20 from adenocarcinoma and 24 from SqCCL patients) were available for analysis. Most specimens were of the pT2 stage group (n=102) while pT1 and pT3/4 group comprised 19 and 12 patients respectively. The clinicopathological characteristics of this cohort are provided in (Appendix 2). The median age of those patients was 67 (45-82); fifty-six of the patients were females and 77 were males.

2.1.1 Cryosectioning

Snap frozen biopsies were cryo-sectioned using OCT embedding matrix (CellPath-UK) to embed frozen blocks for cryosectioning using Cryostat (Thermo Scientific Shandon-UK). Two thicknesses of sections were obtained from each sample; 1st) five μm sections which fixed in 10% buffered formalin (Catalogue no. UN 2209 - AnalaR) and stained using haematoxylin (Catalogue no. 6765003 Thermo Scientific) and eosin (Catalogue no. 6766007 - Thermo Scientific) staining for histopathological examination. 2nd) 10 μm sections utilised for DNA, RNA and protein extractions.

2.2 Cell lines & Growth conditions:

Nine NSCLC cell lines (A549, Calu-3, CALU6, CRL5802, COR-L23, H358, LUDLU-1, SK-LU-1 & SK-MES1) and twelve HNSCC cell lines (BHY, HN5, PE/CA-PJ15, PE/CA-PJ41, UM-SCC-104, UM-SCC-12, UM-SCC-17as, UM-SCC-19, UM-SCC-4, UM-SCC-47, UM-SCC-5, UM-SCC-81b, UPCI-SCC-090 & LIV-7K) (Table 2.1) were tested in this study. They were maintained in Dulbecco's Modified Eagle's Medium (DMEM)/Ham's Nutrient Mixture F-12 (1:1) containing 5% Fetal Bovine Serum (Sigma-Aldrich). Non-tumourigenic immortalised human bronchial epithelial cells (HBEC-3KT) along with their isogenic derivatives; p53 knockouts (HBEC-3KT-53), KRAS mutants (HBEC-3KT-R) and cells with both aberrations (HBEC-3KT-R53) were also employed in this study. HBECs were maintaining in Keratinocyte-SFM medium supplemented with 50µg/mL Bovine Pituitary Extract (BPE) and 5 ng/ml human recombinant Epidermal Growth Factor (rEGF) (Life Technologies). All cell lines were maintained at 37°C, 5% CO2. Cell line authentication was carried out utilising the GenePrint 10 System (Catalogue no. B9510 - Promega) to amplify 10 ng DNA of each cell line. The amplification product was mixed with internal lane standard 600 allele ladder and analysed on a 3130 Genetic Analyzer (Life Technologies) using GeneMapper ID-X Software (Appendex 3). Cell lines were also verified as free from mycoplasma utilising the e-MycoTM plus Mycoplasma PCR Detection Kit (Catalogue no. 17341 - Intron Biotechnology).

2.2.1 Cell growth curves

For growth curve estimation, 10^3 cells were seeded in each well of flat-bottomed 48-well plates in six replicates and cultured in 500 µl of medium. MTT assessments were performed every 24 hrs for 5 subsequent days. The average proliferation rate was

Table 2.1: Cells lines utilised in this study and their histological subtype

Cell Line	Histological origin
NSCLC	
A549	Adenocarcinoma
Calu-3	Adenocarcinoma
CALU6	Adenocarcinoma
COR-L23	large cell carcenoma
CRL5802	SCC
H358	Bronchioloalveolar adenocarcinoma
LUDLU-1	SCC
SK-LU-1	Adenocarcinoma
SK-MES-1	SCC
HNSCC	
BHY	Oral SCC
HN5	SCC
PE/CA-PJ15	Oral SCC
PE/CA-PJ41	Oral SCC
UM SCC-104	SCC
UM SCC-19	SCC
UM SCC-4	SCC
UM-SCC- 47	SCC
UM-SCC-12	Laryngeal SCC
UM-SCC-17as	Supraglottic SCC
UM-SCC-5	Supraglottic SCC
UM-SCC-81B	Laryngeal SCC
UPCI-SCC-090	OPSCC
HBEC	
HBEC-3KT	Non tumourigenic human bronchial epithelial
HBEC-3KT-53	Non tumourigenic human bronchial epithelial
HBEC-3KT-R	Non tumourigenic human bronchial epithelial
HBEC-3KT-R53	Non tumourigenic human bronchial epithelial
LIV-7K	Primary oral SCC (obtained from Dr Janet Risk)

deducted from six independent replicates. This experimental setting was followed according the preliminary results of previous pilot experiments.

2.3 Examination of cell growth

2.3.1 Cellular phenotypic characteristics

EVOS digital inverted microscope (AMG-USA) was used for phenotypic examination of cell lines in addition to monitoring cell growth, confluence and clonal colonies formation.

2.3.2 Exposure to therapeutic agents

Depending on the growth rate of each cell line, (5-8) × 10^4 cells were seeded in each well of flat-bottomed 48-well plates in six replicates and cultured in 500 µl of medium. After overnight incubation, the medium was replaced with media contained a range of concentrations (0-35nM) of Paclitaxel (Catalogue no. T7191 - Sigma-Aldrich), Docetaxel (Catalogue no. 01885 - FLUKA), either separately or synchronously with Alisertib (Catalogue No. S1147 - Selleck Chemicals) (0-11.1 nM), 0-3.2 nM Barasertib-AZD1152 (Catalogue No. S1147 - Selleck Chemicals), 50-200 nM Decitabine (5-Aza-2'-deoxycytidine) (Catalogue No. A3656 - Sigma), or 0.5-8 mM Valproic acid (VPA) (Catalogue No. P4543 - Sigma) and pretreated with 0.5-1 mM VPA. Cells were incubated for 72 hours with replenishment of medium with drug at 36 hours.

2.3.2 MTT proliferation assay

The drug toxicity and viability of the cell lines and knockdown derivative clones were measured using the MTT proliferation assay. Cells already seeded and/or exposed to the chemotherapeutic compounds in 48 well plates, for required time course, were washed with PBS and incubated with fresh medium containing 0.75 mg/ml of MTT (3-(4,5-dimethy1–2-thioazoyl) 2,5-diphenyltetrazolium bromide) (Catalogue No. M5655 - Sigma-

Aldrich) for 3 hours at 37°C supplemented with 5% CO2. The medium was subsequently discarded and the converted formazan was solubilised by lysing the cells by addition 200 ul of 0.04 M HCl in isopropyl alcohol. After five minutes, viability of the cells was determined by measuring the optical density (O.D.) at 590nm with 630nm as reference in a GENios plate reader (Tecan Austria GmBH).

2.4 mRNA expression analyses

2.4.1 RNA extraction

Total RNA was extracted using Direct-zol™ RNA MiniPrep Kit (Zymo Research). Quality and quantity of DNA and RNA were determined using a NanoDrop 2000 Spectrophotometer (Thermo Scientific). RNA extraction from primary tumour tissues was undertaken utilising 10 µm thick sections obtained by cryosectioning. The sections were collected in Precellys ceramic beads prefilled tubes (Catalogue No. KT03961-1-003.2 - Bertin Technologies) 500 µl TRIzol Reagent was added per about 50 mg tissue. The suspension was homogenized using Precellys 24 homogenizer (Bertin Technologies). RNA extraction from cell lines was performed by lysing the cells directly in the culture container by removing liquid medium, washing cells with Dulbecco PBS and replacing with 600 µl TRIzol Reagent. To remove particulates, the mixture was centrifuged at 12,000 x g for 1 minute. One volume ethanol (95-100%) was added directly to one volume sample homogenate (1:1) in TRI Reagent and mixed well by vortexing. The mixture was then loaded into a Zymo-Spin™ IIC Column in a collection tube and centrifuged at 10,000-16,000 x g for 1 minute. The column was transferred into a new collection tube and the collection tube containing the flow-through was discarded. 400 µl Direct-zol™ RNA PreWash reagent was added to the column and centrifuged at aforementioned speed for 1 minute. The flow-through was then discarded.

The previous stage was repeated twice. After that, 700 µl RNA Wash Buffer was added to the column and centrifuged as mentioned above and the flow-through was discarded. To ensure complete removal of the wash buffer, the column was centrifuged for an additional 4 minutes in an emptied collection tube. The column was carefully transferred into an RNase-free tube then 40 µl of DNase/RNase-Free Water was directly added to the column matrix and centrifuged at max speed for 1 minute. Finally, an aliquot of each RNA sample was used for Agilent chip analysis in order to check its quality and quantity while the remaining RNA was stored at -80°C for future use.

2.4.2 Agilent RNA 6000 Nano kit

RNA quality and quantity was assessed by capillary electrophoresis on an Agilent 2100 Bioanalyser (Agilent Technologies). In brief 550 µl of Agilent RNA 6000 Nano gel matrix were placed into the top receptacle of a spin filter. The spin filter was centrifuged for 10 minutes at 1500 g ± 20 % and 65 µl filtered gel were used per each chip. RNA 6000 Nano dye concentrate was vortexed and 1 µl of RNA 6000 Nano dye concentrate was added to a 65 µl aliquot of filtered gel. The gel and dye mix was vortexed thoroughly and spun for 10 minutes at room temperature at 13000 g. 9.0 µl of the gel-dye mix were pipetted at the bottom of the well-marked in a RNA Nano chip. The gel and dye mix was spread throughout the chip under air pressure using a syringe for 30 seconds. After 5 seconds, the plunger of the syringe was slowly pulled back, the chip priming station was opened and 9.0 µl of the gel-dye mix were pipetted in each of the marked wells. Subsequently 5 µl of the RNA 6000 Nano marker were pipetted into the well-marked with the ladder symbol and each of the 12 sample wells. To minimize secondary structure, RNA ladder and samples were heat denatured at 70°C for 2 minutes before loading on the chip. 1 µl of the RNA

ladder was pipetted into the well-marked with the ladder symbol and 1 µl of each sample into each of the 12 sample wells. The chip was placed horizontally in the adapter of the IKA vortex mixer and was vortexed for 60 seconds at 100 g. Finally the chip was inserted in the Agilent 2100 Bioanalyzer and the run started in the following five minutes.

2.4.3 Reverse transcription

RNA was Reverse Transcribed using the High Capacity cDNA Reverse Transcription Kit (Life Technologies). This kit was utilised following the manufacturer's protocol. Briefly (200-300) ng of RNA (10 µl) was heated at 70 °C for 5min then cooled down at 0 0C for 2 minutes. After that, it mixed with 2 µl of 10x RT Buffer, 0.8 µl of dNTP Mix (100 mM), 2 µl of RT Random Primers, 1 µl of MultiScribe™ Reverse Transcriptase and 4.2 µl of Nuclease-free deionised H2O. After mixing by pippeting and centrifugation, the reaction of the reverse transcription took place using a thermal cycler and performing the following steps: 10 min at 25 0C, 120 min at 370C and a last step of 5 sec at 85 0C. cDNAs were diluted five times and 2 µl or 1.5 µl were used for the Quantitative PCR reactions.

2.4.4 Quantitative Real-Time PCR expression assays

The selection of targets among the mitotic spindle genes in this study was based on existing unpublished data; more specifically an expression microarray analysis (ALMAC platform) had been performed on about 4000 genes. Therefore, the mitotic spindle - associated genes demonstrating significant mRNA deregulation were selected for this study (Table 2.2: A: AdC, B: SqCC).

Table 2.2: A: Microarray mRNA expression analysis (ALMAC platform) of mitotic spindle-associated genes

A. Adeno vs normal

Affy Probe ID's	Gene Name	Normal Intensity	SqCCL Intensity	Log (Ratio)	Log (Error)	Fold Change	P-value	GenBank	Orientation
LC3P.5565C1_s_at	*AURKA*	0.8558	3.2300	0.5624	0.1539	3.6506	0.00026	NM_198437	Sense
LCHP.1058-22_s_at	*AURKA*	0.7636	3.0911	0.5928	0.1440	3.9156	0.00004	NM_198437	Sense
LCHP.1130-22_s_at	*AURKB*	0.1183	0.6151	0.7015	0.2249	5.0292	0.00181	NM_004217	Sense
LC3P.9707C1_s_at	*AURKB*	0.1209	0.6866	0.7400	0.2363	5.4953	0.00174	NM_004217	Sense
LC3P.9713C1_at	*DLGAP5*	0.0950	0.5764	0.7684	0.2464	5.8668	0.00181	NM_014750	Sense
LCADNH.6892_at	*KIF11*	0.3177	0.6134	0.2713	0.0983	1.8678	0.00576	AL356128	AntiSense
LCRS.2611_at	*KIF11*	0.4543	1.6643	0.5495	0.1263	3.5436	0.00001	NM_004523	Sense
LCMXR.18640C1_at	*KIF11*	0.2840	1.2394	0.6255	0.1543	4.2216	0.00005	NM_004523	AntiSense
LCHP.701-22_s_at	*TPX2*	0.2574	1.8723	0.8474	0.2065	7.0373	0.00004	NM_012112	Sense
LCHP.1160-22_s_at	*TPX2*	0.0953	0.9198	0.9701	0.2437	9.3342	0.00007	NM_012112	Sense
LCADA.4890_s_at	*TPX2*	0.1198	1.1900	0.9826	0.2369	9.6081	0.00003	NM_012112	Sense
LC3P.10122C1_s_at	*TPX2*	0.1935	1.9712	0.9936	0.2076	9.8547	1.69E-06	NM_012112	Sense
LCHP.442_s_at	*TTK*	0.1420	0.8482	0.7619	0.2174	5.7794	0.00046	NM_003318	Sense
LCHP.442-22_s_at	*TTK*	0.1258	0.7674	0.7710	0.2171	5.9020	0.00038	NM_003318	Sense
LC3P.846C3_at	*TUBB*	1.4783	2.1457	0.1473	0.0473	1.4039	0.00184	NM_178014	Sense
LC3SNG.2461a55_at	*TUBB1*	0.3620	0.1640	-0.3583	0.1045	-2.2821	0.00061	NM_030773	Sense
LC3P.846C4_at	*TUBB3*	0.1577	0.9819	0.7797	0.2270	6.0218	0.00059	NM_006086	Sense

Table 2.2: B: Microarray mRNA expression analysis (ALMAC platform) of mitotic spindle-associated genes

B. Squamous vs normal									
Affy Probe ID's	Gene Name	Normal Intensity	SqCCL Intensity	Log (Ratio)	Log (Error)	Fold Change	P-value	GenBank	Orientation
LC3P.5565C1_s_at	*AURKA*	0.8558	4.0941	0.6627	0.1434	4.5998	2.51E-08	NM_198437	Sense
LCHP.1058-22_s_at	*AURKA*	0.7636	3.8997	0.6911	0.1337	4.9106	2.18E-08	NM_198437	Sense
LCHP.1130-22_s_at	*AURKB*	0.1183	0.8528	0.8408	0.1960	6.9307	1.81E-07	NM_004217	Sense
LC3P.9707C1_s_at	*AURKB*	0.1209	0.9830	0.8932	0.2076	7.8205	2.17E-07	NM_004217	Sense
LC3P.9713C1_at	*DLGAP5*	0.0950	0.9467	0.9813	0.2083	9.5793	5.46E-07	NM_014750	Sense
LCRS.2611_at	*KIF11*	0.4543	2.6259	0.7449	0.1190	5.5580	8.15E-09	NM_004523	Sense
LCMXR.18640C1_at	*KIF11*	0.2840	2.0164	0.8343	0.1429	6.8273	4.71E-08	NM_004523	AntiSense
LCHP.701-22_s_at	*TPX2*	0.2574	2.5100	0.9721	0.1945	9.3781	7.24E-08	NM_012112	Sense
LC3P.10122C1_s_at	*TPX2*	0.1935	2.9047	1.1594	0.1893	14.4353	8.43E-08	NM_012112	Sense
LCHP.1160-22_s_at	*TPX2*	0.0953	1.6204	1.2134	0.2095	16.3461	6.6E-08	NM_012112	Sense
LCADA.4890_s_at	*TPX2*	0.1198	2.0565	1.2176	0.2066	16.5052	8.43E-08	NM_012112	Sense
LCHP.442-22_s_at	*TTK*	0.1258	1.3821	1.0239	0.1887	10.5665	9.5E-07	NM_003318	Sense
LCHP.442_s_at	*TTK*	0.1420	1.5762	1.0284	0.1885	10.6752	1.02E-06	NM_003318	Sense
LC3P.846C3_at	*TUBB*	1.4783	2.5113	0.2131	0.0450	1.6333	2.24E-08	NM_178014	Sense

For qPCR validation, predesigned FAM-MGB labelled Taqman expression assays were utilised in this study (Table 2.3).

Table 2.3: predesigned FAM-MGB labelled Taqman expression assays

Gene name	Catalogue number
AURKA	Hs01582072_m1
AURKB	Hs00945858_g1
AURKC	Hs00152930_m1
CKAP5	Hs01120723_m1
DLGAP5	Hs00207323_m1
KIF11	Hs00189698_m1
TPX2	Hs00201616_m1
TTK	Hs01009870_m1
TUBB	Hs00962419_g1
TUBB3	Hs00964962_g1

A customised expression assay was designed for ACTB gene expression in order to be used as an endogenous control. RT-qPCR primers and probe (labelled with TAMRA-BHQ2 reporter/quencher) were designed using the Primer Express v 3.0 software (Life technologies) (Table 2.4).

Table 2.4: Primers designed for the detection of ACTB RNA sequences.

Target	Forward primer (5'→3')	Reverse primer (5'→3')	probe (TAMRA labelled)
ACTB	GGCACCCAGCACAATGAAG (58.7°C)	CATACTCCTGCTTGCTGATCCA (58.9°C)	CTCCTCCTGAGCGCAAGTACTCCGTG (68.8°C)

The different dyes between my targets (FAM) and endogenous control (TAMRA) enabled multiplexing of the target and endogenous control expression in the same reaction tube. Assays were performed in a final reaction volume of 20 µl containing 10 µl of 2x TaqMan Gene Expression Master Mix (Life Technologies), 900 nM of each primer and 250 nM probe (my targets), 900 nM of each primer and 250 nM probe of the endogenous control ACTB-VIC (Life Technologies). 3 µl of cDNA was then added to the premix (described in section 2.4.3) following the universal (life Technologies term) conditions: [2 min at 50°C (UNG

action), 95°C for 10 min (activation), 45 cycles of 95°C for 15 sec (denaturation), 60°C for 1min (annealing and extension)] on a Life Technologies StepOnePlus Real-Time PCR System. The assays' efficiency regarding reproducibility and robustness was tested over 5-logs of cDNA concentration. The StepOnePlus Software v2.0.1 (Life Technologies) was used for data analysis. RNA levels were expressed as relative quantification values (RQ) which were calculated as: $RQ=2^{-\Delta\Delta Ct}$, where the mRNA expression of HBEC-3KT cells was used as a calibrator in each run. All assays were run in duplicate and the mean values were used for the analysis.

2.5 DNA methylation analysis

2.5.1 DNA extraction

DNA extraction from cell lines and primary lung tumours was performed using DNeasy® Blood and Tissue Kit (QIAGEN) using DNeasy 96 protocol for purification of total DNA from tissues and spin-column protocol for purification of total DNA from cell lines. Quality and quantity of DNA were determined using a NanoDrop 2000 Spectrophotometer (Thermo Scientific).

DNA extraction from primary tumour tissues was undertaken utilising 20 µm thick sections obtained by cryosectioning. The first and last sections underwent pathological review to ensure an at least 80% tumour cell content. DNA extraction of the samples was performed following the manufacturer's protocol. Briefly, tissue was lysed with 360 µl of ATL reagent and 40 µl of Proteinase K solution (Qiagen) and incubated at 55°C overnight in an orbital shaking incubator at 200rpm. 820 µl of premixed AL buffer with ethanol were added and after mixing, lysates were transferred in two "twin" 96-well plates with silica based membranes. The samples were then centrifuged at 4,000 g for 10min and washed once

with 500µl buffer AW1. After centrifugation at 4,000 g the samples were washed again with 500µl buffer AW2. After centrifugation at 4,000 g, 55µl of AE buffer pre-warmed at 60°C were added to each sample and DNA was recovered by centrifugation at 4,000 g for 5 min.

For the DNA extraction from cell lines, a maximum of $5x10^6$ cells were pelleted at 300 x g for 5 minutes and the pellet was re-suspended in 200 µl PBS. 20 µl proteinase K and 4 µl of RNase A (100 mg/ml) (Qiagen) were added, the lysate was then mixed by vortexing and incubated at room temperature for 10 minutes. Subsequently 200 µl Buffer AL were added and the lysate was mixed thoroughly by vortexing and incubated at 56°C for 10 min. 200 µl of ethanol (96–100%) were added to the sample which was mixed thoroughly by vortexing. The mixture was transferred into the DNeasy Mini spin column (which carries a silica based membrane) placed in a 2 ml collection tube, and was centrifuged at 6000 x g for 1 min. 500 µl of Buffer AW1 were added, and the sample was centrifuged for 1 min at 6000 x g . 500 µl of Buffer AW2 were then added and the sample was centrifuged for 3 min at 20,000 x g to dry the DNeasy membrane. The DNeasy mini spin column was then placed in a 1.5 ml microcentrifuge tube and the DNA was recovered into 200 µl Buffer AE with centrifuging at 6000 x g for 1 min. DNA quality and quantity was assessed by spectrophotometry at 260/280 nm wavelength.

2.5.2 DNA methylation

In order to generate positive control for methylation-specific PCR or bisulfate sequencing, reaction of four units SssI per µg of unmethylated DNA for 2 hours was prepared according the modified manufacturing protocol. Briefly, 5µl nuclease free water, 3µl of 10x NEB buffer, 1µl of 1600µM S-adenosylmethionine (SAM), 20µl WBC DNA and 1µl of 4U/1µl SssI

methylase were added in order and mixed properly by pipetting then incubated for 2 hours at 37°C. the reaction was stopped by heating at 65°C for 20 minutes. Standard curve of 20µl two-fold methylated DNA dilutions (5%, 10%, 20%, 40%, and 80%) was prepared by diluting in unmethylated DNA.

2.5.3 Bisulphite treatment of DNA

To investigate the methylation status of the different gene promoters tested in this study, 500 ng DNA from primary tissues was bisulphite treated utilising the EZ-96 DNA Methylation-Gold™ Kit (ZymoResearch) following the manufacturer's protocol.

The CT Conversion Reagent was prepared prior to use by adding 900 µl of water, 50 µl of M-Dissolving Buffer, and 300 µl of M-Dilution buffer. It was then mixed by shaking for 10 minutes at room temperature. The M-Wash Buffer was prepared by adding 144 ml of 100% ethanol to the 36 ml M-Wash Buffer concentrate. 130 µl of the CT Conversion Reagent were added to 20 µl (500 ng) of each DNA tissue sample or 1000 ng DNA from cell lines in a 12 PCR tube strip and samples were mixed by pipetting up and down. The PCR tube strip was locked and transferred to a thermal cycler and the following steps were performed: 98°C for 10 minutes, 64°C for 2.5 hours. The samples from the Conversion step were transferred to Eppendorf tubes containing 600 µl M-Binding Buffer and samples were then mixed by pipetting up and down. Zymo-Spin™ IC Column was placed onto an assembly onto a vacuum manifold and loaded with the sample then the vacuum was turn on the until all of the liquid had passed completely through the column. 1000 µl of M-Wash Buffer were added to each column. Each column was placed into a collection tube and centrifuged at full speed (>10,000 x g) for 30 seconds to eliminate any residue Wash Buffer from the column. 200 µl of M-Desulphonation Buffer were then added to each well and the plate

was left at room temperature (20°C–30°C) for 20 minutes. After the incubation, it was centrifuged at full speed for 30 seconds, and the flow-through was discarded. 800 µl of M-Wash Buffer were added to the column, which was then centrifuged at full speed for 30 seconds, and the flow-through was discarded. Another 800 µl of M-Wash Buffer were added to the column, which was then was spun at full speed for 2 minutes to ensure complete removal of alcohol traces. Finally 10 µl of M-Elution Buffer were added directly to the column matrix, the column was placed into a 1.5 ml tube and spun briefly at full speed to elute the DNA. 3 µl of bisulphite treated DNA was used for each PCR reaction.

2.5.4 Pyrosequencing Methylation Analysis (PMA).

Pyrosequencing (PSQ) is a method that can identify the sequence from small DNAs efficiently and with high fidelity. The procedure of the technique divided into two parts. The first part was the preparation of the samples for pyrosequencing. The targeted DNA sequence was amplified by PCR using forward biontinylated (Fb), reverse (R) and Sequencing (S) primers (Table 2.5). The primers were designed by the PyroMark assay design 2.0 software (Appendix 4). One of the two primers is biotinylated. After the examination of the product's quality in an agarose gel, the PCR products were mixed with the binding buffer, which contained sepharose streptavidin beads and buffer, and then were transferred into a 96 well PSQ plate.

With the help of a tool that used vacuum, the beads, in which the PCR product was bound, were held against a filter. The beads were then washed successively with ethanol, NaOH and wash buffer. NaOH denatured and separated the strands, while the wash buffer neutralised the immobilised strand. As a result, at the end of the above procedure, in the tool remained only the streptavidin beads with the biotinylated strand of the PCR products.

Table 2.5: Pyrosequencing primers of the targeted sequence in the promoter regions of the examined genes.

Gene	Forward biontinylated primer (Fb)	Reverse primer (R)	Sequencing primer (S)
AURKB	5-TTTTTTATTGGGTTTTTATGA 3’	5-ACTTTTCAAATCTCCCCCCC 3’	5-ACCCCATTAAACAAACT 3’
CKAP5	5-GTTTGGTTTAGAGGGAAAT 3’	5-CCATTTAAAAAACCTATAAACA3’	5-TGGTTTAGAGGGAAATA 3’
KIF11	5-TATGGGATGTAGTATTTTTATTGG 3’	5-ACAAACAAACAAACCACCTC 3’	5-AAACAAACCACCTCTTTA 3’
TPX2	5-ATTTTTGTATTATTGGGAAGG 3’	5-TCTCCTTATAATTATACATTATCCC 3’	5-AAATTCAAAAAATTCACTTC 3’
TUBB	5-GAGGGAAAGTAGGTTGGG 3’	5-CCACTAATCAAAACCAAACTC 3’	5-ATAAAACTTTATCTCCCTA 3’

The beads were then released in a new 96 well PSQ plate together with the annealing buffer, which contained the sequencing primers. The first of the four triphosphates (dNTPs) was injected into the reaction. DNA polymerase catalyses the incorporation of the first dNTP into the DNA strand if it was complementary to the base in the template strand. Each incorporation event was accompanied by release of pyrophosphate (PPi) in a quantity equimolar to the amount of incorporated nucleotide. ATP sulfurylase converted PPi to ATP in the presence of Adenosine 5'-phosphosulfate (APS). This ATP drived the lusiferin to oxyluciferin that generated visible light in amounts that were proportional to the amount of the ATP. The light produced in the luciferase- catalysed reaction was detected by a charge coupled device (CCD) camera and seen as a peak in a pyrogram. The height of each peak (light signal) is proportional to the number of nucleotides incorporated (Figure 2.1).

Apyrase, a nucleotide degrading enzyme, continuously degrades ATP and unincorporated dNTPs. This switches off the light and regenerates the reaction solution. The next dNTP is then added. The dNTPs are added one at a time. As the process continuous, the complementary DNA strand is built up and the nucleotide sequence is determined from the signal peaks in the pyrogram. Using the standard treatment of genomic DNA with bisulphite (described in the previous paragraph), unmethylated Cytosine (C) is converted to Uracil (U), whereas methylated Cytosine (mC) remains unchanged. Using PCR, Uracil (U) is amplified to Thymine (T), whereas mC is amplified to Cytosine (C). Discrimination between mC and C is thereby achieved by transforming mC and C to appear as a C/T SNP.

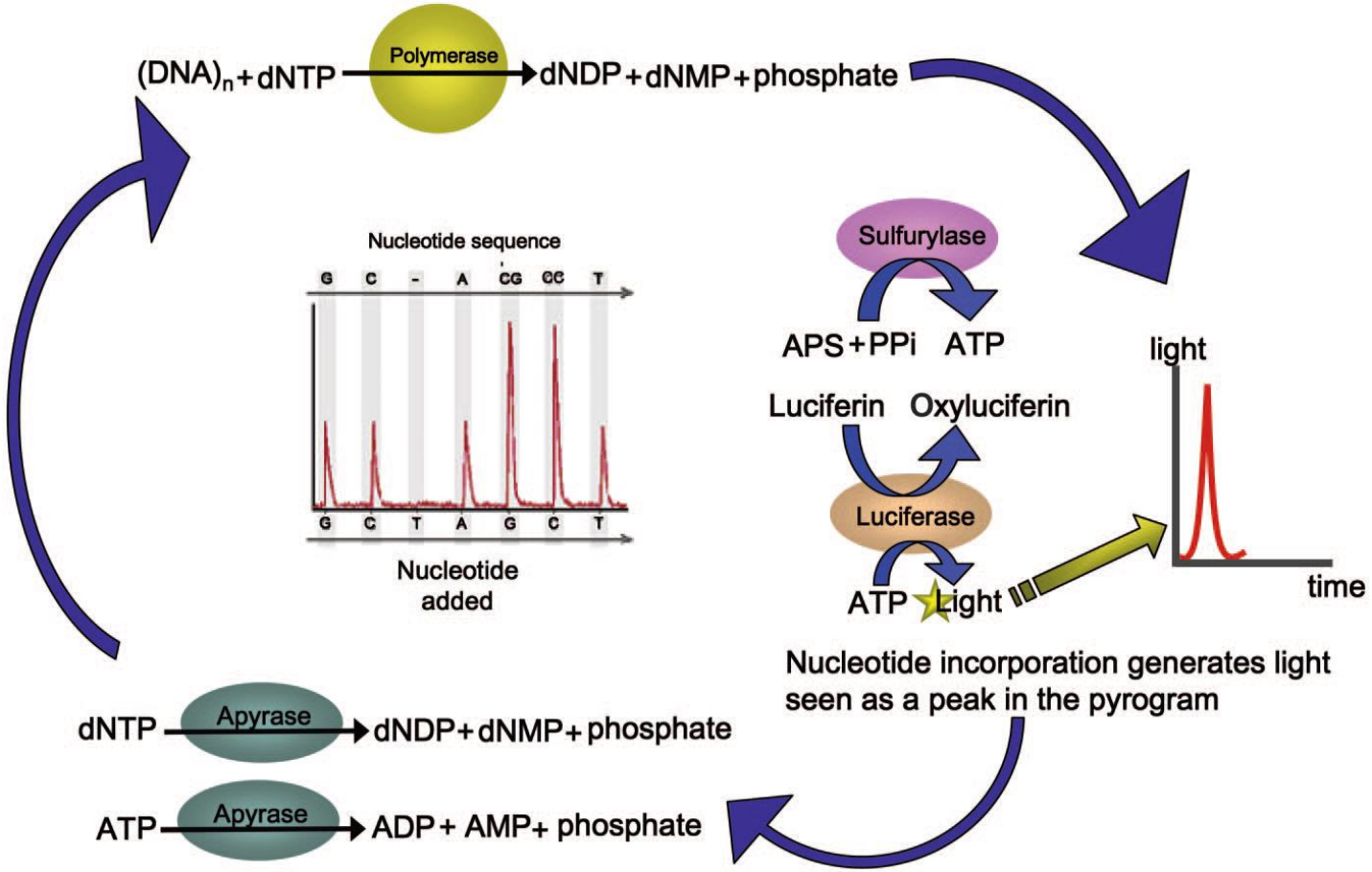

Figure 2.1: Nucleotide incorporation generates light seen as peak in the program. The figure extracted from (Petrosino 2009).

2.5.5 Decitabine efficiency

The previous protocol on Decitabine efficiency in lung cancer cells (Daskalos 2009) was confirmed by assessing global DNA methylation following the cells' treatment. A549 cells were treated with 50, 100, 200 nM 5-aza-20-deoxycytidine (Decitabine; Sigma-Aldrich, cat no11390) for 48 hours. Following a wash with PBS, DNA was extracted as described in section (2.5.1). Decitabine efficiency was determined by measuring global DNA methylation. This was achieved by pyrosequencing-methylation analysis of the LINE-1.2 (Genebank accession no M80343) retrotransposon (Daskalos 2009). Sodium bisulfite conversion as described in section (2.5.3). The primers used were the following:

Promoter	Forward primer (5'→3')	Reverse primer (5'→3')	Sequencing primer (5'→3')
LINE-1	Bio-TAGGGAGTGTTAGATAGTGG	AACTCCCTAACCCCTTAC	CAAATAAAACAATACCTC

PCR amplification was performed using Qiagen HotStarTaq Plus Master Mix Kit, 5µM biotinylated primer, 10 µM non-biotinylated primer and 3 µl (approximately 60ng) of bisulphite treated DNA. The thermal profile for LINE-1 amplification is shown in Table 2.6.

Table 2.6: Thermal profile for LINE-1 amplification PCR reactions

Step	Temperature (^{o}C)	Time	No of cycles
Taq Activation	95	5 min	
Denaturation	94	30 sec	
Annealing	58	45 sec	40 cycle
Extension	72	45 sec	
Final extension	72	10 min	

The PCR product quality and quantity was confirmed by agarose gel (2%) electrophoresis UV visualisation on a UVP VisionWorks LS instrument prior to clean up and Pyrosequencing analysis. For the latter the SQA kit was used following the suppliers protocol (Qiagen) and the reaction was performed on a 96MA Pyrosequencer (Qiagen).

2.6 Transfection

2.6.1 AURKA, AURKB and TPX2 mRNA downregulation

Five different constructs were used to target *AURKA*, *AURKB* or *TPX2* mRNA expression (Catalogue no. SHC202 - Sigma-Aldrich (Table 2.7) that belong to type TRC2-pLKO-puro Vector (Figure 2.2: A) along with a scrambled control construct which is MISSION TRC2 pLKO.5-puro Non-Mammalian shRNA Control Plasmid DNA (Catalogue no. SHC202 - Sigma-Aldrich) (Figure 2.2: B).

2.6.1.1 Propagation of MISSION short hairpin RNA (shRNA) constructs in E. coli

One Shot TOP10 Chemically Competent *E. coli* (Catalogue no. C4040-03 – Life technologies) were transformed with MISSION shRNA constructs utilised in this study. The transformation was followed the Life technologies protocol. Briefly, 2 µl of the DNA was added (100 ng) into a vial of One Shot cells and incubated on ice for 30 minutes. The cells then exposed to Heat-shock for 30 seconds at 42°C without shaking. The vial subsequently placed them on ice for 2 minutes. Aseptically, 500 µl of pre-warmed S.O.C. Medium was added to the vial and then incubated at 37°C for 1 hour at 225 rpm in a shaking incubator. Subsequently, 200 µl from transformation was spread on a pre-warmed selective plate (Luria-Bertani medium contained 100 µg/ml) and incubated overnight at 37°C. After the incubation period, single colonies were selected and analysed by plasmid isolation.

2.6.1.2 shRNA constructs DNA isolation

MISSION shRNA constructs plasmid were isolated utilising Zyppy Plasmid Midiprep Kit (Catalogue no. D4025 - Zymo Research) according to the manufacture protocol. In brief, Six ml of bacterial culture in LB medium was centrifuge at at ≥3,400 x g for 10 minutes. 6 ml of TE was added to the bacterial cell pellet and completely re-suspended by vortexing. 1 ml of 7X

Table 2.7 : shRNA constructs from MISSION library (SIGMA) matching gene transcripts of AURKA, *AURKB* & TPX2

Clone ID	Target Sequence	Target Region
AURKA		
TRCN0000000655	ACGAGAATTGTGCTACTTATA	3UTR
TRCN0000000656	CCTGTCTTACTGTCATTCGAA	CDS
TRCN0000000657	GAGTCTACCTAATTCTGGAAT	CDS
TRCN0000000658	AGGCCACTGAATAACACCCAA	CDS
TRCN0000010533	CACATACCAAGAGACCTACAA	CDS
AURKB		
TRCN0000000776	CTACCTCCTCCTTTGTTTAAT	3UTR
TRCN0000000777	CCTGCGTCTCTACAACTATTT	CDS
TRCN0000000778	TGATGGAGAATAGCAGTGGGA	CDS
TRCN0000010547	GCATCACACAACGAGACCTAT	CDS
TRCN0000000779	GAAGAGCTGCACATTTGACGA	CDS
TPX2		
TRCN0000074533	CCATGTAGTTACTTCCTTTAA	3UTR
TRCN0000074534	CCGAGCCTATTGGCTTTGATT	CDS
TRCN0000074535	CGAGCCTATTGGCTTTGATTT	CDS
TRCN0000074536	CCTTTGAGAAAGGCTAATCTT	CDS
TRCN0000074537	CGTGAACTTGATCCCAGAATA	CDS

Lysis Buffer (Blue) was then added to the sample and mixed by gently inverting the tube 2-4 times. 3.5 ml of cold Neutralization Buffer (Yellow) was added and inverted 4-6 times to mix thoroughly until the sample will turned yellow when the neutralization is completed and a yellowish precipitate formed. Zymo-Midi Filter/Zymo-Spin V-E column assembly was placed onto a vacuum manifold, the entire mixture was then added into the Zymo-Midi Filter column, and the vacuum was then turned on until all of the liquid has passed completely through both columns. The Zymo-Spin V-E column was then transferred to a collection tube and centrifuged at ≥11,000 x g for 30 seconds to remove any retained lysate. Subsequently, 400 µl of Endo-Wash Buffer was added to the Zymo-Spin V-E column and centrifuged at ≥11,000 x g for 30 seconds. 400 µl of Zyppy Wash Buffer was added and centrifuged at ≥11,000 x g for 30 seconds. The Zymo-Spin V-E column was finally transferred into a clean 1.5 ml microcentrifuge tube and then plasmid DNA was eluted by adding 150 µl of Zyppy Elution Buffer at ≥11,000 x g centrifugation for 1 minute.

2.6.1.3 Knock-down of AURKA, AURKB and TPX2 mRNA expression by shRNA

Knock-down of AURKA, AURKB and TPX2 by short hairpin RNA (shRNA); A549, LUDLU1, SKLU1 and SK-MES1 cell lines were transfected with aforementioned shRNA constructs utilising Attractene Transfection Reagent (Catalogue no. 301007 - Qiagen) according the manufacturing protocol. Briefly, 100 mm tissue culture dish was seeded with $5x10^5$ cell/ml and incubated at 37°C overnight. 20 µl of 100 ng/µl plasmid DNA was added to 280 µl free-serum DMEM medium supplemented with 7.5 µl Attractene Transfection Reagent. The mixture was then incubated for 15minute at room temperature to allow transfection complex formation. Meanwhile, the medium of pre-incubated cells was replaced by 2ml of new medium. The transfection complex mixture was added and the cells re-incubated at 37°C overnight. Subsequently, the medium was replaced with new medium containing 4 nM Puromycin. Stable clones were selected by subsequent exposure to 4 nM Puromycin and knockdown efficiency was confirmed by qPCR and western blotting.

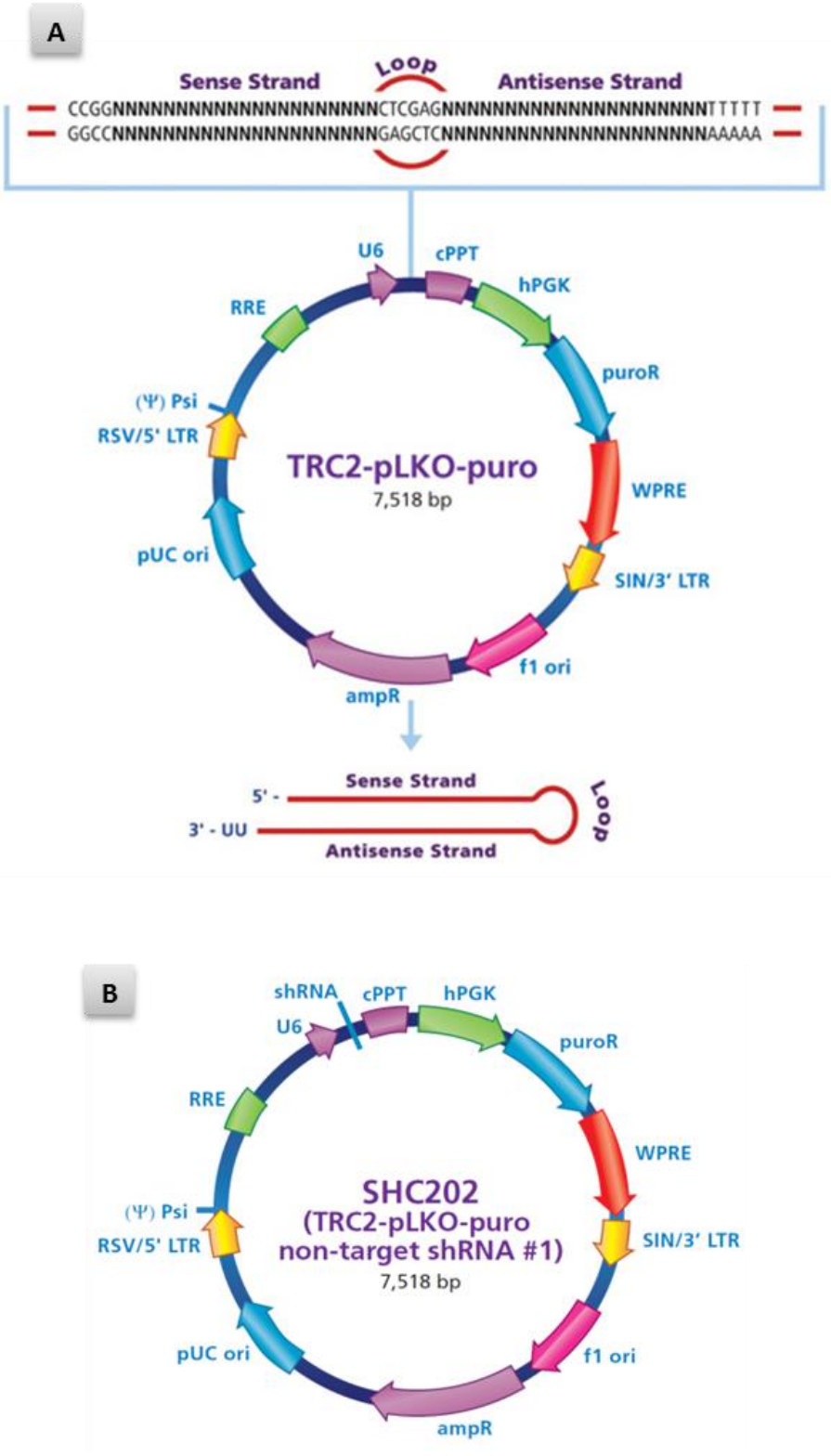

Figure 2.2: (A) TRC2-pLKO-puro plasmid map with shRNA insert, the length is 7,518 bp. (B) MISSION TRC2 pLKO.5-puro Non-mammalian shRNA Control Plasmid DNA map. The figures extracted from (Sigma-Aldrich).

2.6.2 AURKB overexpression by constructed pCMV6-XL4-AURKB/Bsd plasmid

2.6.2.1 pCMV6-XL4 Vector preparation

PCMV6-XL4 plasmid (Catalogue no. PCMV6XL4 – OriGene) (Figure 2.3) which carries human *AURKB* cDNA was used to construct plasmid DNA express *AURKA*-mRNA in mammalian cells and carry Blasticidin resistant gene as a selective marker of successful transfection. PCMV6-XL4 was transformed into One Shot TOP10 Chemically Competent *E. coli* (as mentioned in section (2.6.1.1). The vector was then isolated utilising Zyppy Plasmid Midiprep Kit (as mentioned in section (2.6.1.2).

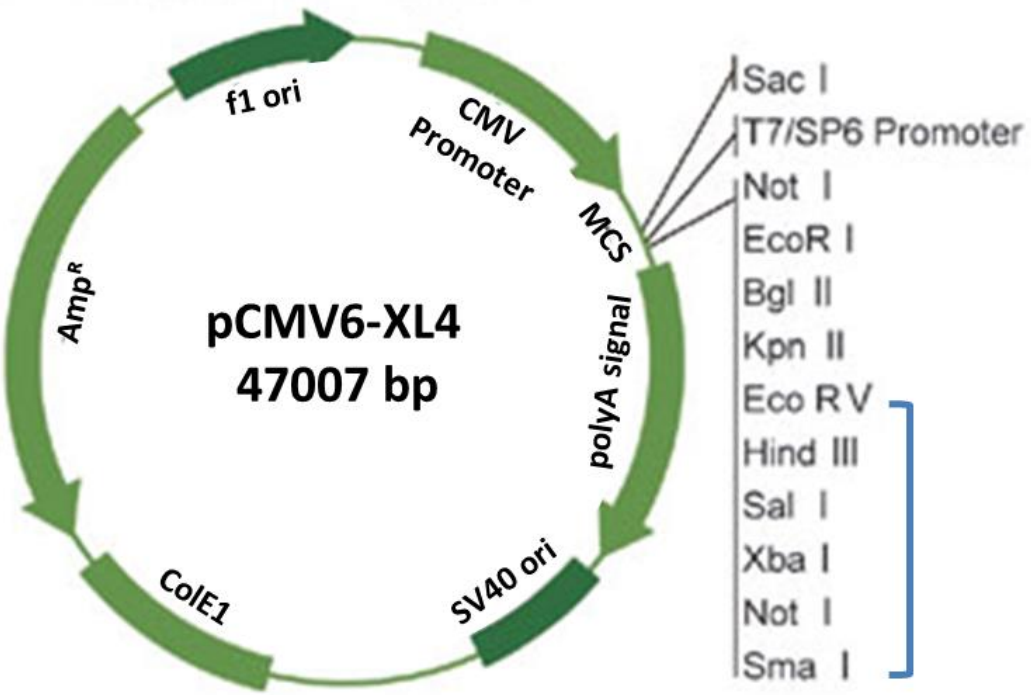

Figure 2.3: SC117526 NM_004217 *AURKB*, Homo sapiens Aurora kinase B as transfection-ready. The figure extracted from (OriGene).

2.6.2.2 pCMV6-XL4 Vector digestion

20 µl of 75ng/µl pCMV6-XL4 Vector was digested with 3 µl of 5 units/µl PsiI (Catalogue no. R0657S - New England Biolabs) in 30 µl restriction buffer2 and incubated at 37°C for

overnight. The digested DNA vector was then cleaned up utilising QIAquick PCR Purification Kit (Catalogue no. 28104 - QIAGENE). The manufacture protocol was followed. Briefly, 250 µl Buffer PB was added to the DNA sample (5:1) until the colour of the mixture turned yellow. The sample was then applied to the QIAquick column and centrifuged at 15000 x g for 60 sec. 750 µl Buffer PE was added to the column and centrifuged at at 15000 x g for 60 sec. the column was placed in a clean 1.5 ml microcentrifuge tube. The ultra-pure DNA was eluted with 30 µl DNA Elution buffer at 15000 x g centrifugation for 30 sec. The purified DNA was analysed by gel electrophoresis.

2.6.2.3 5`-T overhang preparation and 5`- PO_4 group removal of pCMV6-XL4 Vector

In order to avoid vector recircularization and to follow TA overhang cloning strategy, the vector was T overhung and PO4 group was removed (Figure 2.4). PCR amplification step was undertaken on 30 µl DNA vector utilising 1 µl of 100mM dTTP (BIOLINE) and 1 µl of 5U/µl Hot Star Taq Plus DNA polymerase (QIAGEN) in 50 ml reaction volume. The mixture was then incubated for 70°C for 2hr. 50 µl of T-overhung vector was treated with 1 µl of 10U/µl Alkaline Phosphatase, Calf Intestinal (CIP) (Catalogue no. M0290S - New England Biolabs) in 100 µl reaction buffer3. The mixture was then incubated at 37°Cfor 1hr. Final clean-up was performed as mentioned in previous section.

2.6.2.4 pCMV/Bsd plasmid preparation

The pCMV/Bsd plasmid (Catalogue no. V510-20 - Life Technologies), which carries the blasticidin resistance gene under the regulation of a CMV and EM7 promoters followed by

Figure 2.4: This figure demonstrates the TA overhang cloning strategy

an SV40 polyA tail (Figure 2.5), was restricted to obtain the fragment carrying the blasticidin resistance gene and its regulatory sequences flanked by polylinker sequences enabling the excision of the desired fragment using different restriction enzymes. pCMV/Bsd plasmid was transformed into One Shot TOP10 Chemically Competent *E. coli* based on the procedure described in section (2.6.1.1). The vector was then isolated utilising Zyppy Plasmid Midiprep Kit as mentioned in section (2.6.1.2).

2.6.2.4.1 Sequential digestion of the pCMV/Bsd vector to obtain Blasticidin DNA insert

Sequential digestion method was followed to obtain the Blasticidin DNA insert. Briefly, 50 µl of 180 ng/µl pCMV/Bsd vector DNA was digested in 100 µl restriction buffer4 contained 10 µl SmaI and incubated at 30°C for 6hr followed by NH4-acetate/Ethanol purification step with -20°C overnight incubation. Next day, the linear vector DNA was restricted with 10 µl

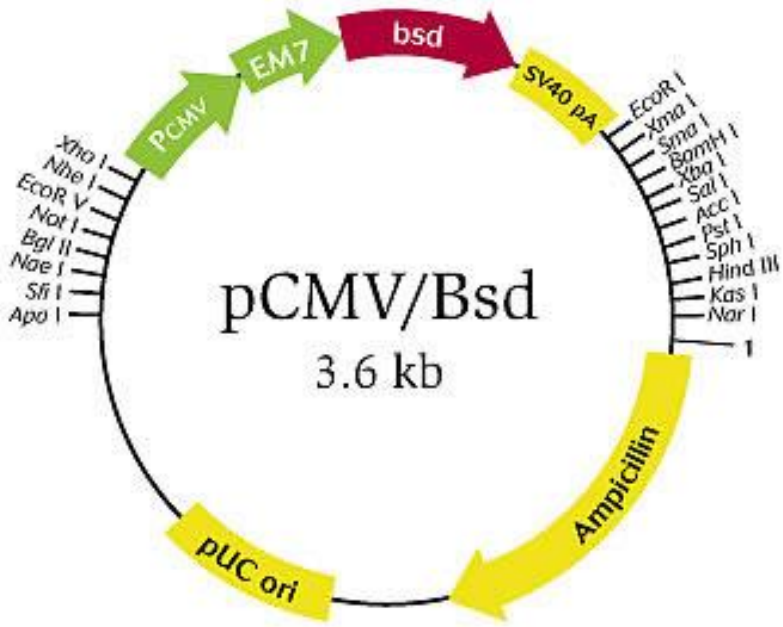

Figure 2.5: Genetic map of the pCMV/Bsd vector, which carries the Blasticidin resistance gene as a selectable marker. The figure extracted from (Invitrogen- Life Technologies).

EcoRV and incubated for 37°C for overnight. Next morning, Ethanol purification step was performed.

Isolation and purification of Blasticidin DNA fragment from low-melt agarose gel was undertaken using QIAquick gel extraction kit (Catalogue no. 28704 – QIAGEN). Gel electrophoresis separated two fragments; the desired fragment carrying the Blasticidin gene (1286 bp) and the rest of pCMV vector. The desired DNA insert was cut out from the gel using a scalpel under low power UV illuminator and obtained using the Qiaquick gel extraction kit according the manufacture protocol. In brief, Blasticidin DNA insert-contained gel was sliced after electrophoresis and three volume of binding buffer was added. The mixture was then incubated at 50°C for 10 min until the gel slice has completely dissolved. The sample was subsequently applied to QIAquick column and centrifuged for 1min at high speed. The binding DNA was washed with buffer PE and the column then centrifuged at

14000 xg for 1 min. finally, the DNA was eluted by 50 µl of buffer EB and then 5 µl was analysed on gel electrophoresis and the rest was stored at 6°C for further use.

2.6.2.4.2 Preparation of 3`-A overhang Blasticidin DNA insert

PCR amplification step was undertaken on 30 µl DNA insert utilising 1 µl of 100mM dATP (BIOLINE) and 1 µl of 5U/µl Hot Star Taq Plus DNA polymerase (QIAGEN) in 50 ml reaction volume. The mixture was then incubated for 70°C for 2hr.

2.6.2.5: Vector construction

TA overhang cloning strategy was followed and pCMV6-XL4-*AURKB*/*Bsd* recombinant plasmid was constructed accordingly.

2.6.2.5.1 DNA quantification

Quant-iT™ dsDNA Assay Kit, broad range (Catalog no. Q-33130 – Life technologies) was utilised to quantify the restricted DNA of pCMV6-XL4-*AURKB* vector and Blasticidin insert according the manufacture protocol. In brief, The Quant-iT working solution was prepared by diluting Quant-iT dsDNA BR reagent 1:200 in Quant-iT dsDNA BR buffer. 200 µl of the working solution was load into each microplate well. 10 µL of each λ DNA standard (Component C) was added to separate wells and mix well as duplicates. 20 µl of each unknown DNA sample was added to separate wells and mix well. The fluorescence measured using a microplate reader. A standard curve was plotted to determine the DNA amounts for the λ DNA standards, plot amount vs. fluorescence, and a straight line was fit to the data points.

2.6.2.5.2 Ligation

The ligation reaction was set up according the 1:3 molar ratio of vector insert. 3 µl pCMV6-XL4 DNA, 7 µl Blasticidin insert DNA and 1 µl T4 DNA ligase was mixed in 20 µl ligation reaction. The mixture was incubated at 16°C for overnight.

2.6.2.5.3 Transformation of E. coli with pCMV6-XL4-AURKB/Bsd recombinant plasmid

In order to propagate the genetically engineered plasmid pCMV6-XL4-*AURKB*/*Bsd*, One Shot TOP10 Chemically Competent *E. coli* cells were transformed with this plasmid based on the procedure mentioned in section (2.6.1.1).

2.6.2.5.4 Restriction mapping of pCMV6-XL4-AURKB/Bsd recombinant plasmid

The sequence of pCMV6-XL4-*AURKB*/*Bsd* recombinant plasmid was predicted according the sequences of pCMV6-XL4 DNA and Blasticidin insert DNA. The suitable restriction enzymes were selected using NEBcutter V2.0 software. NdeI and XmaI were used to confirm the recombination success. 8 µl of 50ng/µl recombinant DNA was double digested by 1 µl NdeI and 1 µl XmaI in 20 µl reaction buffer4. The mixture was incubated at 37°C for overnight. The reaction was deactivated by heating for 20min at 65°C.

2.6.2.5.5 Sequencing of pCMV6-XL4-AURKB/Bsd recombinant plasmid

BigDye Terminator v1.1 Cycle Sequencing Kit (Catalog no. Q-4337449– Life technologies) was utilised for Sequencing of pCMV6-XL4-*AURKB*/*Bsd* recombinant plasmid.

2.6.2.5.5.1 Cycle Sequencing

Sequencing reaction mix was prepared in 4 tubes of recombinant DNA plasmid sequencing primers. The primers were designed using Primer Express Software v3.0:

1. pCMV-xl4/5 *bsd* insert -sequencing F-primer 5`-TCGCCCTTTGACGTTGGA-3`
2. pCMV-xl4/5 *bsd* insert -sequencing R-primer 5`-ATGGAAATTGTAAGCGTTAATA-3`
3. pCMV-xl4/5 *AURKB* insert-sequencing F-primer 5`-ACGGTGGGAGGTCTATATAA-3`
4. pCMV-xl4/5 *AURKB* insert-sequencing R-primer 5`-TATTAGGACAAGGCTGGTGG-3`

4 µl Ready Reaction Premix, 2 µl BigDye Sequencing, 2 µl Sequencing Primer and 6 µl DNA Template/recombinant plasmid was prepared in total volume of 20 µl. The tubes were then placed in a thermal cycler and the volume was set to 20 µl. Cycle Sequencing was performing as shown in Table 2.8.

Table 2.8: Thermal profile for LINE-1 amplification PCR reactions

Step	Temperature (°C)	Time	No of cycles
Taq Activation	95	5 min	
Denaturation	95	30 sec	
Annealing	$53^{\text{F-primer}}$-$60^{\text{R-primer}}$	10 sec	30 cycle
Extension	60	4 min	
Final extension	60	5 min	

2.6.2.5.5.2 Purifyication of extension products

Centri-Sep™ 8-Well Strip (Catalogue no. 4367820 – Life technologies) was utilised in order to efficient removal of excess dye terminators from completed DNA sequencing reactions. The purification was undertaken following the manufacture protocol. Briefly, the strip was first spun down for 2 minutes at 750 x g in a swinging bucket centrifuge to remove interstitial fluid in either of the two ways. 20 µl of sample was added directly to the centre of each well of CENTRI-SEP 8 column. The loaded CENTRI-SEP 8 was placed into an 8-well PCR strip spun down for 2 minutes at 750 x g to collect the sample.

2.6.2.5.5.3 Sequencing analysis

The purified samples were vacuumed until completely dried. The pellet was then resuspended with 10 µl Hi-Di Formamide (Catalogue no. 4311320 – Life technologies). The suspension was heated at 90°C for 5 min and then put in ice path for 1 min. the samples were then analysed by 3130 Genetic Analyzer (Catalogue no. 3130-01R Applied

Biosystems/HITACHI). The sequence of pCMV6-XL4-*AURKB*/*Bsd* recombinant plasmid was then confirmed (Appendix 5; A and B).

2.6.2.6 Transfection of CALU3 cells with pCMV6-XL4-AURKB/Bsd recombinant plasmid

CALU3 cell line was transfected with pCMV6-XL4-*AURKB*/*Bsd* recombinant plasmid according to the method mentioned in section (2.6.1.3). Clonal *AURKB*-mRNA overexpression was confirmed by qPCR (Appendix 6; A) based on method described in section (2.4.4). The modulation of successful clones of taxane response was then analysed (Appendix 6; B) as mentioned in section (2.3.2).

2.7 Western blot

2.7.1 Protein extraction

The cell lines exposed to IC50 concentrations of Aurora inhibitors for (1, 2, 4, 8, 12, 24) hours, AURKA and AURKB knockdown clones as well as their parental cells were washed with DPBS and subsequently lysed by adding Protein Extraction Buffer (PEB) which prepared from material shown in (Table 2.9).

Table 2.9: Protein Extraction Buffer composition

Solution	**ml**	**Provider**	**Cat. no.**
1M Tris-HCl pH=7.4	12.5	Fisher Scientific	BP152-1
Glycerol	12.5	Sigma-Aldrich	G5516
Deoxycholate 6.25%	5	Sigma-Aldrich	D6750
5M NaCl	2.5	Sigma-Aldrich	S9625
0.5M EDTA, pH= 7.4	1	AnalaR	100935V
Triton X-100	1.25	Sigma-Aldrich	T8787
SDS 20%	0.625	Sigma-Aldrich	L3771
ddH20	64.625		
Supplements			
Protease inhibitor cocktail	0.1	Sigma-Aldrich	S8830
Phosphatase inhibitor cocktail	0.1	Sigma-Aldrich	P5726
PMSF (0.3M in DMSO)	0.0035	Sigma-Aldrich	P7626

For each 1 cm^2 of ~80 % confluent growth, 25µl PEB was added. The cell lysate was incubated for 15min on ice bath and then spun at 4°C for 15min at 15000 g. The supernatant was transferred to new tube for additional lysis step by sonication using Bioruptor Sonication System Catalogue no. B01010001 (UCD 200 TM) - Diagenode) following the manufacture protocol. Briefly, 100-250 of cell lysate transferred to 1.5 ml microfuge tube and then placed in the tube holder. Sonication cycle conditions were 30 sec On/90sec off for 6 min. During the sonication time, the temperature was maintaining at 4°C by using ice chilled water and small amounts of crushed ice (no more than 0.5 cm). The sonicated lysate was the centrifuged at 12.000 g for 15 min at 4°C (optional step). The supernatant was stored at -20 oC until further analysis.

2.7.2 The BicinChoninic Acid (BCA) assay for protein quantitation

2.7.2.1 Prepration of bovine serum albumin (BSA) standard curve

Two fold serial dilutions (0.125, 0.25, 0.5, 1, 2, 4, and 8) mg/ml were prepared from 20mg/ml BSA (Catalogue no. A7906 - Sigma-Aldrich) stock dissolved in PEB. A regular assay used a 20:1 reagent / sample volume ratio to detect the BSA concentration range aforementioned according V1.0 User Manual (NanoDrop 2000 Spectrophotometer/ Thermo Fisher Scientific). Briefly, 4 µl of each BSA dilution was mixed thoroughly with 80 µl BCA working reagent by vortexing (1 reagent B: 50 reagent A) (reagent A catalogue no.23228, reagent B catalogue no. 23224 - Thermo Fisher Scientific). The mixture was then incubated at 37°C for 30 minute and subsequently left for 5 minute at room temperature. The BSA standard curve was plotted and the samples were then measured using the NanoDrop 2000 Spectrophotometer according the manufacture instructions.

2.7.2.2 Protein sample preparation

In order to prepare reduced samples for denaturing gel electrophoresis, 40 µg of total protein from cells or clone derivatives were mixed together with 2.5 µl of (4x) NuPAGE LDS Sample Buffer (Catalog no. NP0008 - Life Technologies), 1 µl of (10x) NuPAGE Reducing Agent (Catalog no. NP0004 - Life Technologies), and ddH20 up to a total of 10 µl reaction volume. The mixture was denatured by incubation at 70 0C for 10 minutes.

2.7.2.3 Electrophoresis of NuPAGE® Gels

For the electrophoresing the total protein we have used the NuPAGE Novex Bis-Tris-Acetate (SDS-PAGE) Mini gels (Catalogue no. NP0321PK2 - Novex). Two gels were placed in the electrophoresis tank of XCell SureLock™ Mini-Cell (Catalogue no. EI0001 - Invitrogen). The upper chamber was filled with 200 ml of 1x NuPAGE Tris-Acetate SDS running buffer (Catalogue no. LA0041 - Invitrogen) mixed with 500 µl of NuPAGE Antioxidant (Catalogue no. NP0005 - Invitrogen), while the lower chamber was filled with 600 ml of 1x NuPAGE Tris-Acetate SDS running buffer. After denaturation the samples were loaded on the gels together with SeeBlue® Plus2 Pre-Stained Standard (Catalogue no. LC5925 - Invitrogen). The gels were run at 200 V (110-125) mA/ gel for 35 minute.

2.7.2.4 iBlot Western Detection

For blotting of the electrophoresed proteins we have used the iBlot Dry Blotting System (Catalogue no. IB1001 - Invitrogen). The pre-run gels were released from cassette plates. The 1st gel was rinsed in ddH20 water (3x 5min), stained with the Simple Blue SafeStain (Catalogue no. LC6060 - Invitrogen), destained in water (3x 5 min or more) and pictures were captured using the UVP VisionWorks LS instrument. The 2nd gel was used for blotting where placed onto the PVDF blotting surface of Anode iBlot Gel Transfer Stack (Catalogue no. IB8010-01 - Novex) and covered with pre-soaked (in deionised water) iBlot filter paper.

The Cathode iBlot Gel Transfer Stack was then placed on the top of the filter paper and then toped over with side facing up and aligned to the right edge. The air bubbles removed using blotting roller. A disposable sponge with the metal contact was placed on the upper right corner of the lid. The lid was securely closed and the iBlot Dry Blotting System was switched on at program P3 for 7min.

Subsequently, iBlot Gel Transfer Stacks were dissembled and the PVDF blotting membrane was then blocked in 5ml 1x iBind™ Buffer supplemented with 1x iBind™ additive for 5 minute at room temperature. The iBind Western System (Life Technologies) was employed for application of binding primary and secondary antibodies (at dilution 1:1000) and washing steps. Mouse and rabbit monoclonal primary antibodies to Aurora A (Catalogue no. ab13824 - Abcam), Aurora B (Catalogue no. 3094 - Cell Signaling Technology), total Histone H3 (phospho S10) (Catalogue no. ab14955 - Abcam), α-Tubulin (2144- Cell Signaling Technology) and β-actin (Catalogue no. ab8226 - Abcam) were used, while IRDye 800CW Goat Anti-Mouse IgG (Catalogue no. 925-32210 - LI-COR Biosciences) and DyLight 800 conjugate anti-rabbit IgG (Catalogue no. 5151 - Cell Signaling Technology) antibodies served as secondary. The immune complexes were detected using Odyssey® CLx Infrared Imaging System (Odyssey®- LI-COR Biosciences).

2.8 Data interpretation and Statistical analysis

mRNA levels were expressed as Relative Quantification (RQ) which were calculated as: $RQ=2^{-(\Delta\Delta Ct)}$. Ct values were determined by StepOne software V1.2 (life technologies) and normalized by the corresponding Ct for the endogenous control ACTB, generating ΔCt values (ΔCt = Ct target - Ct ACTB). Sample ΔCt values were further normalised against an immortalised bronchial epithelium cell-line HBEC-3KT (250) calibrator using the formula: ΔΔCt = (ΔCt Sample (Tumour/Normal) - ΔCt HBEC-3KT). RQ was calculated for each target by

the aforementioned formula (RQ=2-(ΔΔCt)). Gene expression in tumour and adjacent normal tissues were compared using Wilcoxon's non-parametric test for paired samples. Overexpression for a tumour sample was designated based on the 95% reference range of normal tissues (mean + 2x SD). The study characteristics were examined using descriptive statistics. Categorical variables were compared using chi-squared test and continuous variables were examined using Mann-Whitney test because of non-normality. Overall survival time was calculated from the date of surgery to the date of death or last follow-up date. Postoperative univariate survival analysis was explored using Kaplan-Meier curves for all the categorical predictors. Tests of equality across strata were also conducted to check the suitability of including potential predictors in the final multivariate model. For the categorical variables, log-rank test of equality across strata was used and univariate Cox proportional hazard regression was used to analyse continuous variables to examine the differences in survival rate. Variables with P value < 0.25 in the univariate analysis were selected for inclusion in the final multivariate model as suggested by Bursac et al. (251). Multivariate Cox proportional hazard model was utilised to examine the association between mRNA expression and other relevant prognostic factors. All statistical analyses were performed using IBM® SPSS® statistical software version 22.0 (Armonk, NY: IBM Corp) and STATA® version 13.1 (StataCorp LP, College Station, Texas). The IC50 values were calculated using Prism 5 (GraphPad) in comparison to untreated cells at time 0.

Chapter 3: AURKA involvement in docetaxel resistance in non-small cell lung cancer

The objectives of this set of experiments were (a) to determine the extent of AURKA expression deregulation in primary human lung tumours and cell lines and (b) to investigate possible associations between AURKA expression and sensitivity to taxane therapy.

The mRNA expression of *AURKA* in 132 cases of NSCLC and 44 normal tissues was determined (Appendix 2). RNA quality analysis using the Agilent Bioanalyzer revealed that almost all RNA samples have RIN values ≥ 7. Out of 176 RNA samples, 158 samples ≥7 and 5≤18 samples<7, which were within the accepted range for qPCR analysis (252) (Figure 3.1). Expression profiling of AURKA mRNA showed a marked overexpression of the gene transcript in lung tumours in comparison to the adjacent normal tissues (Mann-Whitney, test, p=<0001) (Figure 3.2).

The elevated *AURKA* mRNA expression in a panel of nine NSCLC cell lines from different histopathological subtypes was confirmed. The cell lines were distributed among lung adenocarcinoma, squamous carcinoma of the lung and large cell lung carcinoma (Figure 3.3: A &B). *AURKA* mRNA expression was markedly greater than that of non-tumorigenic immortalised bronchial epithelial cells (HBEC-3KT) although the expression was variable in lung cancer cell lines. It was also of note that p53 knockout HBECs (HBEC-3KT-p53 and HBEC-3K-TRp53) demonstrated higher *AURKA* expression (p values = 0.05). LUDLU1 cell line

exhibited the highest mRNA expression of *AURKA*, while Calu-3 showed the lowest expressesion. Kaplan-Meier analysis demonstrates that *AURKA* mRNA expression is a predictor of overall survival (p-value = 0.0079) (Figure 3.4). The p values were derived from Log Rank (Mantel-Cox) test.

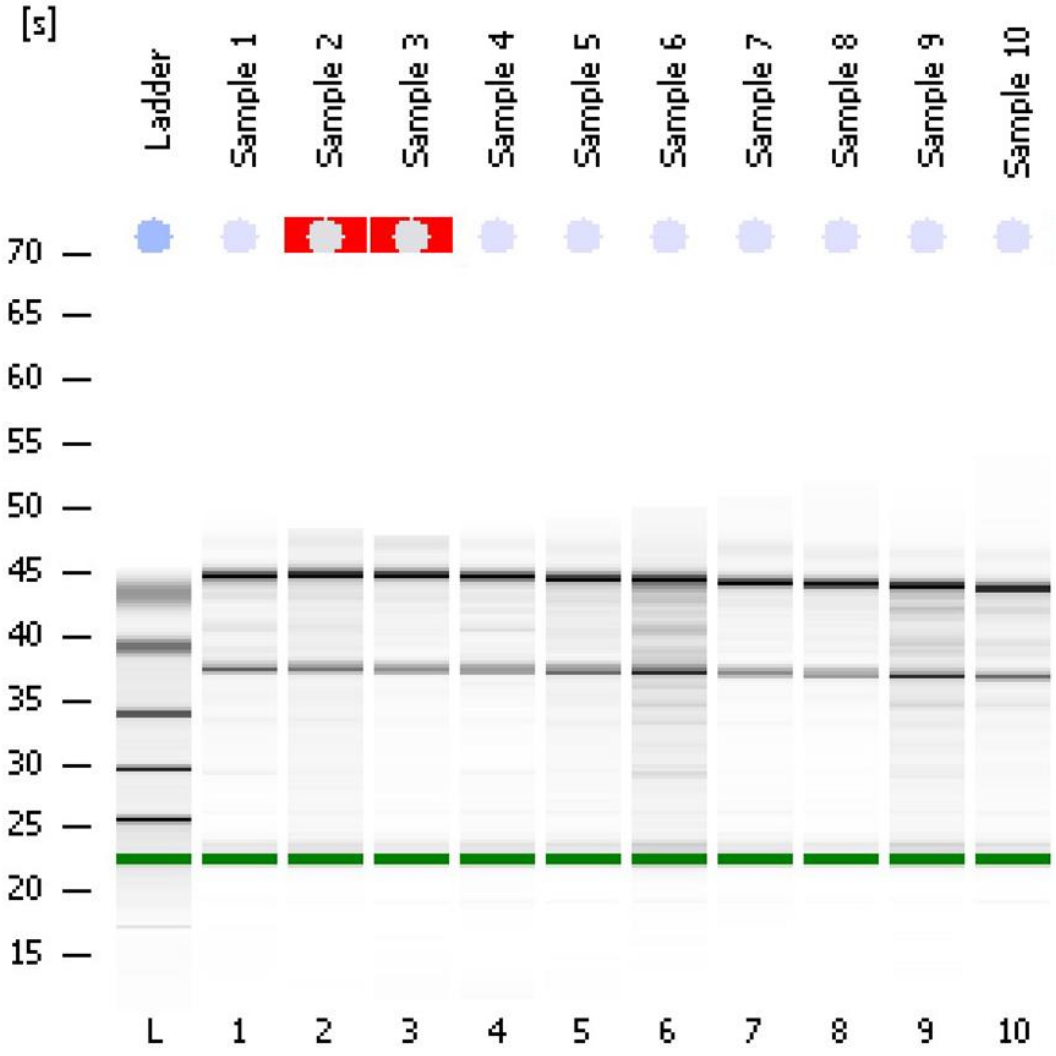

Figure 3.1 Example electropherogram of total RNA by Agilent Bioanalyzer chip shows that the peaks18S and 28S are clearly visible at time 37 and 45 seconds, respectively. The analysed cancer lung cells and tissue RNA set was constructed only for samples with adequate RNA concentration and RIN number 7.7 and above. [s] on y axis represents integration start time.

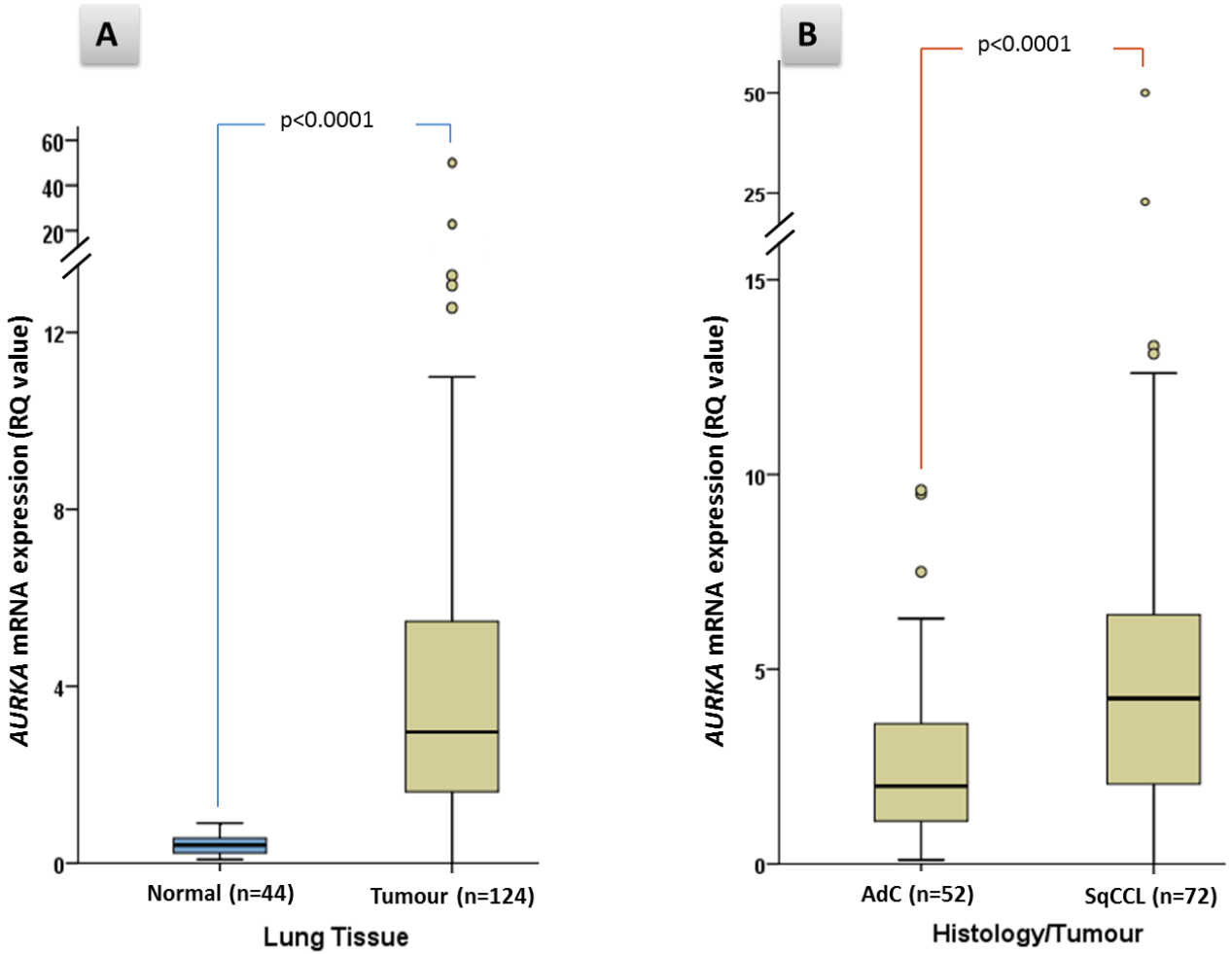

Figure 3.2: (A) Boxplots demonstrating the significantly higher mRNA expression of *AURKA* in primary lung tumours (n= 124) compared to adjacent normal lung tissues (n=44). (B) mRNA expression of *AURKA* is significantly higher in squamous cell carcinomas (SqCC) (n= 72) compared to adenocarcinomas (AdC) (n= 52). P values are derived from Mann-Whitney tests. RQ was calculated using HBEC-3KT cell line RNA as a calibrator.

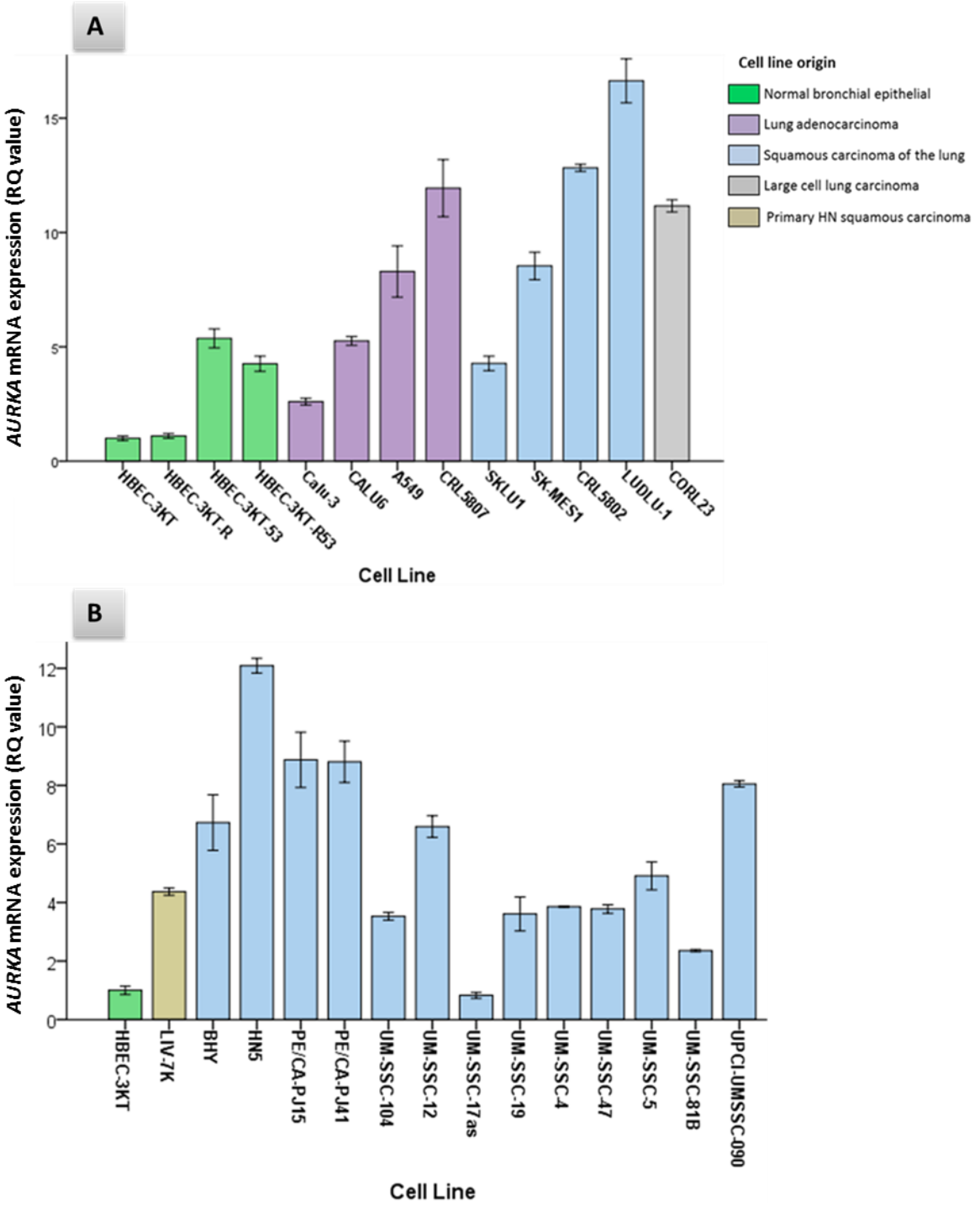

Figure 3.3: (A) *AURKA* mRNA expression in human bronchial epithelial cells (HBEC) and NSCLC cell lines. Cancer cell lines demonstrate variable *AURKA* expression, however, consistently higher than the non-tumorigenic bronchial epithelial cells (HBEC-3KT). It is also of note that p53 knock down derivatives of HBEC-3KT overexpress *AURKA*. Bars represent mean values for four independent repeats and error bars represent standard error of the mean. (B) mRNA expression of *AURKA* in HNSCC cell lines. The expression was variable among the HNSCC cell lines. Bars represent mean values for four independent repeats and error bars represent standard error of the mean. Human bronchial epithelial cell line (HBEC-3KT) was used as a technical calibrator.

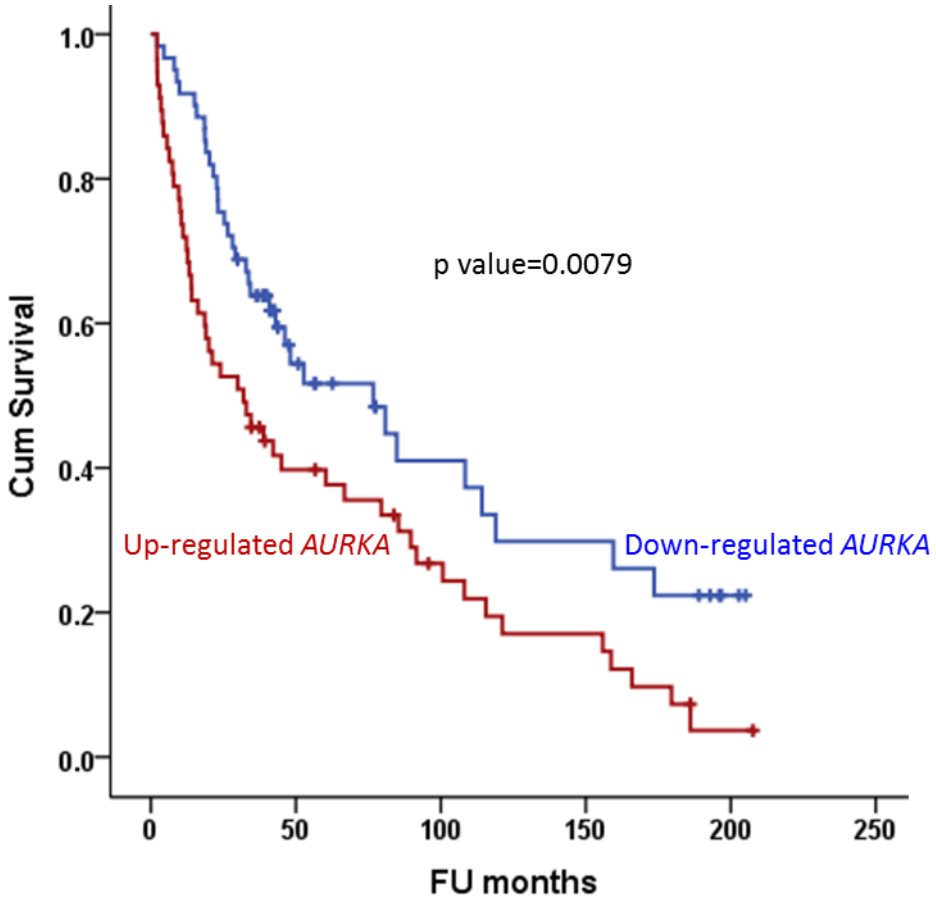

Figure 3.4: Kaplan-Meier analysis of overall survival (OS) of NSCLC cancer patients dichotomised by median *AURKA* mRNA expression. The p values were derived from Log Rank (Mantel-Cox) test. It is evident that high *AURKA* expression is associated with low survival.

Overall survival (OS) analysis of patients in this cohort demonstrates that high expression of *AURKA* mRNA is associated with reduced survival, while worse prognosis was linked with cases whose tumours expressed *AURKA* transcripts at greatest levels (Table 3.1). When NSCLC histological subtypes were analysed separately, association of elevated *AURKA* transcripts with poor prognosis remains significant for both adenocarcinomas (p value = 0.025) and squamous carcinomas (p value = 0.029) (Table 3.1), (Figure 3.5). The data demonstrate that one-year prognostic outcome of 125 cases whom cancerous tissue expresses low levels of *AURKA* transcripts was 75% as opposed to 54% for those with high AURKA-mRNA expression based on median. Five-year survival for low expression of *AURKA* mRNA was 52% as opposed to 36% for high expression based on median. Similarly, ten-year survival was 30% of low expression and 17% of high expression.

When taxane response was examined in NSCLC cell lines and HBEC derivatives, a similar trend was observed for paclitaxel with few differences. In general, all cancer cell lines except SKLU1 exhibited more response to docetaxel compared with paclitaxel (Figures 3.6.1-7). Investigation of the half maximal inhibitory concentration (IC50) after treatment with (1-35 nM) of docetaxel and paclitaxel demonstrated that IC50 values in the cancer cell lines ranged from the more sensitive to docetaxel and paclitaxel which are CRL5807 and CALU6 cell lines respectively, whereas SKLU1 cell line was the most resistant to both taxanes (Table 3.2). Among HBEC isogenic derivatives, KRAS mutants showed higher sensitivity to both taxanes. KRAS wild types were almost twice as resistant as the KRAS mutants to the cytotoxic effect of both taxanes. Docetaxel IC50 values were around 4 nM to KRAS wild types as opposed to about 2 nM to the mutant. Similarly, paclitaxel IC50 values were approximately 10-11 nM for wild type as opposed to 3-5 nM for mutant cells.

Table 3.1: Overall survival analysis in lung cancer patients in relation to AURKA mRNA expression. (a) High *AURKA* expression: >median, Low *AURKA* expression: ≤median. (b) Estimation is limited to the largest survival time if it is censored.

Means and Medians for Survival Time in Months									
		Mean[b]				**Median**			
				95% Confidence Interval				95% Confidence Interval	
Histology	***AURKA* expression**	**Estimate**	**Std. Error**	**Lower Bound**	**Upper Bound**	**Estimate**	**Std. Error**	**Lower Bound**	**Upper Bound**
NSCLC (both histologies) P value= 0.0079	Low[a]	91.7	11.3	69.7	113.8	76.7	20.8	35.8	117.5
	High	61.3	8.6	44.5	78.1	32.0	11.0	10.4	53.6
Adenocarcinoma P value= 0.025	Low	81.3	13.1	55.7	107.0	52.8	19.8	14.0	91.6
	High	40.6	10.5	20.1	61.1	24.0	7.8	8.8	39.2
SqCCL P value= 0.029	Low	107.4	18.6	70.9	143.9	114.1	50.1	15.9	212.4
	High	66.6	10.4	46.3	86.9	38.8	15.6	8.3	69.4

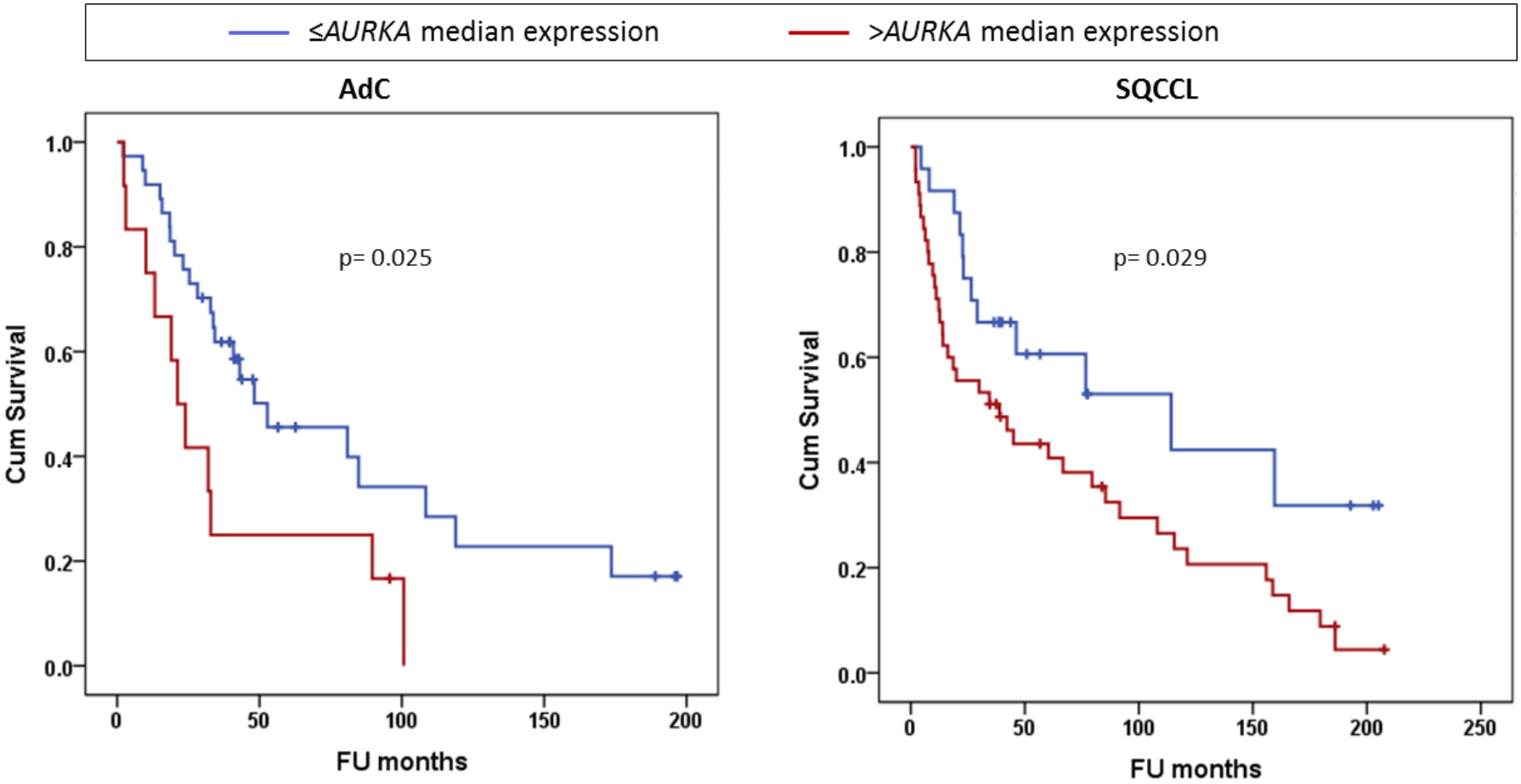

Figure 3.5: Kaplan-Meier analysis of overall survival (OS) of lung cancer patients dichotomised by median *AURKA* mRNA expression. The correlation between *AURKA* expression and OS is significant in both adenocarcinomas (AdC) and squamous cell carcinomas (SqCCL).

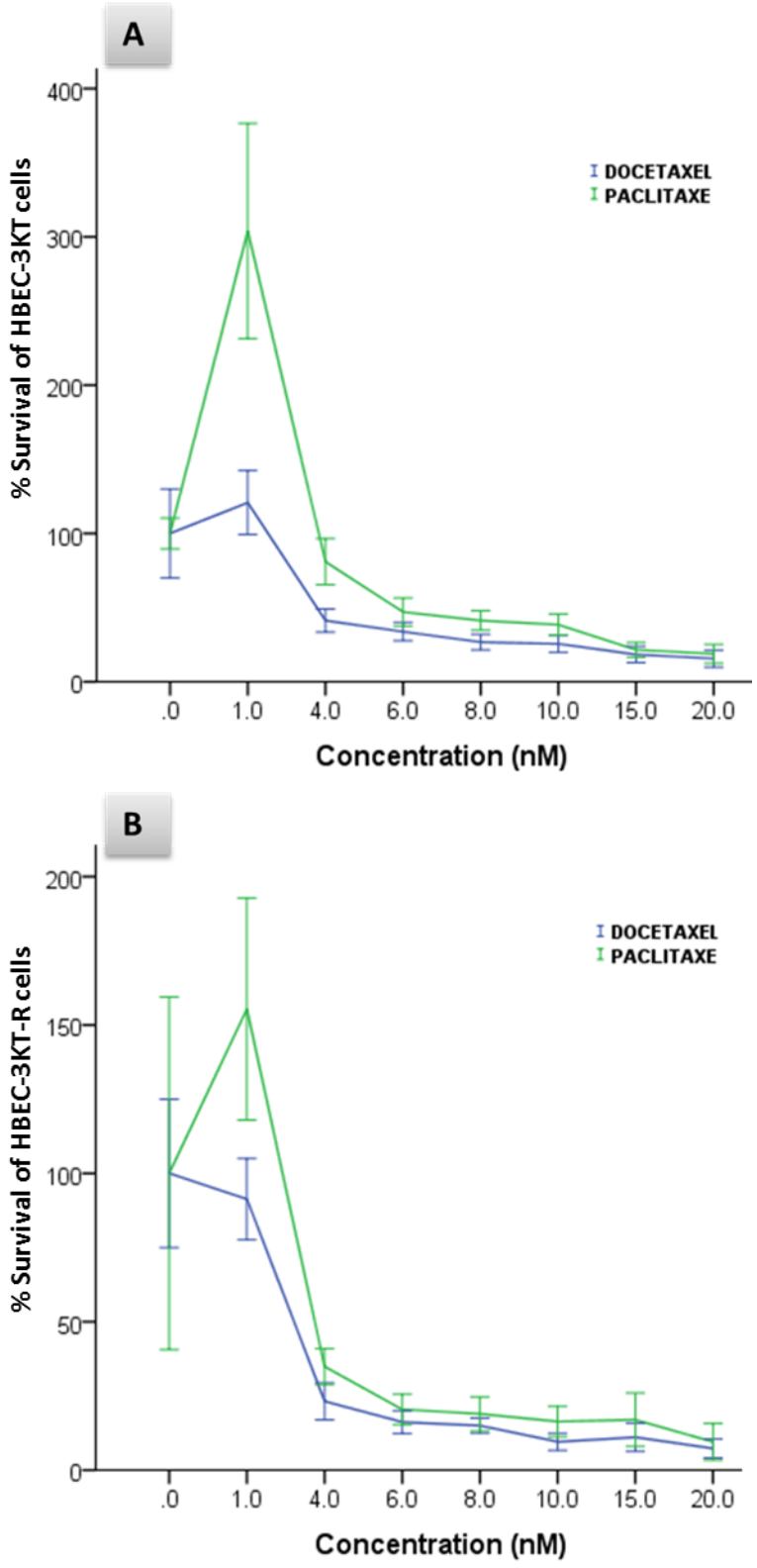

Figure 3.6.1: Taxane response of HBEC isogenic derivative cells, HBEC-3KT (wild type parental) (A) and HBEC-3KT-R (K-ras mutant) (B). Both isogenic derivatives had a similar trend in their response to both taxanes, as both of them are more sensitive to docetaxel than paclitaxel. The mean and error values are for six technical replicates and that one of two independent experiments is shown. Error bars in both line graphs represent 95% confidence intervals.

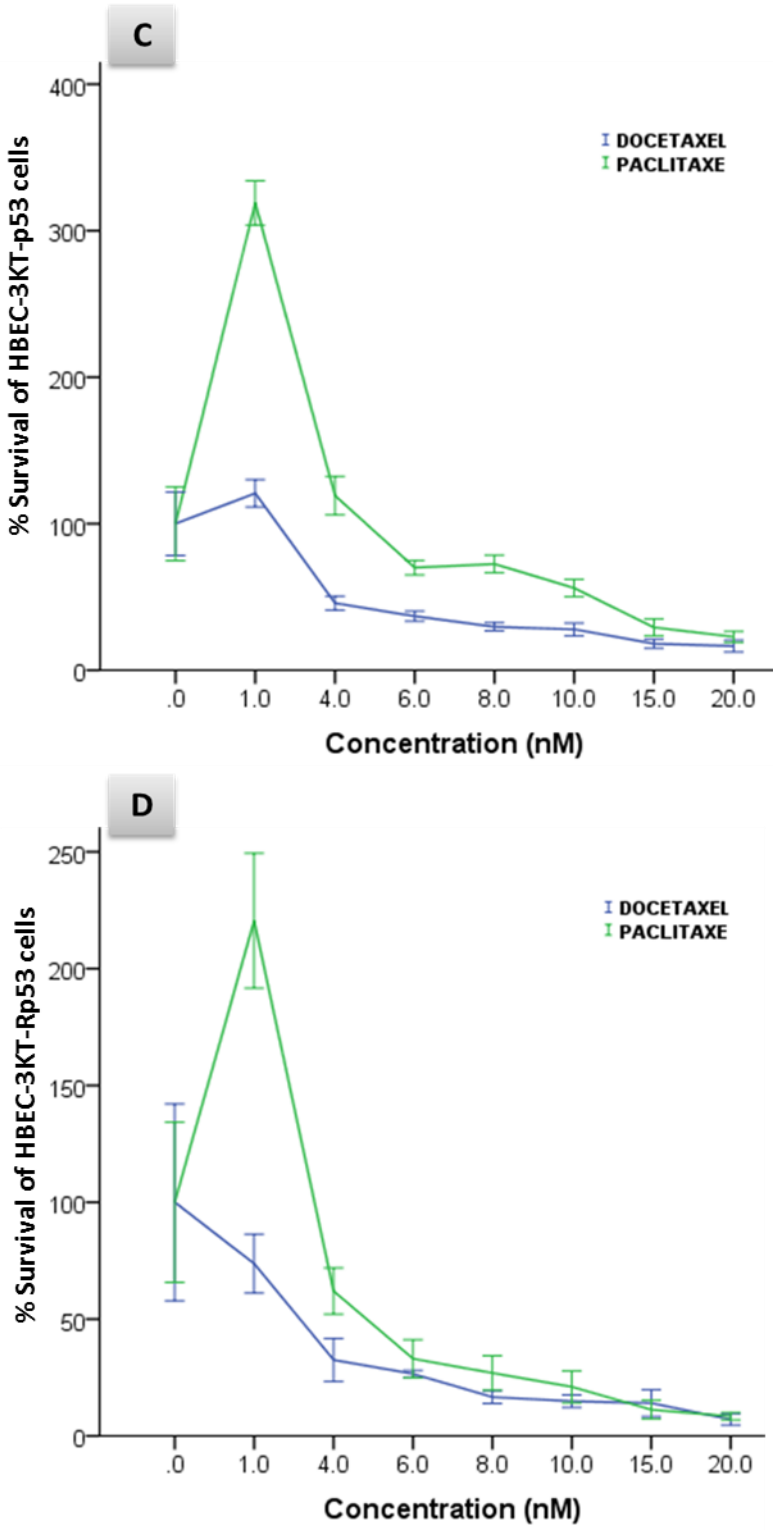

Figure 3.6.2: Taxane response of HBEC isogenic derivative cells, HBEC-3KT-53 (p53 knock out) (C) and HBEC-3KT-R53 with both aberrations (p53 knockout and K-ras mutant) (D). Both isogenic derivatives had a similar trend in their response to both taxanes, as both of them were more sensitive to docetaxel than paclitaxel. The mean and error values are for six technical replicates and that one of two independent experiments is shown. Error bars in both line graphs represent 95% confidence intervals.

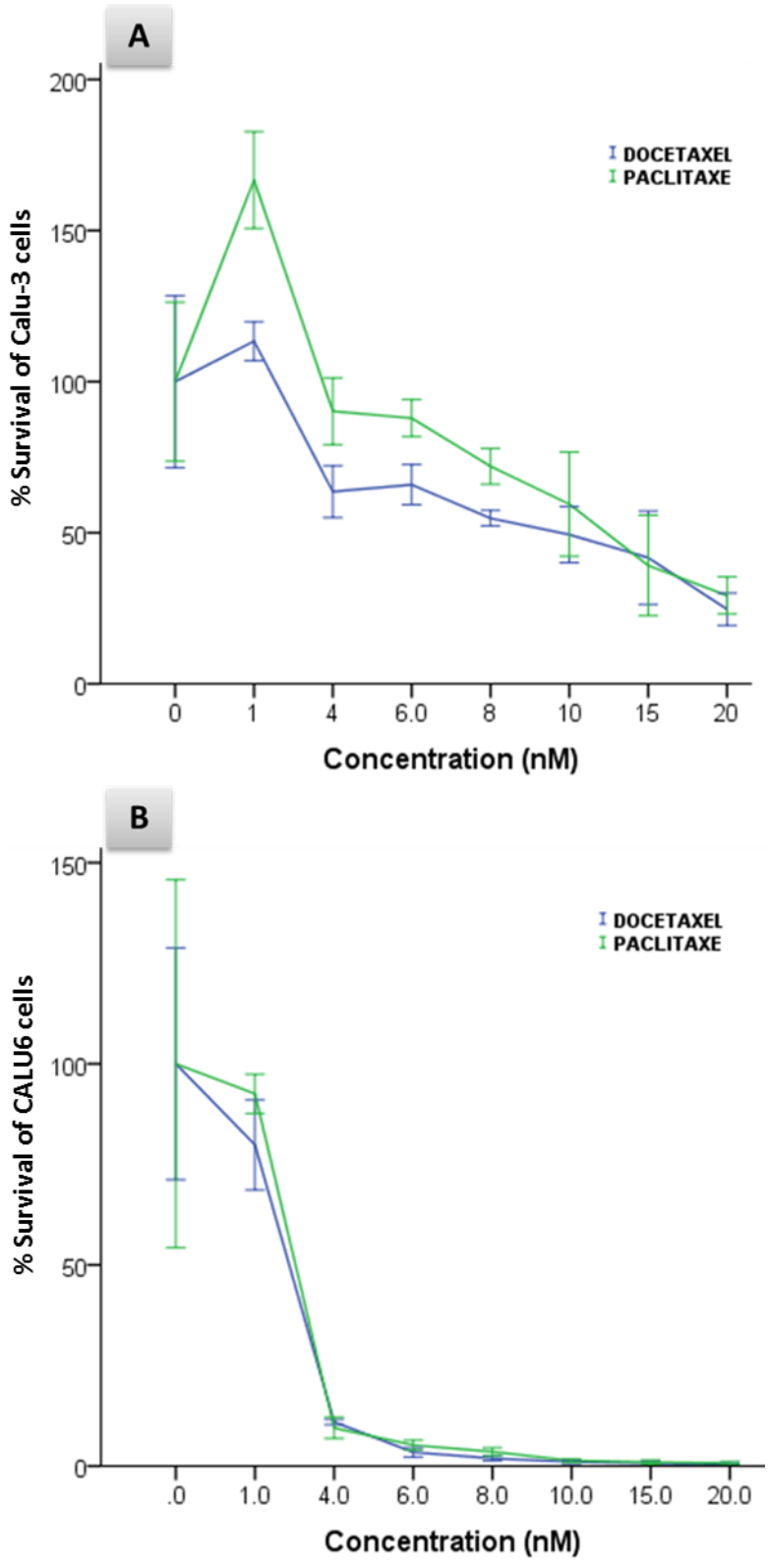

Figure 3.6.3: Taxane response of lung cancer cell lines Calu-3 (A) and CALU6 (B). Calu-3 cells showed more sensitivity to docetaxel than paclitaxel, while CALU6 responded similarly to both taxanes. The mean and error values are for six technical replicates and that one of two independent experiments is shown. Error bars in both line graphs represent 95% confidence intervals.

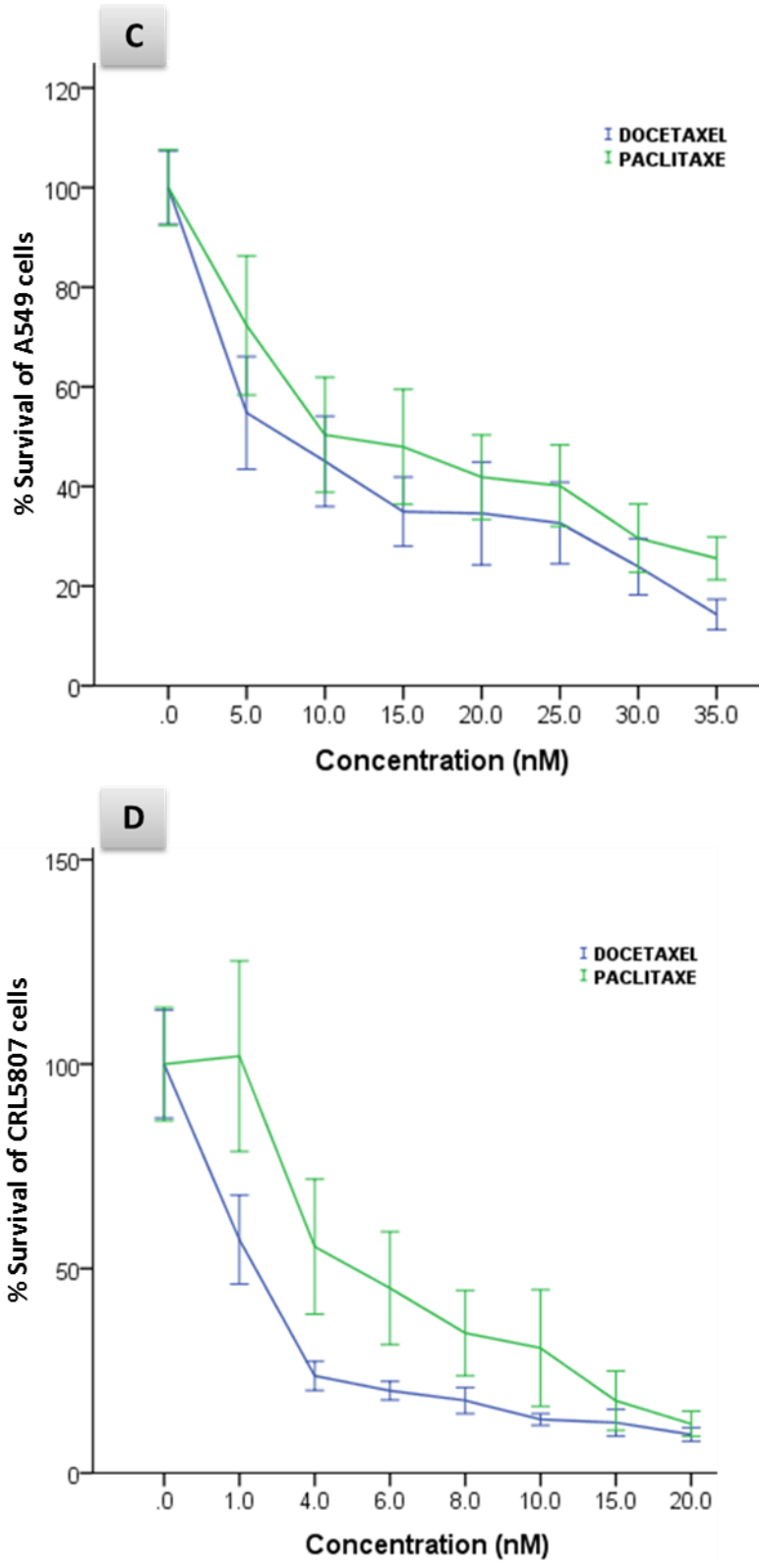

Figure 3.6.4: Taxane response of lung cancer cell lines (C) A549 and (D) CRL5807. Both cell lines demonstrated more sensitivity to docetaxel than paclitaxel. The mean and error values are for six technical replicates and that one of two independent experiments is shown. Error bars in both line graphs represent 95% confidence intervals.

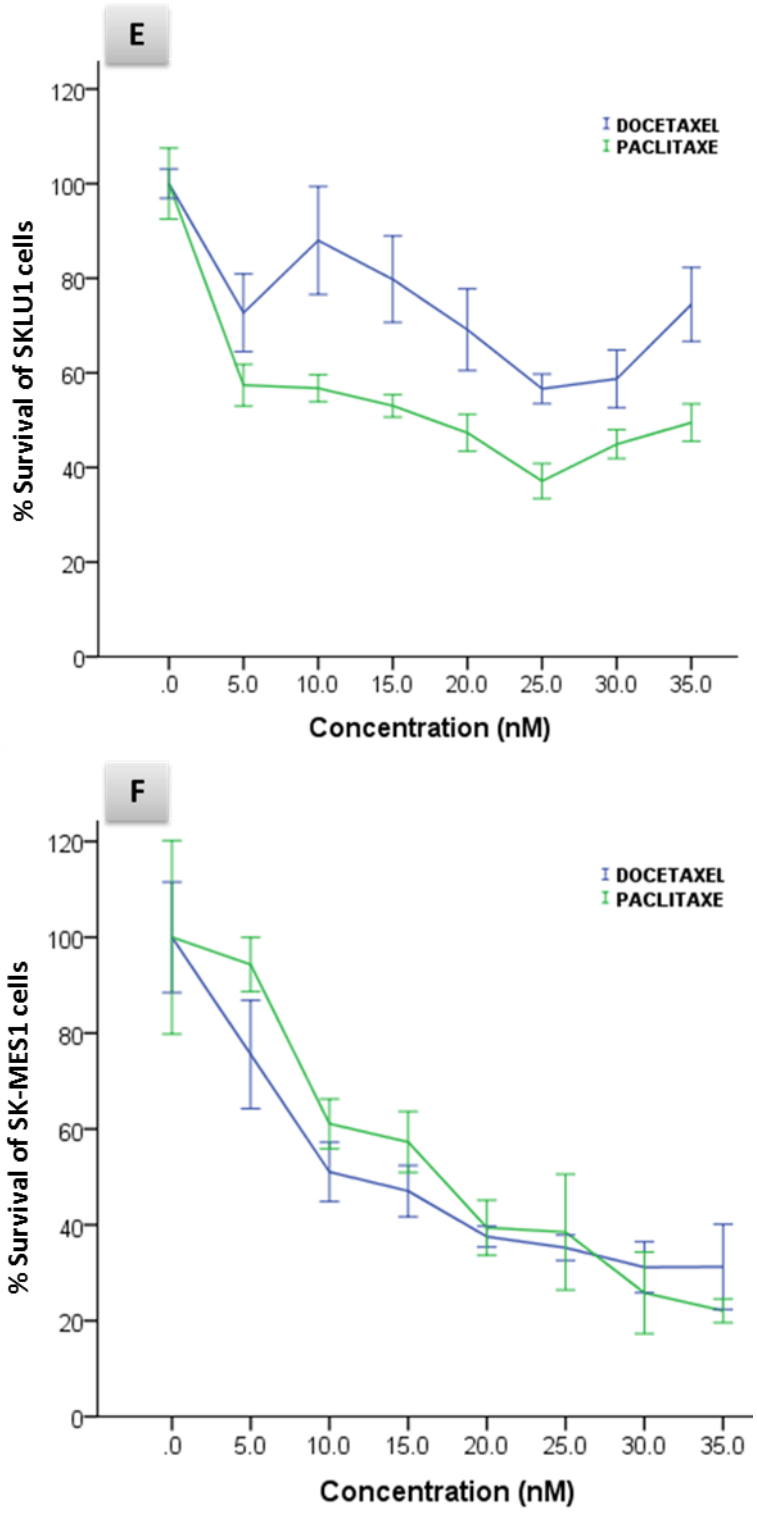

Figure 3.6.5: Taxane response of lung cancer cell lines (E) SKLU1 and (F) SKMES1. SKLU1 exhibited more resistance to docetaxel than paclitaxel, while SKMES1 response to both taxane showed a trend of superior cytotoxicity of docetaxel, with more sensitivity to paclitaxel at doses above 30nM. Both cell lines demonstrated more sensitivity to docetaxel than paclitaxel. The mean and error values are for six technical replicates and that one of two independent experiments is shown. Error bars in both line graphs represent 95% confidence intervals.

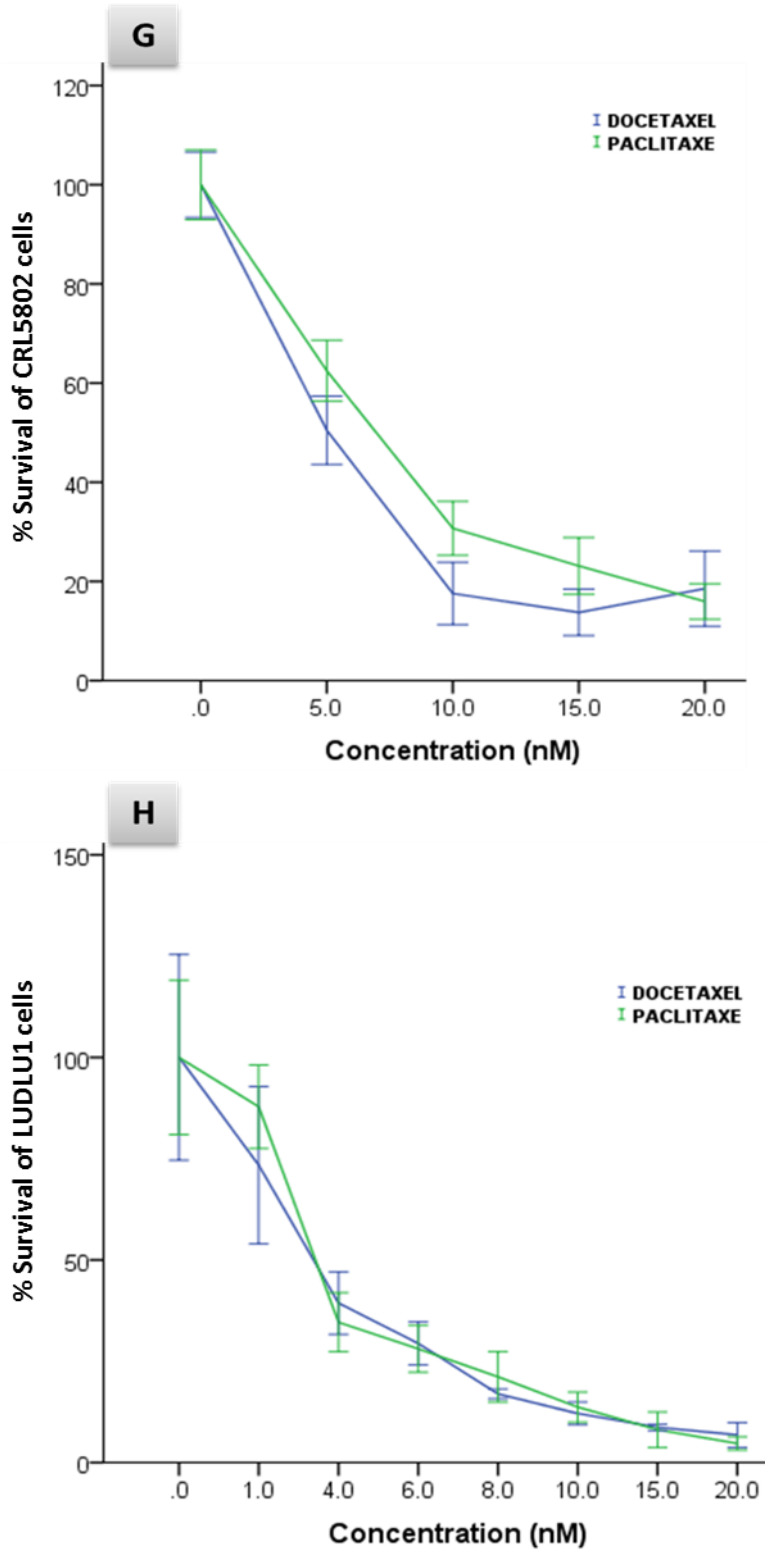

Figure 3.6.6: Taxane response of lung cancer cell lines (G) CRL5082 and (H) LUDLU1. CRL5082 showed more sensitivity to docetaxel than paclitaxel, while LUDLU1 responded similarly to both taxanes. The mean and error values are for six technical replicates and that one of two independent experiments is shown. Error bars in both line graphs represent 95% confidence intervals.

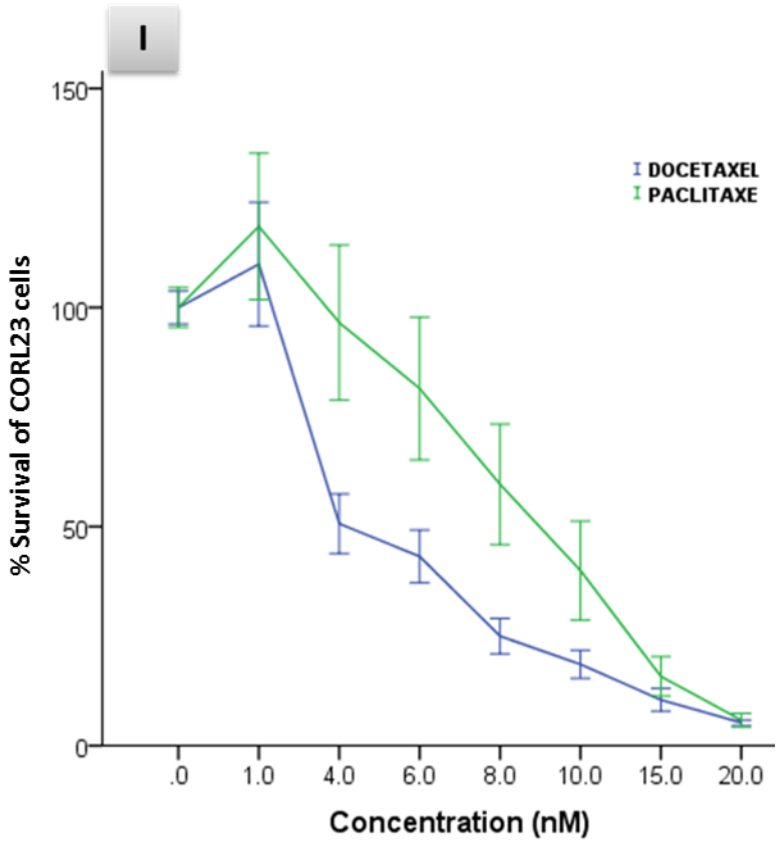

Figure 3.6.7(I): Taxane response of lung cancer cell line CORL23, which showed more sensitivity to docetaxel than paclitaxel. The mean and error values are for six technical replicates and that one of two independent experiments is shown. Error bars in both line graphs represent 95% confidence intervals.

Table 3.2: IC50 values and their respective confidence intervals (95%) in the normal and cancer cell lines after treatment with (1-35 nM) of docetaxel and paclitaxel. A range of sensitivities to both drugs were observed for NSCLC cancer cell lines. In non-tumourigenic cell lines, there was a significant difference to docetaxel response between *KRAS* mutants and *KRAS* wild type cells.

Cell line	IC50-Docetaxel	95% CI	IC50-Paclitaxel	95% CI
A549	**7.3**	*6.0 - 8.9*	**13.6**	12.1 - 15.3
CALU3	**9.0**	*7.3 - 11.2*	**12.8**	8.2 - 20.0
CALU6	**1.7**	*1.7 - 1.8*	**2.1**	2.0 - 2.3
CORL23	**4.7**	*4.1 - 5.4*	**9.0**	8.2 - 9.9
CRL5802	**4.0**	*3.0 - 5.5*	**7.6**	6.0 - 9.6
CRL5807	**1.3**	*1.1 - 1.6*	**5.3**	4.7 - 6.0
LUDLU1	**2.7**	*2.3- 3.1*	**3.0**	2.8 - 3.3
SKLU1	**26.5**	*17.4 - 40.2*	**16.7**	12.8 – 22.0
SK-MES	**9.0**	*7.4 – 11.0*	**15.6**	12.6 - 19.5
HBEC-3KT	**4.3**	*3.0 - 6.2*	**10.4**	*4.1 - 26.2*
HBEC-3KT-53	**4.6**	*3.3 - 6.5*	**11.5**	*3.0 - 43.3*
HBEC-3KT-R	**2.6**	*2.1 - 3.2*	**3.7**	*2.0 - 7.0*
HBEC-3KT-R53	**2.4**	*2.1 – 3.0*	**5.2**	*2.5 - 10.6*

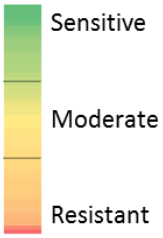

In order to examine whether the cellular response to taxanes is related to growth rate of the studied NSCLC cell lines, cell growth curves were performed and exhibited variability in the growth rate of NSCLC cell lines (Figure 3.7). The data of the growth curves then were employed to calculate the growth doubling time for each cell line with their respective 95% confidence intervals (95%CI). The data demonstrated that the growth doubling time ranged the NSCLC cells from the slowest growing cell line (SKLU1) to the fastest growing one (CALU6) (Table 3.3). When I compared the growth rate values with taxane response in these cell lines using Spearman's rho analysis, the results showed that there was a significant correlation between growth doubling time and cellular response to docetaxel (Spearman's test, rho= 0.71, p value = 0.032). Nevertheless, the growth doubling time was not significantly correlated with the response to paclitaxel.

To investigate the effect of AURKA on the taxane response of NSCLC cell lines, *AURKA* mRNA expression was knocked down in three cancer cell lines (LUDLUE1, SKLU1 and SKMES1). Two shRNAs (TRCN0000000656 and TRCN0000000657) effective at knocking down *AURKA* mRNA expression were identified from five different shRNA constructs by RT-qPCR analysis, with knockdown of *AURKA* transcript at different levels. LUDLU1 cell line was first selected based on the level of *AURKA* mRNA expression, which represents the highest overexpressing *AURKA* cell line, to knock down the expression of this gene. The knock down efficiency was about 50% (Figure 3.8.A). The knock down derivative clone (Aur-KD-LUD) was then exposed to docetaxel and paclitaxel along with parental cells. The exposure data demonstrate that *AURKA* down regulation leads to sensitisation of LUDLU1 to docetaxel and, to a lesser degree, to paclitaxel (Figure 3.8.B). This was the first interesting finding achieved from very beginning pilot transfection experiment.

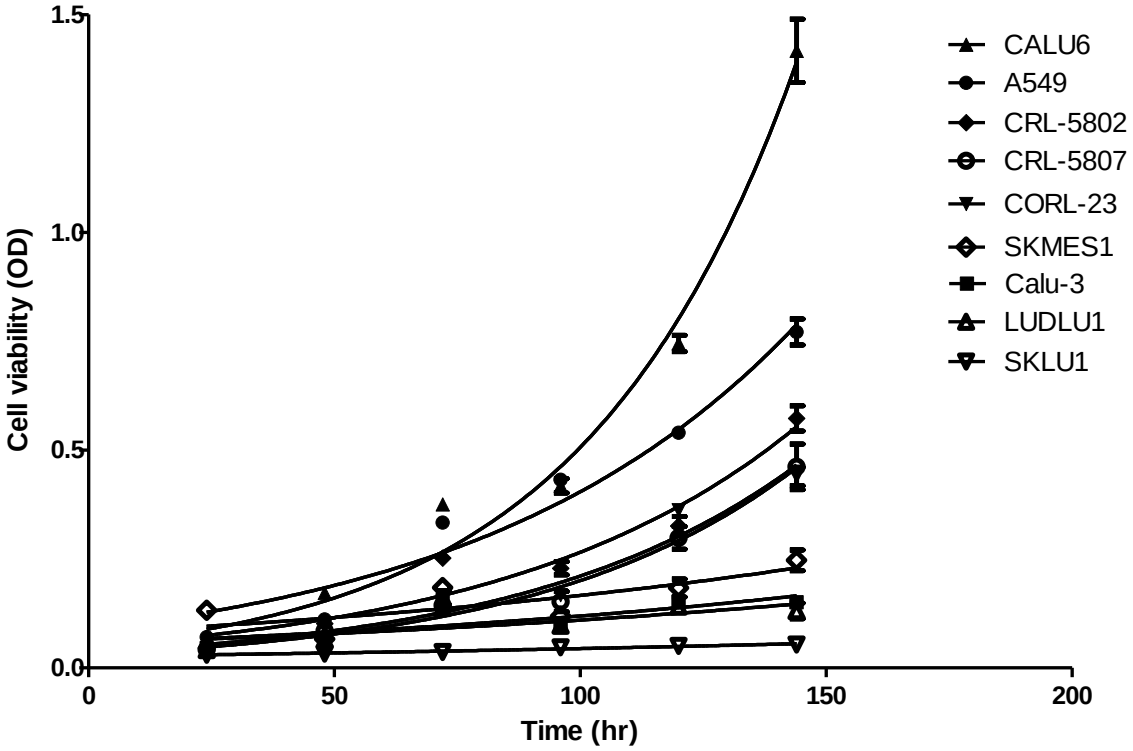

Figure 3.7: Exponential line graphs demonstrating the growth curve for cells grown in DMEM culture medium. The growth analysis covered six days.

Table 3.3: Doubling time values in (hr) and their respective confidence intervals (95%) in the normal and NSCLC cell lines calculated based on growth rate analysis shown in figure 3.7.

Cell Line	Doubling Time(hr)	Doubling Time(hr) at 95%CI
CALU6	30.20	27.59 to 33.36
CRL-5807	36.77	30.77 to 45.69
CORL-23	38.54	33.99 to 44.49
CRL-5802	41.53	36.37 to 48.39
A549	45.73	41.44 to 51.03
Calu-3	92.85	69.69 to 139.1
SKMES1	95.12	68.57 to 155.2
LUDLU1	104.70	73.52 to 182.1
SKLU1	136.40	96.12 to 234.9

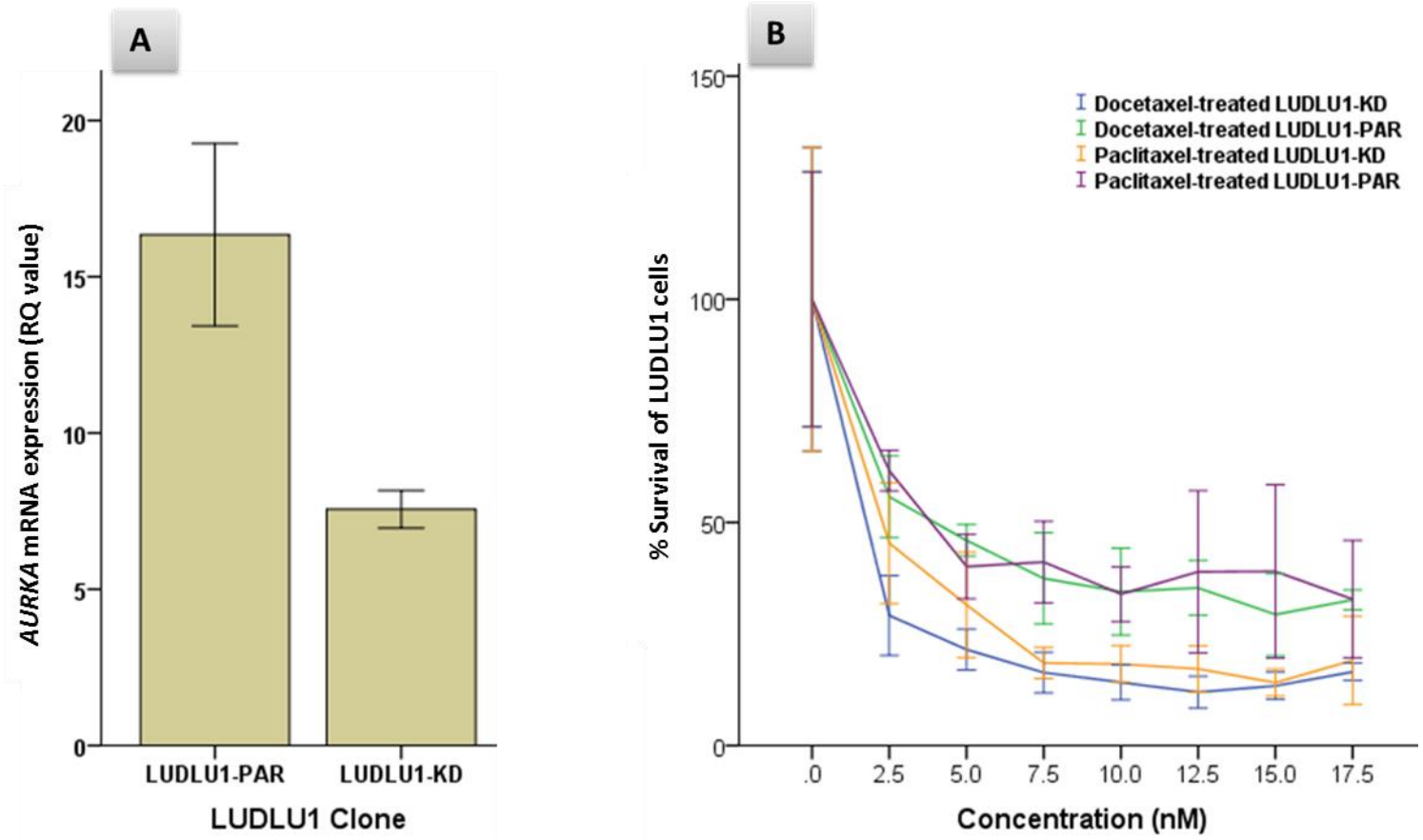

Figure 3.8: *AURKA* mRNA expression of LUDLU1 cell line and its derivative knock down clone (A) in relation to their response to both taxanes (B). Error bars in both the expression bar chart and line graph represent 95% confidence intervals. –PAR: parental, KD: knockdown clone.

Although this cell line was the highest overexpressed *AURKA* among all of the tested cell lines, it was the most sensitive to both taxanes compared with other NSCLC cell lines. I, however, took this issue in consideration and next selected the most resistant cell line (SKLU1) in addition to the second most resistant cell line (SKMES1). One of my objectives for this transfection experiment was to decrease the doses of the antimitotic drugs that would reduce the toxic therapeutic effects. The same dose range of taxanes used with LUDLU1 was, therefore, applied on SKLU1 and SKMES1 cell lines for this investigation. The knock down efficiency of *AURKA* transcript expression in SKLU1 cells was approximately (40-75) %. This result was confirmed by RT-qPCR (Figure 3.9.A). The MTT assay indicates that up to 17.5nM, docetaxel had lower effect on the proliferation of parental SKLU1 and its scrambled control. Interestingly, exposing *AURKA* knock down derivative clones to identical concentrations of docetaxel led to significant proliferative inhibition. Thus, it was possible to sensitise this cell line to docetaxel by reducing *AURKA* mRNA expression (Figure 3.9.B), while the inhibitory effect of exposing to paclitaxel was less significant (data not shown). Similarly, knocking down about (75-80) % of *AURKA* mRNA expression in SKMES1, confirmed by RT-qPCR analysis (Figure 5.10.A), resulted in marked inhibition in viability of knock down derivative clones in comparison of the parental and scrambled controls when exposed to identical concentrations of docetaxel (Figure 3.10.B). Paclitaxel exposure show only borderline significant difference between parental and knock down clones. Down regulation of Aurora kinase A in knock down derivative clones was also confirmed by western blotting analysis of the clones derived from SKLU1 (Figure 3.11 A) and SKMES1 (Figure 3.11.B).

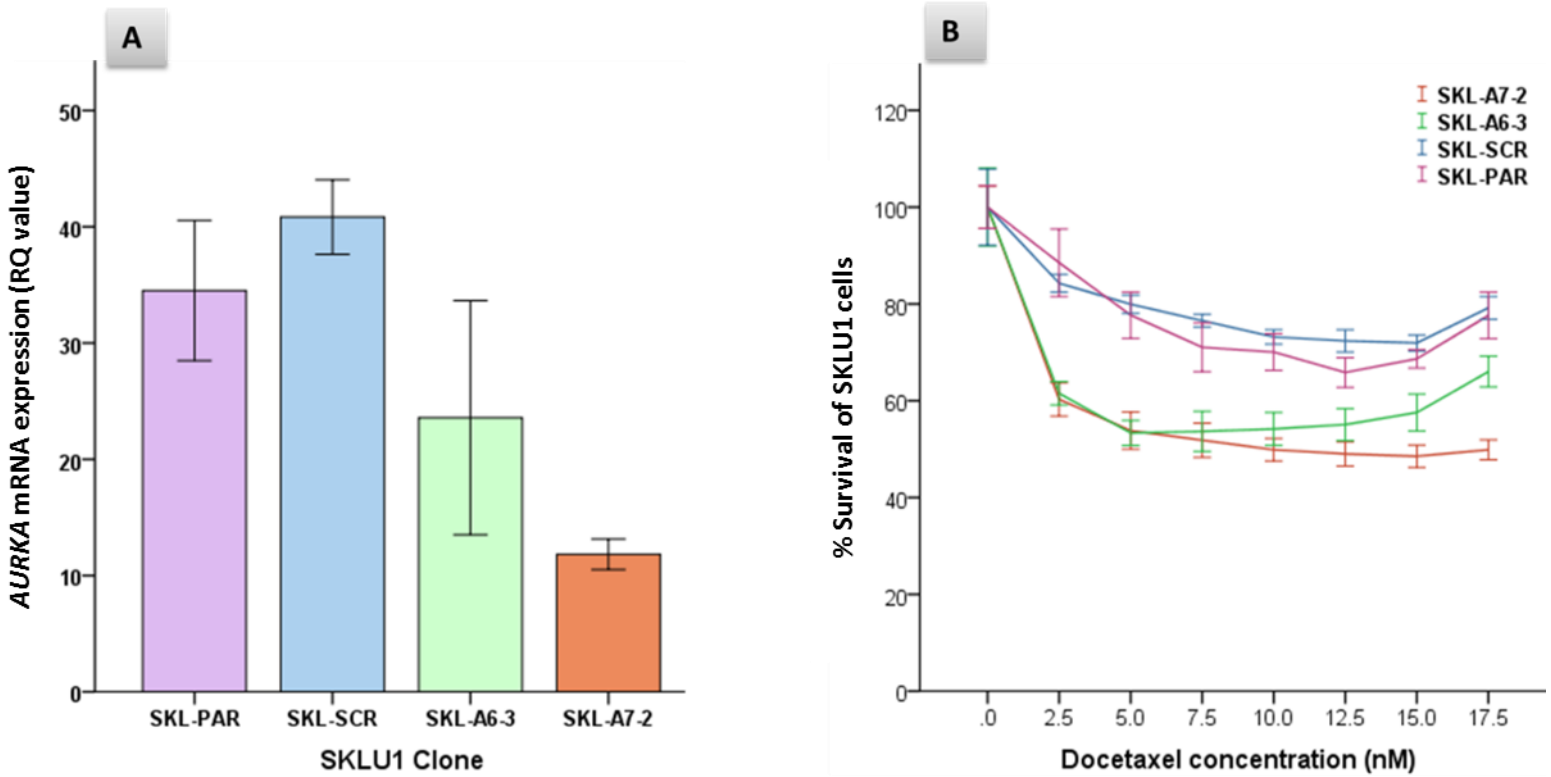

Figure 3.9: AURKA mRNA expression of SK-MES1 cell line and its derivative knock down clones (A) in relation to its response to Docetaxel (B). Error bars in both the expression bar chart and line graph represent 95% confidence intervals. PAR: parental, -SCR: scrambled, -Bx-y: knockdown clones where x is the shRNA construct and y is the clone number from this transfection.

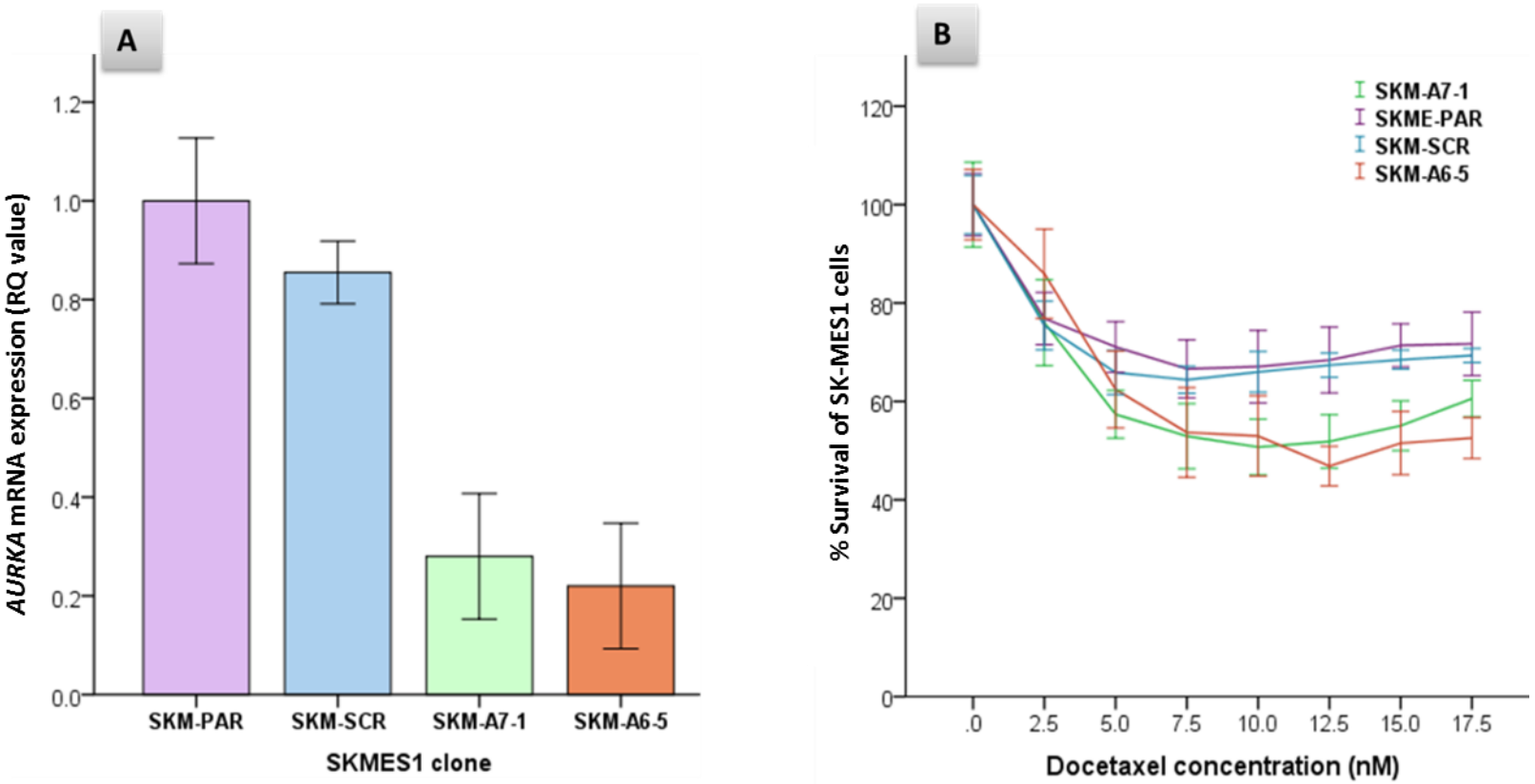

Figure 3.10: *AURKA* mRNA expression of SKLU1 cell line and its derivative knock down clones (A) in relation to its response to Docetaxel (B). Error bars in both the expression bar chart and line graph represent 95% confidence intervals. PAR: parental, -SCR: scrambled, -Bx-y: knockdown clones where x is the shRNA construct and y is the clone number from this transfection.

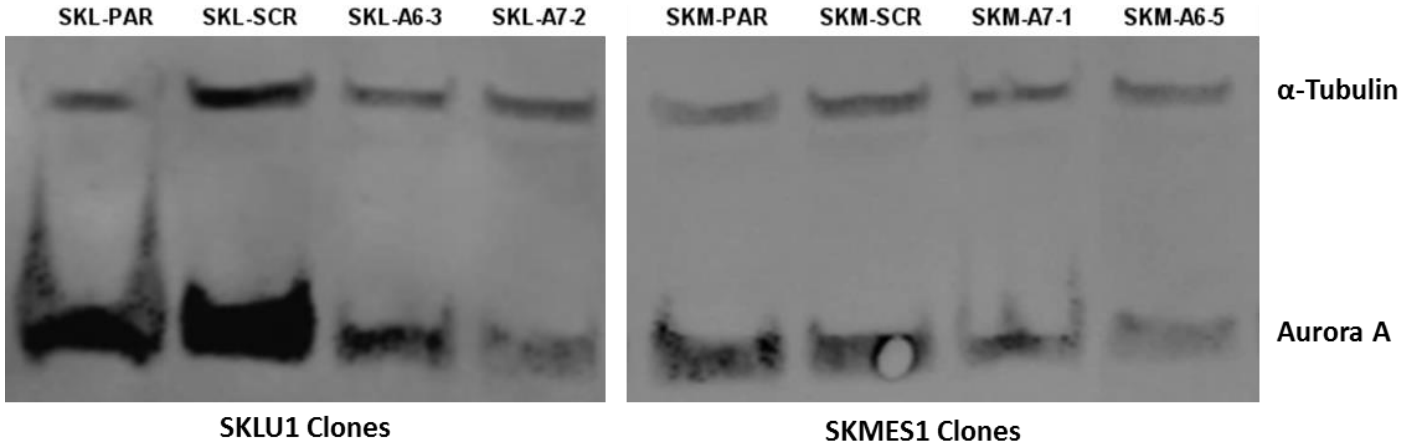

Figure 3.11: Western blot analysis of protein expression of Aurora kinase A and the internal control (α-tubulin) in parental and knockdown derivative clones for SK-MES1 and SKLU1. It is evident that scrambled construct clones (-SCR) have similar Aurora kinase A expression to that of parental (-PAR) cells while lower levels of expression are observed in the shRNA knockdown derivative clones (SKL-A6-3, SKL-A7-2, SKM-A7-1, SKM-A6-5).

In order to gain further evidence of Aurora kinase A down-regulation effect in sensitising NSCLC cells to docetaxel, The cellular response to Alisertib, which is a highly selective Aurora kinase A inhibitor, was first investigated in SKLU1 and SK-MES1 cell lines (Figure 3.12). Accordingly, the IC50 values of this kinase inhibitor were determined (6.3nM and 11.1nM for SKLU1 and SK-MES1 respectively). Expression of AURKA was then determined after treating SKLU1 and SK-MES1 cell lines with alisertib IC50 value of each and in different exposure time points. This kinase inhibitor had no significant effect on the expression level of mRNA transcripts in either cell line (Figure 3.13). After that, the cell lines were exposed to a range of docetaxel and paclitaxel concentrations (0-17.5) nM in combination with different concentrations of Alisertib (0, 5 and 10) nM. MTT analysis of taxane-alisertib treated cells illustrated that increased concentrations of Alisertib resulted in reduced resistance to docetaxel in both NSCLC cell lines but not paclitaxel (Figures 3.14). Although the line graph shows only a trend, the IC50 values docetaxel and their respective 95% CI of were significantly reduced in Alisertib dose-dependent manner in both cell lines (Table 3.4).

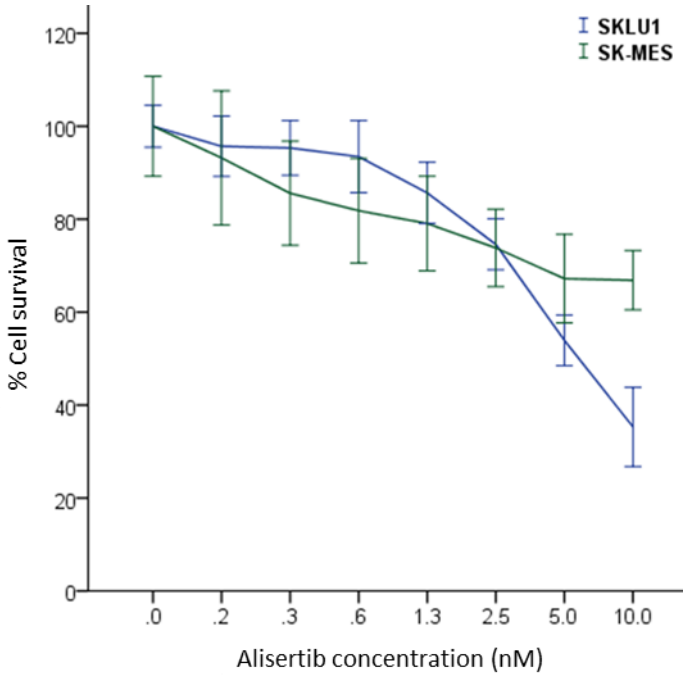

Figure 3.12: Alisertib response of SKLU1 and SKMES1 cell lines. The mean and error values are for six technical replicates and that one of two independent experiments is shown. Error bars in both line graphs represent 95% confidence intervals.

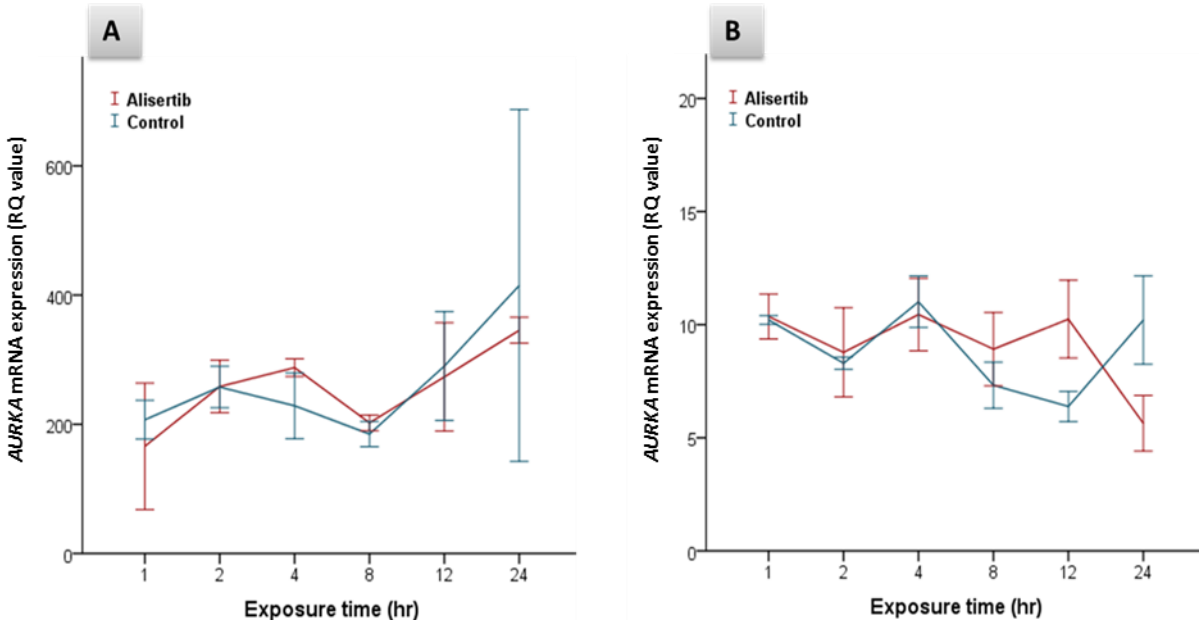

Figure 3.13: *AURKA* mRNA expression after alisertib exposure at IC50 concentrations in (A) SK-MES1 and (B) SKLU1 cell lines. No difference was shown in mRNA expression between alisertib-treated and non-treated cells. The mean and error values are for six technical replicates and that one of two independent experiments is shown. Error bars in both line graphs represent 95% confidence intervals.

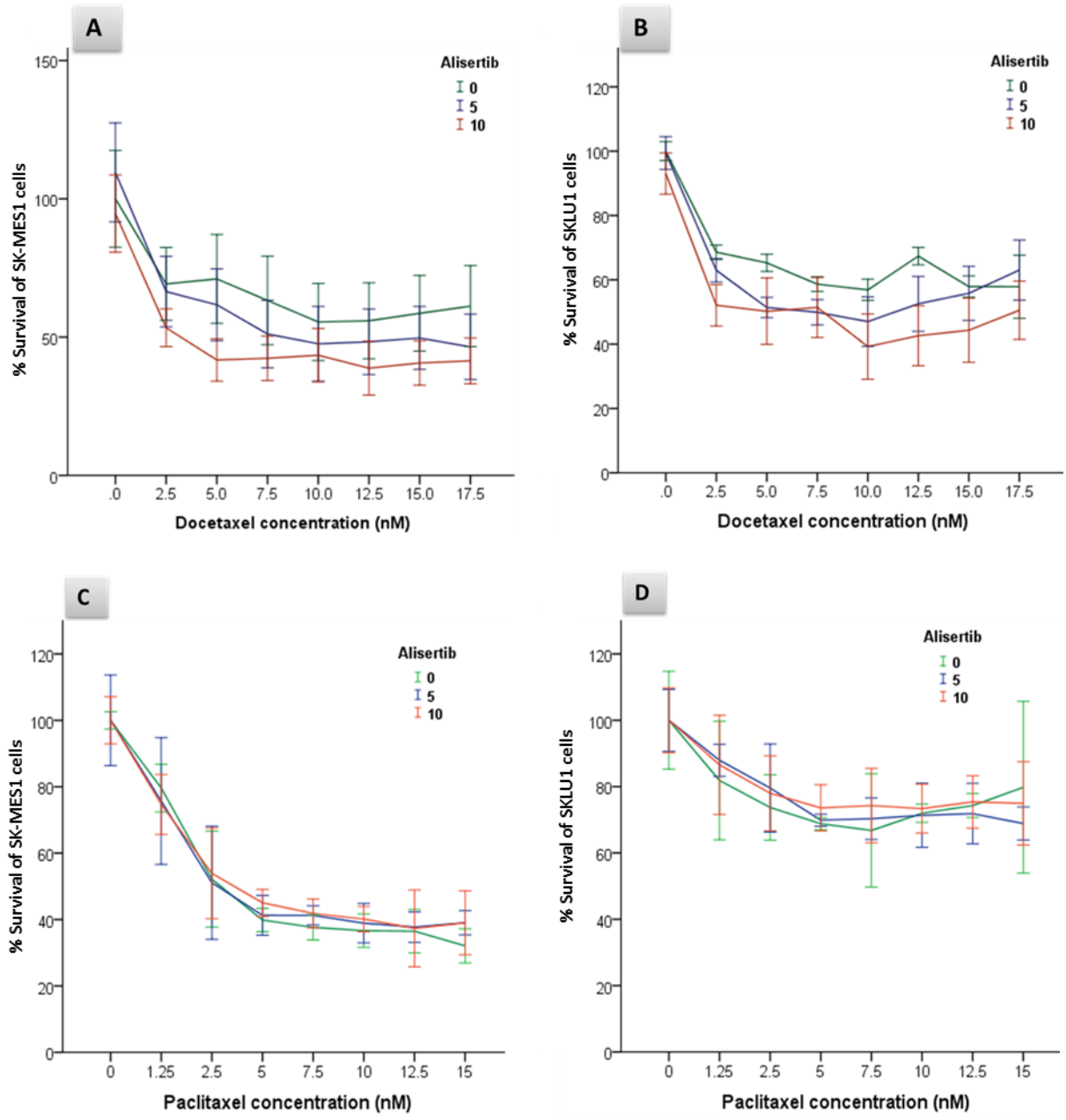

Figure 3.14: Sensitivity of lung cancer cell lines to docetaxel in the presence of the highly selective Aurora kinase A inhibitor (Alisertib). The mean and error values are for six technical replicates and that one of two independent experiments is shown. Error bars in both line graphs represent 95% confidence intervals.

Table 3.4: IC50 values and their respective confidence intervals (95%) in SKMES1 & SKLU1 after treatment with (0-17.5 nM) of docetaxel in presence of (0-10 nM) alisertib.

Cell line	Docetaxel	Alisertib (nM)	IC50	IC50 (95% CI)
	(-)	0	15.8	12.46 to 20.02
SKMES1	(+)	5	10.08	8.304 to 12.23
	(+)	10	6.206	5.249 to 7.338
	(-)	0	15.81	13.92 to 17.95
SKLU1	(+)	5	11.13	9.349 to 13.24
	(+)	10	7.691	6.400 to 9.243

In summary, *AURKA* mRNA expression in primary NSCLC tumours was up-regulated in lung cancer tissues in comparison to the normal adjacent lung tissue. No profile differences were observed in the primary NSCLCs among age, gender, stage or nodal involvement groups. High *AURKA* mRNA expression correlated with reduced survival in both adenocarcinomas and squamous cell carcinomas. The levels of *AURKA* transcripts were variable among NSCLC cell lines. However, they were higher than that in non-tumorigenic bronchial epithelial cell lines, HBEC-3KT. In HBEC isogenic derivatives, p53 knockout increases resistance to both drugs while KRAS mutation appears sensitize cells to treatment. In LUDLU1, SKLU1 and SK-MES1, *AURKA* knock down resulted in a drop of docetaxel IC50 values. Chemical kinase inhibition of AURKA using the selective Aurora A kinase inhibitor, alisertib, was found to augment the cytotoxic efficiency of docetaxel.

Chapter 4: Aurora B expression as a potential predictive biomarker for paclitaxel response in NSCLC

The objective of this set of experiments was to test the AURKB expression in modulating the effectiveness of paclitaxel in NSCLC cells. Supporting evidence for this part of the study was based on the fact that selective inhibition of Aurora B kinase activity using barasertib (the highly selective Aurora B kinase inhibitor) in cancerous cells results in mitotic arrest, endoreplication and polyploidy leading to cell apoptosis (253). This kinase inhibitory effect of treated cells by barasertib may a result of failed mitotic cell division and endoreplication leading to polyploidy due to blocking of Histone H3 phosphorylation on serine 10, the most important substrate of Aurora B (254). Furthermore, polyploidy cells formed by Aurora B inhibition seem to develop cellular resistance to paclitaxel in breast cancer cell lines (255).

mRNA expression profiling of *AURKB* in surgically resected human lung tissues from 132 cases demonstrated significant overexpression of the gene transcript in tumour tissue compared with adjacent normal tissue (Mann-Whitney test, $p<0.0001$) (Figure 4.1: A). This overexpression was more pronounced in SqCCL than AdCs (Mann-Whitney test, $p<0.0001$) (Figure 4.1: B). In addition, mRNA expression of *AURKB* was more elevated in higher pathological T stages (Figure 4.2), however this finding has to be treated with caution as the great majority of tumours in this sample set fall into the pT2 stage group (n=102), while the pT1 and pT3/4 groups comprised 19 and 12 patients respectively. Kaplan-Meier analysis demonstrated that *AURKB* up-regulation

did not incur a significant impact on overall survival (OS) in this clinical cohort, although a non-significant trend was demonstrated in adenocarcinoma patients (p value= 0.0787) (Figure 4.3). The findings show that one-year survival of lung adenocarcinoma patients whose tumours demonstrated decreased levels of *AURKB* mRNA was 79% as opposed to 47% for cases with elevated *AURKB* transcripts based on dichotomy at the median.

Five-year prognostic outcome for low level of *AURKA* mRNA expression was 46% as opposed to 27% for those with high *AURKA* mRNA expression. Ten-year survival showed the worse prognosis, as tumours with low expression level of *AURKA* mRNA represent only 18% of cumulative proportion survival, while no patients were survive after this end of interval. No associations were found between *AURKB* mRNA expression and age, gender, clinical stage or nodal status.

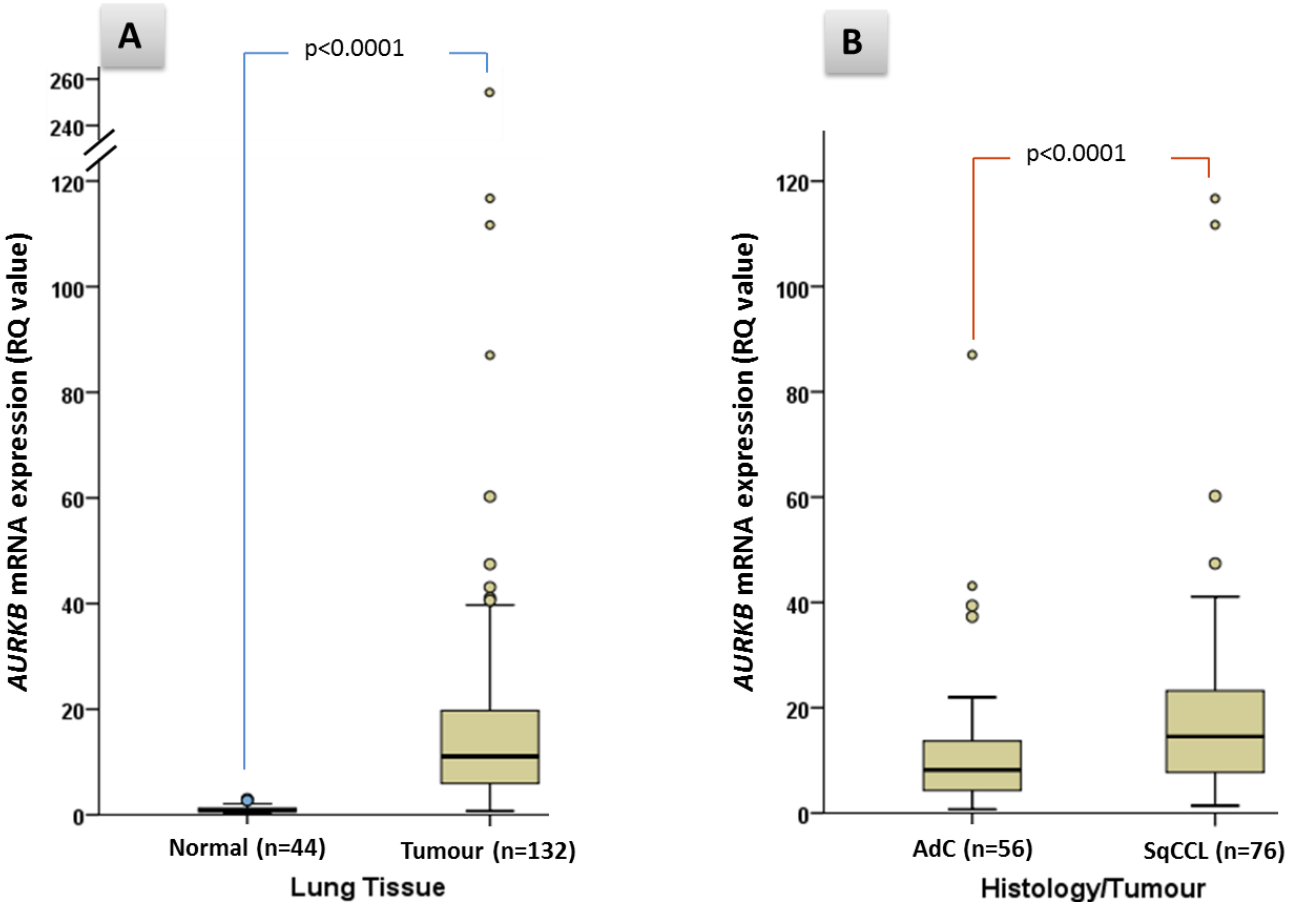

Figure 4.1: Boxplots demonstrating *AURKB* mRNA expression in primary lung tumours compared to adjacent normal lung tissues (right) and in squamous cell carcinomas (SqCC) compared to adenocarcinomas (AdC) (left). *P* values are derived from Mann-Whitney tests. RQ was calculated using HBEC3KT cell line RNA as a calibrator.

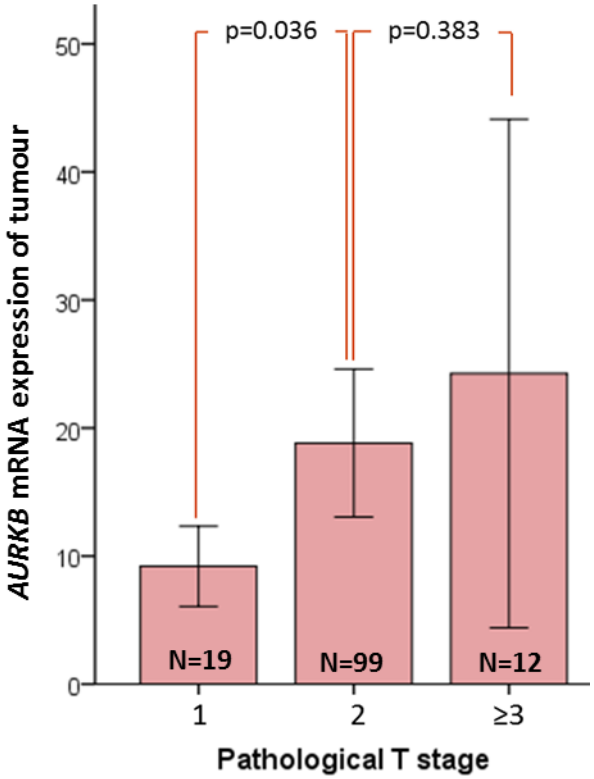

Figure 4.2: *AURKB* mRNA expression in comparison with pathological T stages of lung cancer specimens.

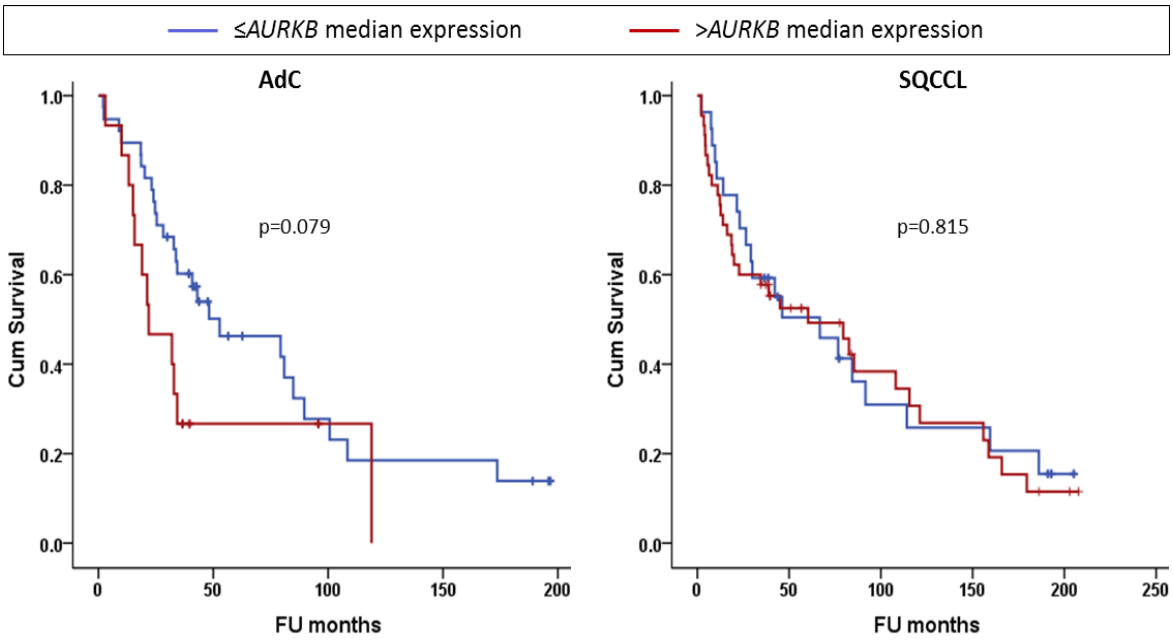

Figure 4.3: Kaplan-Meier analysis of overall survival (OS) of lung cancer patients dichotomised by median *AURKB* mRNA expression. AdC: adenocarcinoma; SqCC: squamous cell carcinoma of the lung.

AURKB mRNA expression profiling was also investigated in the panel of 9 lung cancer cell lines, along with the immortalized normal human bronchial epithelial cells (HBEC-3KT and its isogenic *p53* knockout and *KRAS* mutant derivatives). *AURKB* expression was variable among the lung tumourigenic cell lines, however, markedly higher in comparison to that of non-tumourigenic HBECs (Figure 4.4: A). It is of note that among HBECs, *AURKB* mRNA expression was higher in the p53 knockout derivatives (HBEC3KTp53 and HBEC3KTRp53) while a borderline reduction was seen in *KRAS* mutant cells (HBEC3KTR). Aurora B mRNA expression was also investigated in a panel of 14 HNSCC cell lines (Figure 4.4: B). The expression was also variable among the tested cells. The IC50 values for paclitaxel and docetaxel toxicity among the available lung cell lines along with HBEC isogenic derivatives were determined following treatment with a range of concentrations (1 - 35 nM) of the two drugs as shown in chapter 3 (Figure 3.6.1-7) and (Table 3.2). As previously observed, IC50s for docetaxel were consistently lower than that of paclitaxel with one exception (SKLU1 cell line). Interestingly, mRNA expression of *AURKB* in NSCLC cell lines demonstrated an inverse correlation with resistance to both docetaxel (Spearman's test, rho=- 0.883, $p=1.6\times10^{-3}$) and paclitaxel (rho= -0.800, $p=9.6\times10^{-3}$) (Figure 4.5). However, there was no association between the levels of *AURKB* transcripts in HNSCC cell lines and IC50 values of both taxanes.

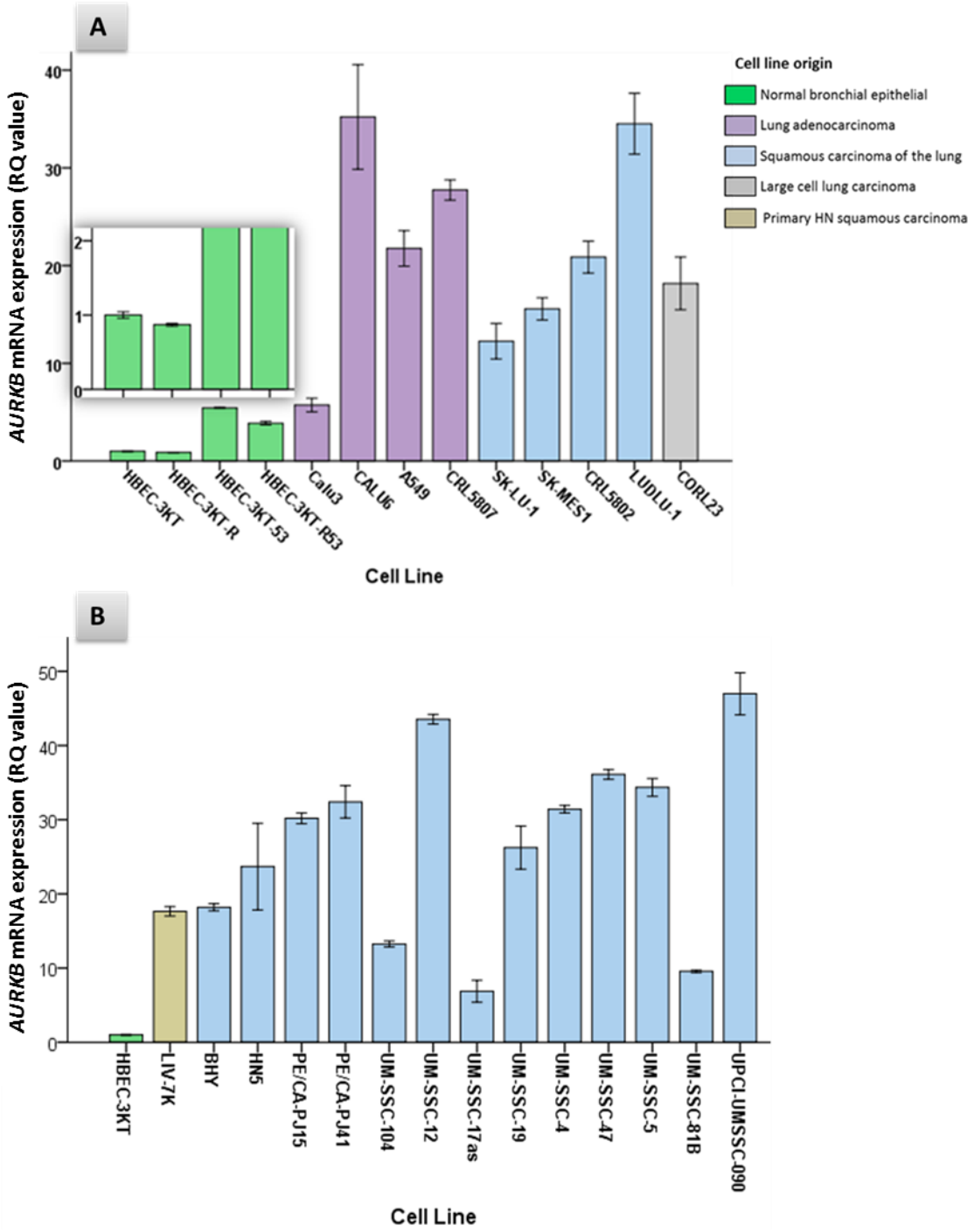

Figure 4.4: *AURKB* mRNA expression in lung cancer and human bronchial epithelial cells (HBEC) cell lines. (A), and HNSCC cell lines (B). In general, the expression was variable among the examined cell lines. In NSCLC cells, the expression was higher than that of HBEC-3KT cells. Among HBECs, the expression was higher in the p53 knockouts (HBEC-3KTp53 and HBEC-3KTRp53) while a borderline reduction was seen in KRAS mutants (HBEC3KTR). HBEC-3KT was used as a technical calibrator in HNSCC cells. Bars represent mean values for four independent repeats and error bars represent standard error of the mean.

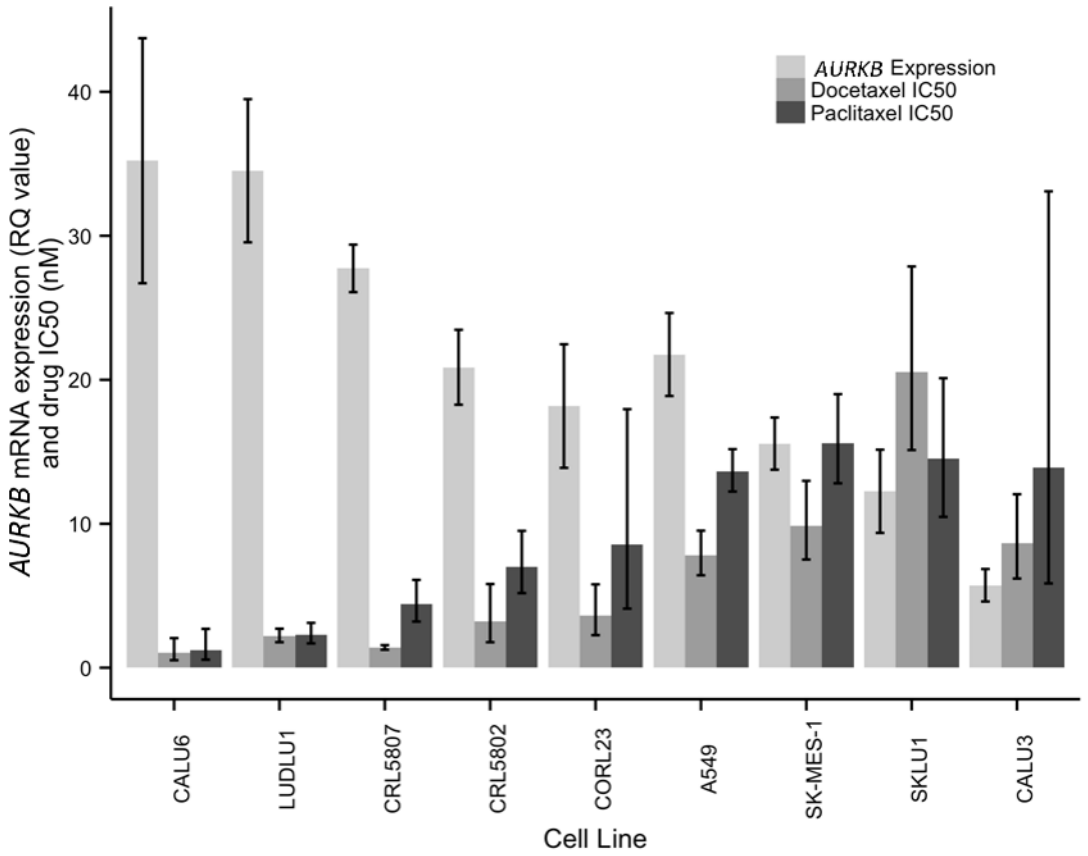

Figure 4.5: *AURKB* mRNA expression (RQ values) in NSCLC cell lines and sensitivity (IC50) to docetaxel and paclitaxel demonstrating an inverse correlation. The mean and error values are for six technical replicates and that one of two independent experiments is shown. Error bars represent 95% confidence intervals.

In order to further explore the possible modulation of taxane response by AURKB, The resistance of lung cancer cell lines to paclitaxel was investigated by (a) knocking down *AURKB* expression and (b) inhibiting its protein activity. Successful *AURKB* knock down clones were derived from A549 and SK-MES1 cells using five different shRNA constructs. Knockdown efficiency of *AURKB* mRNA expression was assessed by qPCR and Aurora kinase B down regulation was confirmed by western blotting (Figure 4.6: A and B). The clones, as expected, demonstrated variable knock down efficiency. This efficiency ranged from 14% to 47% for SKMES1 and from 9% to 44% for A549 cell line. When I exposed these clones to paclitaxel, it was apparent that response to paclitaxel inversely correlated to the level of *AURKB* mRNA expression in a dose-dependent manner. This was true for both clones derived from A549 and 4 clones derived from SK-MES1 ($p= 0.038$, $rho= 0.7$), while scrambled shRNA clones did not demonstrate altered response to paclitaxel when compared to the paternal cells (Figure 4.7).

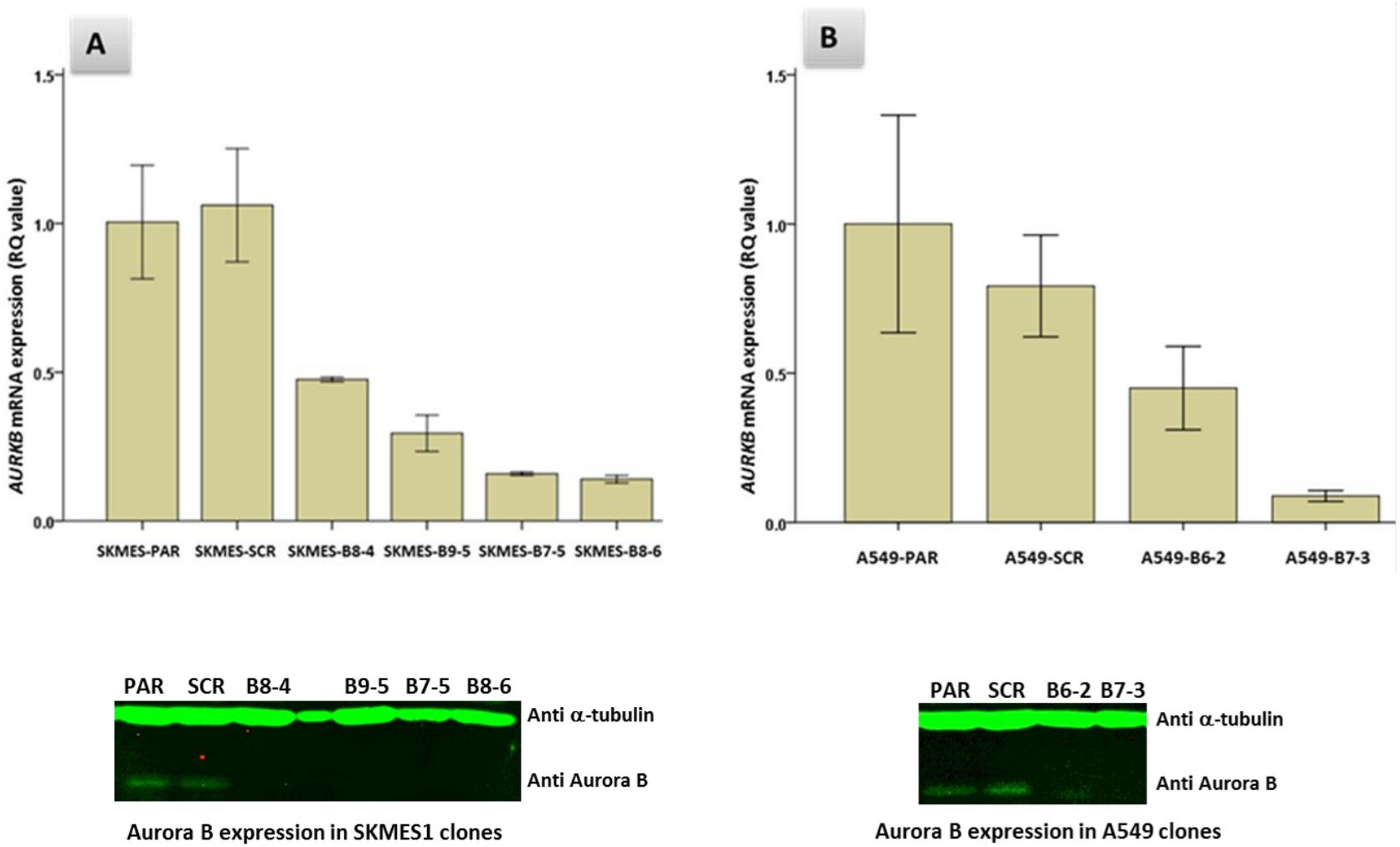

Figure 4.6: *AURKB* mRNA expression of *AURKB* knock down derivative clones (designated –Bx-y, where x is the shRNA construct and y is the clone number from this transfection) and scrambled controls (designated –SCR) relatively to the parental lung cancer cell lines (A) SKMES1 and (B) A549 (designated –PAR). Bars represent mean values for four independent repeats and error bars represent 95% confidence intervals.

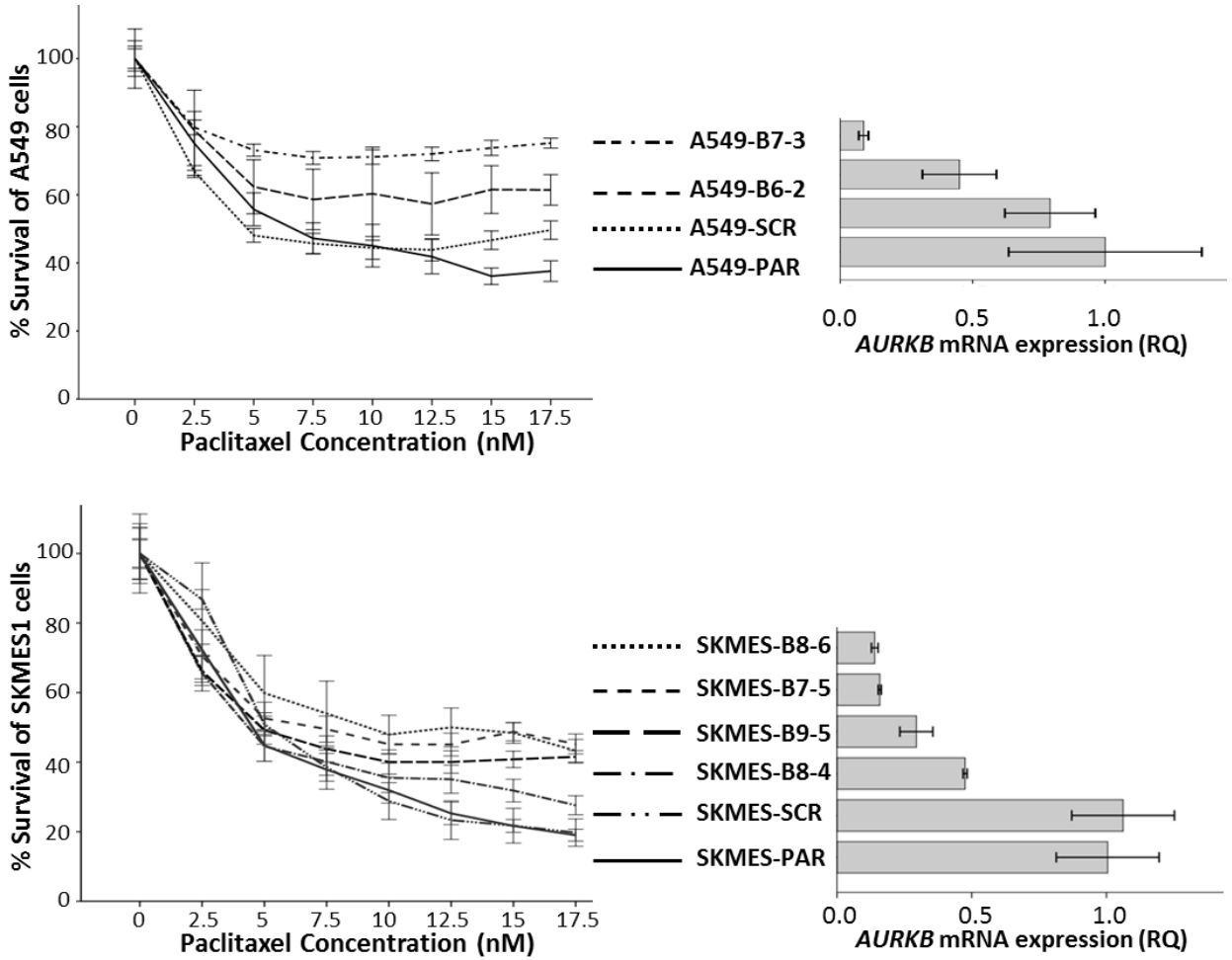

Figure 4.7: Paclitaxel response of lung cancer cell lines A549 and SK-MES1 and their *AURKB* knock down derivative clones in relation to *AURKB* mRNA expression. The figure demonstrates that cellular response to paclitaxel inversely correlated to the level of *AURKB* transcripts in a dose-dependent manner in both tested cell lines. Error bars in the line graphs and expression bar charts represent 95% confidence intervals. –PAR: parental, -SCR: scrambled, -Bx-y: knockdown clones where B is *AURKB*, x is the shRNA construct and y is the clone number from this transfection.

In order to gain additional supporting evidence, selective inhibition of Aurora B protein activity was undertaken using a highly specific Aurora B inhibitor (Barasertib). After experimentally investigating barasertib response in lung cancer cell lines A549, SK-MES1 and SKLU1 (Figure 4.8) and then determining the IC50s of this kinase inhibitor as 0.86 nM, 1.2 nM and 2.3 nM respectively, the cell lines were simultaneously exposed to a range of paclitaxel concentration and different concentrations of barasertib. AURKB inhibition was confirmed by measuring phosphorylation of histone 3 serine 10 (H3S10), which is on one of its prime substrates, using different time-points of exposure (1, 2, 4, 8, 12, and 24) hour. The western blot analysis showed that the peak of barasertib effect was around the 8hr exposure time of A549, while it was 12hr of SK-MES1 (Figure 4.9). In addition, I confirmed that barasertib exposure of A549, SK-MES1 and SKLU1 cell lines did not alter the mRNA expression of *AURKB* at the same exposure time-points (Figure 4.10). Barasertib-mediated AURKB inhibition clearly demonstrated a dose-dependent effect on paclitaxel efficiency; increased barasertib concentrations resulted in increased cellular resistance to paclitaxel in all of the three examined cell lines (Figure 4.11.1 and 2).

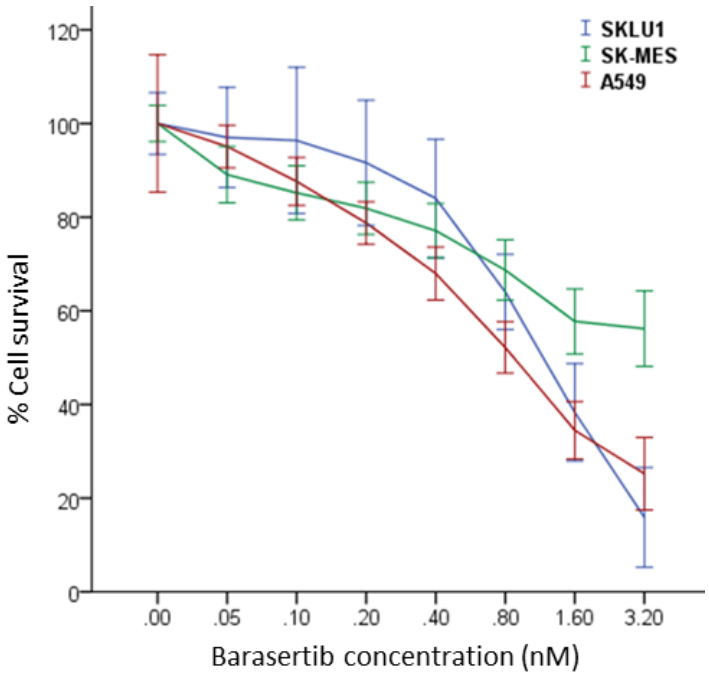

Figure 4.8: Barasertib response of lung cancer cell lines A549 and SK-MES1. The mean and error values are for six technical replicates and that one of two independent experiments is shown. Error bars in the line graphs represent 95% confidence intervals.

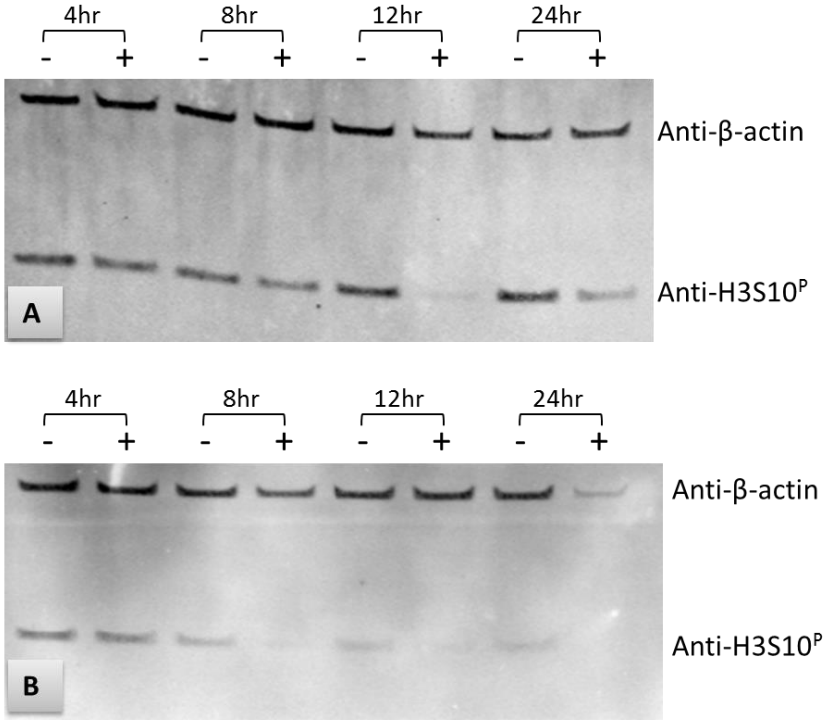

Figure 4.9: Western blot analysis assessing phosphorylated Histone 3 Serine 10 ($H3S10^P$) levels after barasertib exposure for 4-24 hours in A549 (A) and SK-MES1 (B) cell lines. "-": untreated control; "+":barasertib-treated cells.

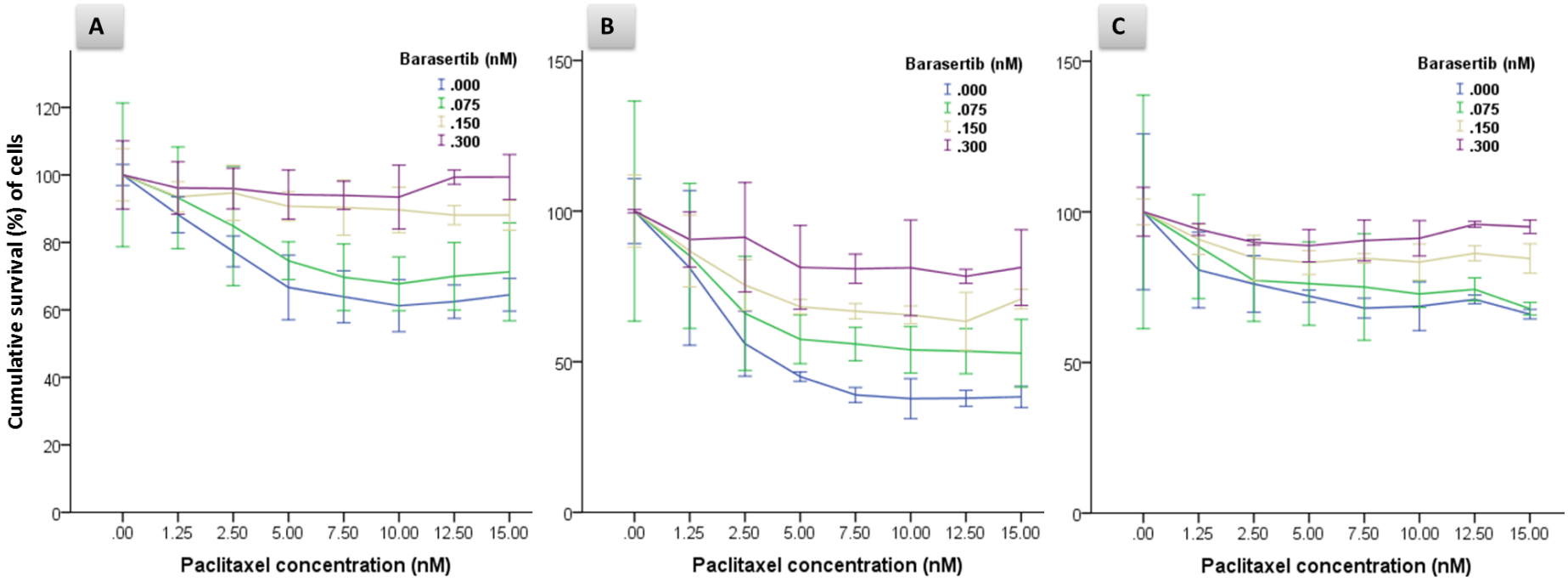

Figure 4.11.1: Sensitivity of lung cancer cell lines (A) A549, (B) SK-MES1 and (C) SKLU1 to paclitaxel in the presence of the highly selective Aurora B inhibitor (Barasertib). Exposed cells simultaneously to a range of paclitaxel concentration and different doses of barasertib showed a dose-dependent effect of barasertib-mediated AURKB inhibition on paclitaxel efficiency; increased barasertib doses led to increased paclitaxel resistance in all of these three cell lines . The mean and error values are for six technical replicates and that one of two independent experiments is shown. Error bars in the line graphs represent 95% confidence intervals.

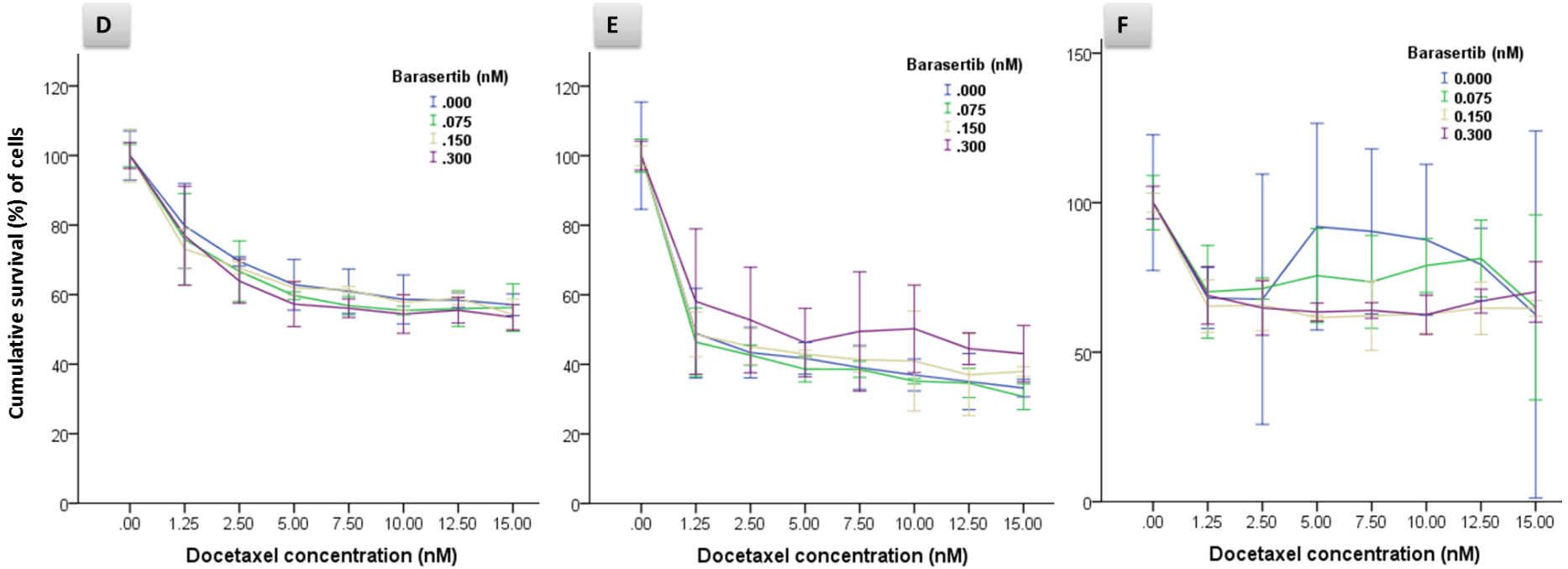

Figure 4.11.2: Sensitivity of lung cancer cell lines (D) A549, (E) SK-MES1 and (F) SKLU1 to Docetaxel in the presence of the highly selective Aurora B inhibitor (Barasertib). Barasertib-mediated AURKB inhibition did not show a synergistic effect on paclitaxel efficiency in the tested cell lines except a trend of increasing SK-MES1 resistance to docetaxel at higher concentration of barasertib. The mean and error values are for six technical replicates and that one of two independent experiments is shown. Error bars in the line graphs represent 95% confidence intervals.

In summary, the present study demonstrated that frequent up-regulation of *AURKB* mRNA was observed in NSCLC tissue in comparison to normal adjacent lung tissue ($p<0.0001$), being more prominent in squamous carcinomas ($p<0.0001$), and higher stages tumors ($p=0.012$). *AURKB* overexpression in NSCLC cell lines strongly correlated with resistance to both docetaxel ($p=0.0016$) and paclitaxel ($p=0.0096$). *AURKB* knock down derivatives of two cell lines consistently showed a dose-dependent association between *AURKB* mRNA expression and resistance to paclitaxel. Inhibition of Aurora B activity by Barasertib also demonstrated a strong dose-dependent efficiency in triggering paclitaxel resistance in all of the cell lines tested.

Chapter 5: *AURKA* mRNA expression is an independent predictor of poor prognosis in patients with NSCLC

Based on the prognostic values of *AURKA* and *AURKB* dysregulation, I analysed mRNA expression levels of further 8 of mitotic spindle associated genes (*AURKC*, *CKAP5*, *TPX2*, *TTK*, *KIF11*, *DLGAP5*, *TUBB* & *TUBB3*) in the available NSCLC tissues (56 adenocarcinomas, 76 squamous cell carcinomas (SqCCL), and 44 adjacent normal tissues from 20 adenocarcinoma and 24 SqCCL patients). The role/effect of their expression status on the prognosis outcome was then tested in these cancer cases by preforming a univariate and multivariate analysis on the mRNA expression levels of all of the ten genes along with the clinicopathological features. In addition, the mRNA expression profiling of aforementioned genes was examined in the available NSCLC cancer cell lines and further thirteen HNSCC cell lines. The taxane response was also tested in these HNSCC cells in order to explore any possible correlation between mRNA expression of the gene and cellular response to taxanes in RTC cell lines.

The results of mRNA expression for both NSCLC tumour samples and cell lines have already been given for *AURKA* and *AURKB* in chapters 3 and 4 respectively. Further qPCR analysis revealed that mRNA expression levels of all of the genes tested in this study (*CKAP5*, *TPX2*, *TTK*, *KIF11*, *DLGAP5*, *TUBB* & *TUBB3*) except *AURKC* were significantly overexpressed in NSCLC tissue compared to normal adjacent lung tissue ($P < 0.0001$) (Figure 5.1.1 and 2).

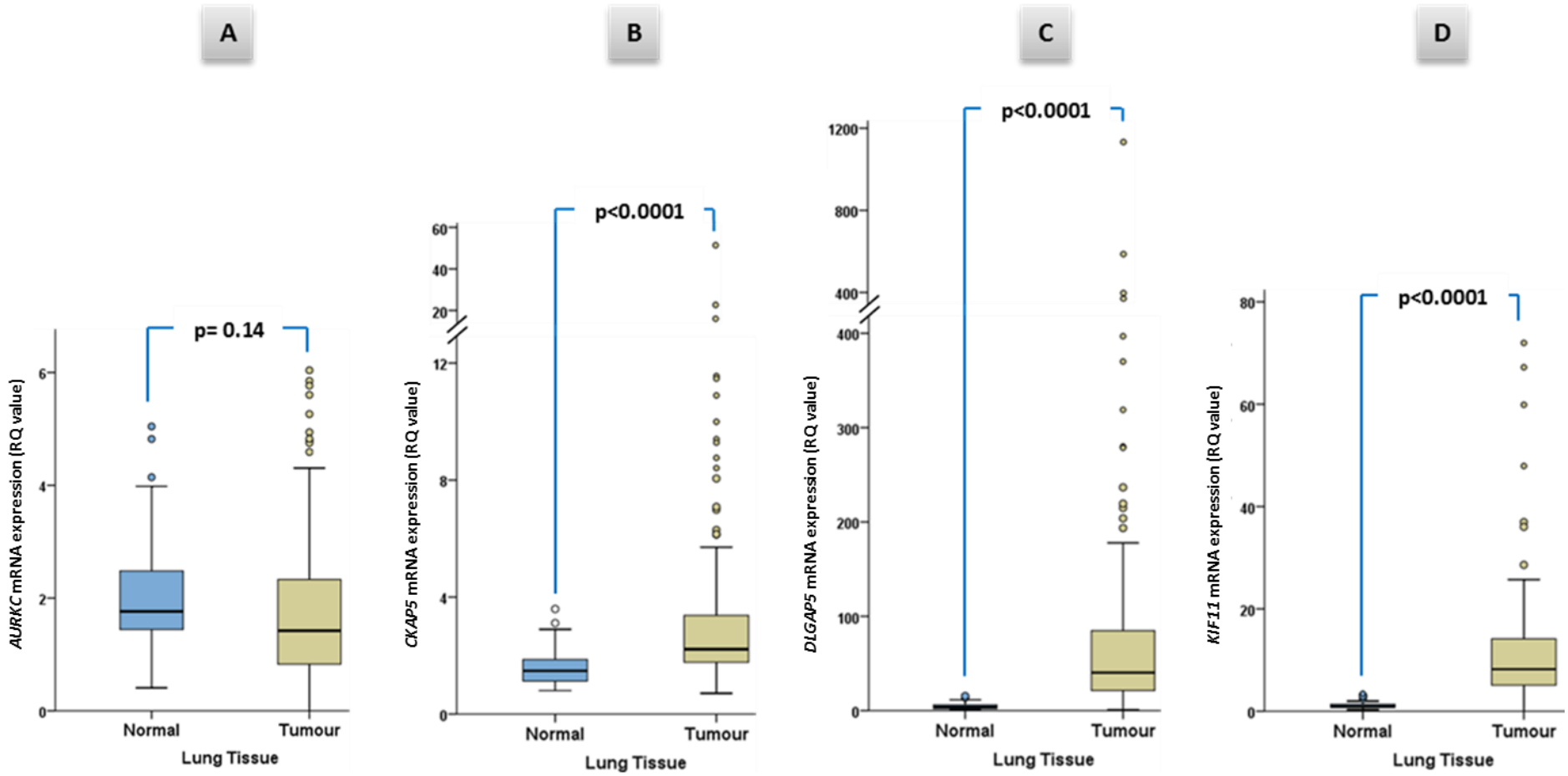

Figure 5.1.1: Box plots showing *AURKC* (A), *CKAP5* (B), *DLGAP5* (C) and *KIF11* (D) mRNA expression in NSCLC tissues and adjacent normal tissues. Comparison between the samples showed that mRNA expression levels of the genes in NSCLC tumours are significantly higher than those in adjacent normal tissues, except that of *AURKC*. *P* values returned from Mann-Whitney test and adjusted for multiple comparisons by Bonferroni correction.

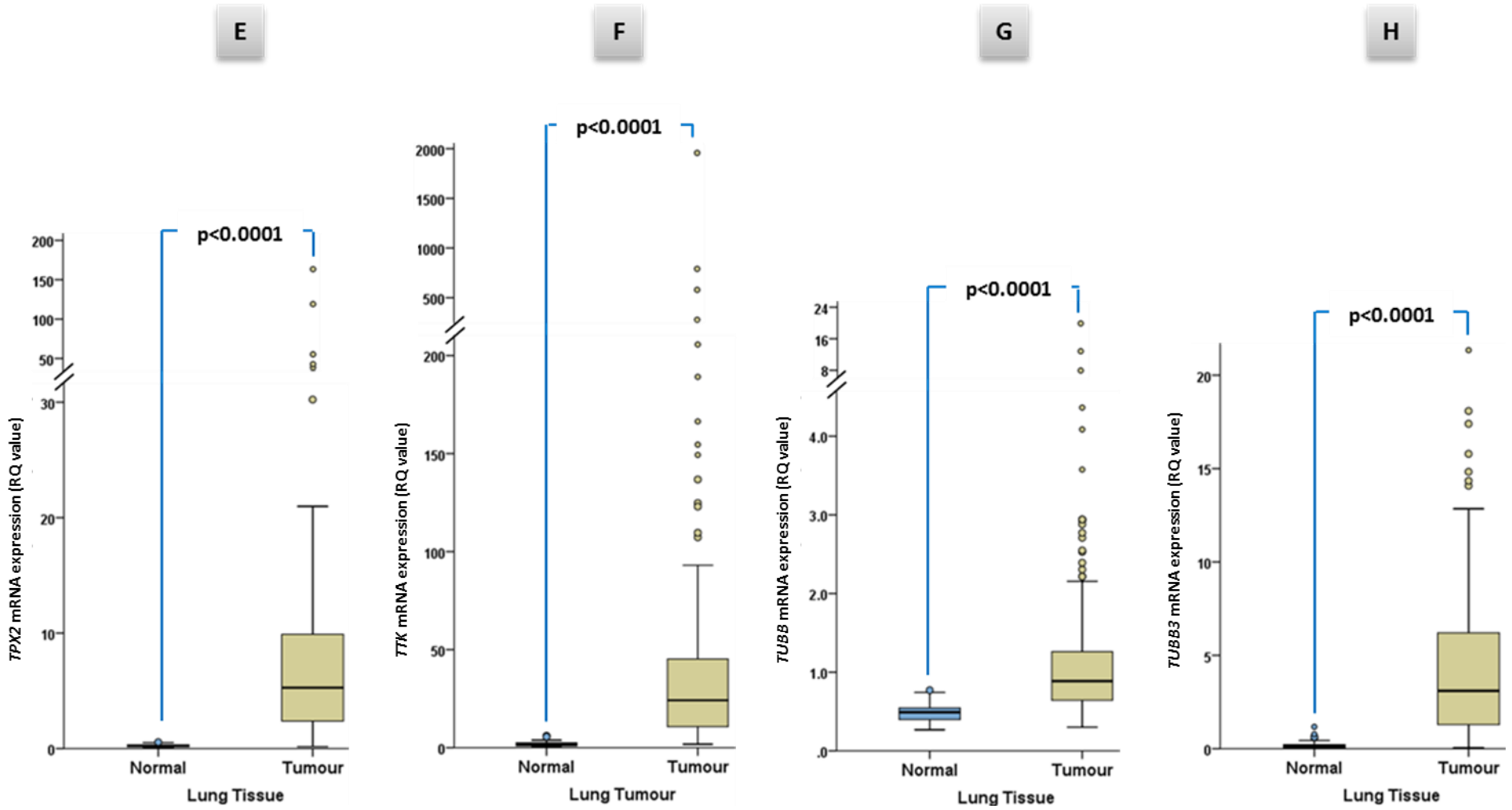

Figure 5.1.2: Box plots showing *TPX2* (E), *TTK* (F), *TUBB* (G) and *TUBB3* (H) mRNA expression in NSCLC tissues and adjacent normal tissues. Comparison between the samples showed that mRNA expression levels of the genes in NSCLC tumours are significantly higher than that in adjacent normal tissues. *P* values returned from Mann-Whitney test and adjusted for multiple comparisons by Bonferroni correction.

Comparison between histology types revealed that the mRNA expression of seven genes; *AURKA*, *AURKB* (already shown in chapters 3 and 4), *DLGAP5*, *TPX2*, *TTK*, *TUBB*, and *KIF11* (Figure 5.2) was more pronounced in squamous cell lung carcinoma (SqCCL) than in adenocarcinoma (AdCs) tissues ($P < 0.0001$; KIF11, p value = 0.01).

The correlation between expression profiles of *AURKA, AURKB, AURKC, CKAP5, TPX2, TTK, KIF11, DLGAP5, TUBB* and *TUBB3* and overall survival was then explored. In addition to the already demonstrated correlation between elevated mRNA expression of *AURKA* and *AURKB* with reduced survival either in whole NSCLC cases or in patients with lung adenocarcinomas respectively (chapters 3 and 4), Kaplan-Meier analysis demonstrates that high TPX2 mRNA expression was borderline correlated with reduced overall survival in all of NSCLC individuals (p=0.055)) (Figure 5.3.A). Analysis of the effect of TPX2 mRNA expression on proportion of patients surviving at the end of different intervals demonstrated that one-year survival of NSCLC cases, whose tumours showed low expression of TPX2 mRNA, was 74% as opposed to 58% for individuals with increased levels of TPX2 mRNA expression (dichotomy based on the median value). Five-year survival for low level of TPX2 mRNA expression was 45% as opposed to 43% for those with higher mRNA expression of TPX2. Similarly, ten-year survival proportion was 30% for those with low mRNA expression and 16% of patients survive with higher levels of TPX2 transcripts.

Elevated levels of CKAP5 mRNA expression were significantly correlated with poor outcome in studied lung cancer individuals (p=0.01) (Figure 5.3.B). No correlation observed between the expression of the rest of the genes and overall survival (Appendix 8, A-H). The proportion of patients with lung adenocarcinoma that pronounced low levels of CKAP5 transcripts surviving one year was 80%, whereas survival was 57% for those patients with tumours expressing high levels of these transcripts.

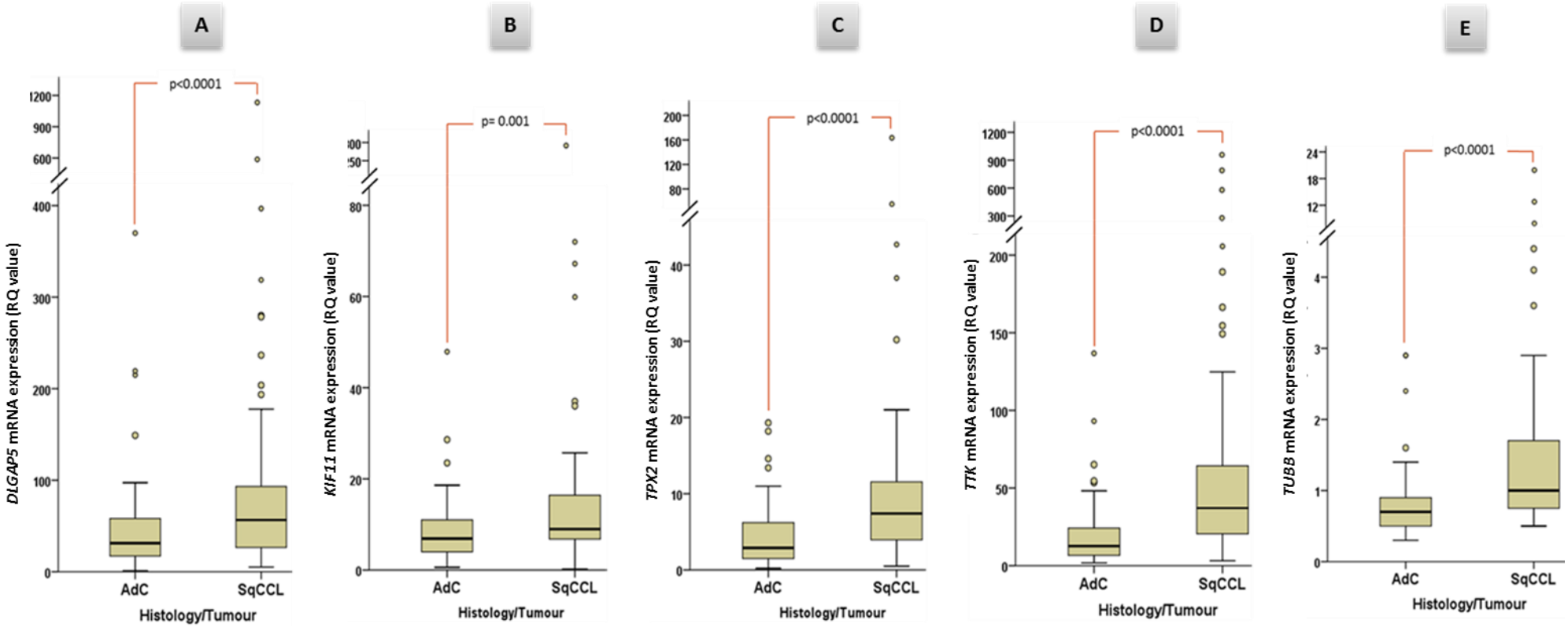

Figure 5.2: Boxplots demonstrating mRNA expressions of *DLGAP5*, *KIF11*, *TPX2*, *TTK* and *TUBB* genes in squamous cell carcinomas (sqCCL) and adenocarcinomas (AdC) of the lung. Comparison between histology types showed that the mRNA expression levels of the genes in sqCCL tumours are significantly higher than that in AdC ones. P values returned from Mann-Whitney test and adjusted for multiple comparisons by Bonferroni correction.

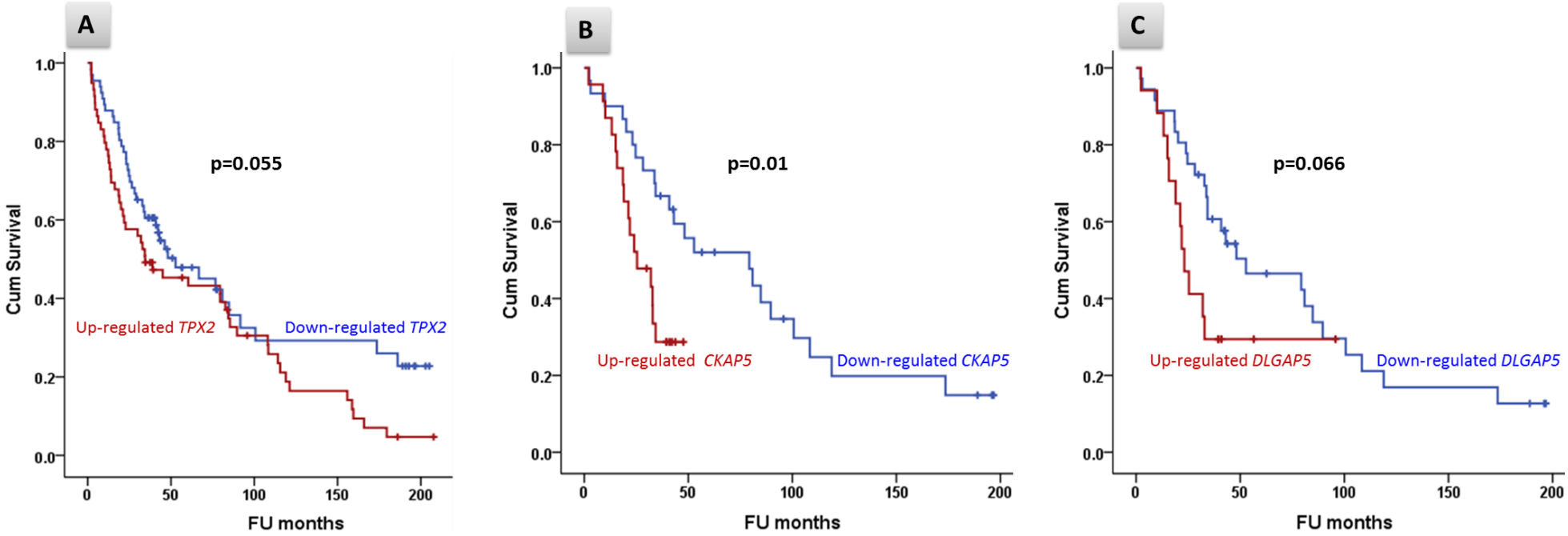

Figure 5.3: Kaplan-Meier analysis of overall survival (OS) of lung cancer patients dichotomised by median mRNA expression of *TPX2* in NSCLC tumours (A), *CKAP5* (B) and *DLGAP5*(C) in adenocarcinomas of the lung.

Five and ten years survival were 52% and 20% respectively in of lung adenocarcinomas with lower CKAP5 mRNA expression, while these 5 and 10 year intervals were censored in highly CKAP5 mRNA expression tumours (i.e. the data about the patients survival duration is incomplete owing to loss to follow-up). Overexpression of *DLGAP5* mRNA was marginally correlated with poor outcome in patients with lung adenocarcinomas (p=0.066) (Figure 5.3.C). One and five year prognostic outcome in those patients whose cancerous tissues express decreased levels of *DLGAP5* mRNA were 81% and 46% respectively as opposed to 47% and 29% respectively for adenocarcinomas patients with higher levels of *DLGAP5* mRNA expression.

Of 132 patients analysed, only 124 had *AURKA* data available for analysis and this expression profile was the only one to show correlation with reduced survival in both adenocarcinomas and squamous cell carcinomas, while no significant correlation was observed of age, gender, tumour stage or nodal status (Table 5.1). This significant correlation with overall survival was observed in both univariate and multivariate analyses (Table 5.2). In univariate analysis, age (Hazard Ratio (HR), 1.02; 1.00-1.05, P=0.066), gender (HR, 1.23; 0.81-1.88, P = 0.326), pathological stages 2 (HR, 2.82; 1.35-5.86, P = 0.006), pathological stage ≥3 (HR, 3.80; 1.42-10.15, P = 0.008), nodal status stage 1 (HR, 1.62; 1.03-2.55, P = 0.037) and nodal status stage 2 (HR, 2.55; 1.35-4.84, P = 0.004) were all predictors of overall survival. Multivariate analysis showed that *AURKA* mRNA expression (Hazard Ratio (HR), 1.81; 95%CI 1.16-2.84, P = 0.009), age (HR 1.03; 95%CI 1.00-1.06, P = 0.020), pathological stage 2 (HR 2.43; 95%CI 1.16-5.10, P = 0.019), and involvement of distal nodes (pN2) (HR 3.14; 95% CI 1.24-7.99, P =0.016) were independent predictors of poor prognosis in patients with NSCLC (Table 5.2).

Table 5.1: Clinicopathological characteristics of patients and *AURKA* mRNA expression

Clinicopathological characteristics	Total number of patients (%)	High expression of Aurora-A mRNA (n=59)	Low expression of Aurora-A mRNA (n=65)	P-values
Mean Age (SD)	124(100)	65.9 (8.5)	67.5 (8.5)	0.223
Gender				0.180
Male	70(56.5)	37 (52.9)	33(47.1)	
Female	54(43.5)	22 (40.7)	32 (59.3)	
Histology				<0.0001
Adenocarcinoma	52(41.9)	13 (25.0)	39 (75.0)	
Squamous cell carcinoma	72(58.1)	46 (63.9)	26 (36.1)	
Tumour stage				0.513
Stage 1	19(15.3)	7 (36.8)	12 (63.2)	
Stage 2	91(73.3)	45 (49.5)	46 (50.6)	
≥Stage 3	12(9.6)	7(58.3)	5(41.7)	
Nodal status				0.975
0	68(54.8)	32 (47.1)	36 (52.9)	
1	38(30.6)	18 (47.4)	20 (52.6)	
2	18(14.6)	9(50.0)	9(50.0)	

Table 5.2: *AURKA* mRNA expression and overall survival of 124 NSCLC patients

	Univariate		**Multivariate**	
Covariates	HR(95%CI)	P-values	HR(95%CI)	P-values
AURKA mRNA	1.79(1.16-2.77)	0.009	1.81(1.16-2.84)	0.009
Age	1.02(1.00-1.05)	0.066	1.03(1.00-1.06)	0.02
Tumour stage				
Stage 1	Reference	Reference	Reference	Reference
Stage 2	2.82(1.35-5.86)	0.006	2.43(1.16-5.10)	0.019
≥Stage 3	3.80(1.42-10.15)	0.008	1.39(0.38-5.09)	0.623
Nodal status				
0	Reference	Reference	Reference	Reference
1	1.62(1.03-2.55)	0.037	1.45(0.90-2.34)	0.128
2	2.55(1.35-4.84)	0.004	3.14(1.24-7.99)	0.016

Univariate and multivariate Cox proportional Hazard regression analysis.

mRNA expression profiling was also tested in RTCs cell lines. The profiling of all of the genes investigated in a panel of 9 NSCLC cell lines from different histological origins (AdC, SqCC and large cell squamous carcinoma) along with non-tumourigenic immortalised bronchial epithelial cells (HBEC-3kt and its isogenic derivatives which are KRAS mutants, p53 knockouts, and cells with both aberrations). mRNA expression profiling of the gene penal (except *AURKC* transcripts) was significantly higher than that in HBEC-3kt in all of these cell lines except *CKAP5* mRNA expression in only Calu-3 cell line. (Figures 5.4.1-4).

In order to expand the sample size of cell lines, the mRNA expression profiling of the studied genes in a panel of thirteen HNSCC cell lines (BHY, HN5, PE/CA-PJ15, PE/CA-PJ41, UM-SCC-104, UM-SCC-12, UM-SCC-17as, UM-SCC-19, UM-SCC-4, UM-SCC-47, UM-SCC-5, UM-SCC-81b and UPCI-SCC-090) in addition to primary HNSCC cells Liv7K (gift of Dr. Janet Risk) (Chapter 2, Table 2.1). Similar to the trend already shown in lung cell lines, mRNA expression profiling of HNSCC showed variable expression levels of gene transcripts, but in most cases was higher than that of the calibrator cell line HBEC-3KT (Figures 5.5.1-4).

MTT analysis was used to measure cellular response to the taxanes after treatment of HNSCC cell lines with (0 -35 nM) of paclitaxel and docetaxel. This showed a similar trend to that seen in lung cancer cells of that docetaxel was superior in its inhibition of cancerous cells with few exceptions (Figures 5.6.1-7). Docetaxel IC50s values at 95% confidence intervals in most cell lines were lower than that of paclitaxel except for UMSCC-17as, UMSCC-104 and UPCI-SCC-090 (Figures 5.6.3 (F), 5.6.4 (H) and 5.6.7 (N)).

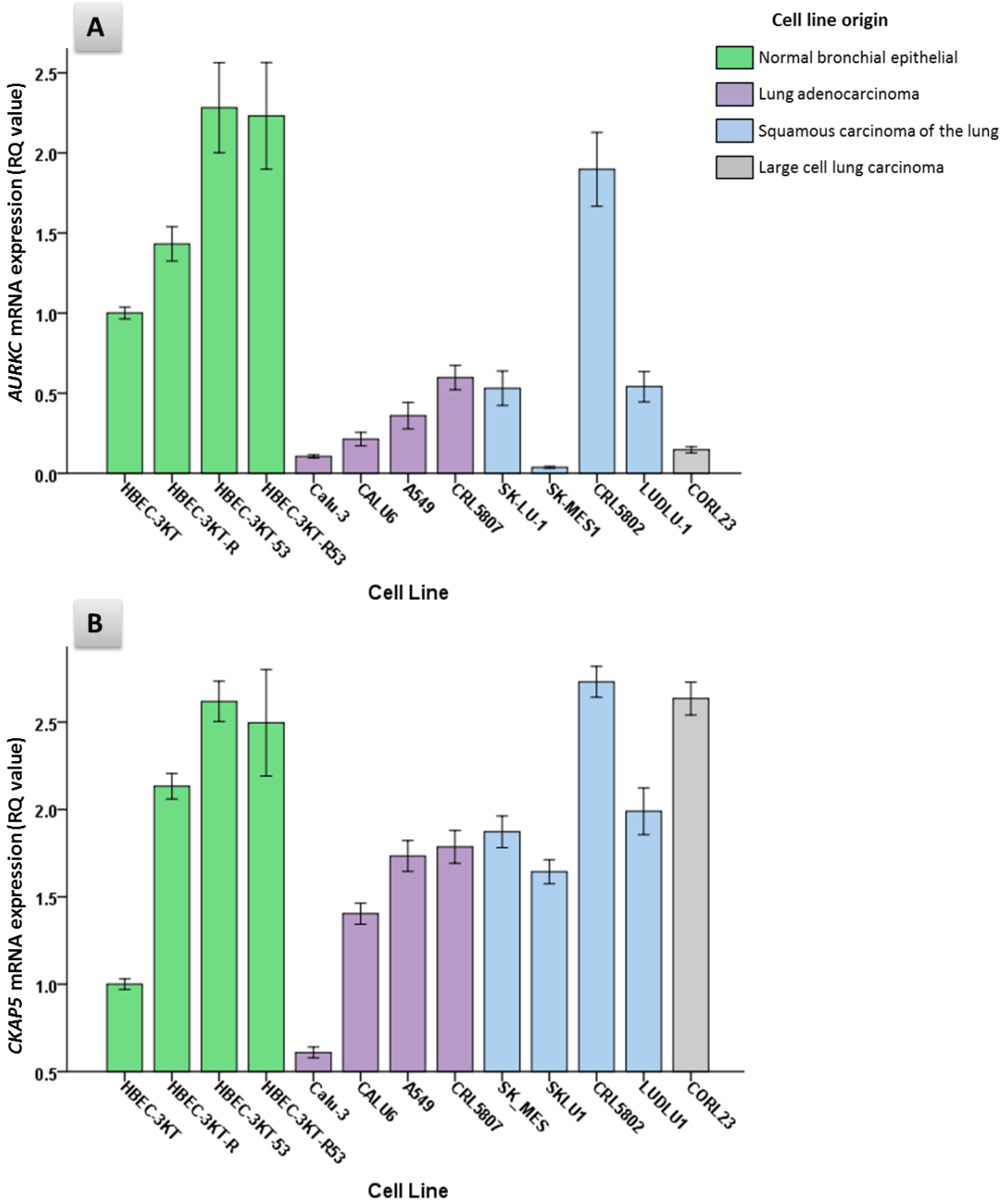

Figure 5.4.1: mRNA expression of *AURKC* (A), and *CKAP5* (B) in human bronchial epithelial cells (HBEC) and lung cancer cell lines. Bars represent mean values for four independent repeats and error bars represent 95% confidence intervals.

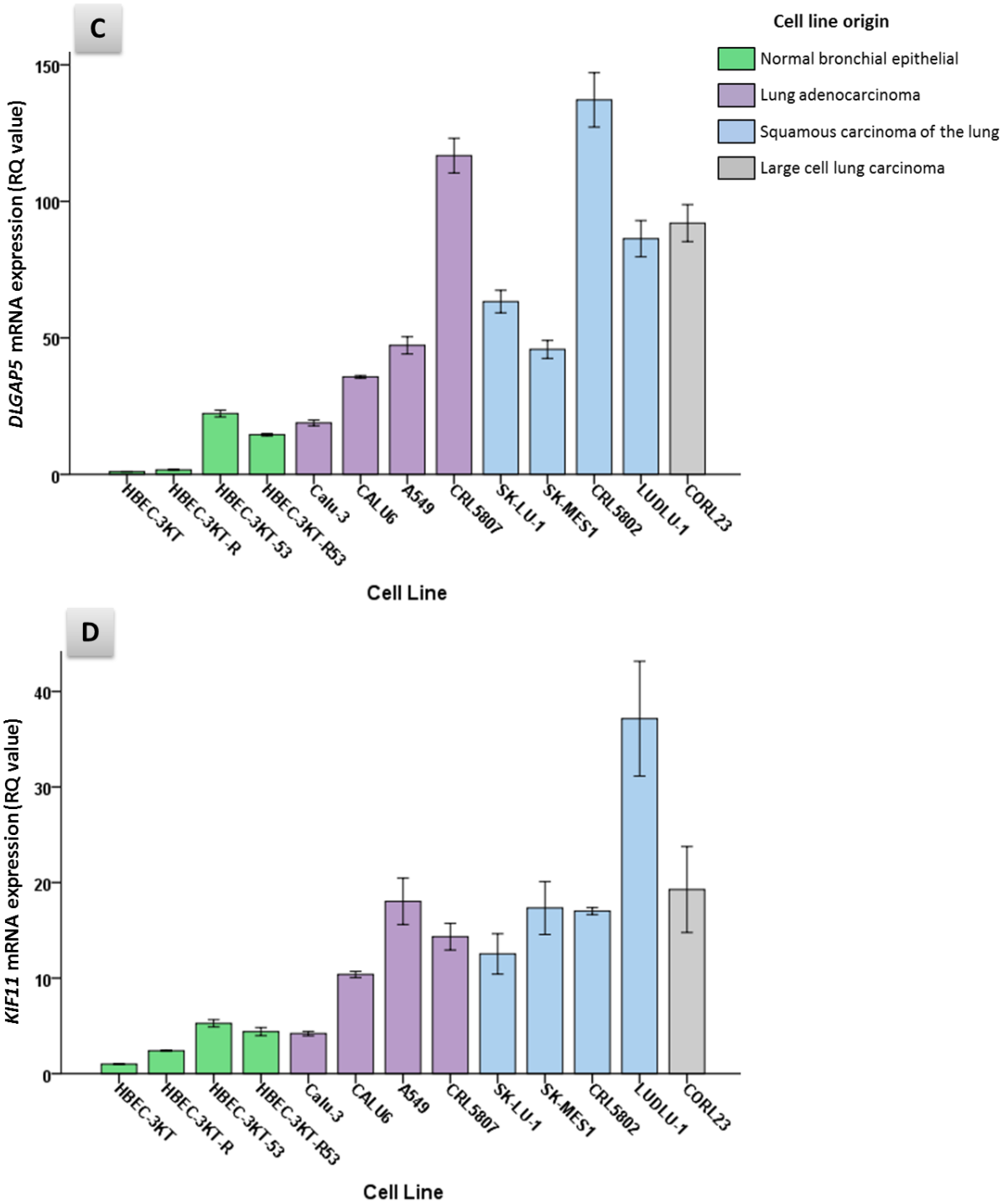

Figure 5.4.2: mRNA expression of *DLGAP5* (C) and *KIF11* (D) in human bronchial epithelial cells (HBEC) and lung cancer cell lines. Bars represent mean values for four independent repeats and error bars represent 95% confidence intervals.

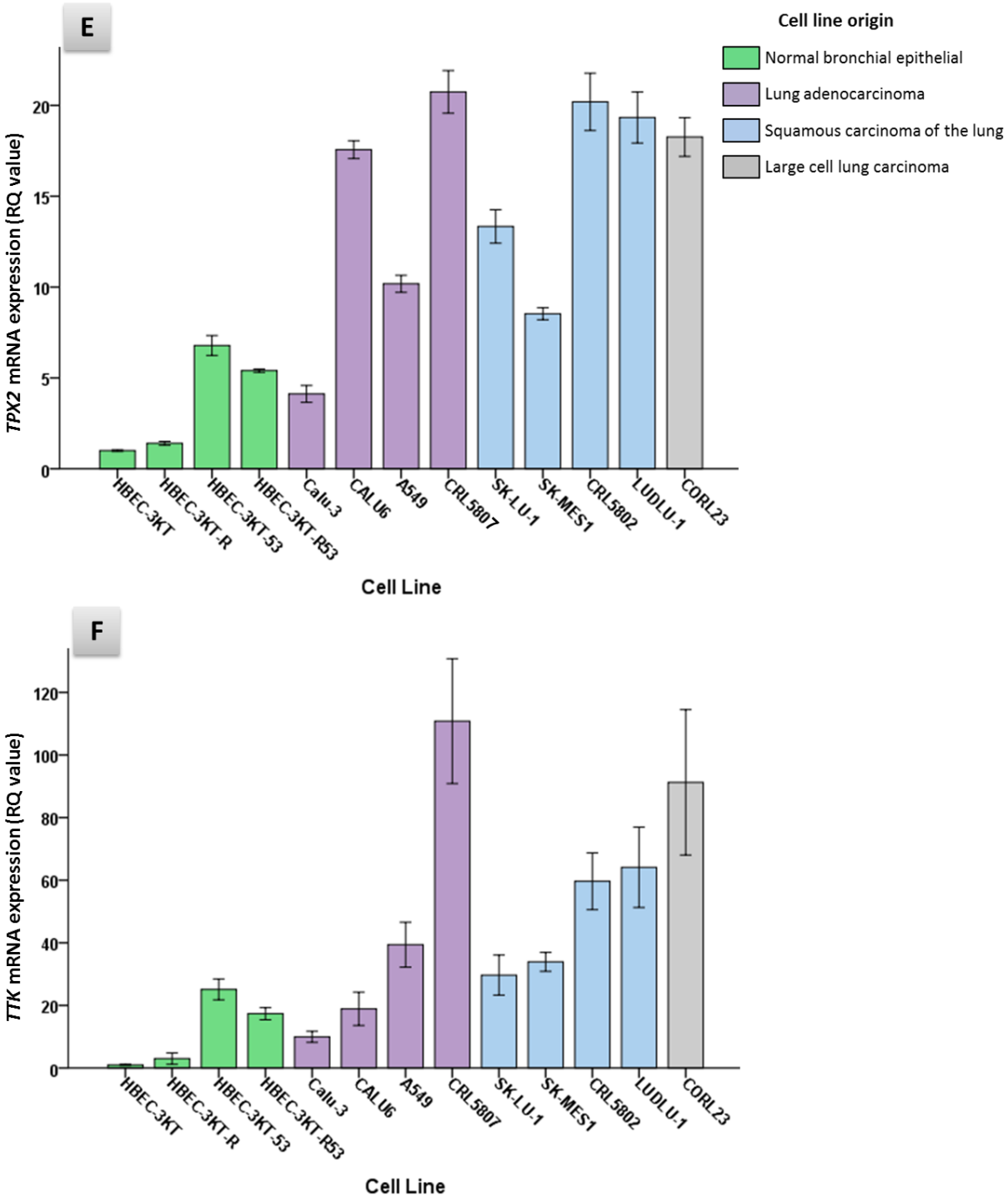

Figure 5.4.3: mRNA expression of *TPX2* (E) and *TTK* (F) in human bronchial epithelial cells (HBEC) and lung cancer cell lines. Bars represent mean values for four independent repeats and error bars represent 95% confidence intervals.

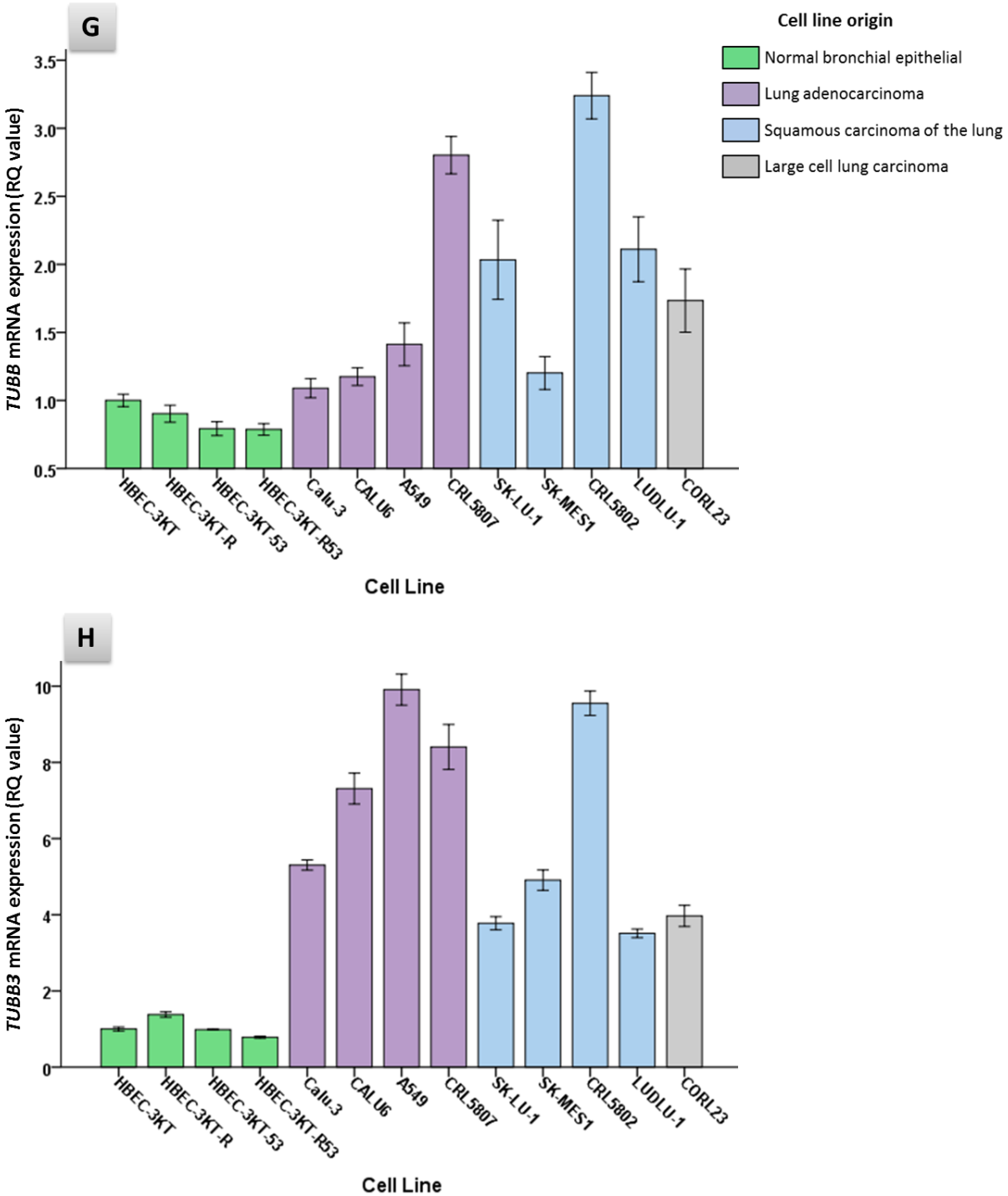

Figure 5.4.4: mRNA expression of *TUBB* (G) and *TUBB3* (H) in human bronchial epithelial cells (HBEC) and lung cancer cell lines. Bars represent mean values for four independent repeats and error bars represent 95% confidence intervals.

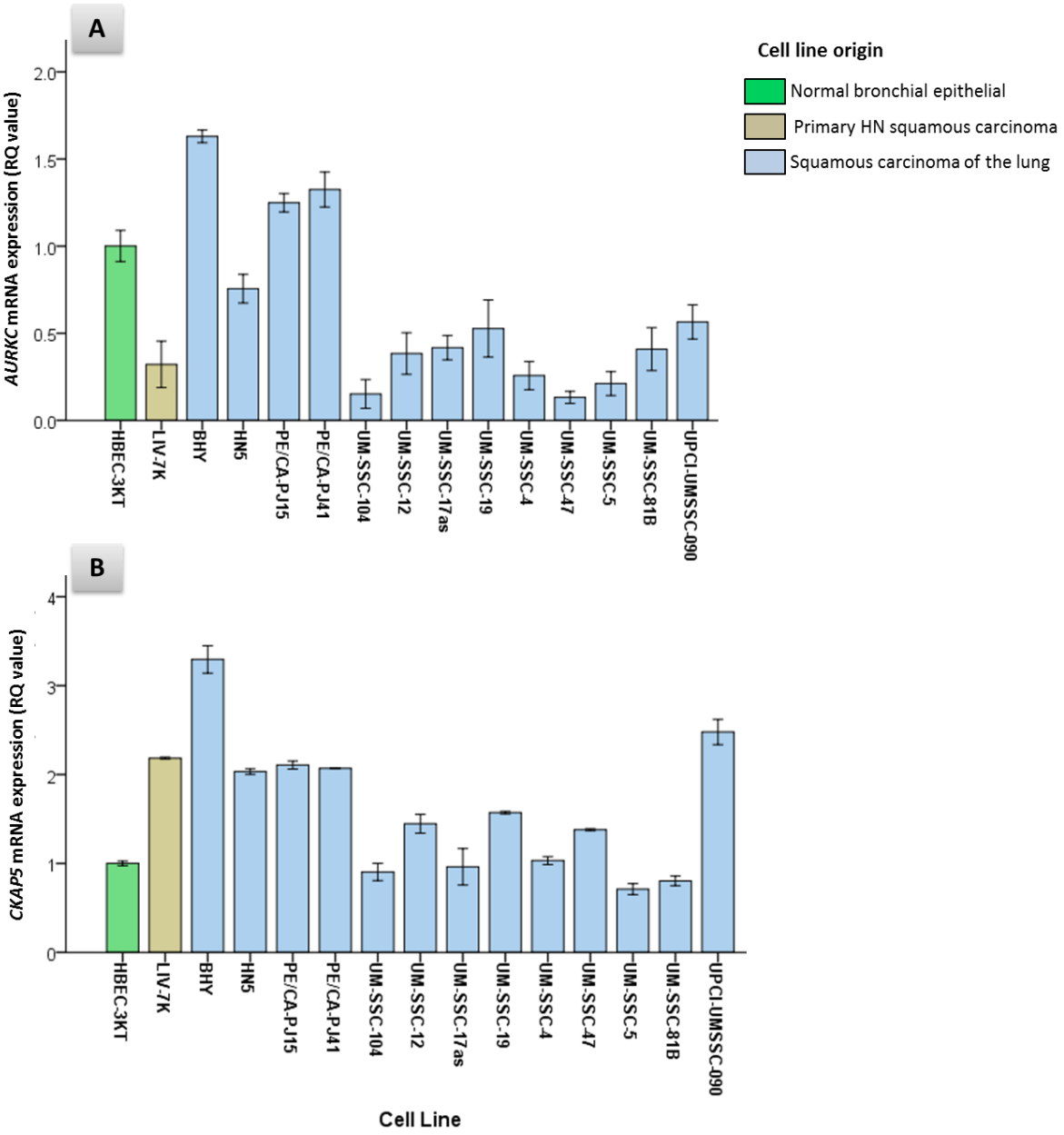

Figure 5.5.1: mRNA expression of *AURKC* (A) and *CKAP5* (B) in HNSCC cell lines. The expression was variable among the cell lines. Bars represent mean values for four independent repeats and error bars represent standard error of the mean. Human bronchial epithelial cell line (HBEC-3KT) was used as a technical calibrator.

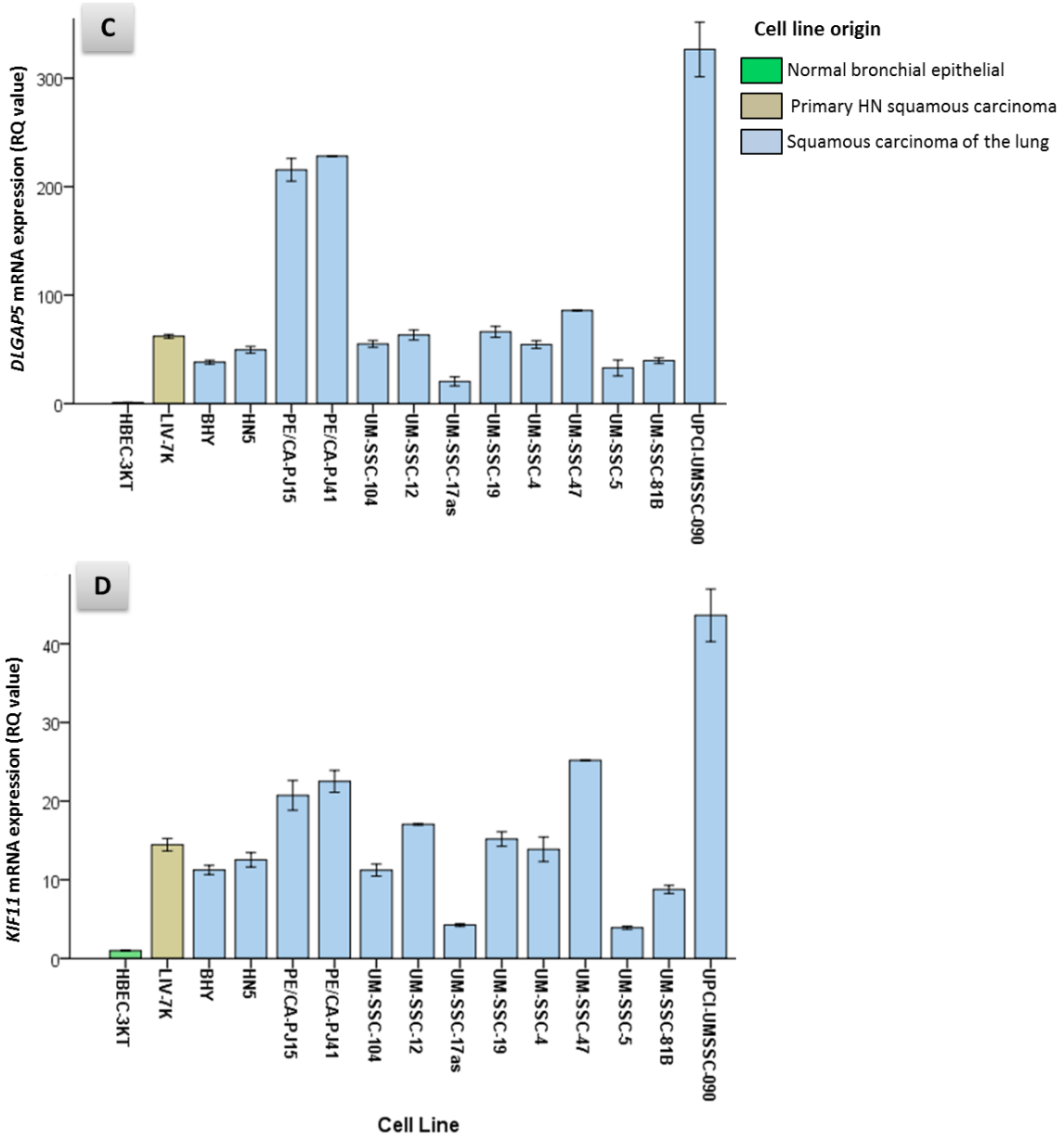

Figure 5.5.2: mRNA expression of *DLGAP5* (C) and *KIF11* (D) in HNSCC cell lines and human bronchial epithelial cells (HBEC-3KT). mRNA expression of both gene was variable among the cell lines. Bars represent mean values for four independent repeats and error bars represent standard error of the mean. Human bronchial epithelial cell line (HBEC-3KT) was used as a technical calibrator.

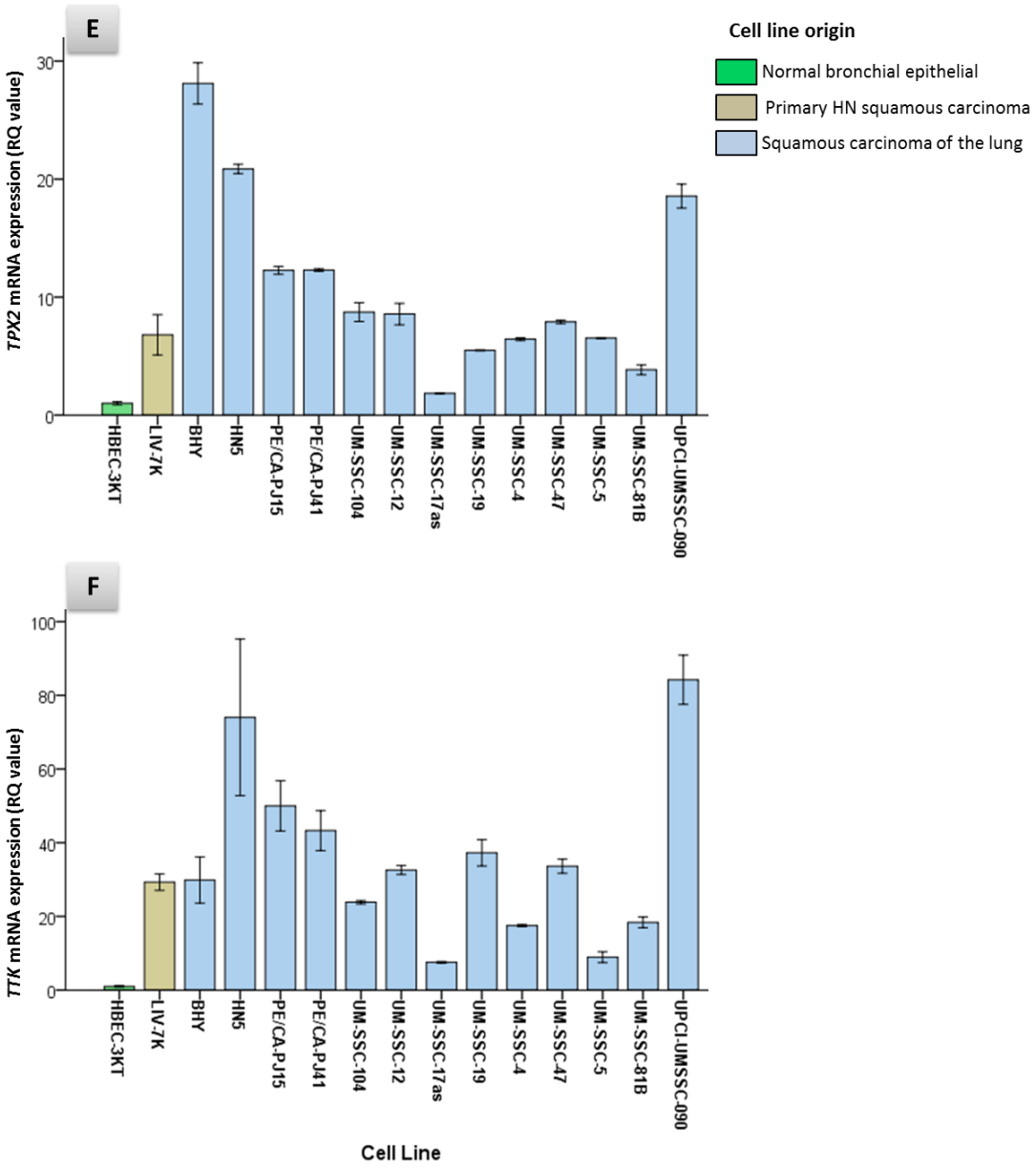

Figure 5.5.3: mRNA expression of *TPX2* (E) and *TTK* (F) in HNSCC cell lines and human bronchial epithelial cells (HBEC-3KT). mRNA expression of both gene was variable among the cell lines. Bars represent mean values for four independent repeats and error bars represent standard error of the mean. Human bronchial epithelial cell line (HBEC-3KT) was used as a technical calibrator.

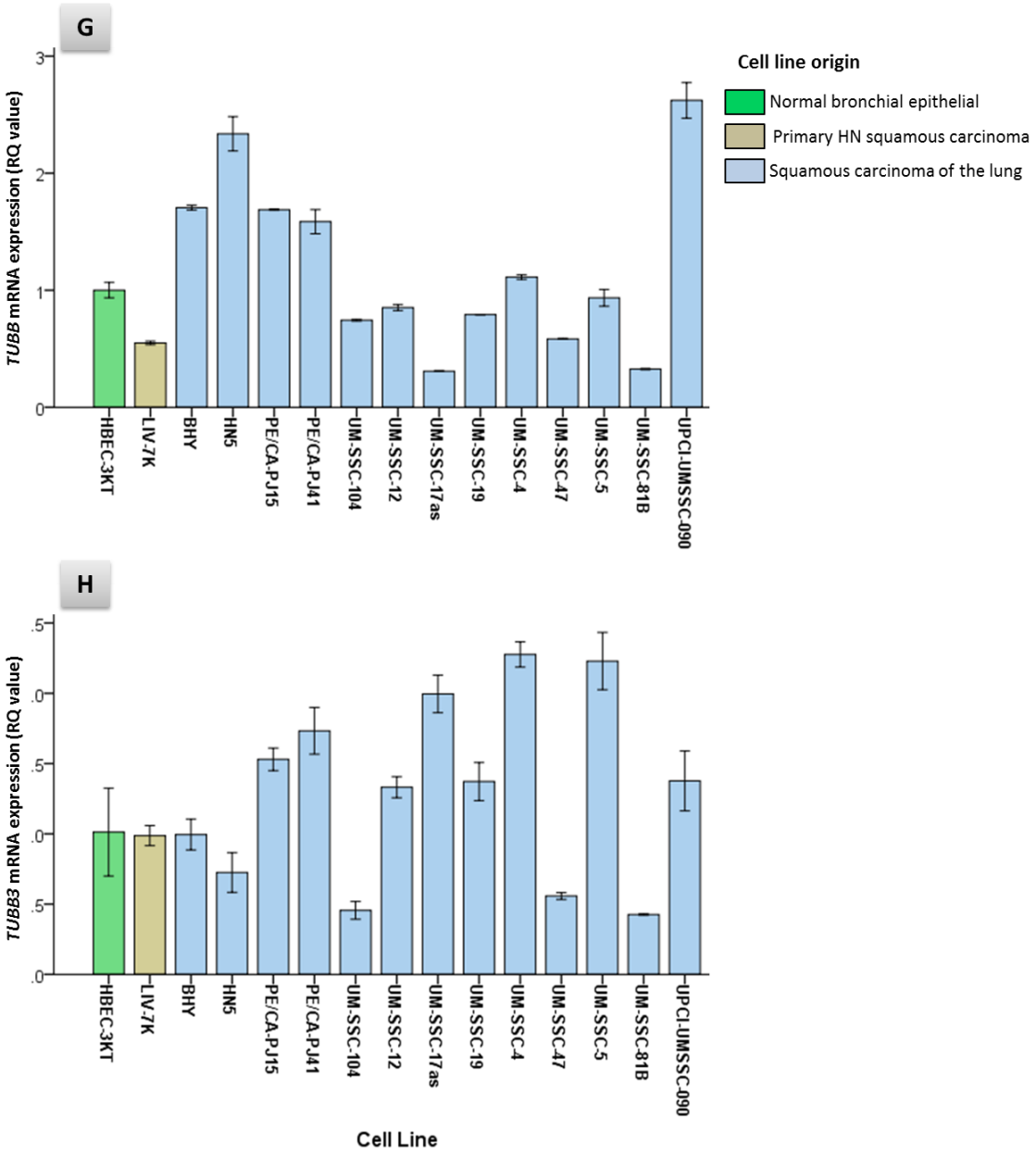

Figure 5.5.4: mRNA expression of *TUBB* (G) and *TUBB3* (H) in HNSCC cell lines and human bronchial epithelial cells (HBEC-3KT). mRNA expression of both gene was variable among the cell lines. Bars represent mean values for four independent repeats and error bars represent standard error of the mean. Human bronchial epithelial cell line (HBEC-3KT) was used as a technical calibrator.

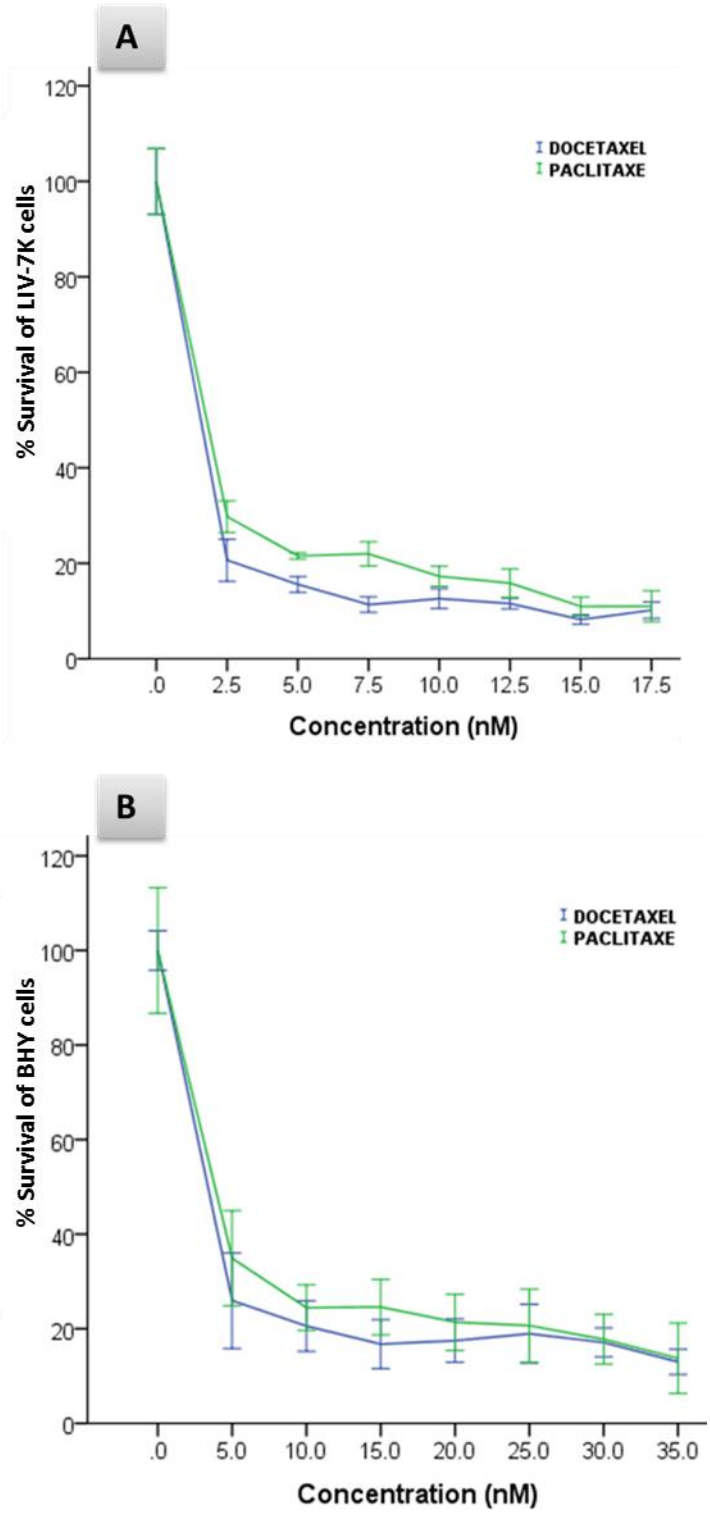

Figure 5.6.1: Taxane response of Head and Neck cancer cell lines (A) primary HNSCC cell line Liv-7K (B) BHY. Among all of studied cell lines (NSCLC, HNSCC and HBEC cells), Liv-7K primary cell line was the most sensitive one to both taxanes. BHY cell line was the 2nd most resistant among HNSCC cells. Generally, both cell lines are more sensitive to docetaxel than paclitaxel. The mean and error values are for six technical replicates and that one of two independent experiments is shown. Error bars in both line graphs represent 95% confidence intervals.

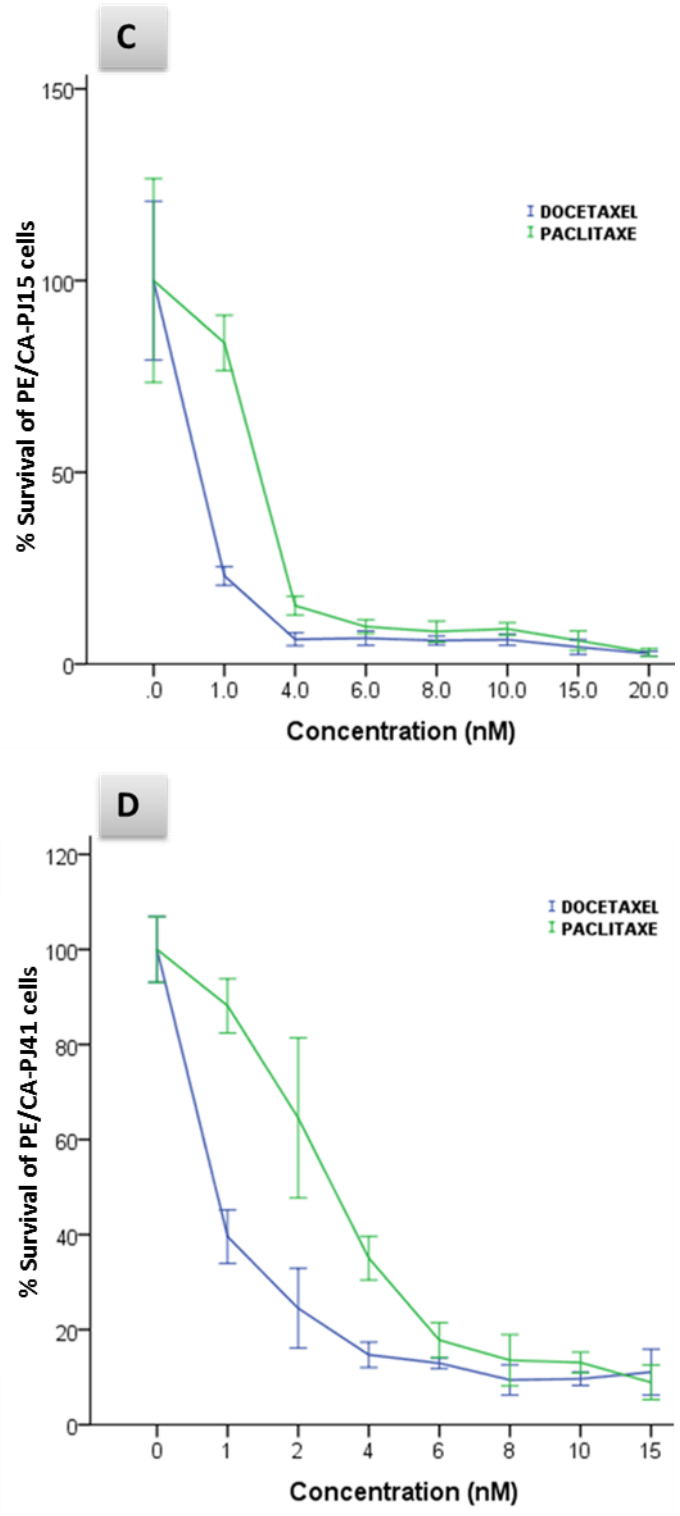

Figure 5.6.2: Taxane response of Head and Neck cancer cell lines (C) PE/CA-PJ15 (D) PE/CA-PJ41. Although PE/CA-PJ15 represents the 2nd most sensitive cell line docetaxel and paclitaxel and PE/CA-PJ41 is the 3rd one among all of studied cell lines, they are similar in their response to both taxanes. Generally, both cell lines are more sensitive to docetaxel than paclitaxel. The mean and error values are for six technical replicates and that one of two independent experiments is shown. Error bars in both line graphs represent 95% confidence intervals.

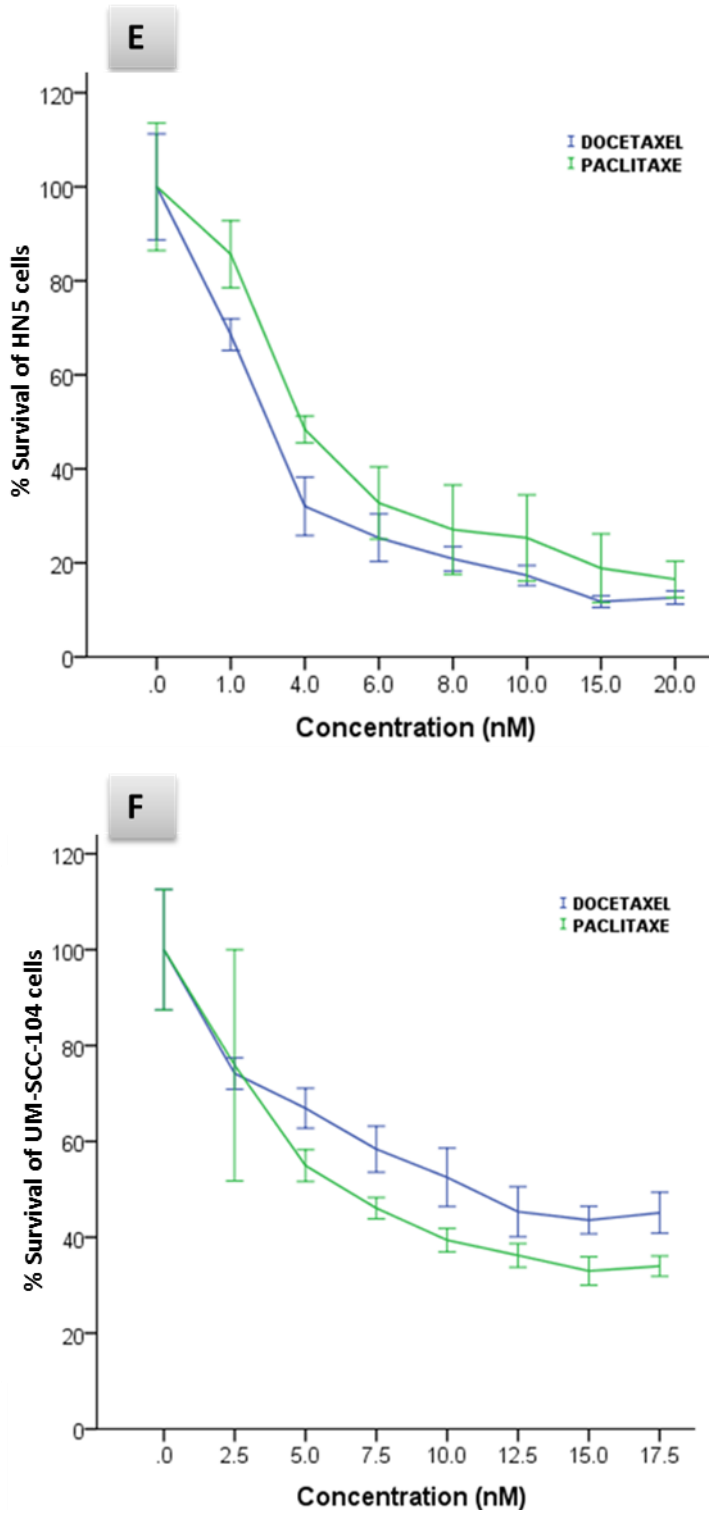

Figure 5.6.3: Taxane response of Head and Neck cancer cell lines (E) HN5 (F) UMSCC-104. While HN5 cell line more sensitive to docetaxel than paclitaxel as same as most other cell lines, UMSCC-104 has opposite trend, as it is more sensitive to paclitaxel than docetaxel. The mean and error values are for six technical replicates and that one of two independent experiments is shown. Error bars in both line graphs represent 95% confidence intervals.

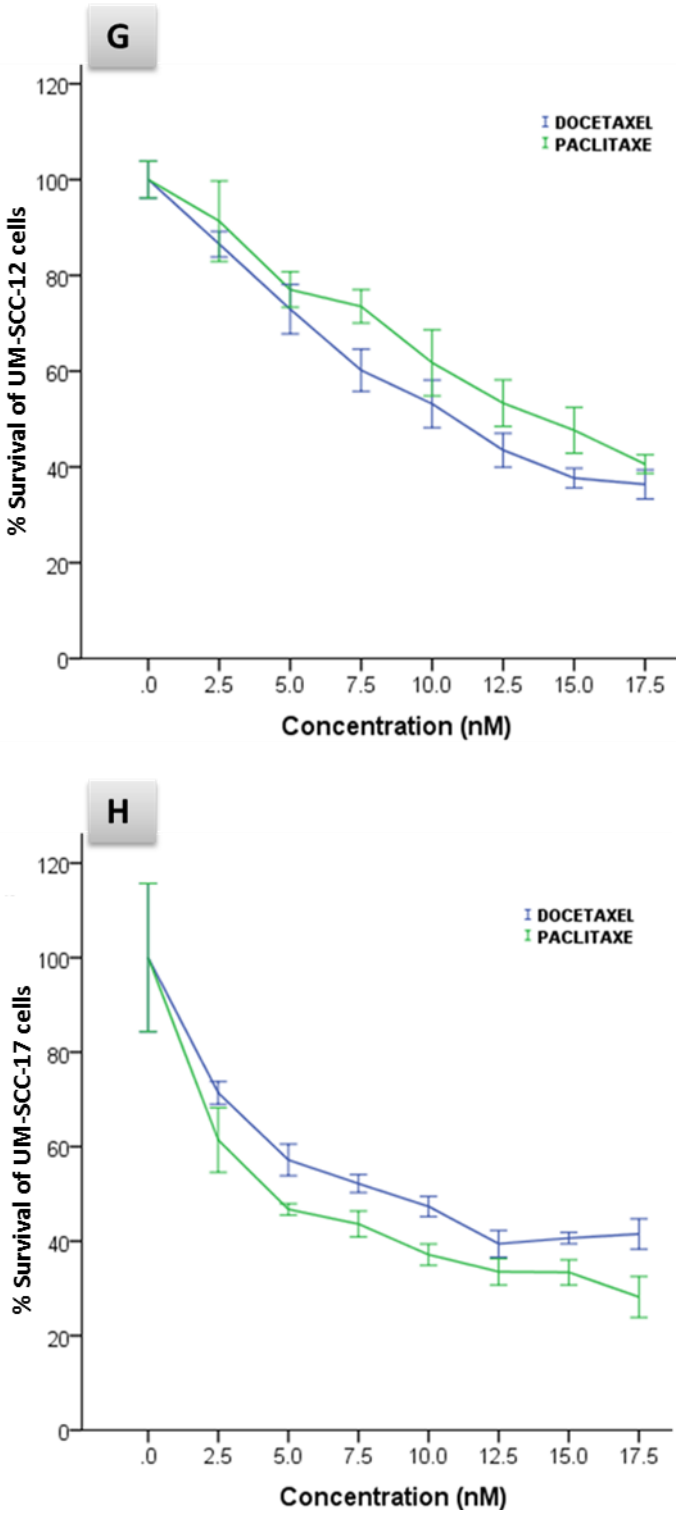

Figure 5.6.4: Taxane response of Head and Neck cancer cell lines (G) UMSCC-12 (H) UMSCC-17. UMSCC-12 cells are more sensitive to docetaxel than paclitaxel similar to most other cell lines. In contrast, UMSCC-17 is more sensitive to paclitaxel than docetaxel. The mean and error values are for six technical replicates and that one of two independent experiments is shown. Error bars in both line graphs represent 95% confidence intervals.

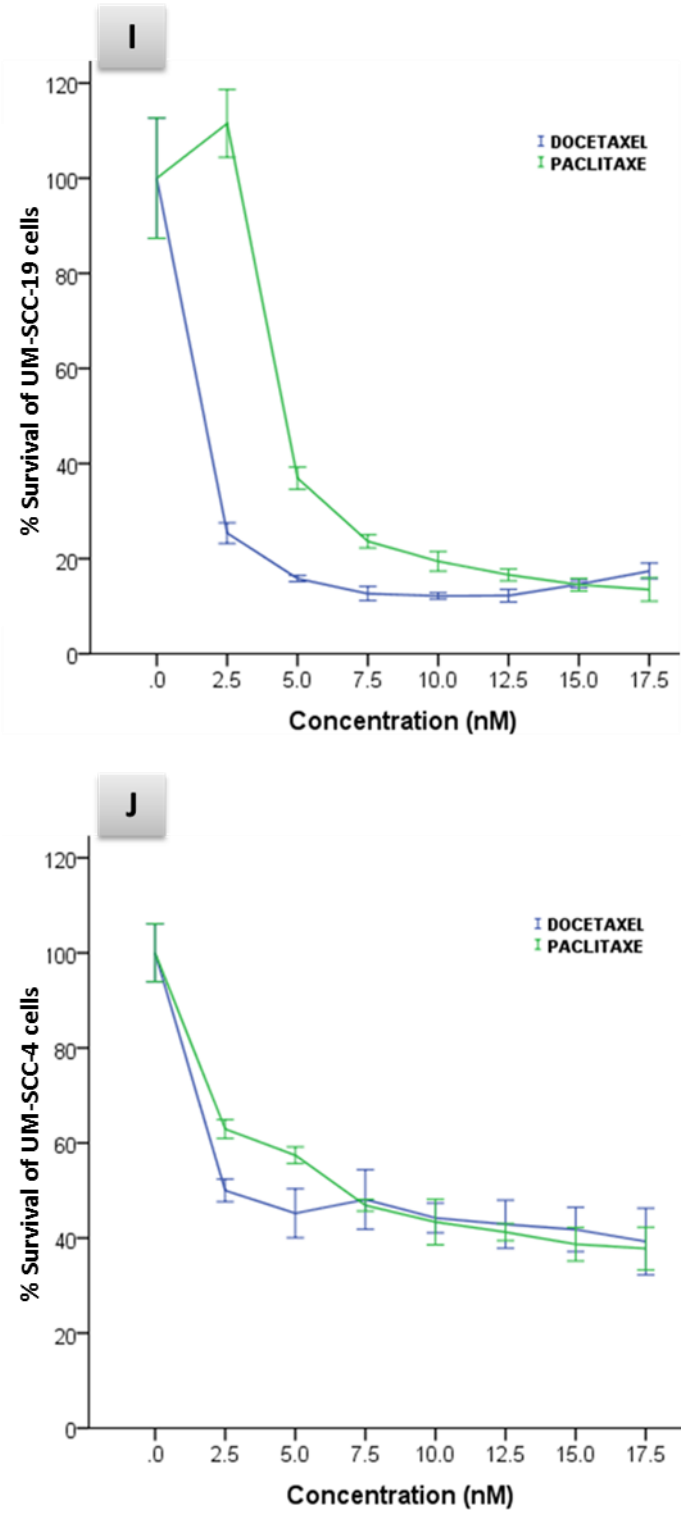

Figure 5.6.5: Taxane response of Head and Neck cancer cell lines (I) UMSCC-19 (J) UMSCC-4. In general, both cell lines are more sensitive to docetaxel than paclitaxel although taxane survival line graphs of UMSCC-4 cells show some overlapping in both taxane concentrations higher than 7.5 nM. The mean and error values are for six technical replicates and that one of two independent experiments is shown. Error bars in both line graphs represent 95% confidence intervals.

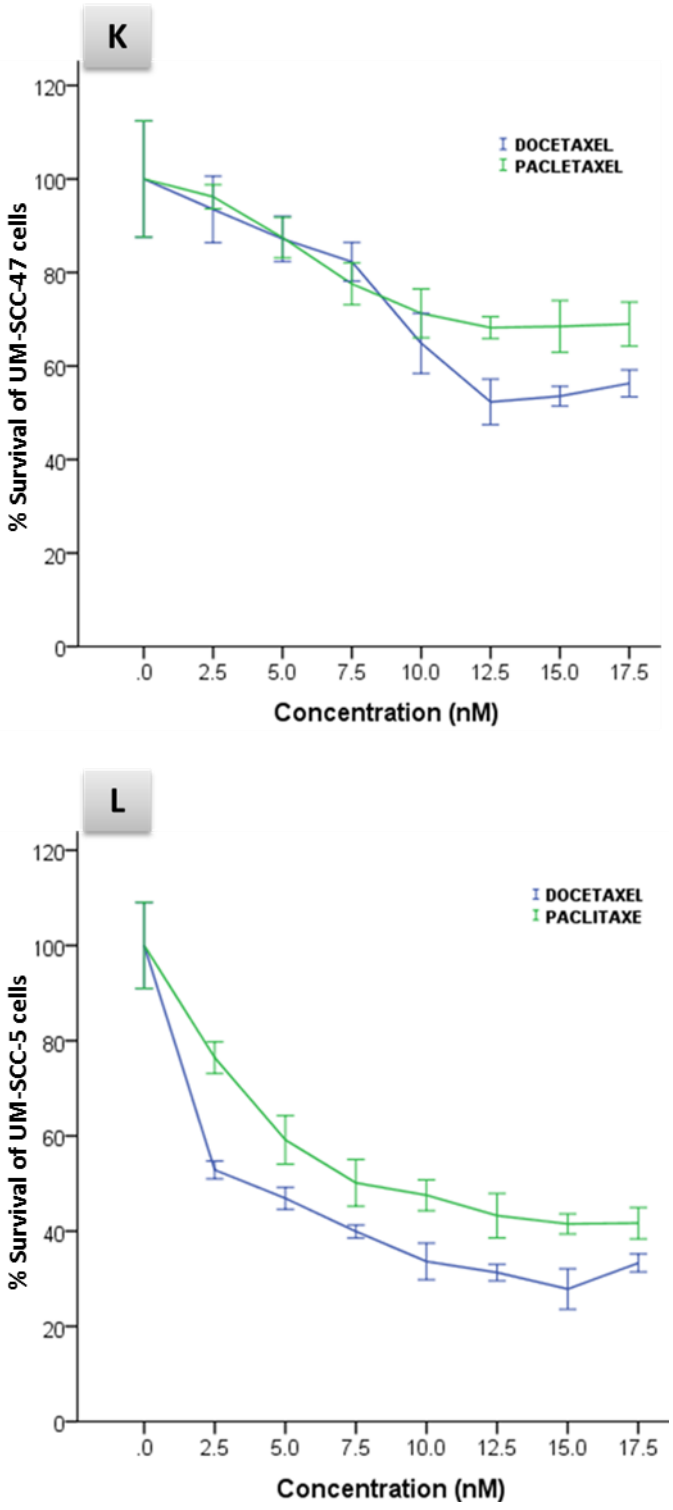

Figure 5.6.6: Taxane response of Head and Neck cancer cell lines (K) UMSCC-47 (L) UMSCC-5. The line graphs show the higher resistance of UMSCC-47 cell line to both taxanes. Generally, both cell lines are more sensitive to docetaxel than paclitaxel although taxane survival line graphs of UMSCC-47 cell line demonstrated some overlapping in response to both taxane at concentrations lower than 12.5 nM. The mean and error values are for six technical replicates and that one of two independent experiments is shown. Error bars in both line graphs represent 95% confidence intervals.

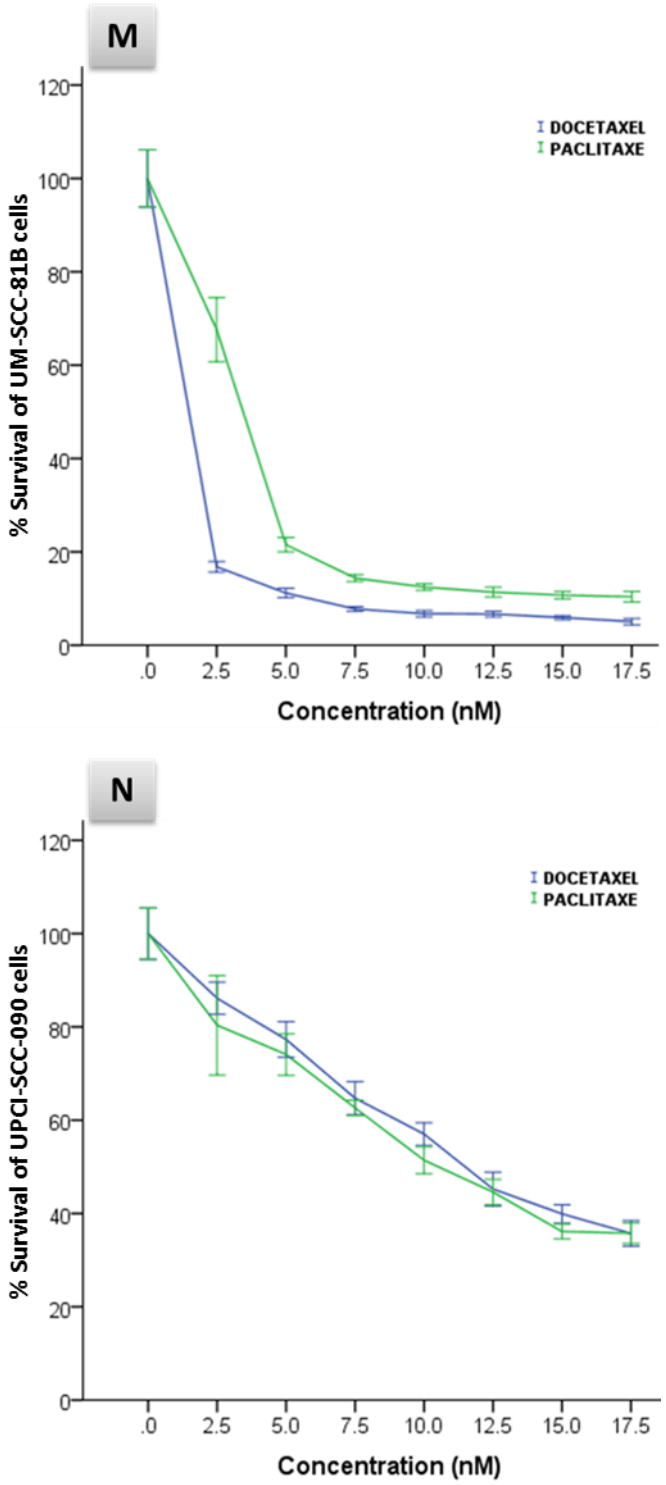

Figure 5.6.7: Taxane response of Head and Neck cancer cell lines (M) UMSCC-81B (N) UPCI-SCC-090. Similar with most other cell line, UMSCC-81B cell line is more sensitive to docetaxel than paclitaxel. However, UPCI-SCC-090 is the 3rd cell line that showing more sensitivity to paclitaxel than docetaxel in HNSCC group. The mean and error values are for six technical replicates and that one of two independent experiments is shown. error bars in both line graphs represent 95%CI.

The MTT analysis demonstrated that the most resistant cell line among all of examined RTCs cells was UMSCC-47 with IC50 values 32.9nM and 17.1nM for paclitaxel and docetaxel respectively, while the primary cell line Liv-7K was the most sensitive one, with IC50 values of 0.1nM for docetaxel and 0.6nM for paclitaxel (Table 5.3).

Based on a significant correlation observed between the expression of TPX2 and the doxetaxal IC50s of tested cell lines (Spearman's test, rho=- 0.78, p=0.013), the effect of modulation of TPX2 mRNA expression on doxetaxal sensitivity in CALU6 cell line was analysed. The data obtained from performing TPX2 mRNA knock down showed that TPX2 down regulation has a lethal effect in these cells (Figure 5.7). Therefore, I was not been able to perform further investigation regarding the effect of TPX2 knock down. The lethal effect of TPX2 knockdown was confirmed through informal communication with Dr Linardopoulos at ICR London.

Table 5.3: Data demonstrating the IC50 values with their respective 95% confidence intervals. The data showed that the HNSCC cells are ranged in their response both taxanes from the most sensitive cell line (Liv-7K) in green to the most resistant one (UMSCC-47) in red. In general, most cell lines were more sensitive to docetaxel than paclitaxel with three exceptions (UMSCC-104, UMSCC-17as and UPCI-SCC-090) where they were more sensitive to paclitaxel than docetaxel.

Cell line	IC50-Docetaxel	95%CI	IC50-Paclitaxel	95%CI
BHY	**11.8**	*10.9 - 12.7*	**14.0**	12.1 - 16.0
HN5	**2.0**	*1.8 - 2.3*	**3.7**	3.2 - 4.3
LIV-7K	**0.1**	*0.0 - 0.5*	**0.6**	0.3 -1.4
PE/CA-PJ15	**0.2**	*0.2 - 0.3*	**2.0**	1.8 - 2.4
PE/CA-PJ41	**0.3**	*0.1 - 1.2*	**2.5**	*1.7- 3.6*
UMSCC-104	**11.5**	*10.0 - 13.1*	**6.9**	*6.0 - 8.0*
UMSCC-12	**10.6**	*10.12- 11.1*	**13.9**	*12.7 - 15.1*
UMSCC-17as	**8.5**	*7.2 - 9.9*	**4.7**	*4.1 - 5.4*
UMSCC-19	**1.1**	*1.1 - 1.6*	**5.2**	*3.5 - 7.8*
UMSCC-4	**2.7**	*1.3 - 5.7*	**6.8**	*6.0 - 7.7*
UMSCC-47	**17.1**	*12.90- 22.6*	**32.9**	*18.2 -59.7*
UMSCC-5	**3.3**	*2.3 - 4.8*	**9.1**	*7.7 - 10.8*
UMSCC-81b	**0.2**	*0.2- 0.4*	**3.3**	*2.5 - 4.3*
UPCI-SCC-090	**11.5**	*10.7 - 12.2*	**10.5**	*9.4 - 11.8*

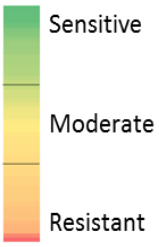

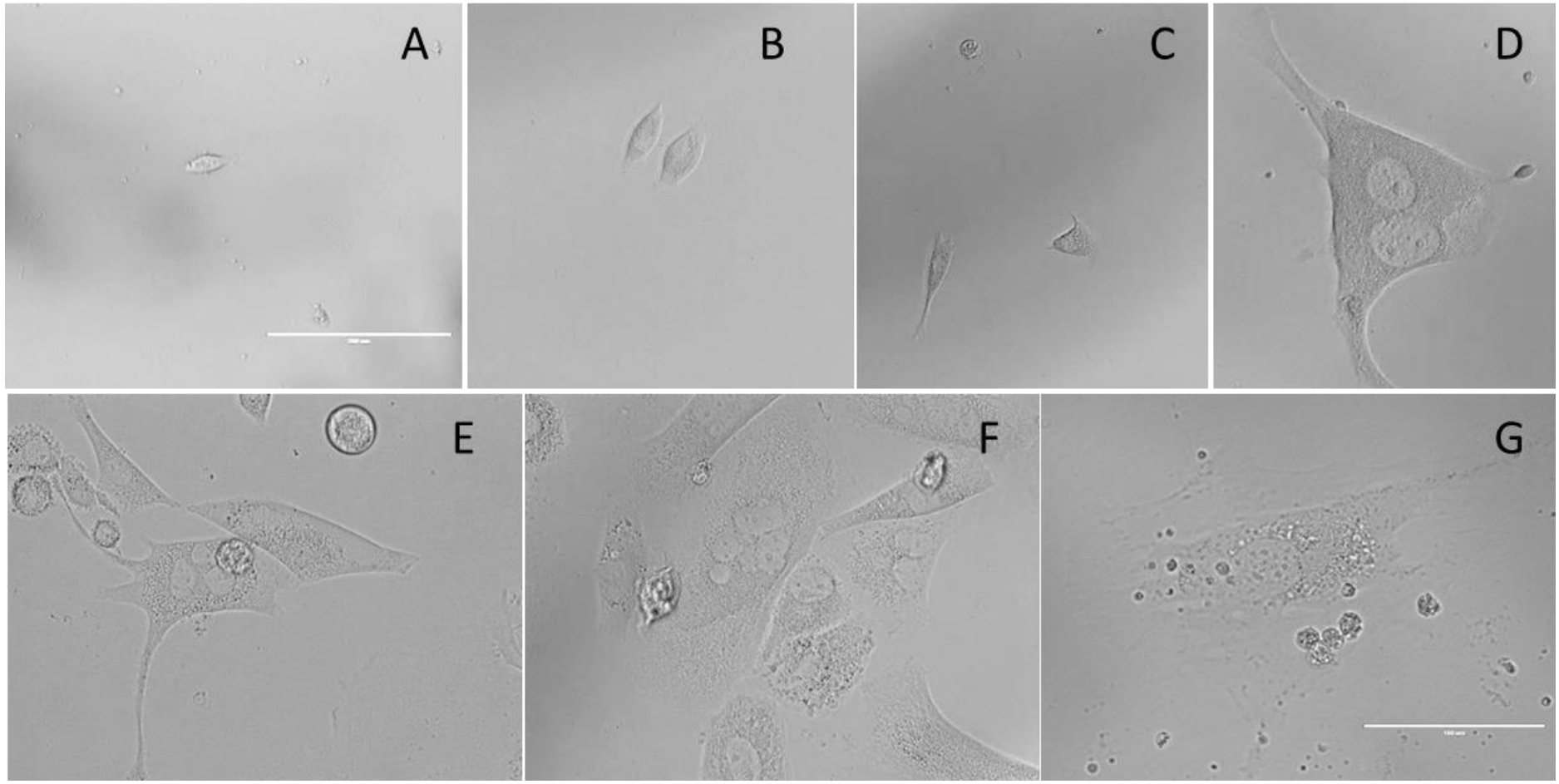

Figure 5.7: Microscopic pictures depicting a clone derived from *TPX2* shRNA-transfected CALU6 cells at different growth stages; (A) successful grown transfected single cell after 1 week of transfection. (B) first mitotic cell division of derived clone at week 2 (C) cell migration at week 3 (D) nuclear division of divided clones at week 4 (E) multi nuclear division with failing in cytoplasmic division at week 5 (F) poly-nucleation and failing in completing mitosis at week 6(G) cell death after 7-8 weeks. The magnification was 200μm for A, B and C, While 100μm for D, E, F and G.

In summary, the findings of the present study showed that of the 10 genes examined, only *AURKA* was significantly associated with prognosis in NSCLC. Multivariate Cox regression analysis showed that *AURKA* mRNA expression (Hazard Ratio (HR), 1.81; 95%CI 1.16-2.84, *P* = 0.009), age (HR 1.03; 95%CI 1.00-1.06, *P* = 0.020), pathological stage 2 (HR 2.43; 95%CI 1.16-5.10, *P* = 0.019), and involvement of distal nodes (pN2) (HR 3.14; 95% CI 1.24-7.99, *P* =0.016) were independent predictors of poor prognosis in patients with NSCLC. Poor prognosis of those patients with high *AURKA* expression suggests they may benefit from therapy with *AURKA* inhibitors. *TPX2* mRNA expression was associated with docetaxel IC50 values of tested cell lines (Spearman's test, rho=0.7, p=0.036).

Chapter 6: Epigenetic sensitization of respiratory tract cancer cells to paclitaxel

As epigenetic therapies have already been introduced into clinical cancer management (256), (257). I examined the potential sensitisation of lung and head and neck cancer cells to paclitaxel by two well-known epigenetic modifiers; the DNA methyltransferase (DNMT) inhibitor Decidabine and histone deacetylase (HDAC) class I inhibitor Valproic acid (VPA). These epigenetic modifiers can alter the response of cancer cells to paclitaxel treatment. Previous evidence suggested that VPA enhances paclitaxel cytotoxic effects in cancerous cells (258) due to HDAC6 deactivation, which results in tubulin hyperacetylation (259) and sensitises lung cancer cells to apoptosis (260). The combinatory effect of VPA-paclitaxel was also tested in HNSCC tumours (261). Aurora kinases also play a transcriptional regulatory role in HDAC inhibitors- mediated cytotoxicity in lung cancer cells (262). Recent reported data showed that enhancing p53 acetylation due to HDAC inhibition leads to enhance paclitaxel-induced apoptosis (263). In addition, a combination of VPA and decitabin has been introduced in clinical trials to treat NSCLC patients (256), (257). Based on aforementioned reported data, I investigated the epigenetic role of both the histone acetylator (VPA) and DNA methylator (decitabin) in sensitising RTC cells to paclitaxel.

I next examined the cellular response to VPA alone in order to select the concentrations below IC50 for further investigation of VPA ability to sensitise cancerous cells to taxanes. MTT analysis of VPA exposure of lung cell lines (A549 and SKLU1) and the 2nd most paclitaxel resistant oral cancer cell line (BHY) demonstrated that these cells are resistant to very high VPA micro-molar concentrations (Figure 6.1) with IC50s of 6.63 mM of A549,

20 mM of SKLU1 and 2.1 mM of BHY) (Table 6.1) at 95% CI. In order to examine the ability of valproate to potentiate the anti-tumour efficacy of paclitaxel in controlling cellular viability, I used two different doses of valproate 0.5 mM and 1 mM that are below IC50s of all of these three cell lines. I utilised a fixed dose of paclitaxel (10 nM) which was also under the IC50s of the studied cell lines; 13.6 nM of A549, 16.7 nM of SKLU1 (Chapter 3, Table 3.2) and 14 nM of BHY (Table 6.1). The growth inhibitory effects of 1 mM VPA and 10 nM paclitaxel were determined as optimal doses utilised either in combination or as successive treatments of the cell lines, A549, SKLU1 and BHY. The synchronous treatment of VPA and paclitaxel produced only a minor additive effect (Data not shown). In contrast, when VPA used to treat the cell for 48 hours prior to paclitaxel addition, a significant increase of the paclitaxel toxicity was observed in the subsequent 72 hours (Figure 6.2).

Interestingly, mRNA expression of *AURKA* in BHY cell line was significantly reduced to around 65% after treatment with 1 mM VPA for 48 h (Figure 6.3). I also examined how the status of tumour suppressor gene *p53* could affect the paclitaxel sensitisation of HBEC cell lines to paclitaxel. The results demonstrated that the VPA exhibited more efficiency in sensitising p53 wild type HBEC cells to paclitaxel than that exhibited in sensitising p53 knockouts and thus p53 expression seems to increase the cytotoxic effect of paclitaxel after course exposure to 0.5 mM VPA although pre-treatment of HBECs with 1 mM VPA shows different trend (Figure 6.4). The efficiency of decitabine treatment of A549 was determined at different concentrations (50, 100 and 200 μM) by measuring the global methylation levels (LINE1 element) (Figure 6.5). This agent showed a dose-dependent efficiency to demethylate A549 cellular DNA (Figure 6.6). Although decitabine was

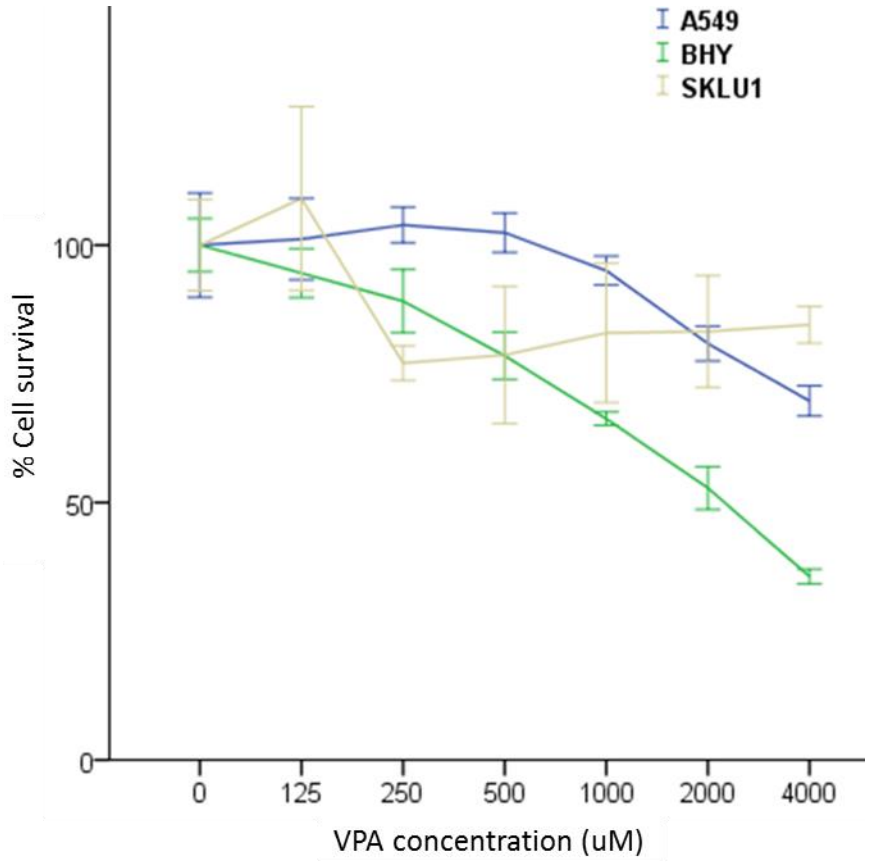

Figure 6.1: MTT line ghraph showing the cellular survival rates of lung (A549 and SKLU1) and HNSCC (BHY) cell lines to VPA. Error bars were represent 95% confidence intervals.

Table 6.1: The data demonstrating the IC50 values of VPA in A549, SKLU1 and BHY cell lines and their respective 95% CI. The results demonstrate that SKLU1 cell line is the most resistant to VPA with IC50 value 20 mM VPA, while BHY is the most sensitive one IC50 value 2.1 mM VPA.

Cell line	VPA IC50 (mM)	95% CI
A549	6.63	5.77 to 7.63
SKLU1	20.00	11.80 to 33.92
BHY	2.10	1.94 to 2.27

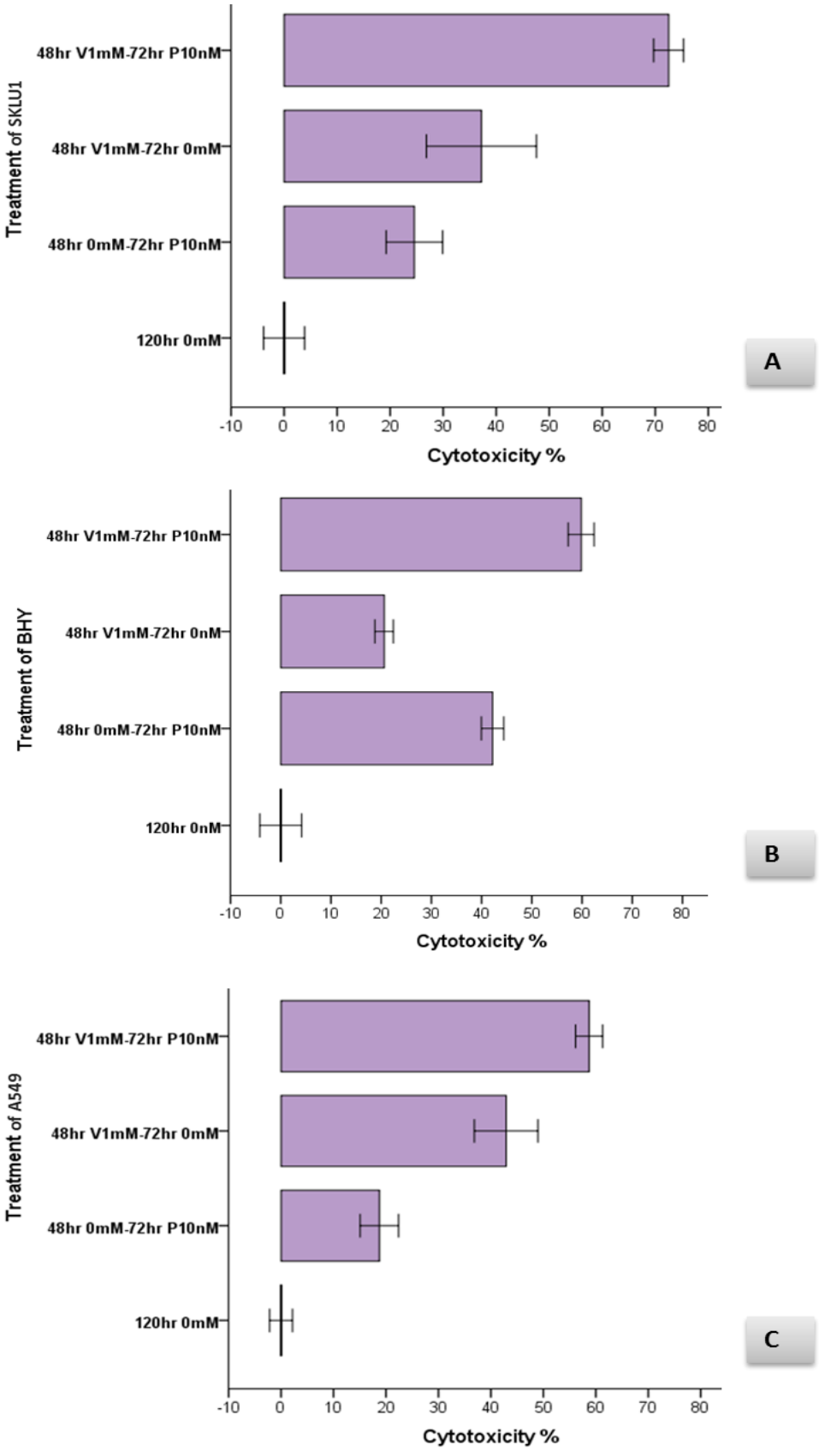

Figure 6.2: Bar charts of cytotoxic effects of 48-hour treatment with 1 mM VPA flowed by 72 hours of 10 nM paclitaxel on A549 (A), BHY (B) and SKLU1 (C) cell lines. Interestingly, SKLU1 cell line exhibited more response to paclitaxel after 48hr exposure to VPA. BHY showed different trend of response to treatment of VPA and paclitaxel separately compared to A549 and SKLU1 cell lines. Error bars represent 95% confidence intervals.

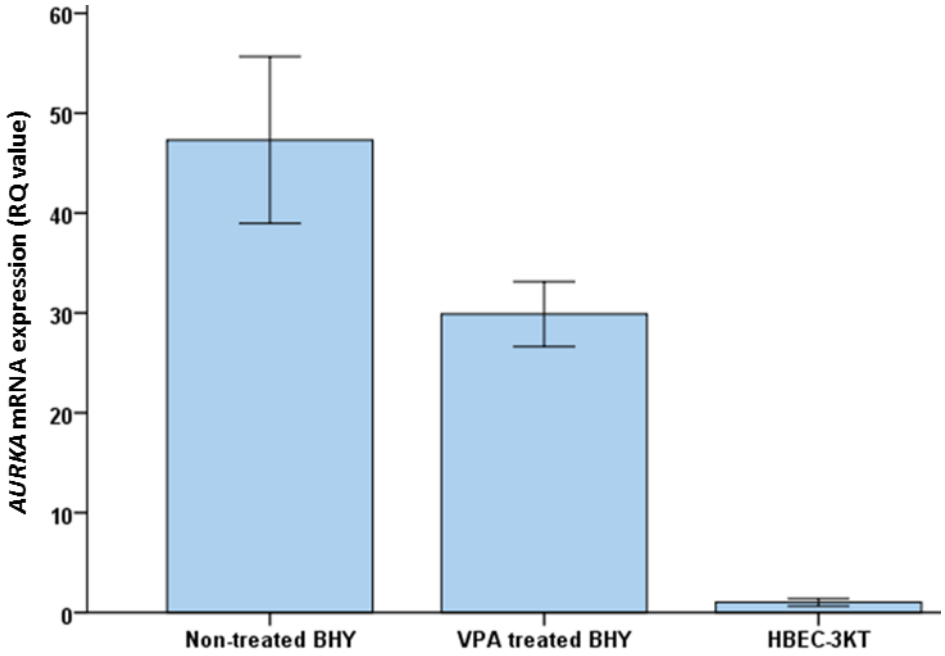

Figure 6.3: *AURKA* mRNA expression in VPA-treated BHY cells with 1mM concentration compared with non-treated in comparison with HBEC-3KT control. VPA treatment seems to reduce *AURKA* expression to around 65%. Error bars were represented 95% confidence intervals.

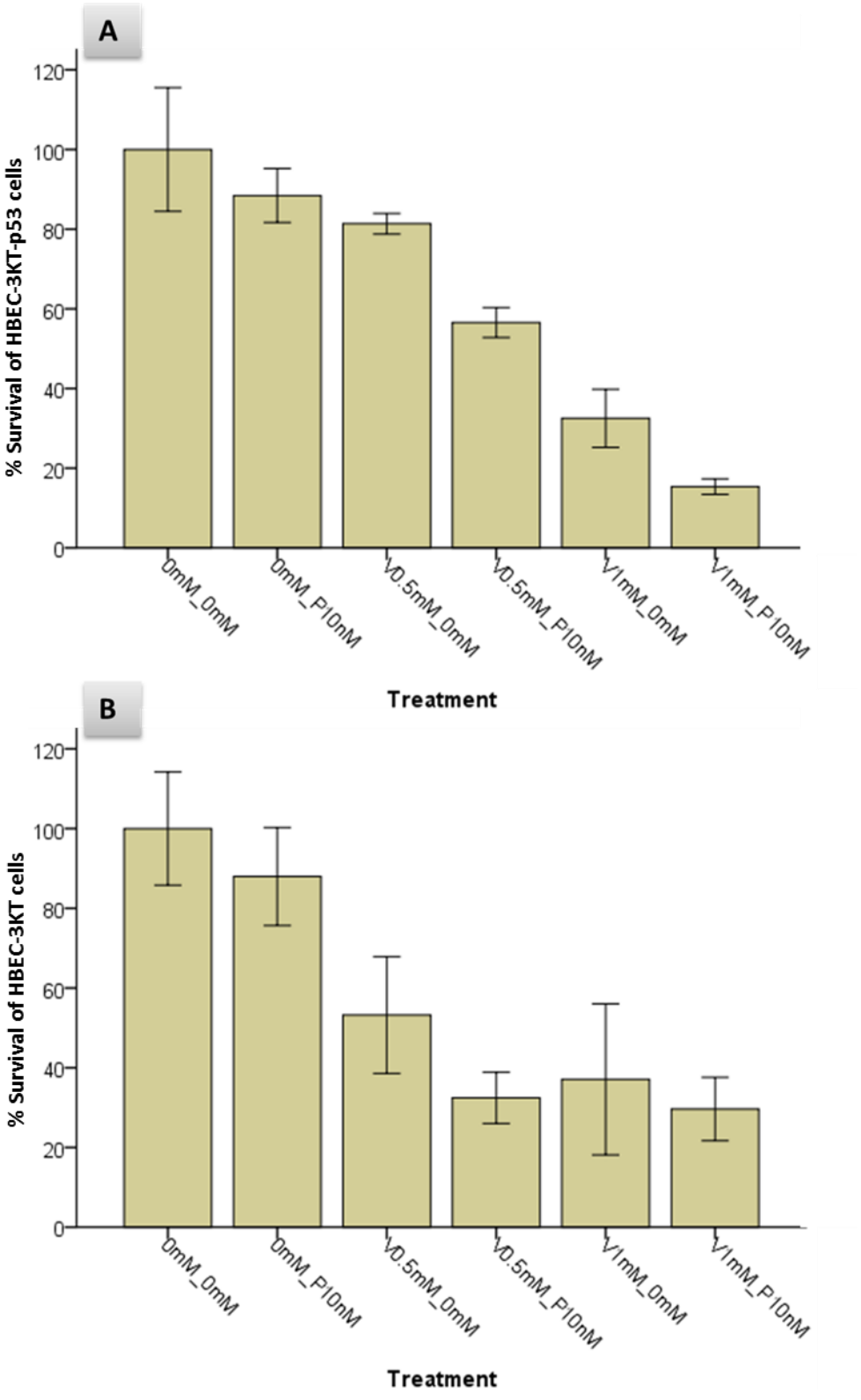

Figure 6.4: Bar charts of cytotoxic effects of 48-hour treatment with 1 and 0.5 mM VPA flowed by 72 hours of 10 nM paclitaxel on HBEC-3KT (A) and HBEC-3KT-p53 (B) cell lines. P53 wild type HBEC cells showed more response to 10nM paclitaxel after 48 hr exposure to 0.5 mM VPA compared to p53 knockouts. However, increasing VPA concentration to 1mM no more effect in HBEC-3KT as opposed to more effect in HBEC-3KT-p53. Error bars were represented 95% confidence intervals.

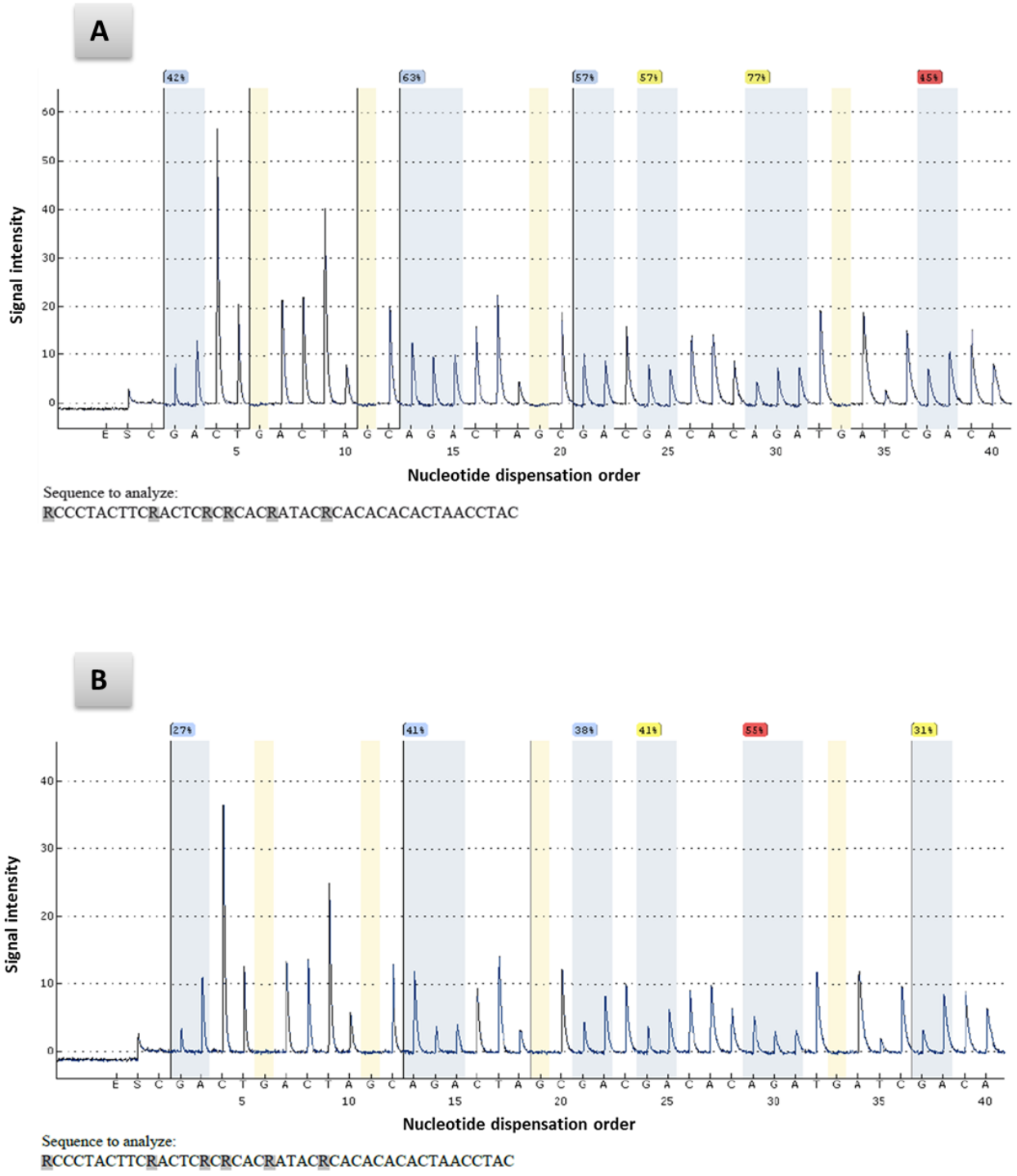

Figure 6.5: Pyrograms of LINE1 global methylation analysis demonstrating the cellular DNA methylation status of A549 cell line in the absence (A) and presence (B) of decitabine at 200 mM.

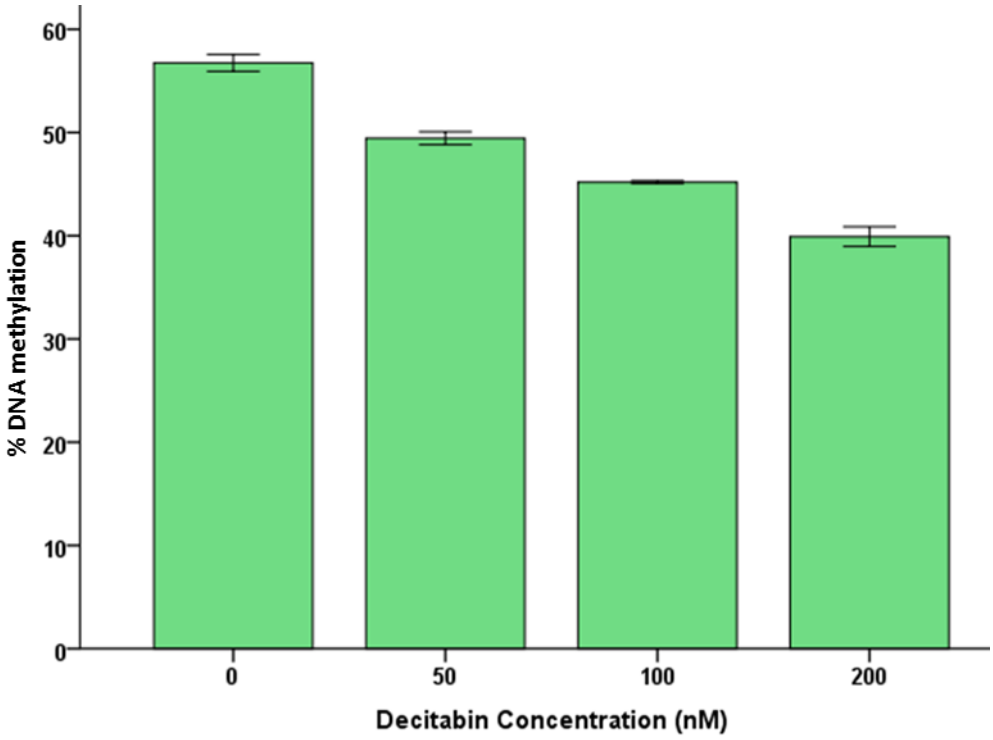

Figure 6.6: The bar chart demonstrating the change in the methylation status of LINE-1 following treatment of A549 with the demethylating agent decitabine at different concentration (0, 50, 100 and 200) μM. The results showed that reduction of the methylation level correlated with increasing decitabine dose. Error bars represent standard error of the mean.

efficient in reducing global LINE methylation, it did not sensitise any of the cell lines to paclitaxel when used either in a synchronous (Figure 6.7) or in a preceding manner (data not shown). In order to provide insight into the inability of decitabine to sensitise cell lines to paclitaxel, I investigated the methylation status of the different gene promoters tested in this study. The pyrosequencing analysis demonstrated that none of the gene promoters examined in this study demonstrated altered methylation status; in fact, all of promoters were unmethylated in all of tumour and normal tissues tested (Figures 6.8).

In summary, VPA was an effective epigenetic sensitizer for treating lung and head and neck cancerous cells (A549, SKLU1 and BHY). 48 hours prior to paclitaxel addition, a significant increase of the paclitaxel toxicity was observed when the cancer cells pre-treated with VPA for 48hr and subsequently with paxlitaxel for 72 hours. Interestingly, mRNA expression of *AURKA* was reduced by VPA treatment. The result also demonstrated that *p53* status was involved in VPA- mediated paclitaxel sensitisation of HBEC cell lines to paclitaxel. VPA seems to potentiate p53 wild type cells (HBEC-3KT) to paclitaxel, while p53 HBEC knockouts showed less cytotoxic effect of paclitaxel after exposure to 0.5 mM VPA.

On the other hand, decitabin was not efficient to sensitise any of the cell lines to paclitaxel when used in either a synchronous or a preceding manner. In addition, the pyrosequencing analysis of the methylation status of the different gene promoters in the lung tumour and normal tissues showed that all of the promoters were unmethylated.

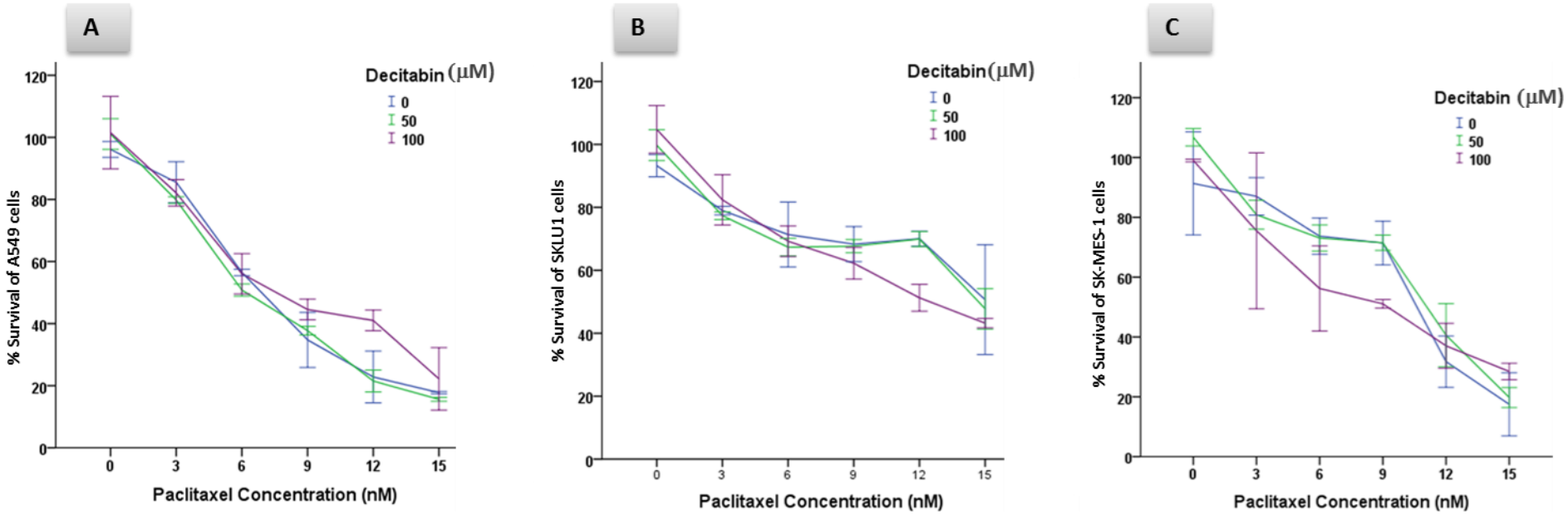

Figure 6.7: MTT line graphs showing the sensitivity of A549 (a), SKLU1 (b) and (c) SKMES1 cell lines to paclitaxel in the presence of differing concentrations of decitabine (0, 50 and 100 μM. The data of showed no significant difference in cellular response to treatment with paclitaxel alone or in combination with decitabine. Error bars were represented 95% confidence intervals.

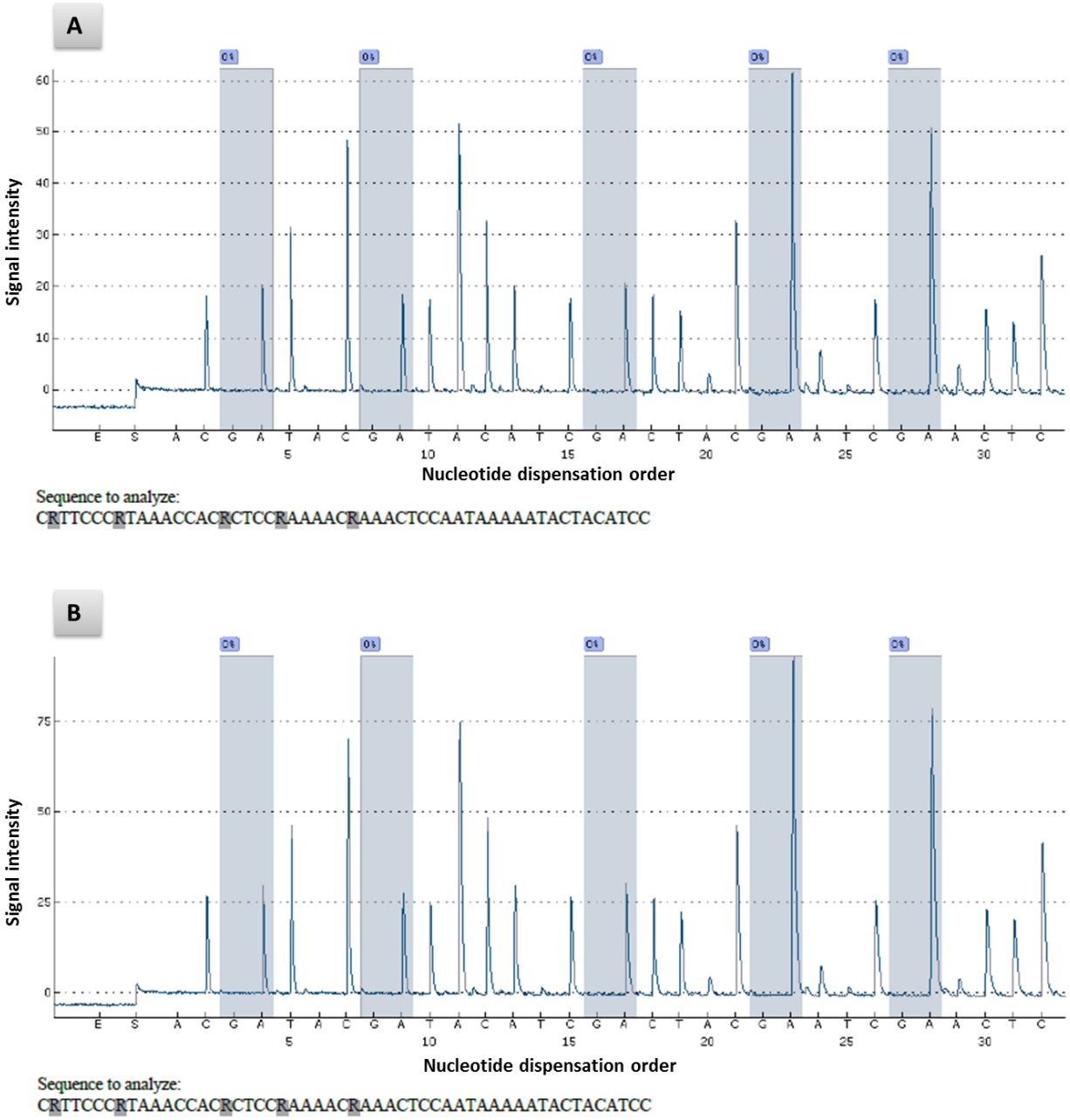

Figure 6.8: representative programs showing DNA methylation status of *KIF11* gene promoter in (A) tumour and (B) normal lung samples. The figures show that the gene promoters were unmethylated in both malignant and normal tissues of the lung.

Chapter 7: Discussion

Mitotic spindle formation and spindle checkpoint are extremely important for the maintenance of correct cell division. The accurate chromosome alignment and their proper attachment to the mitotic spindle are ensured by spindle checkpoint, prior to chromosome segregation (183), (184). Taxanes are anti-mitotic agents, commonly used in a variety of human cancers including those of the lung (138) and head and neck (139). Their limited clinical success is largely due to development of resistance by the neoplastic cells. However, despite the clinical use of taxanes for almost two decades in cancer therapeutics, little is still known about the mechanisms contributing to this resistance and thus potential response predictors to taxane-based regimens. The present study demonstrated that both AURKA and AURKB are potential modulators for taxane resistance in RTCs cells, despite their reciprocal prediction to these antimitotic agents. The findings collectively demonstrated a high potential for further exploitation of the spindle assembly associated genes in developing prediction biomarkers for clinical use.

7.1 Aurora kinase A involvement in docetaxel resistance in NSCLC

Aurora kinase A is frequently upregulated in many malignancies and its oncogenic activity implicated in malignancy transformation of cancerous tissues (196). This study demonstrated the frequent mRNA over-expression of *AURKA* in NSCLC cells and tissues compared with normal ones. My findings confirmed the previously reported data of AURKA overexpression of in NSCLC (264), and similar to other findings (209). *AURKA* mRNA overexpression was more evident in SqCC than AdC. However, the information on the prognostic value of AURKA in this tumour type remains to be examined. In present study a significant correlation was established between the elevated levels of *AURKA* transcripts

and shortened overall survival in NSCLC patients. In contrast to data from (265), the negative prognostic significance of AURKA expression in my data holds true for both histological subtypes. A consensus on this issue is missing, with some groups reporting that levels of Aurora A are associated with poor prognosis in SqCC (210), while others do not (209). Furthermore, perimembrane IHC staining was shown as a strong predictor of poor prognosis in SqCC, but not in AdC patients (206), while recent microarray data analysis demonstrated that *AURKA* mRNA overexpression is associated with poor prognosis in AdC but not SqCC (265). Therefore, recent published data demonstrates the inconsistencies in the field, probably due to differences in the study designs, methodology of Aurora A expression assessment and the occasional inclusion of therapy stratification in the survival outcome. However, in my study, mRNA levels of *AURKA* were associated, and thus may be considered as a candidate prognostic biomarker, in both histological subtypes.

The functional part of this study has clearly demonstrated that suppression of *AURKA* mRNA expression, using shRNA-specific knock down, increased docetaxel response in NSCLC cells. AURKA suppression dependent differential docetaxel cytotoxicity has been previously shown in esophageal squamous cell carcinoma (ESCC) (266), prostate cancer cells in vitro (267) and in vivo (268), renal cell carcinoma (RCC) cells (269) and breast cancer cells (270), however this is the first such report to my knowledge on lung cancer cells. The present study is also in agreement with previously reported data, which showed that combined docetaxel with alisertib-based AURKA deactivation resulted in increased docetaxel anti-tumour activity in upper gastrointestinal adenocarcinomas (271), breast cancer (272) and mantle cell lymphoma (273). It was also reported that co-treatment with docetaxel and MK-5108, another selective Aurora A kinase inhibitor, in NSCLC cell lines, (274) and HeLa cells in in vitro and in vivo (275) enhanced cytotoxic effect of docetaxel.

AURKA suppression induces aneuploidy, polyploidy, and mitotic perturbation in cells and thus cancerous cells exposure to alisertib increases proportion of polyploidy cells leading to mitotic catastrophe (271). Docetaxel perturbs spindle assembly and function due to microtubule stabilisation and activates SAC. It induces either aberrant mitosis then aneuploidy at low concentration or sustained mitotic arrest then mitotic slippage at higher concentrations forming polyploidy cells (276). AURKA overexpression enables the polyploidy cells to abrogate the SAC and confer resistance to taxanes (277). Cellular exposure to docetaxel accumulates cells in the G1 cell cycle stage, activating SAC and then apoptotic pathways (276) accompanying the p53 induction (269). AURKA-overexpressing cells can easily override a transient and weak SAC activation induced by low docetaxel concentrations (278). However, AURKA suppression leads to prolonged activation of docetaxel-induced SAC that subsequently accelerates mitotic exit due to mitotic slippage. These cells re-enter G1 phase with a tetraploid genome and multinucleated phenotype (279). These cells then undergo endoreduplication process due to hyper-karyokinesis forming polyploidy cells (272) And this eventually leads to apoptosis due to induction p53 and its target bax (267). This mechanism was described in NSCLC cell lines as a result to integration of docetaxel treatment and selective Aurora A kinase inhibition by MK-5108 (274).

Despite the fact that the previous studies employed either shRNA-based suppression of *AURKA* mRNA or alisertib-mediated deactivation of Aurora A kinase in enhancement of docetaxel antitumor activity in a number of cancers, employing of which method in sensitising NSCLC cells to docetaxel has not yet been examined. This study, therefore, provide functional evidence demonstrating the AURKA involvement in the efficiency of docetaxel. These results suggest that AURKA could be used two-fold in the clinical

management of lung cancer: (a) as response prediction biomarker for paclitaxel based therapy for NSCLC cancer and (b) by using AURKA selective inhibitors to sensitise tumours to docetaxel treatment. Docetaxel was clinically approved for NSCLC therapy since last decade, (280), while alisertib has very recently clinically approved in treatment of RTC including NSCLC and HNSCC (281). Assuming that my findings in modulation of cellular response to taxanes could be reproduced in NSCLC cases, then a potential scheme of stratifying those patients to taxane-involving schemes could be explained as a scatter plot model (Figure 7.1). As shown in this model, most cases could potentially benefit from integrative therapy of both docetaxel-alisertib combination and paclitaxel-based therapy as an effective therapeutic manoeuvre could apply on NSCLC patients whom tumours overexpressed *AURKA*. This may also give good prognostic outcome. While additional preclinical work can provide further support, alisertib has already gained FDA approval, therefore clinical trials can simultaneously start being designed.

7.2 Aurora kinase B expression can predict response of NSCLC to paclitaxel

Aurora kinase B is an important contributor to the mitotic spindle assembly and its overexpression in human cancer has been frequently reported (282), (283), (284), therefore attracting the interest both in cancer biology and cancer therapeutics fields. In this study, it is hypothesized that Aurora B activity may be implicated in modulating cellular response to taxanes, due to its function in microtubule stabilisation. mRNA profiling of the surgical non-small cell lung tumour cohort confirmed the extensive overexpression of this gene, which has previously reported (207), (211), (212). In contrast to Vischioni et al and Takeshita et al, who profiled NSCLC tumour for Aurora B protein by IHC, I did not observe significant associations between *AURKB* expression and clinicopathological factors (211), (207). This may suggest that post translational regulation may contribute to this difference,

as it is probable that the protein expression may not accurately reflect the level of mRNA expression for a particular gene. Nevertheless, two other studies attempted to correlate *AURKB* mRNA expression with the clinicopathological data; one has not found a significant association between these data and the mRNA expression (212), while the second conducted this correlation by testing more than one cohort; one cohort showed a clear link while the second, however, has not revealed that marked link (213).

I also analysed *AURKB* mRNA expression profiling in nine NSCLC cell lines from different histologic subtypes; SqCCL, LAdC and Large cell lung carcinoma in addition to HNSCC cell lines. This screening intended to confirm the expression patterns identified in primary lung cancer tissues earlier, as well as to investigate the potential involvement of AURKB in cellular resistance to taxanes. In consistence with previously reported data (285), the present study demonstrated that AURKB is frequently overexpressed in lung cancer cells in comparison with immortalised non-tumorigenic HBECs. This may reflect the potency of upregulated Aurora B in overriding mitotic spindle checkpoint and its overexpression seems to be the driving power behind aneuploidy formation during cancer progression via augmented mitotic phosphorylation of histone H3 at Serine-10 (286).

The outcome of taxane response in most RTCs cells showed that the IC50 values for docetaxel were consistently lower to those of paclitaxel except SKLU1 from NSCLC cells and UMSCC-17as, UMSCC-104 and UPCI-SCC-090 from HNSCC cells. These results are in agreement with previously reported data in in vitro, ex vivo and in vivo study (175) as well as randomized phase III clinical study (176). Regarding the HNSCC cell lines (UMSCC-17as, UMSCC-104 and UPCI-SCC-090), the possible explanation for this difference may due to the difference in HPV status in these cell lines. It has been recently investigated HPV status in

these HNSCC cell lines and reported that most of the cells are HPV negative except UPCI-SCC090 and UMSCC-104 (287), (288) but also UMSCC-47. In addition, HPV status of UMSCC-17as is not reported. Therefore, this may partially explain the results and further investigation is warranted in this regard.

The findings have also provided clear evidence of correlation between the AURKB overexpression of NSCLC cell lines with response to paclitaxel. However, there was no correlation detected between the expression and taxane response in HNSCC. This may due to the difference in the origin of both cell types. Interestingly, low levels of mRNA expression of *AURKB* in NSCLC cell lines were observed to correlate with resistance to both taxanes. However, functional experiments involving knockdown and chemical inhibition of AURKB demonstrated a stronger involvement of AURKB in paclitaxel rather than docetaxel cytotoxicity. This may support my hypothesis that AURKB is a potential predictor for paclitaxel-based regimen for treating lung cancer. Docetaxel induced-apoptosis occurs at 100 fold lower concentrations than that of paclitaxel (179) with higher affinity for β-tubulin (180), and broader cell cycle effectiveness in three phases (S/G2/M) compared with two (G2/M) for paclitaxel. However, paclitaxel, occasionally, manifests more anti-tumour activity (177). The reason behind this variation is not fully understood. Docetaxel mainly targets centrosome organization leading to incomplete mitosis and cell damage in S phase with partial toxic effect during mitosis. It is known that AURKA is mainly involved in centrosome maturation (214), (196), whereas paclitaxel affects the mitotic spindle causing cell death (182). This difference in site of action may explain some difference in their efficacy in killing cancer cells and may also give insight on my finding of that the substantial

difference of both Aurora A and B down regulation involvement in taxane-based treatment.

In order to functionally test the hypothesis in this chapter, two different approaches were followed, the cell sensitivity to paclitaxel was first measured after establishing AURKB knockout derivative clones from A549 and SK-MES1 employing multiple shRNA constructs. I then went on to inhibit Aurora B protein activity in these cell lines along with SKLU1 using highly selective Aurora B inhibitor (Barasertib). Similarly to cellular inhibitory effects of other selective Aurora B inhibitors such as Hesperadin (169) and ZM447439 (170), very low levels of barasertib resulted in significant cytotoxicity to lung cancer cells (IC50 0.9-2.3 nM). Barasertib treated cells may undergo failed mitotic cell division and endoreplication leading to polyploidy due to blocking of Histone H3 phosphorylation on serine 10, the most important substrate of Aurora B (254) , (253). The key role of mitotic spindle checkpoint is to ensure that the metaphase-to-anaphase transition is not occurred until an accurate attachment of sister kinetochores to spindle microtubules is happened in correct biorientation (289). This amphitelic attachment is promoting by Aurora kinase B that localises in the inner centromeric gap/region, midway between kinetochore pairs, during mitosis.

Aurora B mutation (290), inhibition using small-molecule inhibitor, or depletion using small inhibitory RNA (169) leads to chromosomal missegregation due to increasing synthetic attachment of microtubules with kinetochore pairs, in spite of remaining a full capability of mitotic spindle to attach to sister kinetochores and pull them on (169), (291).

It was reported that depletion of Aurora B selectively using Hesperadin in presence of paclitaxel leads to abrogating this checkpoint (169). It was also reported that Aurora kinase

B inhibition using AT9283 could be targeted to increase cellular response to antimitotic agents. This kinase inhibition causes slowing or arrest of the cell growth during mitosis when co-treating either with paclitaxel (292) or with docetaxel (293). AT9283, however, is a dual kinase inhibitor of both Aurora A & B. This combinatory effect could be due to inhibitory effect of AT9283 on both kinases. While Curry et al do not consider the possibility of Aurora A inhibition by AT9283 and suggest employing Aurora B inhibition to potentiate paclitaxel's effect, Qi et al referred to a possible role for Aurora A inhibitory effect of AT9283 in sensitising cells to docetaxel. Likewise, I could argue that (294) study of depicting the enhancing of taxane antitumor activity by AMG 900, the pan Aurora kinase inhibitor, was merely caused by inhibiting Aurora B kinase activity. In addition, all of the three aforementioned studies lack of supporting evidence that could further prove their explanation in favour of Aurora B, for instance using specific Aurora B-RNA interference (RNAi) to gain that evidence. Therefore, identifying ATP competitive molecules that inhibit Aurora B selectively may make the high homology degree among Aurora kinases (295) less challenging.

The selective Aurora kinase B inhibitors, such as barasertib (254) Hesperadin (169) and ZM447439 (170), induce mitotic arrest and polyploidy leading to apoptosis in leukaemia cells. This occurs in the same Aurora B inhibition dependent manner regardless of the Aurora B expression level. The kinase inhibitory effect of each selective inhibitor is different, for example the inhibitory effect of barasertib is higher than that of ZM447439 (296). Supporting evidence from (169) and (170) studies can assist interpretation of my findings, i.e. that both AURKB down-regulated clones and barasertib-treated cells demonstrated resistance to paclitaxel. Paclitaxel arrests cells by activating mitotic spindle

checkpoint in the presence of Aurora b activity, which maintains a dynamic rhythm between attached kinetochore with those unattached (169), (170). Anaphase onset is initiated by activating anaphase-promoting complex (APC). This activated complex is supressed by the mitotic spindle checkpoint if any sister kinetochore is incorrectly attached with spindle microtubules. This improper attachment recruits mitotic spindle checkpoint components, such as kinetochore-associated protein Mad2, to deactivate APC (169). Like other spindle checkpoint regulators, Mad2 localises to unattached kinetochores and this localisation is indispensable for spindle assembly checkpoint signalling (221), Although Aurora B inhibition reduces high proportion of kinetochore-associated protein Mad2 (297), the residual attached protein may be sufficient to maintain the mitotic checkpoint in absence of kinetochore–microtubule interactions and/or tension. If microtubule occupancy is adequate for unattached kinetochore then this could inactivate MSC and, in turn, activate APC to promote anaphase onset (170).

Accordingly, the possible explanation of why paclitaxel-treated cells cannot be arrested in the absence of Aurora B function could be that the stabilising syntelic kinetochore, and may be monotelic, attachments increase the possibility of inhibiting mitotic checkpoint signalling in paclitaxel-exposed cells caused by Aurora b deactivation using Barasertib. This is possibly because all kinetochores gradually accumulate depolymerized attached microtubules (298). Therefore, no free-attached Mad2 that could inhibit APC by the mitotic checkpoint thus co-treated cells enter anaphase and, eventually, exit mitosis.

In addition to the qualitative Aurora B inhibition that could results in abolishing the spindle assembly checkpoint in paclitaxel-arrested cells, the findings clearly demonstrated the quantitative effect of this inhibition in paclitaxel efficacy. Lower levels of Aurora B

decreased response to paclitaxel in all of the three cell lines, but intermediate levels of Aurora B had an intermediate effect on paclitaxel resistance. Therefore, the response to paclitaxel seems to rely on the level of Aurora B activity. The outcomes are keeping with (90); this study reported that decreased Aurora B activity, using either selective inhibition or mutation, raised the cellular resistance to paclitaxel. Interestingly, when Aurora B activity is only slightly increased (in the kinase activation defective mutant compared to the kinase-binding defective mutant), it appears to intensify the response to low dose paclitaxel, but Aurora B activity is not necessary for response to high doses of paclitaxel (90).

In conclusion, the results confirm previous reports on the significant overexpression of the AURKB in NSCLC tissue and its association with NSCLC patient survival, pointing to a potential exploitation for therapeutic stratification of NSCLC patients into taxane-involving regimens. I have shown that high *AURKB* expression is associated with sensitivity to paclitaxel and that AURKB inhibition or down-regulation leads to paclitaxel resistance.

The important translational message from this study is that; while AURKA inhibitors could be utilised in combination with docetaxel to overcome the resistance demonstrated by many lung tumours that overexpress Aurora kinase A, AURKB inhibitors should be avoided if treating with paclitaxe. Nontheless, high AURKB expression could benefit as a candidate biomarker for stratification of lung cancer patients to paclitaxel therapy (Figure 7.1). The molecular basis of these interactions is described in my proposed model presented in Figure 7.2.

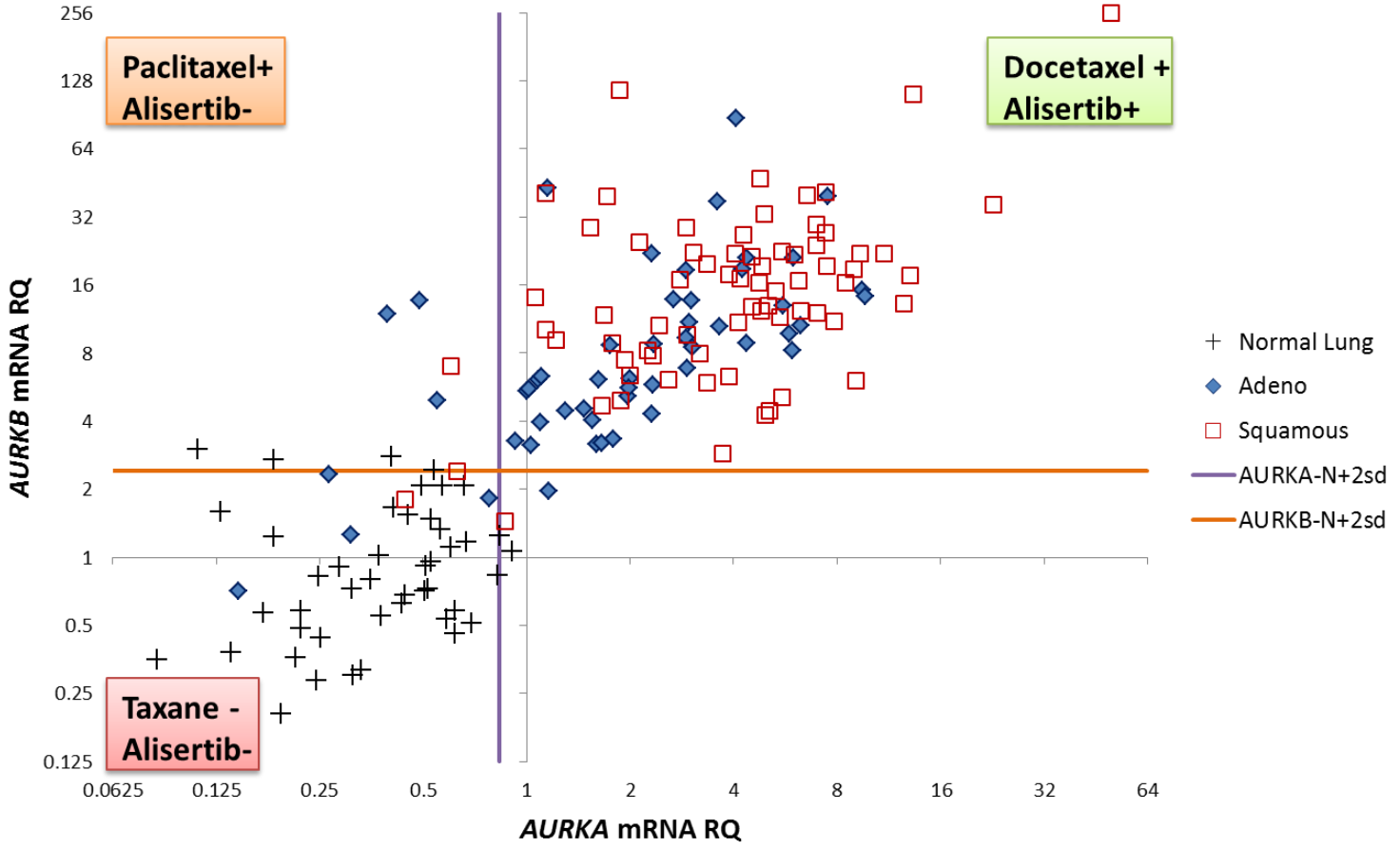

Figure 7.1: A scatter plot demonstrating potential taxane therapeutic scheme based on the coordinated mRNA expression of both *AURKA* and *AURKB* in the screened NSCLC tissues. The top left quartile represents the NSCLC tissues cases with high level of mRNA *AURKB* expression and low *AURKA* transcripts. These cases would benefit from paclitaxel only involving regimen. Most cases are located in the top right quartile. These tumours overexpress both kinases and may require simultaneous treatment with combination of docetaxel and alisertib. NSCLC cases at the bottom left quartile would not be eligible for neither taxane nor alisertib therapies.

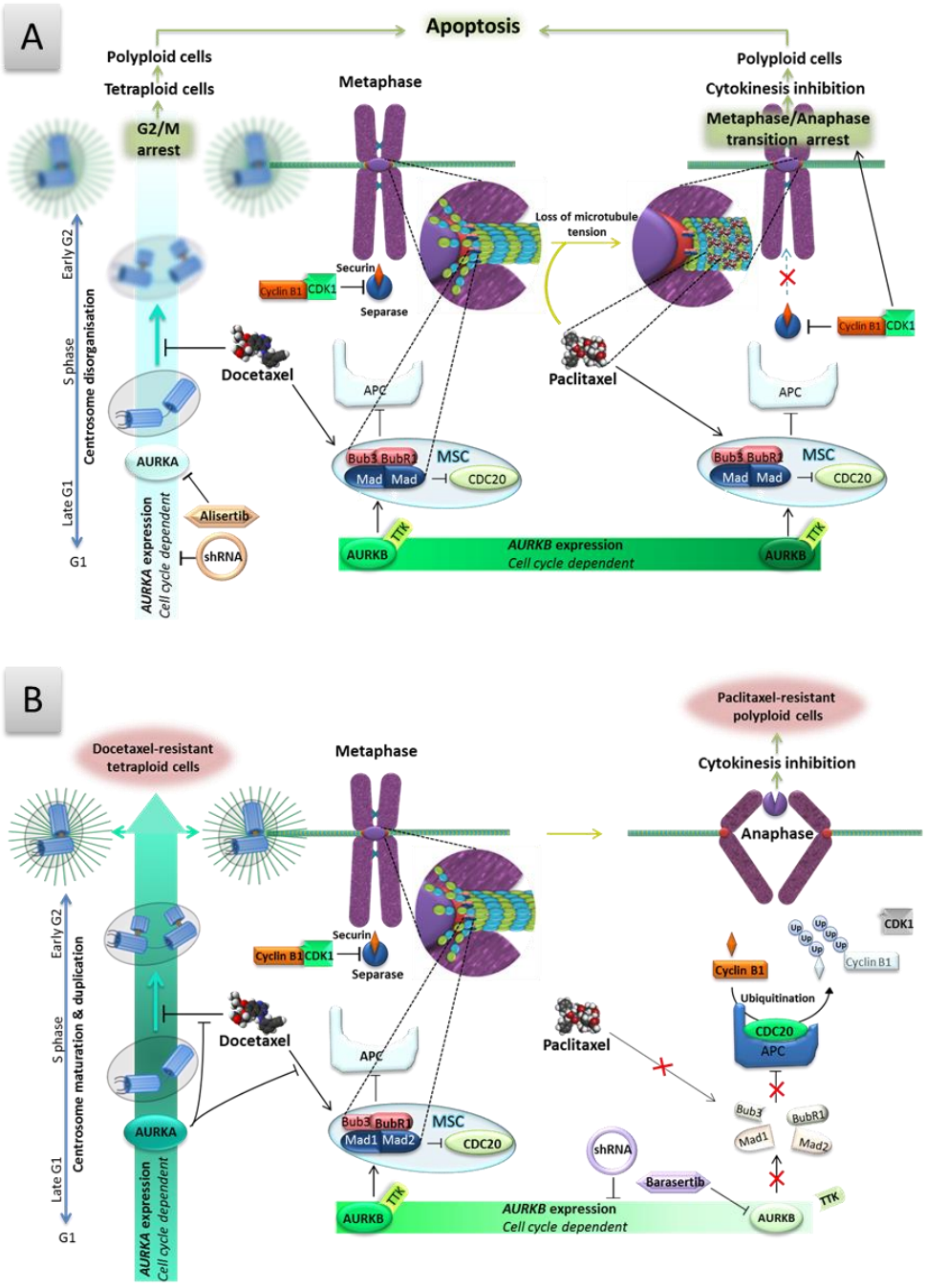

Figure 7.2: Proposed model explaining the different roles of AURKA and AURKB in molecular modulation of docetaxel and paclitaxel cytotoxicity respectively in lung cancer cells: (A) Both AURKA inhibition by alisertib (or down-regulation by shRNA) and docetaxel treatment affect centrosome organisation in the S phase resulting in G2/M arrest and forming tetraploid and polyploid cells that undergo apoptosis. Meanwhile, both paclitaxel and up-regulated AURKB activate mitotic spindle checkpoint in metaphase causing mitotic arrest and eventually apoptosis; (B) AURKA over expression overrides the mitotic spindle checkpoint activated by docetaxel leading to docetaxel-resistant tetraploid cells that continue to divide. On the other hand, AURKB inhibition by barasertib (or down-regulation by shRNA) results in MSC disassembly leading to cellular resistance to paclitaxel.

7.3 *AURKA* mRNA expression is an independent predictor of poor prognosis in patients with NSCLC

Mitotic spindle formation is a key process for cell proliferation (199). It is well known that spindle assembly aberrations lead to aneuploidy and are heavily involved in cancer development (190). I thus hypothesised that the expression of genes related to this process may be indicative of the aggressiveness of a tumour and therefore might be used for prognostication.

In the present study, the mRNA expression profiling of *AURKA, AURKAB, AURKC, CKAP5, DLGAP5, KIF11, TPX2, TTK, TUBB* and *TUBB3* was investigated in a large cohort of human NSCLC and queried potential associations between expression profiles and clinicopathological characteristics including survival. All of the genes, except AURKC, were overexpressed in malignant tissues compared to normal adjacent ones. Taken together, my results suggest that up-regulation of mitotic spindle genes is a common abnormality in NSCLC and may explain its important contribution in lung tumour aggressiveness (196).

Of the 10 genes examined, only *AURKA* overexpression was associated with poor prognosis. Multivariate Cox regression analysis showed that *AURKA* mRNA expression, age, pathological stage and involvement of distal nodes were independent predictors of poor prognosis in patients with NSCLC.

AURKA overexpression may play an important role in cancer aggressiveness through a range of mechanisms. Elevated levels of AURKA perturb mitotic spindle formation and thus cytokinesis due to centrosome amplification, aneuploidy and chromosomal instability (214), (196). When overexpressed, AURKA also inactivates the activity of several tumour suppressor genes including p53 (215). The association between AURKA overexpression and p53 mutation as well as high tumour grade and high cancer stage was also reported in

patients with hepatocellular carcinoma (216) and with clinically aggressive disease and reduced survival in ovarian cancer (217). These AURKA-related events, the perturbation of spindle formation and inactivation of tumour suppressor genes by elevated AURKA, may explain my established association between up-regulated AURKA and poor outcome of NSCLC patients. Nonetheless, the notion that up-regulated AURKA contributes to a poor outcome in lung cancer has been debated, presumably because NSCLC represents a set of heterogeneous malignancies (218), with differing outcomes, even amongst those with the same clinopathological features.

The kinase activity of Aurora A is regulated by Targeting Protein for Xenopus kinesin-like protein 2 (TPX2) through their interaction during mitosis (240). At the end of mitotic cell division, both Aurora A (241) and TPX2 (242) are degraded by the anaphase promoting cyclosome/complex E3 ubiquitin ligase. TPX2 expression was differentially detected in cancerous lung tissues and not in normal lung tissue (243). Investigation of the distinctively higher expression of TPX2 in mitotic phases of cell cycle led to the suggestion it may serve as a biomarker for cancer prognosis (244). Several studies on TPX2 expression have demonstrated the potential prognostic value of this gene when overexpressed in lung cancer using different approaches either as independent marker by immunohistochemistry (245), or as a part of 5 gene cluster/ panel signature ($P < 0.001$, $HR = 2.84$) employing lung adenocarcinoma microarray data sets (69), (208). Nevertheless, *TPX2* mRNA involvement in NSCLC prognosis has not been previously investigated independently in lung cancer cases.

Aurora A recruits the interaction between the *CKAP5* encoded protein, colonic and hepatic Tumour Over-expressed Gene (ch-TOG), and TACC3 to centrosomes and proximal spindle microtubules (229). ch-TOG up regulation in cancer was first demonstrated by Charrasse et

al 1995 in liver and colon tumours compared with the corresponding normal tissues (230). However, no reported data that show such association between CKAP5 expression and survival in cancer patients or could potentially prognosticate the disease outcome. Therefore, my results warrant further investigation of exporting the CKAP5 role in predicting survival in cancer patients including lung cases.

DLGAP5, which reported as the most closely related to AURKA expression (233), was first described by Tsou et al 2003 as an up-regulated transcript in hepatocellular cancer and called Hepatoma Up Regulated Protein (HURP) (232). HURP is a kinetochore microtubule-associated protein that mediates Ran-GTP-dependent mitotic spindle assembly, promoting microtubule polymerization and spindle formation, activating chromosome congregation and alignment during mitosis in normal and cancer cells (233). Increased expression levels of DLGAP5 are related to tumour aggressiveness in several cancers such as hepatocellular carcinoma (234), adrenocortical tumours (235), and meningioma (23). Up-regulation of DLGAP5, which is correlated with poor prognosis in liver (237) and prostate (238) cancers, showed a borderline trend (p=0.067) with poor outcome in lung cancer cases involved in my study. My data, therefore, may suggest further investigation of the potential prognostic value of *DLGAP5*-mRNA expression in lung cancer.

In conclusion, Overexpression of *AURKA*, AURKB, *CKAP5, DLGAP5* and *TPX2* were associated with poor prognosis of NSCLC patients in different degrees. However, only *AURKA* mRNA overexpression can prognosticate the clinical outcome in NSCLC patients using univariate and multivariate models could be useful in the management of NSCLC. This may also have application for developing of targeted therapy for lung carcinoma; patients with high *AURKA* expression may benefit from therapy with *AURKA* inhibitors to have good prognosis.

7.4 Epigenetic sensitization of respiratory tract cancer cells to paclitaxel

Epigenetic therapies and epigenetic sensitization of cancer cells to common chemotherapeutics have come to focus in the last decade (30), (176). As sensitization to taxanes was a major objective in my thesis, I examined the potential of modulating paclitaxel efficiency using two epigenetic modifiers; valproic acid to induce histone acetylation and decitabin to induce global DNA hypomethylation. Both epigenetic drugs in used as a combination treating patients with lung and head and neck in phase I clinical studies (256), (257) which demonstrated that decreased DNA methylation and induction of histone acetylation were associated with prolonged stable disease for 6 months as a median (4-12 months).

This part of the study commenced later in year three and produced only pilot data that warrant further investigation. The data obtained demonstrated that pre-treatment of three different RTC cell lines with VPA sensitised these cells to paclitaxel, while decitabin has no such sensitising effect. The maximum concentration that has been used in this study was corresponded to levels in the plasma of patient treated for epilepsy that ranged from (30-111) mg/L as opposed to (0.2 – 0.8) mM and exhibited low risk side effects (299), while resulting in histone acetylation (300). These findings are consistent with Chen *et al,* who established that VPA enhanced paclitaxel response in resistant human lung adenocarcinoma cells but in dose-dependent manner (218), but in contrast to Erlich et al, who could not deduce that VPA can potentiate the cytotoxic effect to paclitaxel in HNSCC cells (261). This inconsistency probably exists because the researchers did not try to pre-treat the cells with VPA prior paclitaxel treatment rather they examined only the VPA-paclitaxel combination. However, my finding demonstrated a minor effect of VPA and paclitaxel in RTC cells. This epigenetic sensitisation of cancer cells to paclitaxel might result

through induction of apoptosis due to enhancement of tubulin acetylation (259). Although paclitaxel–induced apoptosis in NSCLC is well documented and p53-independent, (301), (302), (303), (304), following the finding that VPA pre-treatment potentiates paclitaxel cytotoxic effect in RTC cell lines, I investigated whether VPA-mediated paclitaxel cytotoxicity is associated with p53 status. The results indicated that p53 status was a determinant of epigenetic sensitisation of HBEC cells to paclitaxel cytotoxicity. It was evident that 0.5 mM VPA enhanced paclitaxel activity in p53 wild type HBEC cells but to a lesser extent in the p53-knockout derivatives. However, increased VPA dose to 1mM showed similar paclitaxel sensitising effect in both p53 wild type and p53 null cells. Further investigation is required to provide compelling evidence on the exact mechanism of p53 involvement on VPA-based sensitization of paclitaxel.

The present study also demonstrated that VPA exposure of BHY cells led to the reduction of *AURKA* mRNA expression. This suggests that *AURKA* transcription is under epigenetic control (305). While the mechanism behind VPA-mediated sensitisation to paclitaxel is still unclear, the reduction of *AURKA* expression may be one of the mediators as thoroughly discussed in the previous chapters.

In conclusion, the results indicate that HDAC inhibitors could be beneficial in sensitising RTC cells to paclitaxel, which is a very common and inexpensive chemotherapeutic agent. Such sensitisation could lead to lowering the effective dose of paclitaxel and subsequently reducing the adverse effects of this drug to the patient. Additional preclinical and clinical evidence is required to provide further support to my observation. The great advantage of VPA is that it is in routine clinical use for many years demonstrating minor side effects.

Further research is required to establish the exact molecular mechanisms modulating this epigenetic sensitisation of cancer cells to paclitaxel.

Refrences

1. Michikawa C, Uzawa N, Sato H, Ohyama Y, Okada N, Amagasa T. Epidermal growth factor receptor gene copy number aberration at the primary tumour is significantly associated with extracapsular spread in oral cancer. British journal of cancer. 2011;104(5):850-5. Epub 2011/02/10.
2. Fox E, Curt GA, Balis FM. Clinical trial design for target-based therapy. The oncologist. 2002;7(5):401-9. Epub 2002/10/29.
3. Tost J, Gut IG. DNA methylation analysis by pyrosequencing. Nature protocols. 2007;2(9):2265-75. Epub 2007/09/15.
4. Ferlay J, Soerjomataram I, Dikshit R, Eser S, Mathers C, Rebelo M, et al. Cancer incidence and mortality worldwide: sources, methods and major patterns in GLOBOCAN 2012. International journal of cancer Journal international du cancer. 2015;136(5):E359-86. Epub 2014/09/16.
5. Ettinger DS, Akerley W, Borghaei H, Chang AC, Cheney RT, Chirieac LR, et al. Non-small cell lung cancer, version 2.2013. Journal of the National Comprehensive Cancer Network : JNCCN. 2013;11(6):645-53; quiz 53. Epub 2013/06/08.
6. Travis WD, Brambilla E, Noguchi M, Nicholson AG, Geisinger KR, Yatabe Y, et al. International association for the study of lung cancer/american thoracic society/european respiratory society international multidisciplinary classification of lung adenocarcinoma. Journal of thoracic oncology : official publication of the International Association for the Study of Lung Cancer. 2011;6(2):244-85. Epub 2011/01/22.
7. Travis WD, Brambilla E, Riely GJ. New pathologic classification of lung cancer: relevance for clinical practice and clinical trials. Journal of clinical oncology : official journal of the American Society of Clinical Oncology. 2013;31(8):992-1001. Epub 2013/02/13.
8. Maeshima AM, Tochigi N, Yoshida A, Asamura H, Tsuta K, Tsuda H. Histological scoring for small lung adenocarcinomas 2 cm or less in diameter: a reliable prognostic indicator. Journal of thoracic oncology : official publication of the International Association for the Study of Lung Cancer. 2010;5(3):333-9. Epub 2010/02/04.
9. Yoshizawa A, Motoi N, Riely GJ, Sima CS, Gerald WL, Kris MG, et al. Impact of proposed IASLC/ATS/ERS classification of lung adenocarcinoma: prognostic subgroups and implications for further revision of staging based on analysis of 514 stage I cases. Modern pathology : an official journal of the United States and Canadian Academy of Pathology, Inc. 2011;24(5):653-64. Epub 2011/01/22.
10. Zugazagoitia J, Enguita AB, Nunez JA, Iglesias L, Ponce S. The new IASLC/ATS/ERS lung adenocarcinoma classification from a clinical perspective: current concepts and future prospects. Journal of thoracic disease. 2014;6(Suppl 5):S526-36. Epub 2014/10/29.
11. Wistuba, II. Genetics of preneoplasia: lessons from lung cancer. Current molecular medicine. 2007;7(1):3-14. Epub 2007/02/22.
12. Jackman DM, Johnson BE. Small-cell lung cancer. The Lancet. 2005;366(9494):1385-96.
13. Travis WD. Update on small cell carcinoma and its differentiation from squamous cell carcinoma and other non-small cell carcinomas. Modern pathology : an official journal of the United States and Canadian Academy of Pathology, Inc. 2012;25 Suppl 1:S18-30. Epub 2012/01/11.

14. Travis WD. Pathology and diagnosis of neuroendocrine tumors: lung neuroendocrine. Thoracic surgery clinics. 2014;24(3):257-66. Epub 2014/07/30.
15. Travis WD. Advances in neuroendocrine lung tumors. Annals of oncology : official journal of the European Society for Medical Oncology / ESMO. 2010;21 Suppl 7:vii65-71. Epub 2010/10/15.
16. Gazdar AF, Brambilla E. Preneoplasia of lung cancer. Cancer biomarkers : section A of Disease markers. 2010;9(1-6):385-96. Epub 2011/11/25.
17. Ruffini E, Bongiovanni M, Cavallo A, Filosso PL, Giobbe R, Mancuso M, et al. The significance of associated pre-invasive lesions in patients resected for primary lung neoplasms. European journal of cardio-thoracic surgery : official journal of the European Association for Cardio-thoracic Surgery. 2004;26(1):165-72. Epub 2004/06/18.
18. Wistuba, II, Gazdar AF. Lung cancer preneoplasia. Annual review of pathology. 2006;1:331-48. Epub 2007/11/28.
19. Kerr KM. Pulmonary preinvasive neoplasia. Journal of clinical pathology. 2001;54(4):257-71. Epub 2001/04/18.
20. Lantuejoul S, Salameire D, Salon C, Brambilla E. Pulmonary preneoplasia--sequential molecular carcinogenetic events. Histopathology. 2009;54(1):43-54. Epub 2009/02/04.
21. Mireskandari M, Abdirad A, Zhang Q, Dietel M, Petersen I. Association of small foci of diffuse idiopathic pulmonary neuroendocrine cell hyperplasia (DIPNECH) with adenocarcinoma of the lung. Pathology, research and practice. 2013;209(9):578-84. Epub 2013/08/31.
22. Owonikoko TK, Ragin CC, Belani CP, Oton AB, Gooding WE, Taioli E, et al. Lung cancer in elderly patients: an analysis of the surveillance, epidemiology, and end results database. Journal of clinical oncology : official journal of the American Society of Clinical Oncology. 2007;25(35):5570-7. Epub 2007/12/11.
23. Gajra A, Lichtman SM. Treatment of advanced lung cancer in the elderly. Hospital practice (1995). 2011;39(2):107-15. Epub 2011/05/18.
24. Smith BD, Smith GL, Hurria A, Hortobagyi GN, Buchholz TA. Future of cancer incidence in the United States: burdens upon an aging, changing nation. Journal of clinical oncology : official journal of the American Society of Clinical Oncology. 2009;27(17):2758-65. Epub 2009/05/01.
25. Jemal A, Thun MJ, Ries LA, Howe HL, Weir HK, Center MM, et al. Annual report to the nation on the status of cancer, 1975-2005, featuring trends in lung cancer, tobacco use, and tobacco control. Journal of the National Cancer Institute. 2008;100(23):1672-94. Epub 2008/11/27.
26. McKay JD, Hung RJ, Gaborieau V, Boffetta P, Chabrier A, Byrnes G, et al. Lung cancer susceptibility locus at 5p15.33. Nature genetics. 2008;40(12):1404-6. Epub 2008/11/04.
27. Hung RJ, McKay JD, Gaborieau V, Boffetta P, Hashibe M, Zaridze D, et al. A susceptibility locus for lung cancer maps to nicotinic acetylcholine receptor subunit genes on 15q25. Nature. 2008;452(7187):633-7. Epub 2008/04/04.
28. Lips EH, Gaborieau V, McKay JD, Chabrier A, Hung RJ, Boffetta P, et al. Association between a 15q25 gene variant, smoking quantity and tobacco-related cancers among 17 000 individuals. International journal of epidemiology. 2010;39(2):563-77. Epub 2009/09/25.

29. McKay JD, Truong T, Gaborieau V, Chabrier A, Chuang SC, Byrnes G, et al. A genome-wide association study of upper aerodigestive tract cancers conducted within the INHANCE consortium. PLoS genetics. 2011;7(3):e1001333. Epub 2011/03/26.
30. Timofeeva MN, Hung RJ, Rafnar T, Christiani DC, Field JK, Bickeboller H, et al. Influence of common genetic variation on lung cancer risk: meta-analysis of 14 900 cases and 29 485 controls. Human molecular genetics. 2012;21(22):4980-95. Epub 2012/08/18.
31. Sun C, Chan F, Briassouli P, Linardopoulos S. Aurora kinase inhibition downregulates NF-kappaB and sensitises tumour cells to chemotherapeutic agents. Biochemical and biophysical research communications. 2007;352(1):220-5. Epub 2006/11/23.
32. Thun MJ, Hannan LM, Adams-Campbell LL, Boffetta P, Buring JE, Feskanich D, et al. Lung cancer occurrence in never-smokers: an analysis of 13 cohorts and 22 cancer registry studies. PLoS medicine. 2008;5(9):e185. Epub 2008/09/16.
33. Subramanian J, Govindan R. Lung cancer in never smokers: a review. Journal of clinical oncology : official journal of the American Society of Clinical Oncology. 2007;25(5):561-70. Epub 2007/02/10.
34. Boch C, Kollmeier J, Roth A, Stephan-Falkenau S, Misch D, Gruning W, et al. The frequency of EGFR and KRAS mutations in non-small cell lung cancer (NSCLC): routine screening data for central Europe from a cohort study. BMJ open. 2013;3(4). Epub 2013/04/06.
35. Xu J, He J, Yang H, Luo X, Liang Z, Chen J, et al. Somatic mutation analysis of EGFR, KRAS, BRAF and PIK3CA in 861 patients with non-small cell lung cancer. Cancer biomarkers : section A of Disease markers. 2011;10(2):63-9. Epub 2011/01/01.
36. Janjigian YY, McDonnell K, Kris MG, Shen R, Sima CS, Bach PB, et al. Pack-years of cigarette smoking as a prognostic factor in patients with stage IIIB/IV nonsmall cell lung cancer. Cancer. 2010;116(3):670-5. Epub 2009/12/24.
37. Kawaguchi T, Takada M, Kubo A, Matsumura A, Fukai S, Tamura A, et al. Performance status and smoking status are independent favorable prognostic factors for survival in non-small cell lung cancer: a comprehensive analysis of 26,957 patients with NSCLC. Journal of thoracic oncology : official publication of the International Association for the Study of Lung Cancer. 2010;5(5):620-30. Epub 2010/04/01.
38. Forrest LF, Sowden S, Rubin G, White M, Adams J. Socio-economic inequalities in patient, primary care, referral, diagnostic, and treatment intervals on the lung cancer care pathway: protocol for a systematic review and meta-analysis. Systematic reviews. 2014;3:30. Epub 2014/03/29.
39. Bagan P, Berna P, De Dominicis F, Das Neves Pereira JC, Mordant P, De La Tour B, et al. Nutritional status and postoperative outcome after pneumonectomy for lung cancer. The Annals of thoracic surgery. 2013;95(2):392-6. Epub 2012/07/31.
40. Fiorelli A, Vicidomini G, Mazzella A, Messina G, Milione R, Di Crescenzo VG, et al. The influence of body mass index and weight loss on outcome of elderly patients undergoing lung cancer resection. The Thoracic and cardiovascular surgeon. 2014;62(7):578-87. Epub 2014/06/25.
41. Prosch H, Schaefer-Prokop C. Screening for lung cancer. Current opinion in oncology. 2014;26(2):131-7. Epub 2014/01/21.
42. Brett GZ. The value of lung cancer detection by six-monthly chest radiographs. Thorax. 1968;23(4):414-20. Epub 1968/07/01.
43. Frost JK, Ball WC, Jr., Levin ML, Tockman MS, Baker RR, Carter D, et al. Early lung cancer detection: results of the initial (prevalence) radiologic and cytologic screening in the

Johns Hopkins study. The American review of respiratory disease. 1984;130(4):549-54. Epub 1984/10/01.
44. Pastorino U, Bellomi M, Landoni C, De Fiori E, Arnaldi P, Picchio M, et al. Early lung-cancer detection with spiral CT and positron emission tomography in heavy smokers: 2-year results. Lancet (London, England). 2003;362(9384):593-7. Epub 2003/08/29.
45. Yang H, Zhao H, Garfield DH, Teng J, Han B, Sun J. Endobronchial ultrasound-guided transbronchial needle aspiration in the diagnosis of non-lymph node thoracic lesions. Annals of thoracic medicine. 2013;8(1):14-21. Epub 2013/02/27.
46. Dincer HE. Linear EBUS in staging non-small cell lung cancer and diagnosing benign diseases. Journal of bronchology & interventional pulmonology. 2013;20(1):66-76. Epub 2013/01/19.
47. Lennon AM, Rintoul RC, Penman ID. Competition for EUS (a) EBUS-TBNA (b) video assisted thoracoscopy. Endoscopy. 2006;38 Suppl 1:S80-3. Epub 2006/06/28.
48. Moreira AL, Thornton RH. Personalized medicine for non-small-cell lung cancer: implications of recent advances in tissue acquisition for molecular and histologic testing. Clinical lung cancer. 2012;13(5):334-9. Epub 2012/03/20.
49. Tsuchiya T, Nagayasu T, Yamasaki N, Matsumoto K, Miyazaki T, Tagawa T, et al. A multicenter phase II study of adjuvant chemotherapy with oral fluoropyrimidine S-1 for non-small-cell lung cancer: high completion and survival rates. Clinical lung cancer. 2012;13(6):464-9. Epub 2012/03/20.
50. Hwang Y, Kang CH, Kim HS, Jeon JH, Park IK, Kim YT. Comparison of thoracoscopic segmentectomy and thoracoscopic lobectomy on the patients with non-small cell lung cancer: a propensity score matching studydagger. European journal of cardio-thoracic surgery : official journal of the European Association for Cardio-thoracic Surgery. 2015;48(2):273-8. Epub 2014/11/20.
51. McElnay P, Lim E. Adjuvant or neoadjuvant chemotherapy for NSCLC. Journal of thoracic disease. 2014;6 Suppl 2:S224-7. Epub 2014/05/29.
52. Wang S, Wang Z, Boise L, Dent P, Grant S. Loss of the bcl-2 phosphorylation loop domain increases resistance of human leukemia cells (U937) to paclitaxel-mediated mitochondrial dysfunction and apoptosis. Biochemical and biophysical research communications. 1999;259(1):67-72. Epub 1999/05/21.
53. Marzo I, Naval J. Antimitotic drugs in cancer chemotherapy: promises and pitfalls. Biochemical pharmacology. 2013;86(6):703-10. Epub 2013/07/28.
54. Zhang X, Lu J, Xu J, Li H, Wang J, Qin Y, et al. Pemetrexed plus platinum or gemcitabine plus platinum for advanced non-small cell lung cancer: final survival analysis from a multicentre randomized phase II trial in the East Asia region and a meta-analysis. Respirology. 2013;18(1):131-9. Epub 2012/08/14.
55. Capasso A. Vinorelbine in cancer therapy. Current drug targets. 2012;13(8):1065-71. Epub 2012/05/19.
56. Tabaczar S, Koceva-Chyla A, Matczak K, Gwozdzinski K. [Molecular mechanisms of antitumor activity of taxanes. I. Interaction of docetaxel with microtubules]. Postepy higieny i medycyny doswiadczalnej (Online). 2010;64:568-81. Epub 2010/11/27. Molekularne mechanizmy aktywnosci przeciwnowotworowej taksanow. I. Oddzialywanie docetakselu na mikrotubule.
57. Visentin M, Zhao R, Goldman ID. The antifolates. Hematology/oncology clinics of North America. 2012;26(3):629-48, ix. Epub 2012/04/24.

58. Plunkett W, Huang P, Xu YZ, Heinemann V, Grunewald R, Gandhi V. Gemcitabine: metabolism, mechanisms of action, and self-potentiation. Seminars in oncology. 1995;22(4 Suppl 11):3-10. Epub 1995/08/01.
59. Shepherd FA, Rodrigues Pereira J, Ciuleanu T, Tan EH, Hirsh V, Thongprasert S, et al. Erlotinib in previously treated non-small-cell lung cancer. The New England journal of medicine. 2005;353(2):123-32. Epub 2005/07/15.
60. Inoue A, Kobayashi K, Usui K, Maemondo M, Okinaga S, Mikami I, et al. First-line gefitinib for patients with advanced non-small-cell lung cancer harboring epidermal growth factor receptor mutations without indication for chemotherapy. Journal of clinical oncology : official journal of the American Society of Clinical Oncology. 2009;27(9):1394-400. Epub 2009/02/20.
61. Passaro A, Gori B, de Marinis F. Afatinib as first-line treatment for patients with advanced non-small-cell lung cancer harboring EGFR mutations: focus on LUX-Lung 3 and LUX-Lung 6 phase III trials. Journal of thoracic disease. 2013;5(4):383-4. Epub 2013/08/31.
62. Spaans JN, Goss GD. Trials to Overcome Drug Resistance to EGFR and ALK Targeted Therapies - Past, Present, and Future. Frontiers in oncology. 2014;4:233. Epub 2014/09/16.
63. Haasbeek CJ, Slotman BJ, Senan S. Radiotherapy for lung cancer: clinical impact of recent technical advances. Lung Cancer. 2009;64(1):1-8. Epub 2008/09/06.
64. Murai T, Shibamoto Y, Baba F, Hashizume C, Mori Y, Ayakawa S, et al. Progression of non-small-cell lung cancer during the interval before stereotactic body radiotherapy. International journal of radiation oncology, biology, physics. 2012;82(1):463-7. Epub 2010/11/26.
65. van der Drift MA, Karim-Kos HE, Siesling S, Groen HJ, Wouters MW, Coebergh JW, et al. Progress in standard of care therapy and modest survival benefits in the treatment of non-small cell lung cancer patients in the Netherlands in the last 20 years. Journal of thoracic oncology : official publication of the International Association for the Study of Lung Cancer. 2012;7(2):291-8. Epub 2011/12/14.
66. Carnio S, Novello S, Mele T, Levra MG, Scagliotti GV. Extending survival of stage IV non-small cell lung cancer. Seminars in oncology. 2014;41(1):69-92. Epub 2014/02/26.
67. Sad LM, Younis SG, Elity MM. Prognostic and predictive role of ERCC1 protein expression in locally advanced stage III non-small cell lung cancer. Med Oncol. 2014;31(7):58. Epub 2014/06/18.
68. Sudhindra A, Ochoa R, Santos ES. Biomarkers, prediction, and prognosis in non-small-cell lung cancer: a platform for personalized treatment. Clinical lung cancer. 2011;12(6):360-8. Epub 2011/07/07.
69. Kadara H, Lacroix L, Behrens C, Solis L, Gu X, Lee JJ, et al. Identification of gene signatures and molecular markers for human lung cancer prognosis using an in vitro lung carcinogenesis system. Cancer prevention research (Philadelphia, Pa). 2009;2(8):702-11. Epub 2009/07/30.
70. Balgkouranidou I, Liloglou T, Lianidou ES. Lung cancer epigenetics: emerging biomarkers. Biomarkers in medicine. 2013;7(1):49-58. Epub 2013/02/08.
71. Han M, Dai J, Zhang Y, Lin Q, Jiang M, Xu X, et al. Support vector machines coupled with proteomics approaches for detecting biomarkers predicting chemotherapy resistance in small cell lung cancer. Oncol Rep. 2012;28(6):2233-8. Epub 2012/09/21.

72. Indovina P, Marcelli E, Pentimalli F, Tanganelli P, Tarro G, Giordano A. Mass spectrometry-based proteomics: the road to lung cancer biomarker discovery. Mass spectrometry reviews. 2013;32(2):129-42. Epub 2012/07/26.
73. Pirozzi G, Tirino V, Camerlingo R, La Rocca A, Martucci N, Scognamiglio G, et al. Prognostic value of cancer stem cells, epithelial-mesenchymal transition and circulating tumor cells in lung cancer. Oncol Rep. 2013;29(5):1763-8. Epub 2013/02/22.
74. Braakhuis BJ, Tabor MP, Kummer JA, Leemans CR, Brakenhoff RH. A genetic explanation of Slaughter's concept of field cancerization: evidence and clinical implications. Cancer research. 2003;63(8):1727-30. Epub 2003/04/19.
75. Amit M, Yen TC, Liao CT, Chaturvedi P, Agarwal JP, Kowalski LP, et al. Improvement in survival of patients with oral cavity squamous cell carcinoma: An international collaborative study. Cancer. 2013;119(24):4242-8. Epub 2013/10/12.
76. Speight PM. Update on oral epithelial dysplasia and progression to cancer. Head and neck pathology. 2007;1(1):61-6. Epub 2007/09/01.
77. Dakubo GD, Jakupciak JP, Birch-Machin MA, Parr RL. Clinical implications and utility of field cancerization. Cancer cell international. 2007;7:2. Epub 2007/03/17.
78. Slaughter DP, Southwick HW, Smejkal W. Field cancerization in oral stratified squamous epithelium; clinical implications of multicentric origin. Cancer. 1953;6(5):963-8. Epub 1953/09/01.
79. Mehanna HM, Rattay T, Smith J, McConkey CC. Treatment and follow-up of oral dysplasia - a systematic review and meta-analysis. Head Neck. 2009;31(12):1600-9. Epub 2009/05/21.
80. Leemans CR, Braakhuis BJ, Brakenhoff RH. The molecular biology of head and neck cancer. Nature reviews Cancer. 2011;11(1):9-22. Epub 2010/12/17.
81. Sy SM, Wong N, Lai PB, To KF, Johnson PJ. Regional over-representations on chromosomes 1q, 3q and 7q in the progression of hepatitis B virus-related hepatocellular carcinoma. Modern pathology : an official journal of the United States and Canadian Academy of Pathology, Inc. 2005;18(5):686-92. Epub 2004/12/18.
82. van Zeeburg HJ, Graveland AP, Brink A, Nguyen M, Leemans CR, Bloemena E, et al. Generation of precursor cell lines from preneoplastic fields surrounding head and neck cancers. Head Neck. 2013;35(4):568-74. Epub 2012/06/21.
83. Gillison ML. Human papillomavirus-related diseases: oropharynx cancers and potential implications for adolescent HPV vaccination. The Journal of adolescent health : official publication of the Society for Adolescent Medicine. 2008;43(4 Suppl):S52-60. Epub 2008/10/01.
84. Schache AG, Liloglou T, Risk JM, Filia A, Jones TM, Sheard J, et al. Evaluation of human papilloma virus diagnostic testing in oropharyngeal squamous cell carcinoma: sensitivity, specificity, and prognostic discrimination. Clinical cancer research : an official journal of the American Association for Cancer Research. 2011;17(19):6262-71. Epub 2011/10/05.
85. Maier H, Dietz A, Gewelke U, Heller WD, Weidauer H. Tobacco and alcohol and the risk of head and neck cancer. The Clinical investigator. 1992;70(3-4):320-7. Epub 1992/03/01.
86. Dahlstrom KR, Little JA, Zafereo ME, Lung M, Wei Q, Sturgis EM. Squamous cell carcinoma of the head and neck in never smoker-never drinkers: a descriptive epidemiologic study. Head Neck. 2008;30(1):75-84. Epub 2007/08/19.

87. Ho MW, Risk JM, Woolgar JA, Field EA, Field JK, Steele JC, et al. The clinical determinants of malignant transformation in oral epithelial dysplasia. Oral oncology. 2012;48(10):969-76. Epub 2012/05/15.
88. Bachar G, Hod R, Goldstein DP, Irish JC, Gullane PJ, Brown D, et al. Outcome of oral tongue squamous cell carcinoma in patients with and without known risk factors. Oral oncology. 2011;47(1):45-50. Epub 2010/12/21.
89. Sturgis EM, Cinciripini PM. Trends in head and neck cancer incidence in relation to smoking prevalence: an emerging epidemic of human papillomavirus-associated cancers? Cancer. 2007;110(7):1429-35. Epub 2007/08/29.
90. Heck JE, Berthiller J, Vaccarella S, Winn DM, Smith EM, Shan'gina O, et al. Sexual behaviours and the risk of head and neck cancers: a pooled analysis in the International Head and Neck Cancer Epidemiology (INHANCE) consortium. International journal of epidemiology. 2010;39(1):166-81. Epub 2009/12/22.
91. Chaturvedi AK, Engels EA, Pfeiffer RM, Hernandez BY, Xiao W, Kim E, et al. Human papillomavirus and rising oropharyngeal cancer incidence in the United States. Journal of clinical oncology : official journal of the American Society of Clinical Oncology. 2011;29(32):4294-301. Epub 2011/10/05.
92. Upile T, Jerjes W, Al-Khawalde M, Radhi H, Sudhoff H. Oral sex, cancer and death: sexually transmitted cancers. Head & neck oncology. 2012;4:31. Epub 2012/06/08.
93. Deschler DG, Richmon JD, Khariwala SS, Ferris RL, Wang MB. The "new" head and neck cancer patient-young, nonsmoker, nondrinker, and HPV positive: evaluation. Otolaryngology--head and neck surgery : official journal of American Academy of Otolaryngology-Head and Neck Surgery. 2014;151(3):375-80. Epub 2014/06/14.
94. Rogers SN, Brown JS, Woolgar JA, Lowe D, Magennis P, Shaw RJ, et al. Survival following primary surgery for oral cancer. Oral oncology. 2009;45(3):201-11. Epub 2008/08/05.
95. Pignon JP, le Maitre A, Maillard E, Bourhis J. Meta-analysis of chemotherapy in head and neck cancer (MACH-NC): an update on 93 randomised trials and 17,346 patients. Radiotherapy and oncology : journal of the European Society for Therapeutic Radiology and Oncology. 2009;92(1):4-14. Epub 2009/05/19.
96. Toner M, O'Regan EM. Head and neck squamous cell carcinoma in the young: a spectrum or a distinct group? Part 2. Head and neck pathology. 2009;3(3):249-51. Epub 2010/07/03.
97. Awan KH, Morgan PR, Warnakulasuriya S. Evaluation of an autofluorescence based imaging system (VELscope) in the detection of oral potentially malignant disorders and benign keratoses. Oral oncology. 2011;47(4):274-7. Epub 2011/03/15.
98. Keereweer S, Sterenborg HJ, Kerrebijn JD, Van Driel PB, Baatenburg de Jong RJ, Lowik CW. Image-guided surgery in head and neck cancer: current practice and future directions of optical imaging. Head Neck. 2012;34(1):120-6. Epub 2011/02/02.
99. Nagata S, Hamada T, Yamada N, Yokoyama S, Kitamoto S, Kanmura Y, et al. Aberrant DNA methylation of tumor-related genes in oral rinse: a noninvasive method for detection of oral squamous cell carcinoma. Cancer. 2012;118(17):4298-308. Epub 2012/01/19.
100. Langevin SM, Stone RA, Bunker CH, Grandis JR, Sobol RW, Taioli E. MicroRNA-137 promoter methylation in oral rinses from patients with squamous cell carcinoma of the head and neck is associated with gender and body mass index. Carcinogenesis. 2010;31(5):864-70. Epub 2010/03/04.

101. Hu S, Arellano M, Boontheung P, Wang J, Zhou H, Jiang J, et al. Salivary proteomics for oral cancer biomarker discovery. Clinical cancer research : an official journal of the American Association for Cancer Research. 2008;14(19):6246-52. Epub 2008/10/03.
102. Righini CA, de Fraipont F, Timsit JF, Faure C, Brambilla E, Reyt E, et al. Tumor-specific methylation in saliva: a promising biomarker for early detection of head and neck cancer recurrence. Clinical cancer research : an official journal of the American Association for Cancer Research. 2007;13(4):1179-85. Epub 2007/02/24.
103. Demokan S, Chang X, Chuang A, Mydlarz WK, Kaur J, Huang P, et al. KIF1A and EDNRB are differentially methylated in primary HNSCC and salivary rinses. International journal of cancer Journal international du cancer. 2010;127(10):2351-9. Epub 2010/02/18.
104. Schussel J, Zhou XC, Zhang Z, Pattani K, Bermudez F, Jean-Charles G, et al. EDNRB and DCC salivary rinse hypermethylation has a similar performance as expert clinical examination in discrimination of oral cancer/dysplasia versus benign lesions. Clinical cancer research : an official journal of the American Association for Cancer Research. 2013;19(12):3268-75. Epub 2013/05/03.
105. Arantes LM, de Carvalho AC, Melendez ME, Centrone CC, Gois-Filho JF, Toporcov TN, et al. Validation of methylation markers for diagnosis of oral cavity cancer. European journal of cancer (Oxford, England : 1990). 2015;51(5):632-41. Epub 2015/02/18.
106. Bhide SA, Nutting CM. Advances in chemotherapy for head and neck cancer. Oral oncology. 2010;46(6):436-8. Epub 2010/04/20.
107. Sakuraba M, Miyamoto S, Kimata Y, Nakatsuka T, Harii K, Ebihara S, et al. Recent advances in reconstructive surgery: head and neck reconstruction. International journal of clinical oncology. 2013;18(4):561-5. Epub 2012/12/28.
108. Adelstein DJ, Li Y, Adams GL, Wagner H, Jr., Kish JA, Ensley JF, et al. An intergroup phase III comparison of standard radiation therapy and two schedules of concurrent chemoradiotherapy in patients with unresectable squamous cell head and neck cancer. Journal of clinical oncology : official journal of the American Society of Clinical Oncology. 2003;21(1):92-8. Epub 2002/12/31.
109. Brizel DM, Albers ME, Fisher SR, Scher RL, Richtsmeier WJ, Hars V, et al. Hyperfractionated irradiation with or without concurrent chemotherapy for locally advanced head and neck cancer. The New England journal of medicine. 1998;338(25):1798-804. Epub 1998/06/19.
110. Bourhis J, Sire C, Graff P, Gregoire V, Maingon P, Calais G, et al. Concomitant chemoradiotherapy versus acceleration of radiotherapy with or without concomitant chemotherapy in locally advanced head and neck carcinoma (GORTEC 99-02): an open-label phase 3 randomised trial. The Lancet Oncology. 2012;13(2):145-53. Epub 2012/01/21.
111. Blanchard P, Bourhis J, Lacas B, Posner MR, Vermorken JB, Hernandez JJ, et al. Taxane-cisplatin-fluorouracil as induction chemotherapy in locally advanced head and neck cancers: an individual patient data meta-analysis of the meta-analysis of chemotherapy in head and neck cancer group. Journal of clinical oncology : official journal of the American Society of Clinical Oncology. 2013;31(23):2854-60. Epub 2013/07/10.
112. Georges P, Rajagopalan K, Leon C, Singh P, Ahmad N, Nader K, et al. Chemotherapy advances in locally advanced head and neck cancer. World journal of clinical oncology. 2014;5(5):966-72. Epub 2014/12/11.
113. Soulieres D, Senzer NN, Vokes EE, Hidalgo M, Agarwala SS, Siu LL. Multicenter phase II study of erlotinib, an oral epidermal growth factor receptor tyrosine kinase inhibitor, in

patients with recurrent or metastatic squamous cell cancer of the head and neck. Journal of clinical oncology : official journal of the American Society of Clinical Oncology. 2004;22(1):77-85. Epub 2004/01/01.
114. Siu LL, Soulieres D, Chen EX, Pond GR, Chin SF, Francis P, et al. Phase I/II trial of erlotinib and cisplatin in patients with recurrent or metastatic squamous cell carcinoma of the head and neck: a Princess Margaret Hospital phase II consortium and National Cancer Institute of Canada Clinical Trials Group Study. Journal of clinical oncology : official journal of the American Society of Clinical Oncology. 2007;25(16):2178-83. Epub 2007/06/01.
115. Argiris A, Ghebremichael M, Gilbert J, Lee JW, Sachidanandam K, Kolesar JM, et al. Phase III randomized, placebo-controlled trial of docetaxel with or without gefitinib in recurrent or metastatic head and neck cancer: an eastern cooperative oncology group trial. Journal of clinical oncology : official journal of the American Society of Clinical Oncology. 2013;31(11):1405-14. Epub 2013/03/06.
116. Abdul Razak AR, Soulieres D, Laurie SA, Hotte SJ, Singh S, Winquist E, et al. A phase II trial of dacomitinib, an oral pan-human EGF receptor (HER) inhibitor, as first-line treatment in recurrent and/or metastatic squamous-cell carcinoma of the head and neck. Annals of oncology : official journal of the European Society for Medical Oncology / ESMO. 2013;24(3):761-9. Epub 2012/10/31.
117. Chau NG, Perez-Ordonez B, Zhang K, Pham NA, Ho J, Zhang T, et al. The association between EGFR variant III, HPV, p16, c-MET, EGFR gene copy number and response to EGFR inhibitors in patients with recurrent or metastatic squamous cell carcinoma of the head and neck. Head & neck oncology. 2011;3:11. Epub 2011/03/01.
118. Cohen RB. Current challenges and clinical investigations of epidermal growth factor receptor (EGFR)- and ErbB family-targeted agents in the treatment of head and neck squamous cell carcinoma (HNSCC). Cancer treatment reviews. 2014;40(4):567-77. Epub 2013/11/13.
119. Argiris A, Karamouzis MV, Raben D, Ferris RL. Head and neck cancer. Lancet (London, England). 2008;371(9625):1695-709. Epub 2008/05/20.
120. Shaw RJ, Lowe D, Woolgar JA, Brown JS, Vaughan ED, Evans C, et al. Extracapsular spread in oral squamous cell carcinoma. Head Neck. 2010;32(6):714-22. Epub 2009/10/15.
121. Chung CH, Zhang Q, Kong CS, Harris J, Fertig EJ, Harari PM, et al. p16 protein expression and human papillomavirus status as prognostic biomarkers of nonoropharyngeal head and neck squamous cell carcinoma. Journal of clinical oncology : official journal of the American Society of Clinical Oncology. 2014;32(35):3930-8. Epub 2014/10/01.
122. Schiff PB, Fant J, Horwitz SB. Promotion of microtubule assembly in vitro by taxol. Nature. 1979;277(5698):665-7. Epub 1979/02/22.
123. Wiernik PH, Schwartz EL, Einzig A, Strauman JJ, Lipton RB, Dutcher JP. Phase I trial of taxol given as a 24-hour infusion every 21 days: responses observed in metastatic melanoma. Journal of clinical oncology : official journal of the American Society of Clinical Oncology. 1987;5(8):1232-9. Epub 1987/08/01.
124. Wiernik PH, Schwartz EL, Strauman JJ, Dutcher JP, Lipton RB, Paietta E. Phase I clinical and pharmacokinetic study of taxol. Cancer research. 1987;47(9):2486-93. Epub 1987/05/01.

125. Donehower RC, Rowinsky EK, Grochow LB, Longnecker SM, Ettinger DS. Phase I trial of taxol in patients with advanced cancer. Cancer treatment reports. 1987;71(12):1171-7. Epub 1987/12/01.
126. Grem JL, Tutsch KD, Simon KJ, Alberti DB, Willson JK, Tormey DC, et al. Phase I study of taxol administered as a short i.v. infusion daily for 5 days. Cancer treatment reports. 1987;71(12):1179-84. Epub 1987/12/01.
127. Longnecker SM, Donehower RC, Cates AE, Chen TL, Brundrett RB, Grochow LB, et al. High-performance liquid chromatographic assay for taxol in human plasma and urine and pharmacokinetics in a phase I trial. Cancer treatment reports. 1987;71(1):53-9. Epub 1987/01/01.
128. McGuire WP, Rowinsky EK, Rosenshein NB, Grumbine FC, Ettinger DS, Armstrong DK, et al. Taxol: a unique antineoplastic agent with significant activity in advanced ovarian epithelial neoplasms. Annals of internal medicine. 1989;111(4):273-9. Epub 1989/08/15.
129. Murphy WK, Fossella FV, Winn RJ, Shin DM, Hynes HE, Gross HM, et al. Phase II study of taxol in patients with untreated advanced non-small-cell lung cancer. Journal of the National Cancer Institute. 1993;85(5):384-8. Epub 1993/03/03.
130. Chang AY, Kim K, Glick J, Anderson T, Karp D, Johnson D. Phase II study of taxol, merbarone, and piroxantrone in stage IV non-small-cell lung cancer: The Eastern Cooperative Oncology Group Results. Journal of the National Cancer Institute. 1993;85(5):388-94. Epub 1993/03/03.
131. Forastiere AA, Neuberg D, Taylor SGt, DeConti R, Adams G. Phase II evaluation of Taxol in advanced head and neck cancer: an Eastern Cooperative Oncology group trial. Journal of the National Cancer Institute Monographs. 1993(15):181-4. Epub 1993/01/01.
132. Ringel I, Horwitz SB. Studies with RP 56976 (taxotere): a semisynthetic analogue of taxol. Journal of the National Cancer Institute. 1991;83(4):288-91. Epub 1991/02/20.
133. Fossella FV, Lee JS, Murphy WK, Lippman SM, Calayag M, Pang A, et al. Phase II study of docetaxel for recurrent or metastatic non-small-cell lung cancer. Journal of clinical oncology : official journal of the American Society of Clinical Oncology. 1994;12(6):1238-44. Epub 1994/06/01.
134. Francis PA, Rigas JR, Kris MG, Pisters KM, Orazem JP, Woolley KJ, et al. Phase II trial of docetaxel in patients with stage III and IV non-small-cell lung cancer. Journal of clinical oncology : official journal of the American Society of Clinical Oncology. 1994;12(6):1232-7. Epub 1994/06/01.
135. Del Mastro L, Fabi A, Mansutti M, De Laurentiis M, Durando A, Merlo DF, et al. Randomised phase 3 open-label trial of first-line treatment with gemcitabine in association with docetaxel or paclitaxel in women with metastatic breast cancer: a comparison of different schedules and treatments. BMC cancer. 2013;13:164. Epub 2013/03/30.
136. Isonishi S, Suzuki M, Nagano H, Takagi K, Shimauchi M, Kawabata M, et al. A feasibility study on maintenance of docetaxel after paclitaxel-carboplatin chemotherapy in patients with advanced ovarian cancer. Journal of gynecologic oncology. 2013;24(2):154-9. Epub 2013/05/09.
137. Van Veldhuizen PJ, Reed G, Aggarwal A, Baranda J, Zulfiqar M, Williamson S. Docetaxel and ketoconazole in advanced hormone-refractory prostate carcinoma: a phase I and pharmacokinetic study. Cancer. 2003;98(9):1855-62. Epub 2003/10/30.

138. Maemondo M, Inoue A, Sugawara S, Harada T, Minegishi Y, Usui K, et al. Randomized phase II trial comparing carboplatin plus weekly paclitaxel and docetaxel alone in elderly patients with advanced non-small cell lung cancer: north japan lung cancer group trial 0801. The oncologist. 2014;19(4):352-3. Epub 2014/04/01.
139. Behera M, Owonikoko TK, Kim S, Chen Z, Higgins K, Ramalingam SS, et al. Concurrent therapy with taxane versus non-taxane containing regimens in locally advanced squamous cell carcinomas of the head and neck (SCCHN): a systematic review. Oral oncology. 2014;50(9):888-94. Epub 2014/07/26.
140. Tsao AS, Liu S, Fujimoto J, Wistuba, II, Lee JJ, Marom EM, et al. Phase II trials of imatinib mesylate and docetaxel in patients with metastatic non-small cell lung cancer and head and neck squamous cell carcinoma. Journal of thoracic oncology : official publication of the International Association for the Study of Lung Cancer. 2011;6(12):2104-11. Epub 2011/09/06.
141. Oh IJ, Kim KS, Kim YC, Ban HJ, Kwon YS, Kim YI, et al. A phase III concurrent chemoradiotherapy trial with cisplatin and paclitaxel or docetaxel or gemcitabine in unresectable non-small cell lung cancer: KASLC 0401. Cancer chemotherapy and pharmacology. 2013;72(6):1247-54. Epub 2013/10/05.
142. Herbst RS, Sun Y, Eberhardt WE, Germonpre P, Saijo N, Zhou C, et al. Vandetanib plus docetaxel versus docetaxel as second-line treatment for patients with advanced non-small-cell lung cancer (ZODIAC): a double-blind, randomised, phase 3 trial. The Lancet Oncology. 2010;11(7):619-26. Epub 2010/06/24.
143. Chu Q, Vincent M, Logan D, Mackay JA, Evans WK. Taxanes as first-line therapy for advanced non-small cell lung cancer: a systematic review and practice guideline. Lung Cancer. 2005;50(3):355-74. Epub 2005/09/06.
144. Hitt R, Lopez-Pousa A, Martinez-Trufero J, Escrig V, Carles J, Rizo A, et al. Phase III study comparing cisplatin plus fluorouracil to paclitaxel, cisplatin, and fluorouracil induction chemotherapy followed by chemoradiotherapy in locally advanced head and neck cancer. Journal of clinical oncology : official journal of the American Society of Clinical Oncology. 2005;23(34):8636-45. Epub 2005/11/09.
145. Pointreau Y, Garaud P, Chapet S, Sire C, Tuchais C, Tortochaux J, et al. Randomized trial of induction chemotherapy with cisplatin and 5-fluorouracil with or without docetaxel for larynx preservation. Journal of the National Cancer Institute. 2009;101(7):498-506. Epub 2009/03/26.
146. Paccagnella A, Ghi MG, Loreggian L, Buffoli A, Koussis H, Mione CA, et al. Concomitant chemoradiotherapy versus induction docetaxel, cisplatin and 5 fluorouracil (TPF) followed by concomitant chemoradiotherapy in locally advanced head and neck cancer: a phase II randomized study. Annals of oncology : official journal of the European Society for Medical Oncology / ESMO. 2010;21(7):1515-22. Epub 2009/12/25.
147. Lorch JH, Goloubeva O, Haddad RI, Cullen K, Sarlis N, Tishler R, et al. Induction chemotherapy with cisplatin and fluorouracil alone or in combination with docetaxel in locally advanced squamous-cell cancer of the head and neck: long-term results of the TAX 324 randomised phase 3 trial. The Lancet Oncology. 2011;12(2):153-9. Epub 2011/01/15.
148. Marquez B, Van Bambeke F. ABC multidrug transporters: target for modulation of drug pharmacokinetics and drug-drug interactions. Current drug targets. 2011;12(5):600-20. Epub 2010/11/03.

149. Oguri T, Ozasa H, Uemura T, Bessho Y, Miyazaki M, Maeno K, et al. MRP7/ABCC10 expression is a predictive biomarker for the resistance to paclitaxel in non-small cell lung cancer. Molecular cancer therapeutics. 2008;7(5):1150-5. Epub 2008/05/01.
150. Glaysher S, Yiannakis D, Gabriel FG, Johnson P, Polak ME, Knight LA, et al. Resistance gene expression determines the in vitro chemosensitivity of non-small cell lung cancer (NSCLC). BMC cancer. 2009;9:300. Epub 2009/08/29.
151. Zhao Y, Lu H, Yan A, Yang Y, Meng Q, Sun L, et al. ABCC3 as a marker for multidrug resistance in non-small cell lung cancer. Scientific reports. 2013;3:3120. Epub 2013/11/02.
152. Che CL, Zhang YM, Zhang HH, Sang YL, Lu B, Dong FS, et al. DNA microarray reveals different pathways responding to paclitaxel and docetaxel in non-small cell lung cancer cell line. International journal of clinical and experimental pathology. 2013;6(8):1538-48. Epub 2013/08/08.
153. Jinturkar KA, Anish C, Kumar MK, Bagchi T, Panda AK, Misra AR. Liposomal formulations of Etoposide and Docetaxel for p53 mediated enhanced cytotoxicity in lung cancer cell lines. Biomaterials. 2012;33(8):2492-507. Epub 2011/12/28.
154. Guntur VP, Waldrep JC, Guo JJ, Selting K, Dhand R. Increasing p53 protein sensitizes non-small cell lung cancer to paclitaxel and cisplatin in vitro. Anticancer research. 2010;30(9):3557-64. Epub 2010/10/15.
155. Taguchi T, Kato Y, Baba Y, Nishimura G, Tanigaki Y, Horiuchi C, et al. Protein levels of p21, p27, cyclin E and Bax predict sensitivity to cisplatin and paclitaxel in head and neck squamous cell carcinomas. Oncol Rep. 2004;11(2):421-6. Epub 2004/01/14.
156. Eberhard DA, Johnson BE, Amler LC, Goddard AD, Heldens SL, Herbst RS, et al. Mutations in the epidermal growth factor receptor and in KRAS are predictive and prognostic indicators in patients with non-small-cell lung cancer treated with chemotherapy alone and in combination with erlotinib. Journal of clinical oncology : official journal of the American Society of Clinical Oncology. 2005;23(25):5900-9. Epub 2005/07/27.
157. Furugaki K, Iwai T, Shirane M, Kondoh K, Moriya Y, Mori K. Schedule-dependent antitumor activity of the combination with erlotinib and docetaxel in human non-small cell lung cancer cells with EGFR mutation, KRAS mutation or both wild-type EGFR and KRAS. Oncol Rep. 2010;24(5):1141-6. Epub 2010/09/30.
158. Jiang Y, Yuan Q, Fang Q. Schedule-dependent synergistic interaction between docetaxel and gefitinib in NSCLC cell lines regardless of the mutation status of EGFR and KRAS and its molecular mechanisms. Journal of cancer research and clinical oncology. 2014;140(7):1087-95. Epub 2014/04/15.
159. Kaira K, Takahashi T, Murakami H, Shukuya T, Kenmotsu H, Ono A, et al. The role of betaIII-tubulin in non-small cell lung cancer patients treated by taxane-based chemotherapy. International journal of clinical oncology. 2013;18(3):371-9. Epub 2012/02/24.
160. Kavallaris M, Burkhart CA, Horwitz SB. Antisense oligonucleotides to class III beta-tubulin sensitize drug-resistant cells to Taxol. British journal of cancer. 1999;80(7):1020-5. Epub 1999/06/11.
161. Koh Y, Kim TM, Jeon YK, Kwon TK, Hah JH, Lee SH, et al. Class III beta-tubulin, but not ERCC1, is a strong predictive and prognostic marker in locally advanced head and neck squamous cell carcinoma. Annals of oncology : official journal of the European Society for Medical Oncology / ESMO. 2009;20(8):1414-9. Epub 2009/05/27.

162. Pillai RN, Brodie SA, Sica GL, Shaojin Y, Li G, Nickleach DC, et al. CHFR protein expression predicts outcomes to taxane-based first line therapy in metastatic NSCLC. Clinical cancer research : an official journal of the American Association for Cancer Research. 2013;19(6):1603-11. Epub 2013/02/07.
163. Kris MG, Johnson BE, Berry LD, Kwiatkowski DJ, Iafrate AJ, Wistuba, II, et al. Using multiplexed assays of oncogenic drivers in lung cancers to select targeted drugs. Jama. 2014;311(19):1998-2006. Epub 2014/05/23.
164. Cagle PT, Chirieac LR. Advances in treatment of lung cancer with targeted therapy. Archives of pathology & laboratory medicine. 2012;136(5):504-9. Epub 2012/05/01.
165. Cottini F, Lautenschlaeger T. Predictors of biomarkers guiding targeted therapeutic strategies in locally advanced lung cancer. Cancer journal (Sudbury, Mass). 2013;19(3):263-71. Epub 2013/05/28.
166. Monzo M, Rosell R, Sanchez JJ, Lee JS, O'Brate A, Gonzalez-Larriba JL, et al. Paclitaxel resistance in non-small-cell lung cancer associated with beta-tubulin gene mutations. Journal of clinical oncology : official journal of the American Society of Clinical Oncology. 1999;17(6):1786-93. Epub 1999/11/24.
167. Abal M, Andreu JM, Barasoain I. Taxanes: microtubule and centrosome targets, and cell cycle dependent mechanisms of action. Current cancer drug targets. 2003;3(3):193-203. Epub 2003/05/29.
168. Ibrado AM, Kim CN, Bhalla K. Temporal relationship of CDK1 activation and mitotic arrest to cytosolic accumulation of cytochrome C and caspase-3 activity during Taxol-induced apoptosis of human AML HL-60 cells. Leukemia. 1998;12(12):1930-6. Epub 1998/12/09.
169. Hauf S, Cole RW, LaTerra S, Zimmer C, Schnapp G, Walter R, et al. The small molecule Hesperadin reveals a role for Aurora B in correcting kinetochore-microtubule attachment and in maintaining the spindle assembly checkpoint. J Cell Biol. 2003;161(2):281-94. Epub 2003/04/23.
170. Ditchfield C. Aurora B couples chromosome alignment with anaphase by targeting BubR1, Mad2, and Cenp-E to kinetochores. The Journal of Cell Biology. 2003;161(2):267-80.
171. Berchem GJ, Bosseler M, Mine N, Avalosse B. Nanomolar range docetaxel treatment sensitizes MCF-7 cells to chemotherapy induced apoptosis, induces G2M arrest and phosphorylates bcl-2. Anticancer research. 1999;19(1A):535-40. Epub 1999/05/05.
172. Weaver BA. How Taxol/paclitaxel kills cancer cells. Molecular biology of the cell. 2014;25(18):2677-81. Epub 2014/09/13.
173. Carter DL, Garfield D, Hathorn J, Mundis R, Boehm KA, Ilegbodu D, et al. A randomized phase III trial of combined paclitaxel, carboplatin, and radiation therapy followed by weekly paclitaxel or observation for patients with locally advanced inoperable non-small-cell lung cancer. Clinical lung cancer. 2012;13(3):205-13. Epub 2011/12/06.
174. Garon EB, Cao D, Alexandris E, John WJ, Yurasov S, Perol M. A randomized, double-blind, phase III study of Docetaxel and Ramucirumab versus Docetaxel and placebo in the treatment of stage IV non-small-cell lung cancer after disease progression after 1 previous platinum-based therapy (REVEL): treatment rationale and study design. Clinical lung cancer. 2012;13(6):505-9. Epub 2012/08/03.
175. Grant DS, Williams TL, Zahaczewsky M, Dicker AP. Comparison of antiangiogenic activities using paclitaxel (taxol) and docetaxel (taxotere). International journal of cancer Journal international du cancer. 2003;104(1):121-9. Epub 2003/01/18.

176.Jones SE, Erban J, Overmoyer B, Budd GT, Hutchins L, Lower E, et al. Randomized phase III study of docetaxel compared with paclitaxel in metastatic breast cancer. Journal of clinical oncology : official journal of the American Society of Clinical Oncology. 2005;23(24):5542-51. Epub 2005/08/20.
177.Izbicka E, Campos D, Marty J, Carrizales G, Mangold G, Tolcher A. Molecular determinants of differential sensitivity to docetaxel and paclitaxel in human pediatric cancer models. Anticancer research. 2006;26(3A):1983-8. Epub 2006/07/11.
178.Hanauske AR, Degen D, Hilsenbeck SG, Bissery MC, Von Hoff DD. Effects of Taxotere and taxol on in vitro colony formation of freshly explanted human tumor cells. Anti-cancer drugs. 1992;3(2):121-4. Epub 1992/04/01.
179.Haldar S, Basu A, Croce CM. Bcl2 is the guardian of microtubule integrity. Cancer research. 1997;57(2):229-33. Epub 1997/01/15.
180.Diaz JF, Andreu JM. Assembly of purified GDP-tubulin into microtubules induced by taxol and taxotere: reversibility, ligand stoichiometry, and competition. Biochemistry. 1993;32(11):2747-55. Epub 1993/03/23.
181.Gligorov J, Lotz JP. Preclinical pharmacology of the taxanes: implications of the differences. The oncologist. 2004;9 Suppl 2:3-8. Epub 2004/05/27.
182.Hennequin C, Giocanti N, Favaudon V. S-phase specificity of cell killing by docetaxel (Taxotere) in synchronised HeLa cells. British journal of cancer. 1995;71(6):1194-8. Epub 1995/06/01.
183.Walczak CE. Molecular mechanisms of spindle function. Genome biology. 2000;1(1):REVIEWS101. Epub 2000/12/06.
184.De Souza CP, Hashmi SB, Yang X, Osmani SA. Regulated inactivation of the spindle assembly checkpoint without functional mitotic spindles. The EMBO journal. 2011;30(13):2648-61. Epub 2011/06/07.
185.Desai A, Mitchison TJ. Microtubule polymerization dynamics. Annual review of cell and developmental biology. 1997;13:83-117. Epub 1997/01/01.
186.Tanaka TU. Chromosome bi-orientation on the mitotic spindle. Philosophical transactions of the Royal Society of London Series B, Biological sciences. 2005;360(1455):581-9. Epub 2005/05/18.
187.Dumont S, Mitchison TJ. Force and length in the mitotic spindle. Current biology : CB. 2009;19(17):R749-61. Epub 2009/11/13.
188.Bieche I, Vacher S, Lallemand F, Tozlu-Kara S, Bennani H, Beuzelin M, et al. Expression analysis of mitotic spindle checkpoint genes in breast carcinoma: role of NDC80/HEC1 in early breast tumorigenicity, and a two-gene signature for aneuploidy. Molecular cancer. 2011;10:23. Epub 2011/03/01.
189.McIntosh JR. Motors or dynamics: what really moves chromosomes? Nature cell biology. 2012;14(12):1234. Epub 2012/12/01.
190.Cimini D, Degrassi F. Aneuploidy: a matter of bad connections. Trends in cell biology. 2005;15(8):442-51. Epub 2005/07/19.
191.Tanaka K, Hirota T. Chromosome segregation machinery and cancer. Cancer science. 2009;100(7):1158-65. Epub 2009/05/13.
192.Musacchio A. Spindle assembly checkpoint: the third decade. Philosophical transactions of the Royal Society of London Series B, Biological sciences. 2011;366(1584):3595-604. Epub 2011/11/16.

193. Bakhoum SF, Silkworth WT, Nardi IK, Nicholson JM, Compton DA, Cimini D. The mitotic origin of chromosomal instability. Current biology : CB. 2014;24(4):R148-9. Epub 2014/02/22.
194. Mathew P, Dipaola R. Taxane refractory prostate cancer. The Journal of urology. 2007;178(3 Pt 2):S36-41. Epub 2007/07/24.
195. Wassmann K, Benezra R. Mitotic checkpoints: from yeast to cancer. Current opinion in genetics & development. 2001;11(1):83-90. Epub 2001/02/13.
196. Fu J, Bian M, Jiang Q, Zhang C. Roles of Aurora kinases in mitosis and tumorigenesis. Molecular cancer research : MCR. 2007;5(1):1-10. Epub 2007/01/30.
197. Martens-de Kemp SR, Nagel R, Stigter-van Walsum M, van der Meulen IH, van Beusechem VW, Braakhuis BJ, et al. Functional genetic screens identify genes essential for tumor cell survival in head and neck and lung cancer. Clinical cancer research : an official journal of the American Association for Cancer Research. 2013;19(8):1994-2003. Epub 2013/02/28.
198. Sankaran S, Parvin JD. Centrosome function in normal and tumor cells. Journal of cellular biochemistry. 2006;99(5):1240-50. Epub 2006/07/04.
199. Tanenbaum ME, Medema RH. Mechanisms of centrosome separation and bipolar spindle assembly. Developmental cell. 2010;19(6):797-806. Epub 2010/12/15.
200. Royle SJ. The role of clathrin in mitotic spindle organisation. Journal of cell science. 2012;125(Pt 1):19-28. Epub 2012/02/02.
201. Manning AL, Compton DA. Structural and regulatory roles of nonmotor spindle proteins. Current opinion in cell biology. 2008;20(1):101-6. Epub 2008/01/08.
202. Leandro-Garcia LJ, Leskela S, Landa I, Montero-Conde C, Lopez-Jimenez E, Leton R, et al. Tumoral and tissue-specific expression of the major human beta-tubulin isotypes. Cytoskeleton (Hoboken, NJ). 2010;67(4):214-23. Epub 2010/03/02.
203. Jelluma N, Brenkman AB, van den Broek NJ, Cruijsen CW, van Osch MH, Lens SM, et al. Mps1 phosphorylates Borealin to control Aurora B activity and chromosome alignment. Cell. 2008;132(2):233-46. Epub 2008/02/05.
204. Nguyen HG, Makitalo M, Yang D, Chinnappan D, St Hilaire C, Ravid K. Deregulated Aurora-B induced tetraploidy promotes tumorigenesis. FASEB journal : official publication of the Federation of American Societies for Experimental Biology. 2009;23(8):2741-8. Epub 2009/04/01.
205. Slattery SD, Mancini MA, Brinkley BR, Hall RM. Aurora-C kinase supports mitotic progression in the absence of Aurora-B. Cell Cycle. 2009;8(18):2984-94. Epub 2009/08/29.
206. Ogawa E, Takenaka K, Katakura H, Adachi M, Otake Y, Toda Y, et al. Perimembrane Aurora-A expression is a significant prognostic factor in correlation with proliferative activity in non-small-cell lung cancer (NSCLC). Annals of surgical oncology. 2008;15(2):547-54. Epub 2007/11/29.
207. Takeshita M, Koga T, Takayama K, Ijichi K, Yano T, Maehara Y, et al. Aurora-B overexpression is correlated with aneuploidy and poor prognosis in non-small cell lung cancer. Lung Cancer. 2013;80(1):85-90. Epub 2013/01/15.
208. Kadara H, Behrens C, Yuan P, Solis L, Liu D, Gu X, et al. A five-gene and corresponding protein signature for stage-I lung adenocarcinoma prognosis. Clinical cancer research : an official journal of the American Association for Cancer Research. 2011;17(6):1490-501. Epub 2010/12/18.

209. Lo Iacono M, Monica V, Saviozzi S, Ceppi P, Bracco E, Papotti M, et al. Aurora Kinase A expression is associated with lung cancer histological-subtypes and with tumor de-differentiation. Journal of translational medicine. 2011;9:100. Epub 2011/07/02.
210. Takeshita M, Koga T, Takayama K, Kouso H, Nishimura-Ikeda Y, Yoshino I, et al. CHFR expression is preferentially impaired in smoking-related squamous cell carcinoma of the lung, and the diminished expression significantly harms outcomes. International journal of cancer Journal international du cancer. 2008;123(7):1623-30. Epub 2008/07/16.
211. Vischioni B, Oudejans JJ, Vos W, Rodriguez JA, Giaccone G. Frequent overexpression of aurora B kinase, a novel drug target, in non-small cell lung carcinoma patients. Molecular cancer therapeutics. 2006;5(11):2905-13. Epub 2006/11/24.
212. Smith SL, Bowers NL, Betticher DC, Gautschi O, Ratschiller D, Hoban PR, et al. Overexpression of aurora B kinase (AURKB) in primary non-small cell lung carcinoma is frequent, generally driven from one allele, and correlates with the level of genetic instability. British journal of cancer. 2005;93(6):719-29. Epub 2005/10/14.
213. Perumal D, Singh S, Yoder SJ, Bloom GC, Chellappan SP. A novel five gene signature derived from stem-like side population cells predicts overall and recurrence-free survival in NSCLC. PloS one. 2012;7(8):e43589. Epub 2012/09/07.
214. Marumoto T, Zhang D, Saya H. Aurora-A - a guardian of poles. Nature reviews Cancer. 2005;5(1):42-50. Epub 2005/01/05.
215. Katayama H, Sasai K, Kawai H, Yuan ZM, Bondaruk J, Suzuki F, et al. Phosphorylation by aurora kinase A induces Mdm2-mediated destabilization and inhibition of p53. Nature genetics. 2004;36(1):55-62. Epub 2004/01/01.
216. Jeng YM, Peng SY, Lin CY, Hsu HC. Overexpression and amplification of Aurora-A in hepatocellular carcinoma. Clinical cancer research : an official journal of the American Association for Cancer Research. 2004;10(6):2065-71. Epub 2004/03/26.
217. Lassmann S, Shen Y, Jutting U, Wiehle P, Walch A, Gitsch G, et al. Predictive value of Aurora-A/STK15 expression for late stage epithelial ovarian cancer patients treated by adjuvant chemotherapy. Clinical cancer research : an official journal of the American Association for Cancer Research. 2007;13(14):4083-91. Epub 2007/07/20.
218. Chen J, Liu J. Spatial-temporal model for silencing of the mitotic spindle assembly checkpoint. Nature communications. 2014;5:4795. Epub 2014/09/13.
219. Xu Z, Ogawa H, Vagnarelli P, Bergmann JH, Hudson DF, Ruchaud S, et al. INCENP-aurora B interactions modulate kinase activity and chromosome passenger complex localization. J Cell Biol. 2009;187(5):637-53. Epub 2009/12/03.
220. Carmena M, Wheelock M, Funabiki H, Earnshaw WC. The chromosomal passenger complex (CPC): from easy rider to the godfather of mitosis. Nature reviews Molecular cell biology. 2012;13(12):789-803. Epub 2012/11/24.
221. van der Waal MS, Hengeveld RC, van der Horst A, Lens SM. Cell division control by the Chromosomal Passenger Complex. Experimental cell research. 2012;318(12):1407-20. Epub 2012/04/05.
222. Beussel S, Hasenburg A, Bogatyreva L, Hauschke D, Werner M, Lassmann S. Aurora-B protein expression is linked to initial response to taxane-based first-line chemotherapy in stage III ovarian carcinoma. Journal of clinical pathology. 2012;65(1):29-35. Epub 2011/10/21.
223. Sasai K, Katayama H, Stenoien DL, Fujii S, Honda R, Kimura M, et al. Aurora-C kinase is a novel chromosomal passenger protein that can complement Aurora-B kinase function in mitotic cells. Cell motility and the cytoskeleton. 2004;59(4):249-63. Epub 2004/10/23.

224.Tang CJ, Lin CY, Tang TK. Dynamic localization and functional implications of Aurora-C kinase during male mouse meiosis. Developmental biology. 2006;290(2):398-410. Epub 2006/01/03.
225.Tseng TC, Chen SH, Hsu YP, Tang TK. Protein kinase profile of sperm and eggs: cloning and characterization of two novel testis-specific protein kinases (AIE1, AIE2) related to yeast and fly chromosome segregation regulators. DNA and cell biology. 1998;17(10):823-33. Epub 1998/11/11.
226.Yazarloo F, Shirkoohi R, Mobasheri MB, Emami A, Modarressi MH. Expression analysis of four testis-specific genes AURKC, OIP5, PIWIL2 and TAF7L in acute myeloid leukemia: a gender-dependent expression pattern. Med Oncol. 2013;30(1):368. Epub 2013/01/08.
227.Zekri A, Lesan V, Ghaffari SH, Tabrizi MH, Modarressi MH. Gene amplification and overexpression of Aurora-C in breast and prostate cancer cell lines. Oncology research. 2012;20(5-6):241-50. Epub 2012/01/01.
228.Tsou JH, Chang KC, Chang-Liao PY, Yang ST, Lee CT, Chen YP, et al. Aberrantly expressed AURKC enhances the transformation and tumourigenicity of epithelial cells. The Journal of pathology. 2011;225(2):243-54. Epub 2011/06/29.
229.Conte N, Delaval B, Ginestier C, Ferrand A, Isnardon D, Larroque C, et al. TACC1-chTOG-Aurora A protein complex in breast cancer. Oncogene. 2003;22(50):8102-16. Epub 2003/11/07.
230.Charrasse S, Mazel M, Taviaux S, Berta P, Chow T, Larroque C. Characterization of the cDNA and pattern of expression of a new gene over-expressed in human hepatomas and colonic tumors. European journal of biochemistry / FEBS. 1995;234(2):406-13. Epub 1995/12/01.
231.Wong J, Lerrigo R, Jang CY, Fang G. Aurora A regulates the activity of HURP by controlling the accessibility of its microtubule-binding domain. Molecular biology of the cell. 2008;19(5):2083-91. Epub 2008/03/07.
232.Tsou AP, Yang CW, Huang CY, Yu RC, Lee YC, Chang CW, et al. Identification of a novel cell cycle regulated gene, HURP, overexpressed in human hepatocellular carcinoma. Oncogene. 2003;22(2):298-307. Epub 2003/01/16.
233.Koffa MD, Casanova CM, Santarella R, Kocher T, Wilm M, Mattaj IW. HURP is part of a Ran-dependent complex involved in spindle formation. Current biology : CB. 2006;16(8):743-54. Epub 2006/04/25.
234.Zhao L, Qin LX, Ye QH, Zhu XQ, Zhang H, Wu X, et al. KIAA0008 gene is associated with invasive phenotype of human hepatocellular carcinoma--a functional analysis. Journal of cancer research and clinical oncology. 2004;130(12):719-27. Epub 2004/09/02.
235.de Reynies A, Assie G, Rickman DS, Tissier F, Groussin L, Rene-Corail F, et al. Gene expression profiling reveals a new classification of adrenocortical tumors and identifies molecular predictors of malignancy and survival. Journal of clinical oncology : official journal of the American Society of Clinical Oncology. 2009;27(7):1108-15. Epub 2009/01/14.
236.Stuart JE, Lusis EA, Scheck AC, Coons SW, Lal A, Perry A, et al. Identification of gene markers associated with aggressive meningioma by filtering across multiple sets of gene expression arrays. Journal of neuropathology and experimental neurology. 2011;70(1):1-12. Epub 2010/12/16.
237.Chang ML, Lin SM, Yeh CT. HURP expression-assisted risk scores identify prognosis distinguishable subgroups in early stage liver cancer. PloS one. 2011;6(10):e26323. Epub 2011/10/25.

238. Gomez CR, Kosari F, Munz JM, Schreiber CA, Knutson GJ, Ida CM, et al. Prognostic value of discs large homolog 7 transcript levels in prostate cancer. PloS one. 2013;8(12):e82833. Epub 2013/12/19.
239. Woodcock SA, Rushton HJ, Castaneda-Saucedo E, Myant K, White GR, Blyth K, et al. Tiam1-Rac signaling counteracts Eg5 during bipolar spindle assembly to facilitate chromosome congression. Current biology : CB. 2010;20(7):669-75. Epub 2010/03/30.
240. Kufer TA, Sillje HH, Korner R, Gruss OJ, Meraldi P, Nigg EA. Human TPX2 is required for targeting Aurora-A kinase to the spindle. J Cell Biol. 2002;158(4):617-23. Epub 2002/08/15.
241. Littlepage LE, Ruderman JV. Identification of a new APC/C recognition domain, the A box, which is required for the Cdh1-dependent destruction of the kinase Aurora-A during mitotic exit. Genes & development. 2002;16(17):2274-85. Epub 2002/09/05.
242. Stewart S, Fang G. Anaphase-promoting complex/cyclosome controls the stability of TPX2 during mitotic exit. Molecular and cellular biology. 2005;25(23):10516-27. Epub 2005/11/17.
243. Manda R, Kohno T, Matsuno Y, Takenoshita S, Kuwano H, Yokota J. Identification of genes (SPON2 and C20orf2) differentially expressed between cancerous and noncancerous lung cells by mRNA differential display. Genomics. 1999;61(1):5-14. Epub 1999/10/08.
244. Heidebrecht HJ, Buck F, Steinmann J, Sprenger R, Wacker HH, Parwaresch R. p100: a novel proliferation-associated nuclear protein specifically restricted to cell cycle phases S, G2, and M. Blood. 1997;90(1):226-33. Epub 1997/07/01.
245. Ma Y, Lin D, Sun W, Xiao T, Yuan J, Han N, et al. Expression of targeting protein for xklp2 associated with both malignant transformation of respiratory epithelium and progression of squamous cell lung cancer. Clinical cancer research : an official journal of the American Association for Cancer Research. 2006;12(4):1121-7. Epub 2006/02/21.
246. Hewitt L, Tighe A, Santaguida S, White AM, Jones CD, Musacchio A, et al. Sustained Mps1 activity is required in mitosis to recruit O-Mad2 to the Mad1-C-Mad2 core complex. J Cell Biol. 2010;190(1):25-34. Epub 2010/07/14.
247. Saurin AT, van der Waal MS, Medema RH, Lens SM, Kops GJ. Aurora B potentiates Mps1 activation to ensure rapid checkpoint establishment at the onset of mitosis. Nature communications. 2011;2:316. Epub 2011/05/19.
248. Daniel J, Coulter J, Woo JH, Wilsbach K, Gabrielson E. High levels of the Mps1 checkpoint protein are protective of aneuploidy in breast cancer cells. Proceedings of the National Academy of Sciences of the United States of America. 2011;108(13):5384-9. Epub 2011/03/16.
249. Magnani M, Ortuso F, Soro S, Alcaro S, Tramontano A, Botta M. The betaI/betaIII-tubulin isoforms and their complexes with antimitotic agents. Docking and molecular dynamics studies. The FEBS journal. 2006;273(14):3301-10. Epub 2006/06/29.
250. Sato M, Vaughan MB, Girard L, Peyton M, Lee W, Shames DS, et al. Multiple oncogenic changes (K-RAS(V12), p53 knockdown, mutant EGFRs, p16 bypass, telomerase) are not sufficient to confer a full malignant phenotype on human bronchial epithelial cells. Cancer research. 2006;66(4):2116-28. Epub 2006/02/21.
251. Bursac Z, Gauss CH, Williams DK, Hosmer DW. Purposeful selection of variables in logistic regression. Source code for biology and medicine. 2008;3:17. Epub 2008/12/18.

252.Schroeder A, Mueller O, Stocker S, Salowsky R, Leiber M, Gassmann M, et al. The RIN: an RNA integrity number for assigning integrity values to RNA measurements. BMC molecular biology. 2006;7:3. Epub 2006/02/02.
253.Yang J, Ikezoe T, Nishioka C, Tasaka T, Taniguchi A, Kuwayama Y, et al. AZD1152, a novel and selective aurora B kinase inhibitor, induces growth arrest, apoptosis, and sensitization for tubulin depolymerizing agent or topoisomerase II inhibitor in human acute leukemia cells in vitro and in vivo. Blood. 2007;110(6):2034-40. Epub 2007/05/15.
254.Wilkinson RW, Odedra R, Heaton SP, Wedge SR, Keen NJ, Crafter C, et al. AZD1152, a selective inhibitor of Aurora B kinase, inhibits human tumor xenograft growth by inducing apoptosis. Clinical cancer research : an official journal of the American Association for Cancer Research. 2007;13(12):3682-8. Epub 2007/06/19.
255.Sharma S, Zeng JY, Zhuang CM, Zhou YQ, Yao HP, Hu X, et al. Small-molecule inhibitor BMS-777607 induces breast cancer cell polyploidy with increased resistance to cytotoxic chemotherapy agents. Molecular cancer therapeutics. 2013;12(5):725-36. Epub 2013/03/08.
256.Braiteh F, Soriano AO, Garcia-Manero G, Hong D, Johnson MM, Silva Lde P, et al. Phase I study of epigenetic modulation with 5-azacytidine and valproic acid in patients with advanced cancers. Clinical cancer research : an official journal of the American Association for Cancer Research. 2008;14(19):6296-301. Epub 2008/10/03.
257.Chu BF, Karpenko MJ, Liu Z, Aimiuwu J, Villalona-Calero MA, Chan KK, et al. Phase I study of 5-aza-2'-deoxycytidine in combination with valproic acid in non-small-cell lung cancer. Cancer chemotherapy and pharmacology. 2013;71(1):115-21. Epub 2012/10/12.
258.Roy Choudhury S, Karmakar S, Banik NL, Ray SK. Valproic acid induced differentiation and potentiated efficacy of taxol and nanotaxol for controlling growth of human glioblastoma LN18 and T98G cells. Neurochemical research. 2011;36(12):2292-305. Epub 2011/07/26.
259.Catalano MG, Poli R, Pugliese M, Fortunati N, Boccuzzi G. Valproic acid enhances tubulin acetylation and apoptotic activity of paclitaxel on anaplastic thyroid cancer cell lines. Endocrine-related cancer. 2007;14(3):839-45. Epub 2007/10/05.
260.Tesei A, Brigliadori G, Carloni S, Fabbri F, Ulivi P, Arienti C, et al. Organosulfur derivatives of the HDAC inhibitor valproic acid sensitize human lung cancer cell lines to apoptosis and to cisplatin cytotoxicity. Journal of cellular physiology. 2012;227(10):3389-96. Epub 2012/01/04.
261.Erlich RB, Rickwood D, Coman WB, Saunders NA, Guminski A. Valproic acid as a therapeutic agent for head and neck squamous cell carcinomas. Cancer chemotherapy and pharmacology. 2009;63(3):381-9. Epub 2008/04/10.
262.Bailey VJ, Easwaran H, Zhang Y, Griffiths E, Belinsky SA, Herman JG, et al. MS-qFRET: a quantum dot-based method for analysis of DNA methylation. Genome research. 2009;19(8):1455-61. Epub 2009/05/16.
263.Kim CH. Druggable targets of squamous cell lung cancer. Tuberculosis and respiratory diseases. 2013;75(6):231-5. Epub 2014/01/15.
264.Xu HT, Ma L, Qi FJ, Liu Y, Yu JH, Dai SD, et al. Expression of serine threonine kinase 15 is associated with poor differentiation in lung squamous cell carcinoma and adenocarcinoma. Pathology international. 2006;56(7):375-80. Epub 2006/06/24.
265.Tang H, Xiao G, Behrens C, Schiller J, Allen J, Chow CW, et al. A 12-gene set predicts survival benefits from adjuvant chemotherapy in non-small cell lung cancer patients.

Clinical cancer research : an official journal of the American Association for Cancer Research. 2013;19(6):1577-86. Epub 2013/01/30.
266. Tanaka E, Hashimoto Y, Ito T, Kondo K, Higashiyama M, Tsunoda S, et al. The suppression of aurora-A/STK15/BTAK expression enhances chemosensitivity to docetaxel in human esophageal squamous cell carcinoma. Clinical cancer research : an official journal of the American Association for Cancer Research. 2007;13(4):1331-40. Epub 2007/02/24.
267. He W, Zhang MG, Wang XJ, Zhong S, Shao Y, Zhu Y, et al. AURKA suppression induces DU145 apoptosis and sensitizes DU145 to docetaxel treatment. American journal of translational research. 2013;5(3):359-67. Epub 2013/05/02.
268. Kumano M, Miyake H, Terakawa T, Furukawa J, Fujisawa M. Suppressed tumour growth and enhanced chemosensitivity by RNA interference targeting Aurora-A in the PC3 human prostate cancer model. BJU international. 2010;106(1):121-7. Epub 2009/11/17.
269. Terakawa T, Miyake H, Kumano M, Fujisawa M. Growth inhibition and enhanced chemosensitivity induced by down-regulation of Aurora-A in human renal cell carcinoma Caki-2 cells using short hairpin RNA. Oncology letters. 2011;2(4):713-7. Epub 2012/08/01.
270. Lee HH, Zhu Y, Govindasamy KM, Gopalan G. Downregulation of Aurora-A overrides estrogen-mediated growth and chemoresistance in breast cancer cells. Endocrine-related cancer. 2008;15(3):765-75. Epub 2008/05/13.
271. Sehdev V, Katsha A, Ecsedy J, Zaika A, Belkhiri A, El-Rifai W. The combination of alisertib, an investigational Aurora kinase A inhibitor, and docetaxel promotes cell death and reduces tumor growth in preclinical cell models of upper gastrointestinal adenocarcinomas. Cancer. 2013;119(4):904-14. Epub 2012/09/14.
272. Huck JJ, Zhang M, Mettetal J, Chakravarty A, Venkatakrishnan K, Zhou X, et al. Translational exposure-efficacy modeling to optimize the dose and schedule of taxanes combined with the investigational Aurora A kinase inhibitor MLN8237 (alisertib). Molecular cancer therapeutics. 2014;13(9):2170-83. Epub 2014/07/02.
273. Qi W, Cooke LS, Liu X, Rimsza L, Roe DJ, Manziolli A, et al. Aurora inhibitor MLN8237 in combination with docetaxel enhances apoptosis and anti-tumor activity in mantle cell lymphoma. Biochemical pharmacology. 2011;81(7):881-90. Epub 2011/02/05.
274. Chinn DC, Holland WS, Mack PC. Anticancer activity of the Aurora A kinase inhibitor MK-5108 in non-small-cell lung cancer (NSCLC) in vitro as monotherapy and in combination with chemotherapies. Journal of cancer research and clinical oncology. 2014;140(7):1137-49. Epub 2014/04/24.
275. Shimomura T, Hasako S, Nakatsuru Y, Mita T, Ichikawa K, Kodera T, et al. MK-5108, a highly selective Aurora-A kinase inhibitor, shows antitumor activity alone and in combination with docetaxel. Molecular cancer therapeutics. 2010;9(1):157-66. Epub 2010/01/08.
276. Hernandez-Vargas H, Palacios J, Moreno-Bueno G. Telling cells how to die: docetaxel therapy in cancer cell lines. Cell Cycle. 2007;6(7):780-3. Epub 2007/03/23.
277. Anand S, Penrhyn-Lowe S, Venkitaraman AR. AURORA-A amplification overrides the mitotic spindle assembly checkpoint, inducing resistance to Taxol. Cancer cell. 2003;3(1):51-62. Epub 2003/02/01.
278. Manfredi MG, Ecsedy JA, Chakravarty A, Silverman L, Zhang M, Hoar KM, et al. Characterization of Alisertib (MLN8237), an investigational small-molecule inhibitor of aurora A kinase using novel in vivo pharmacodynamic assays. Clinical cancer research :

an official journal of the American Association for Cancer Research. 2011;17(24):7614-24. Epub 2011/10/22.
279. Yamada HY, Gorbsky GJ. Spindle checkpoint function and cellular sensitivity to antimitotic drugs. Molecular cancer therapeutics. 2006;5(12):2963-9. Epub 2006/12/19.
280. Montero A, Fossella F, Hortobagyi G, Valero V. Docetaxel for treatment of solid tumours: a systematic review of clinical data. The Lancet Oncology. 2005;6(4):229-39. Epub 2005/04/07.
281. Melichar B, Adenis A, Lockhart AC, Bennouna J, Dees EC, Kayaleh O, et al. Safety and activity of alisertib, an investigational aurora kinase A inhibitor, in patients with breast cancer, small-cell lung cancer, non-small-cell lung cancer, head and neck squamous-cell carcinoma, and gastro-oesophageal adenocarcinoma: a five-arm phase 2 study. The Lancet Oncology. 2015;16(4):395-405. Epub 2015/03/03.
282. Sorrentino R, Libertini S, Pallante PL, Troncone G, Palombini L, Bavetsias V, et al. Aurora B overexpression associates with the thyroid carcinoma undifferentiated phenotype and is required for thyroid carcinoma cell proliferation. The Journal of clinical endocrinology and metabolism. 2005;90(2):928-35. Epub 2004/11/25.
283. Lin ZZ, Jeng YM, Hu FC, Pan HW, Tsao HW, Lai PL, et al. Significance of Aurora B overexpression in hepatocellular carcinoma. Aurora B Overexpression in HCC. BMC cancer. 2010;10:461. Epub 2010/08/31.
284. Pohl A, Azuma M, Zhang W, Yang D, Ning Y, Winder T, et al. Pharmacogenetic profiling of Aurora kinase B is associated with overall survival in metastatic colorectal cancer. The pharmacogenomics journal. 2011;11(2):93-9. Epub 2010/04/07.
285. Hayama S, Daigo Y, Yamabuki T, Hirata D, Kato T, Miyamoto M, et al. Phosphorylation and activation of cell division cycle associated 8 by aurora kinase B plays a significant role in human lung carcinogenesis. Cancer research. 2007;67(9):4113-22. Epub 2007/05/08.
286. Ota T, Suto S, Katayama H, Han ZB, Suzuki F, Maeda M, et al. Increased mitotic phosphorylation of histone H3 attributable to AIM-1/Aurora-B overexpression contributes to chromosome number instability. Cancer research. 2002;62(18):5168-77. Epub 2002/09/18.
287. Kawakami H, Okamoto I, Terao K, Sakai K, Suzuki M, Ueda S, et al. Human papillomavirus DNA and p16 expression in Japanese patients with oropharyngeal squamous cell carcinoma. Cancer medicine. 2013;2(6):933-41. Epub 2014/01/10.
288. Arenz A, Ziemann F, Mayer C, Wittig A, Dreffke K, Preising S, et al. Increased radiosensitivity of HPV-positive head and neck cancer cell lines due to cell cycle dysregulation and induction of apoptosis. Strahlentherapie und Onkologie : Organ der Deutschen Rontgengesellschaft [et al]. 2014;190(9):839-46. Epub 2014/04/10.
289. Rieder CL, Cole RW. Entry into mitosis in vertebrate somatic cells is guarded by a chromosome damage checkpoint that reverses the cell cycle when triggered during early but not late prophase. J Cell Biol. 1998;142(4):1013-22. Epub 1998/08/29.
290. Biggins S, Severin FF, Bhalla N, Sassoon I, Hyman AA, Murray AW. The conserved protein kinase Ipl1 regulates microtubule binding to kinetochores in budding yeast. Genes & development. 1999;13(5):532-44. Epub 1999/03/11.
291. Dewar H, Tanaka K, Nasmyth K, Tanaka TU. Tension between two kinetochores suffices for their bi-orientation on the mitotic spindle. Nature. 2004;428(6978):93-7. Epub 2004/02/13.

292. Curry J, Angove H, Fazal L, Lyons J, Reule M, Thompson N, et al. Aurora B kinase inhibition in mitosis: strategies for optimising the use of aurora kinase inhibitors such as AT9283. Cell Cycle. 2009;8(12):1921-9. Epub 2009/05/15.
293. Qi W, Liu X, Cooke LS, Persky DO, Miller TP, Squires M, et al. AT9283, a novel aurora kinase inhibitor, suppresses tumor growth in aggressive B-cell lymphomas. International journal of cancer Journal international du cancer. 2012;130(12):2997-3005. Epub 2011/07/29.
294. Bush TL, Payton M, Heller S, Chung G, Hanestad K, Rottman JB, et al. AMG 900, a small-molecule inhibitor of aurora kinases, potentiates the activity of microtubule-targeting agents in human metastatic breast cancer models. Molecular cancer therapeutics. 2013;12(11):2356-66. Epub 2013/08/31.
295. Lens SM, Voest EE, Medema RH. Shared and separate functions of polo-like kinases and aurora kinases in cancer. Nature reviews Cancer. 2010;10(12):825-41. Epub 2010/11/26.
296. Walsby E, Walsh V, Pepper C, Burnett A, Mills K. Effects of the aurora kinase inhibitors AZD1152-HQPA and ZM447439 on growth arrest and polyploidy in acute myeloid leukemia cell lines and primary blasts. Haematologica. 2008;93(5):662-9. Epub 2008/03/28.
297. Carvalho A, Carmena M, Sambade C, Earnshaw WC, Wheatley SP. Survivin is required for stable checkpoint activation in taxol-treated HeLa cells. Journal of cell science. 2003;116(Pt 14):2987-98. Epub 2003/06/05.
298. Waters JC, Chen RH, Murray AW, Salmon ED. Localization of Mad2 to kinetochores depends on microtubule attachment, not tension. J Cell Biol. 1998;141(5):1181-91. Epub 1998/06/12.
299. Zighetti ML, Fontana G, Lussana F, Chiesa V, Vignoli A, Canevini MP, et al. Effects of chronic administration of valproic acid to epileptic patients on coagulation tests and primary hemostasis. Epilepsia. 2015;56(5):e49-52. Epub 2015/03/12.
300. Tremolizzo L, Difrancesco JC, Rodriguez-Menendez V, Riva C, Conti E, Galimberti G, et al. Valproate induces epigenetic modifications in lymphomonocytes from epileptic patients. Progress in neuro-psychopharmacology & biological psychiatry. 2012;39(1):47-51. Epub 2012/05/16.
301. King TC, Akerley W, Fan AC, Moore T, Mangray S, Hsiu Chen M, et al. p53 mutations do not predict response to paclitaxel in metastatic nonsmall cell lung carcinoma. Cancer. 2000;89(4):769-73. Epub 2000/08/22.
302. Vogt U, Zaczek A, Klinke F, Granetzny A, Bielawski K, Falkiewicz B. p53 Gene status in relation to ex vivo chemosensitivity of non-small cell lung cancer. Journal of cancer research and clinical oncology. 2002;128(3):141-7. Epub 2002/04/06.
303. Das GC, Holiday D, Gallardo R, Haas C. Taxol-induced cell cycle arrest and apoptosis: dose-response relationship in lung cancer cells of different wild-type p53 status and under isogenic condition. Cancer letters. 2001;165(2):147-53. Epub 2001/03/29.
304. Duarte ML, de Moraes E, Pontes E, Schluckebier L, de Moraes JL, Hainaut P, et al. Role of p53 in the induction of cyclooxygenase-2 by cisplatin or paclitaxel in non-small cell lung cancer cell lines. Cancer letters. 2009;279(1):57-64. Epub 2009/02/17.
305. Zhang XH, Rao M, Loprieato JA, Hong JA, Zhao M, Chen GZ, et al. Aurora A, Aurora B and survivin are novel targets of transcriptional regulation by histone deacetylase inhibitors in non-small cell lung cancer. Cancer biology & therapy. 2008;7(9):1388-97. Epub 2008/08/19.

Web References

1. Cummings 2003

http://cmapspublic3.ihmc.us/rid=1176137552531_1405028108_13786/cell%20reproduction.cmap).

2. genecards.org

(http://www.genecards.org/).

3. NCRI HN Ca CSG Ann Rep 2013/2014

(http://csg.ncri.org.uk/wp-content/uploads/2014/11/NCRI-Head-Neck-CSG-Annual-Report-2013-14.pdf).

4. practice.sph.umich.edu

(http://practice.sph.umich.edu/micphp/epicentral/index.php).

5. study.com

(http://study.com/academy/lesson/telophase-definition-lesson-quiz.html).

6. surveillance.cancer.gov

(http://surveillance.cancer.gov/statistics/types/incidence.html).

7. UK clinical trials

(http://www.nhs.uk/Conditions/Cancer-of-the-lung/Pages/clinical-trial.aspx?CT=0&Rec=1&Countries=United+Kingdom&Condition=Cancer%2c+lung~NSCLC~paclitaxel&pn=1).

8. WHO Report on the Global Tobacco Epidemic, 2008

(http://www.who.int/tobacco/mpower/2008/en/).

9. www.cancer.gov

(http://www.cancer.gov/publications/dictionaries/cancer-terms?cdrid=618612).

10. www.nature.com

(http://www.nature.com/subjects).

Appendices

Appendix 1: Publication/communication material out of this study.

1. A manuscript on AURKB modulation has been recently reviewed by the Journal of Thoracic Oncology and the comments are currently dealt with.
2. Four posters have been presented in the following conferences:

- A Al-Khafaji, P Pantazi, J Risk, R Shaw, J Field, T Liloglou. mRNA signature of the mitotic spindle gene members in predicting taxane response for non-small cell lung carcinomas. B14. NCRI Cancer Conference, 3-6 Nov 2013, Liverpool, UK.
- P Pantazi, A Al-Khafaji, A Acha Sagredo, A Schache, T Liloglou. Upregulation of HURP gene expression in Head and Neck cancer and its clinical impact. v international symposium “advances in oral cancer”, 10-11 Jul 2014, Bilbao, Spain.
- A Al-Khafaji, S Ali, J Field, T Liloglou. AURKA involvement in paclitaxel resistance in non-small cell lung cancer. B54. NCRI Cancer Conference, 2 - 5 Nov 2014, Liverpool, UK.
- A Al-Khafaji, J Risk, R Shaw, J Field, T Liloglou. Epigenetic sensitization of respiratory tract cancer cells to paclitaxel. 627. EAS2015 conference, 20-23 Jun 2015, Florence, Italy.

Appendix 2: Clinicopathological characteristics of the patients included in this study.

No.	Sex	Age	Histology	pT	pN	Clinical stage
1	Female	70	AdC	1	0	IA
2	Male	50	AdC	1	0	IA
3	Male	67	AdC	1	0	IA
4	Female	77	AdC	1	0	IA
5	Female	80	AdC	1	0	IA
6	Female	77	AdC	1	0	IA
7	Female	79	AdC	1	0	IA
8	Female	63	AdC	1	0	IA
9	Male	67	AdC	2	0	IB
10	Female	66	AdC	2	0	IB
11	Female	65	AdC	2	0	IB
12	Female	67	AdC	2	0	IB
13	Female	69	AdC	2	0	IB
14	Female	71	AdC	2	0	IB
15	Male	49	AdC	2	0	IB
16	Male	54	AdC	2	0	IB
17	Male	76	AdC	2	0	IB
18	Male	73	AdC	2	0	IB
19	Female	69	AdC	2	0	IB
20	Male	76	AdC	2	0	IB
21	Male	74	AdC	2	0	IB
22	Female	74	AdC	2	0	IB
23	Female	74	AdC	2	0	IB
24	Male	74	AdC	2	0	IB
25	Male	75	AdC	2	0	IB
26	Female	75	AdC	2	0	IB
27	Female	78	AdC	2	0	IB
28	Female	49	AdC	2	0	IB
29	Female	55	AdC	2	0	IB
30	Male	62	AdC	2	0	IB
31	Male	68	AdC	2	0	IB
32	Female	61	AdC	1	1	IIA
33	Male	73	AdC	2	1	IIA
34	Male	60	AdC	2	1	IIB
35	Female	61	AdC	2	1	IIB
36	Female	60	AdC	2	1	IIB
37	Female	66	AdC	2	1	IIB
38	Male	70	AdC	2	1	IIB
39	Female	73	AdC	2	1	IIB
40	Male	63	AdC	2	1	IIB
41	Male	67	AdC	2	1	IIB

42	Male	78	AdC	2	1	IIB
43	Female	68	AdC	2	1	IIB
44	Male	64	AdC	3	0	IIB
45	Male	70	AdC	2	1	IIB
46	Male	70	AdC	2	2	IIIA
47	Male	67	AdC	3	1	IIIA
48	Female	66	AdC	2	2	IIIA
49	Male	71	AdC	3	2	IIIA
50	Male	47	AdC	2	2	IIIA
51	Male	67	AdC	2	2	IIIA
52	Female	60	AdC	3	2	IIIA
53	Female	73	AdC	2	2	IIIA
54	Female	68	AdC	3	2	IIIA
55	Male	68	AdC	4	2	IIIB
56	Female	71	AdC	2	1	IIIB
57	Female	69	SqCCL	1	0	IA
58	Male	54	SqCCL	1	0	IA
59	Male	55	SqCCL	1	0	IA
60	Male	77	SqCCL	1	0	IA
61	Male	57	SqCCL	1	0	IA
62	Male	73	SqCCL	1	0	IA
63	Female	73	SqCCL	1	0	IA
64	Female	58	SqCCL	2	0	IB
65	Female	79	SqCCL	2	0	IB
66	Male	70	SqCCL	2	0	IB
67	Female	69	SqCCL	2	0	IB
68	Female	71	SqCCL	2	0	IB
69	Male	66	SqCCL	2	0	IB
70	Male	63	SqCCL	2	0	IB
71	Male	57	SqCCL	2	0	IB
72	Male	69	SqCCL	2	0	IB
73	Male	74	SqCCL	2	0	IB
74	Male	73	SqCCL	2	0	IB
75	Female	56	SqCCL	2	0	IB
76	Male	73	SqCCL	2	0	IB
77	Female	50	SqCCL	2	0	IB
78	Male	66	SqCCL	2	0	IB
79	Male	71	SqCCL	2	0	IB
80	Male	76	SqCCL	2	0	IB
81	Female	61	SqCCL	2	0	IB
82	Male	77	SqCCL	2	0	IB
83	Male	80	SqCCL	2	0	IB
84	Male	71	SqCCL	2	0	IB
85	Male	54	SqCCL	2	0	IB
86	Female	71	SqCCL	2	0	IB
87	Male	77	SqCCL	2	0	IB
88	Female	70	SqCCL	2	0	IB

89	Female	71	SqCCL	2	0	IB
90	Male	76	SqCCL	2	0	IB
91	Male	75	SqCCL	2	0	IB
92	Female	78	SqCCL	2	0	IB
93	Male	63	SqCCL	2	0	IB
94	Male	76	SqCCL	2	0	IB
95	Male	70	SqCCL	2	0	IB
96	Male	60	SqCCL	2	0	IB
97	Male	65	SqCCL	2	0	IB
98	Male	75	SqCCL	1	1	IIA
99	Female	54	SqCCL	1	1	IIA
100	Male	46	SqCCL	1	1	IIA
101	Female	51	SqCCL	2	1	IIB
102	Female	60	SqCCL	2	1	IIB
103	Female	50	SqCCL	2	1	IIB
104	Male	70	SqCCL	2	1	IIB
105	Male	79	SqCCL	2	1	IIB
106	Male	74	SqCCL	2	1	IIB
107	Male	70	SqCCL	2	1	IIB
108	Female	70	SqCCL	2	1	IIB
109	Male	56	SqCCL	2	1	IIB
110	Male	69	SqCCL	3	0	IIB
111	Female	45	SqCCL	2	1	IIB
112	Male	73	SqCCL	2	1	IIB
113	Female	60	SqCCL	2	1	IIB
114	Male	68	SqCCL	2	1	IIB
115	Male	59	SqCCL	2	1	IIB
116	Female	73	SqCCL	2	1	IIB
117	Male	82	SqCCL	2	1	IIB
118	Male	58	SqCCL	2	1	IIB
119	Female	66	SqCCL	2	1	IIB
120	Female	63	SqCCL	2	1	IIB
121	Female	77	SqCCL	2	1	IIB
122	Male	51	SqCCL	2	1	IIB
123	Male	64	SqCCL	2	2	IIIA
124	Male	69	SqCCL	3	1	IIIA
125	Male	62	SqCCL	3	2	IIIA
126	Male	63	SqCCL	3	2	IIIA
127	Female	66	SqCCL	3	2	IIIA
128	Male	50	SqCCL	2	2	IIIA
129	Male	74	SqCCL	2	2	IIIA
130	Female	58	SqCCL	3	2	IIIA
131	Male	68	SqCCL	2	2	IIIA
132	Female	71	SqCCL	2	2	IIIA

MPI: master patient index, AdC: adenocarcinoma of the lung, SqCCL: squamous cell carcinoma of the lung.

Appendix 3: Representative data of cell line authentication determined by DNA fragmentation analysis using GenePrint 10 System

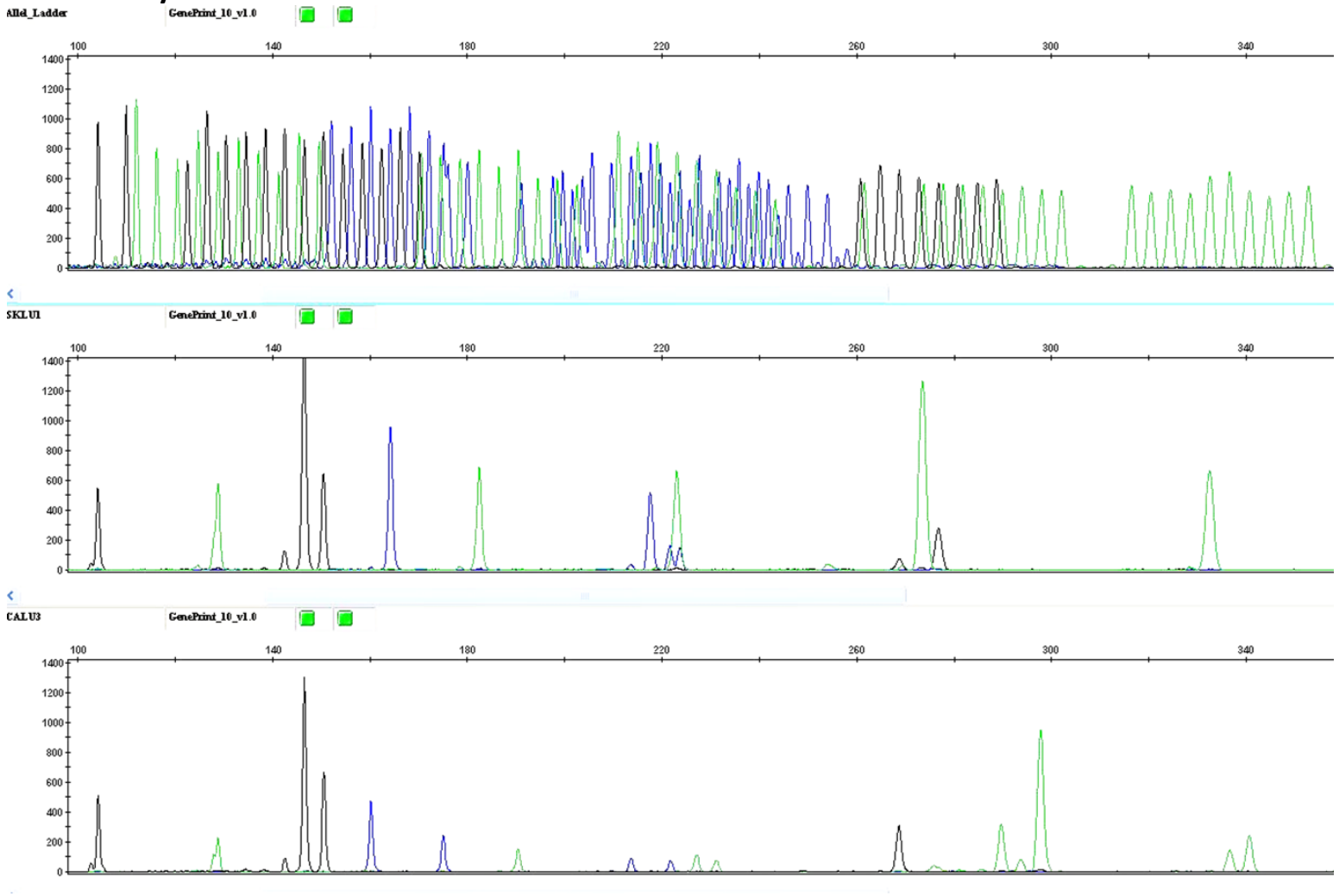

Appendix 4: Representative pyrosequencing assay design and its analysis report for detection methylation status of KIF11 gene promoter. The forward biontinylated (Fb), reverse (R) and Sequencing (S) primers were designed using PyroMark assay design 2.0 software.

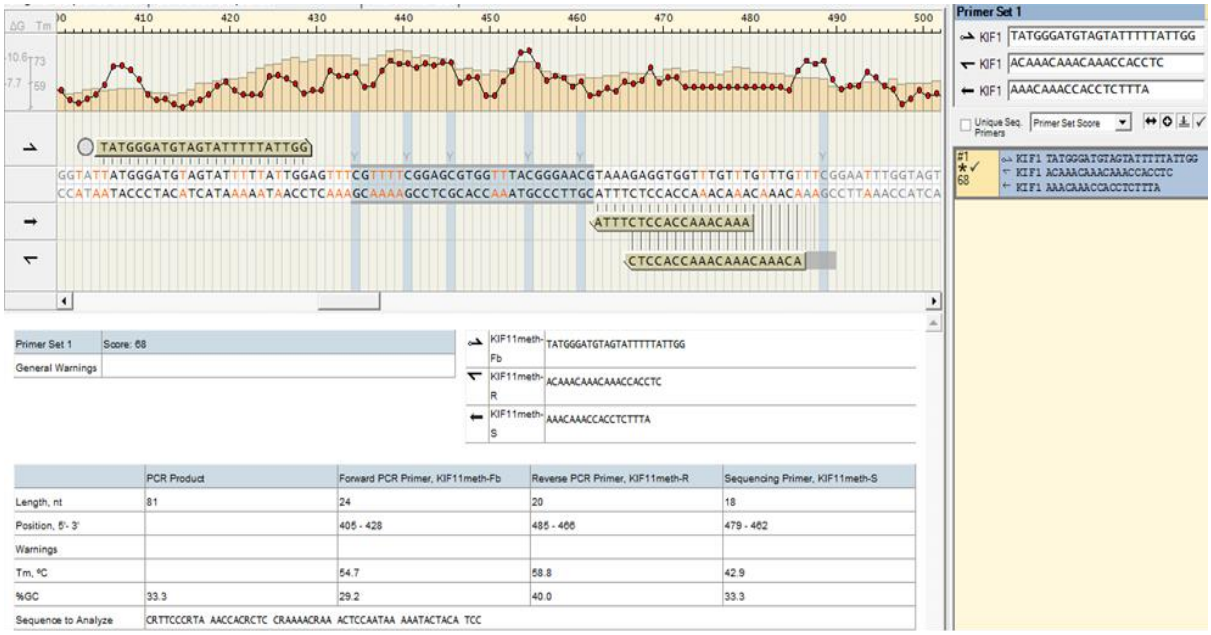

Primer Set 1			Score: 68 Quality: Medium		
Primer	**Id**	**Sequence**	**Nt**	**Tm, °C**	**%GC**
PCR	KIF11meth-Fb	TATGGGATGTAGTATTTTTATTGG	24	54.7	29.2
PCR	KIF11meth-R	ACAAACAAACAAACCACCTC	20	58.8	40.0
Sequencing	KIF11meth-S	AAACAAACCACCTCTTTA	18	42.9	33.3
Target Polymorphisms	Position41, Position42, Position43, Position44, Position45				
Sequence to Analyze	CRTTCCCRTA AACCACRCTC CRAAAACRAA ACTCCAATAA AAATACTACA TCC				
Analysis Steps	Name: **Biotinylated PCR Primer Hairpin Analysis** Description: Evaluates hairpin structures on the biotinylated PCR primer. Penalty: 0				
	Name: **Duplex Formation Analysis** Description: Identifies possible annealing between the sequencing primer and the biotinylated PCR primer. Penalty: 0				
	Name: **Mispriming Analysis** Description: Identifies alternate annealing sites for the sequencing primer on the amplicon. Penalty: 0				
	Name: **Template Loop Analysis** Description: Identifies possible template loops on the amplicon. Penalty: 0				

Appendix 5 (A): The sequencing confirmation of *AURKB* cDNA sequence on pCMV6-XL4-*AURKB*/*Bsd* recombinant plasmid analysed on 3130 Genetic Analyzer.

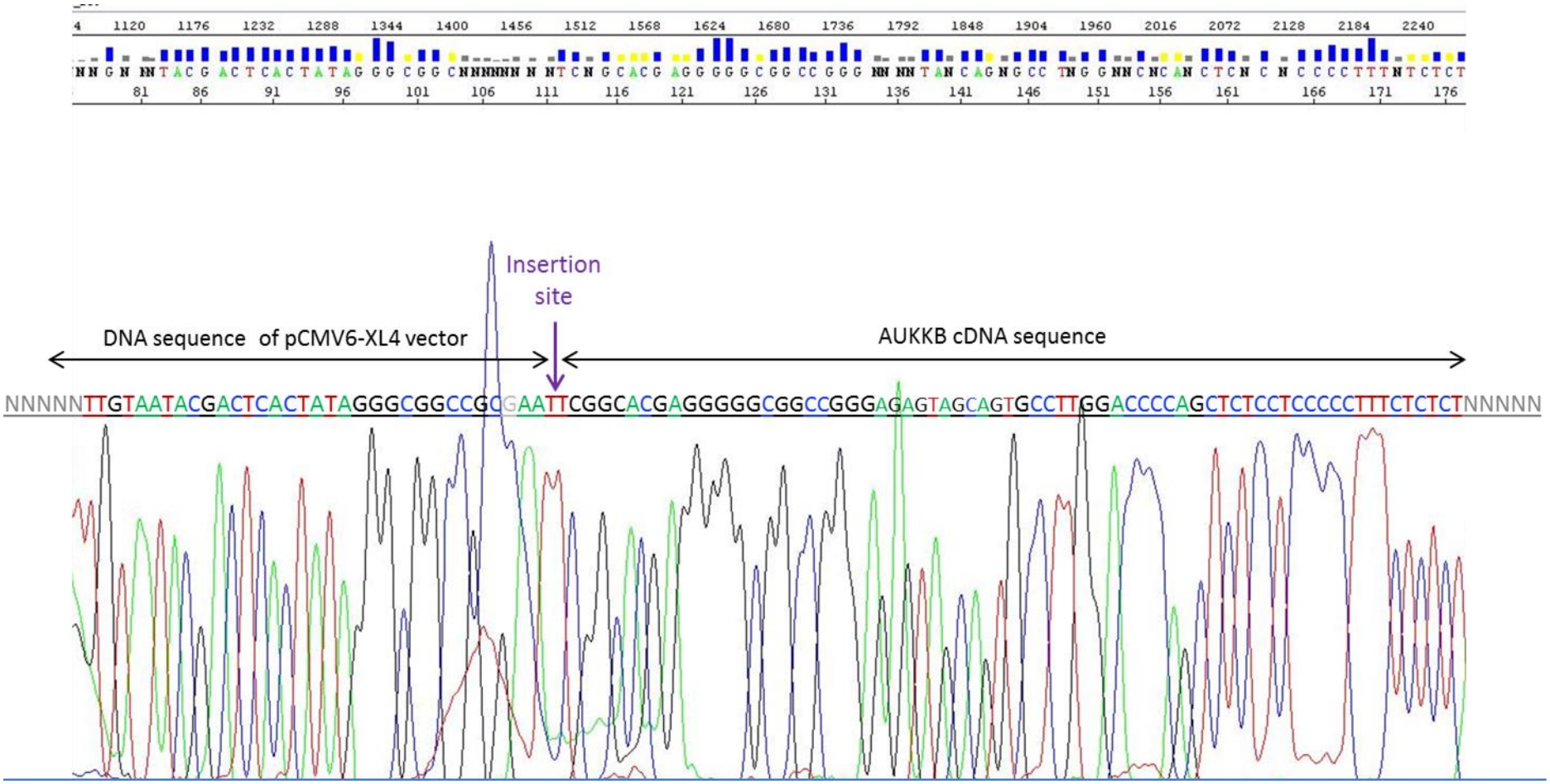

Appendix 5 (B): The map of genetically engineered plasmid pCMV6-XL4-*AURKB-Bsd* highlighting the insertion site of *BSD* gene.

GGGCCATCGCCCTGATAGACGGTTTTTCGCCCTTTGACGTTGGAGTCCACGTTCTTTAATAGTGGACTCTTGTTCCAAACTGG
AACAACACTCAACCCTATCTCGGTCTATTCTTTTGATTTAT**GGGAATTCAGACATGATAAGATACATTGATGAGTTTGGACAA**
ACCACAACTAGAATGCAGTGAAAAAAATGCTTTATTTGTGAAATTTGTGATGCTATTGCTTTATTTGTAACCATTATAAGCTG
CAATAAACAAGTTTCGAGGTCGAGTGTCAGTCCTGCTCCTCGGCCACGAAGTGCTTAGCCCTCCCACACATAACCAGAGGGCA
GCAATTCACGAATCCCAACTGCCGTCGGCTGTCCATCACTGTCCTTCACTATGGCTTTGATCCCAGGATGCAGATCGAGAAGC
ACCTGTCGGCACCGTCCGCAGGGGCTCAAGATGCCCCTGTTCTCATTTCCGATCGCGACGATACAAGTCAGGTTGCCAGCTGC
CGCAGCAGCAGCAGTGCCCAGCACCACGAGTTCTGCACAAGGTCCCCCAGTAAAATGATATACATTGACACCAGTGAAGATGC
GGCCGTCGCTAGAGAGAGCTGCGCTGGCGACGCTGTAGTCTTCAGAGATGGGGATGCTGTTGATTGTAGCCGTTGCTCTTTCA
ATGAGGGTGGATTCTTCTTGAGACAAAGGCTTGGCCATGGTTTAGTTCCTCACCTTGTCGTATTATACTATGCCGATATACTA
TGCCGATGATTAATTGTCAACACGGTCCGTTCCAATGCACCGTTCCCGGCCGCGGAGGCTGGATCGGTCCCGGTGTCTTCTAT
GGAGGTCAAAACAGCGTGGATGGCGTCTCCAGGCGATCTGACGGTTCACTAAACGAGCTCTGCTTATATAGACCTCCCACCGT
ACACGCCTACCGCCCATTTGCGTCAATGGGGCGGAGTTGTTACGACATTTTGGAAAGTCCCGTTGATTTTGGTGCCAAAACAA
ACTCCCATTGACGTCAATGGGGTGGAGACTTGGAAATCCCCGTGAGTCAAACCGCTATCCACGCCCATTGATGTACTGCCAAA
ACCGCATCACCATGGTAATAGCGATGACTAATACGTAGATGTACTGCCAAGTAGGAAAGTCCCATAAGGTCATGTACTGGGCA
TAATGCCAGGCGGGCCATTTACCGTCATTGACGTCAATAGGGGGCGTACTTGGCATATGATACACTTGATGTACTGCCAAGTG
GGCAGTTTACCGTAAATACTCCACCCATTGACGTCAATGGAAAGTCCCTATTGGCGTTACTATGGGAACATACGTCATTATTG
ACGTCAATGGGCGGGGGTCGTTGGGCGGTCAGCCAGGCGGGCCATTTACCGTAAGTTATGTAACGGACCTCGAGCTAGCGATA
TAAGGGATTTTGCCGATTTCGGCCTATTGGTTAAAAAATGAGCTGATTTAACAAAAATTTAACGCGAATTTTAACAAAATATT

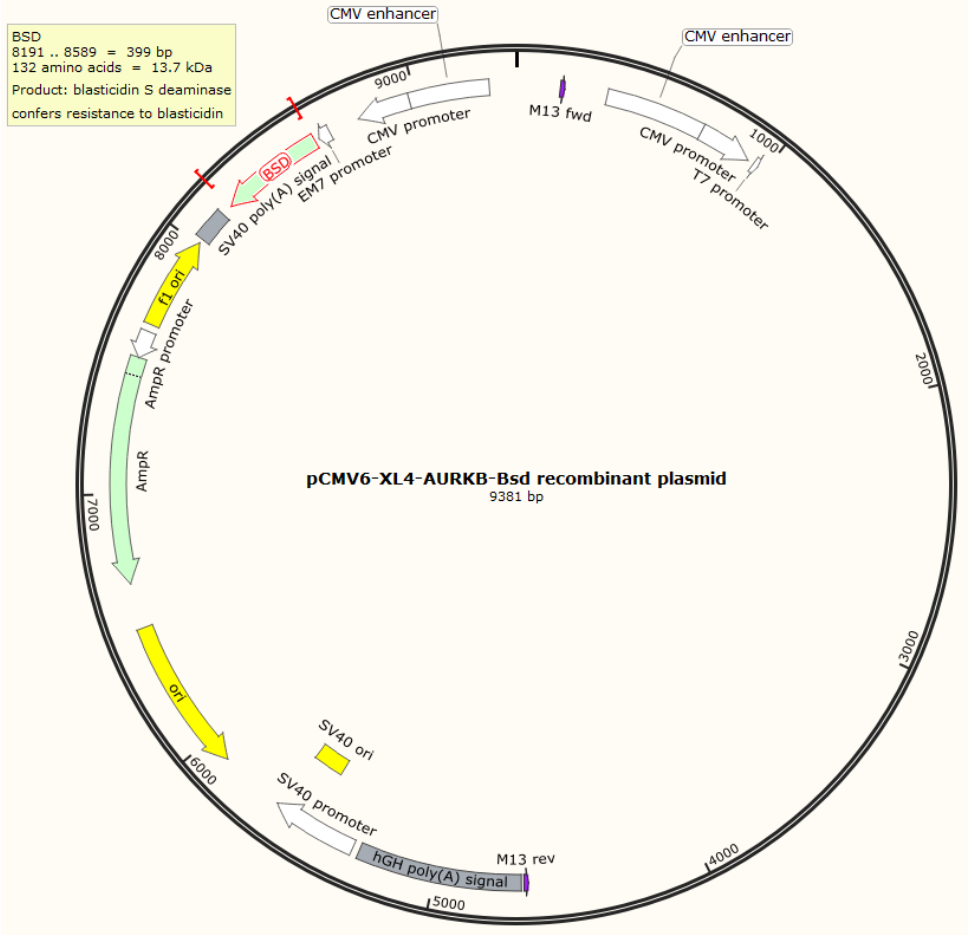

The inserted sequence above include CMV promoter, EM7 promoter, *BSD* gene SV40 polyadenylation signal sequences. *BSD* gene carries the blasticidin resistant characteristic as a selective marker that employed to select *AURKB* overexpressed clones derived from transfected parental Calu-3 cell line. The map was build using SnapGene Viewer software.

Appendix 6: *AURKB* mRNA expression of Calu-3 cell line and its derivative overexpressed clones (A) in relation to their response to both taxanes (B).

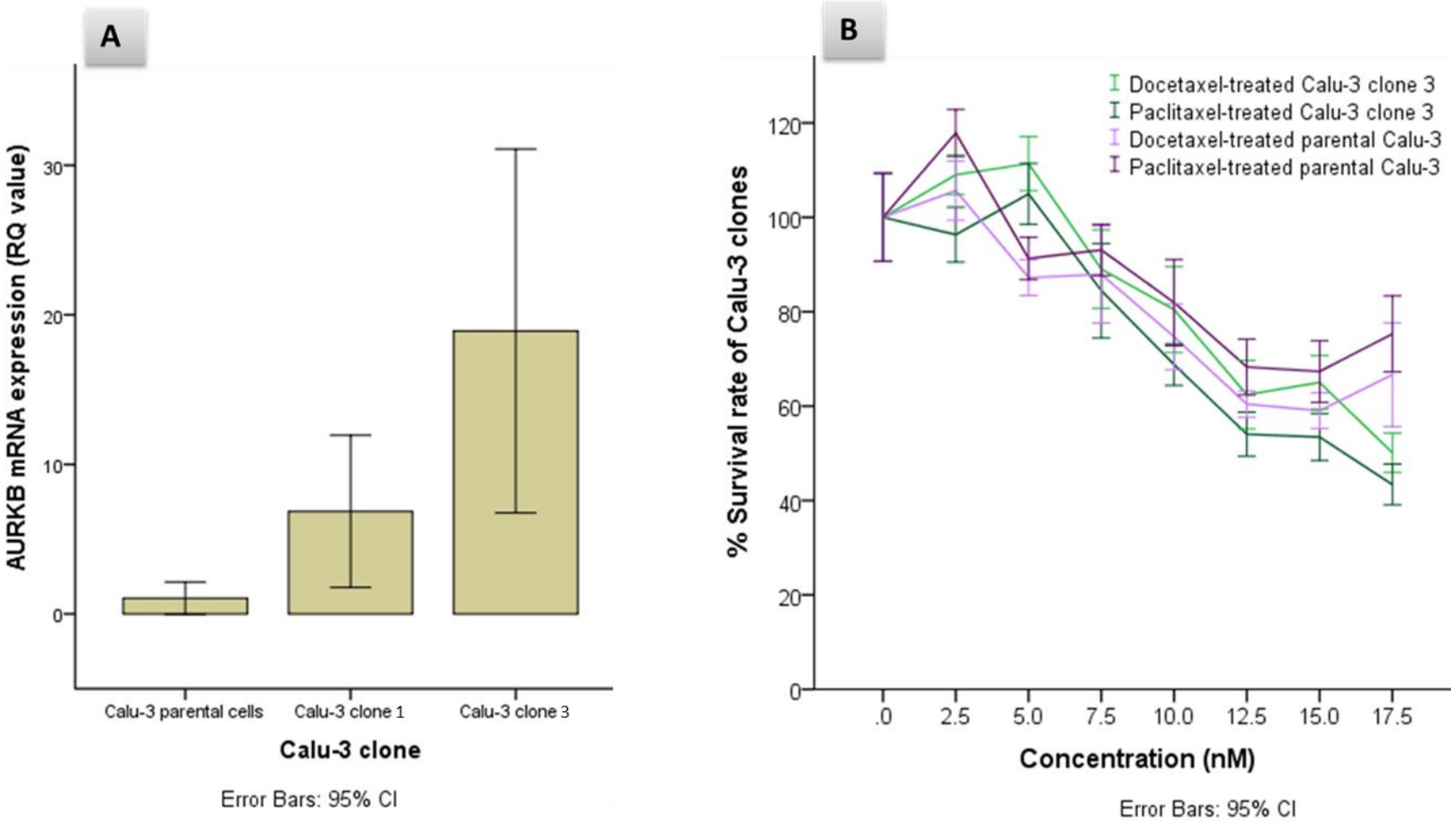

Appendix 7: mRNA expression of *AURKC*, CKAP5 and *TUBB3* in lung cancer tissues.

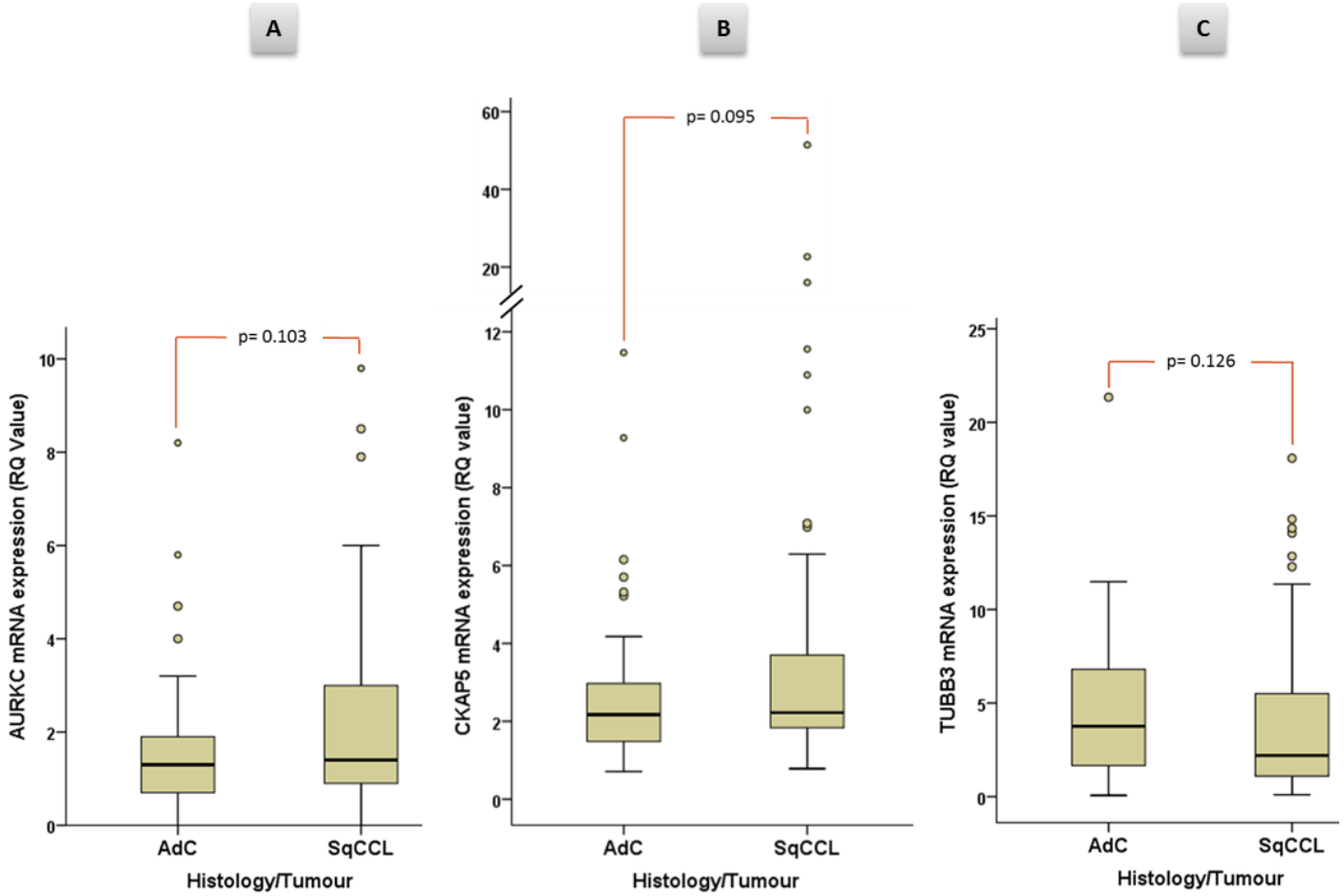

Boxplots demonstrating mRNA expressions of *AURKC* (A), *CKAP5* (B) and *TUBB3* (C) genes in squamous cell carcinomas (sqCCL) and adenocarcinomas (AdC) of the lung.

Appendix 8(A): Kaplan-Meier analysis of overall survival (OS) of NSCLC cancer patients dichotomised by median *AURKB* mRNA expression. The p value was derived from Log Rank (Mantel-Cox) test.

Means and Medians for Survival Time

aurkb_m	Mean[a]				Median			
			95% Confidence Interval				95% Confidence Interval	
	Estimate	Std. Error	Lower Bound	Upper Bound	Estimate	Std. Error	Lower Bound	Upper Bound
0	78.868	9.357	60.529	97.207	52.770	17.731	18.017	87.523
1	73.074	9.775	53.916	92.233	34.430	15.725	3.609	65.251
Overall	76.277	6.833	62.885	89.669	46.230	14.175	18.448	74.012

a. Estimation is limited to the largest survival time if it is censored.

Overall Comparisons

	Chi-Square	df	Sig.
Log Rank (Mantel-Cox)	.755	1	.385

Test of equality of survival distributions for the different levels of aurkb_m.

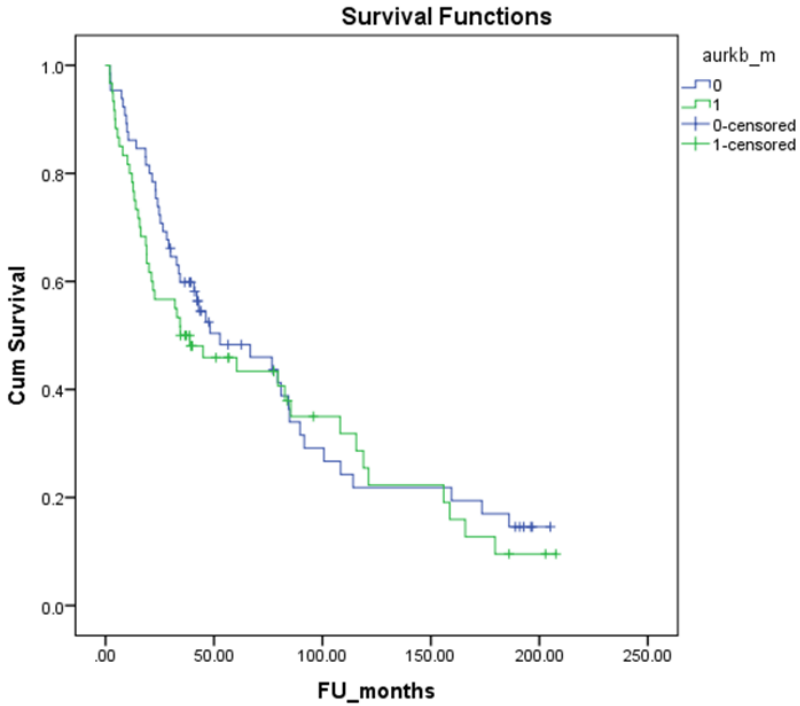

Appendix 8(B): Kaplan-Meier analysis of overall survival (OS) of NSCLC cancer patients dichotomised by median *AURKC* mRNA expression. The p value was derived from Log Rank (Mantel-Cox) test.

Means and Medians for Survival Time

	Mean[a]				Median			
			95% Confidence Interval				95% Confidence Interval	
aurkc_m	Estimate	Std. Error	Lower Bound	Upper Bound	Estimate	Std. Error	Lower Bound	Upper Bound
0	70.948	8.843	53.617	88.280	34.300	9.750	15.190	53.410
1	80.027	10.567	59.315	100.738	79.330	19.974	40.180	118.480
Overall	76.277	6.833	62.885	89.669	46.230	14.175	18.448	74.012

a. Estimation is limited to the largest survival time if it is censored.

Overall Comparisons

	Chi-Square	df	Sig.
Log Rank (Mantel-Cox)	.941	1	.332

Test of equality of survival distributions for the different levels of aurkc_m.

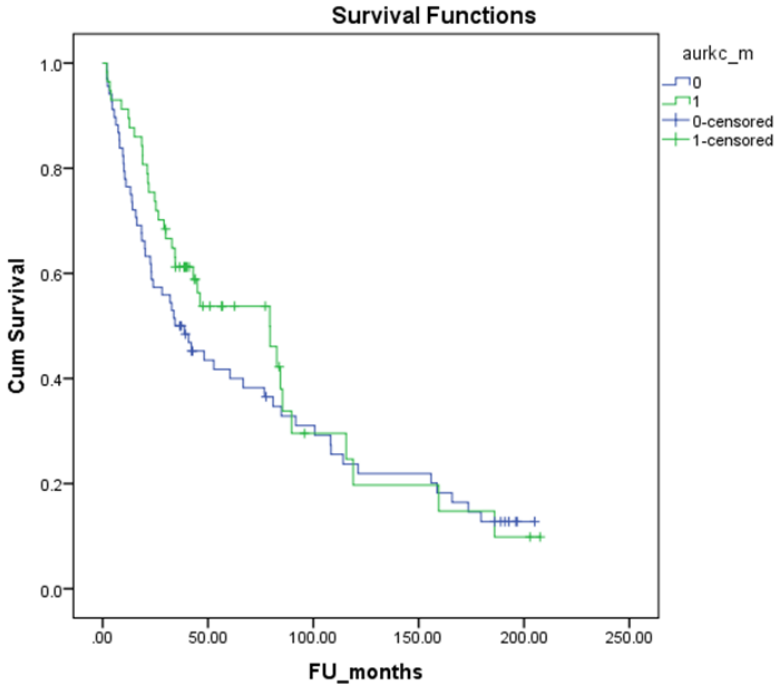

Appendix 8(C): Kaplan-Meier analysis of overall survival (OS) of NSCLC cancer patients dichotomised by median *CKAP5* mRNA expression. The p value was derived from Log Rank (Mantel-Cox) test.

Means and Medians for Survival Time

	Mean[a]				Median			
			95% Confidence Interval				95% Confidence Interval	
ckap5_m	Estimate	Std. Error	Lower Bound	Upper Bound	Estimate	Std. Error	Lower Bound	Upper Bound
0	76.487	8.584	59.662	93.311	48.130	18.864	11.156	85.104
1	78.148	11.653	55.308	100.988	45.000	15.193	15.222	74.778
Overall	76.277	6.833	62.885	89.669	46.230	14.175	18.448	74.012

a. Estimation is limited to the largest survival time if it is censored.

Overall Comparisons

	Chi-Square	df	Sig.
Log Rank (Mantel-Cox)	.067	1	.795

Test of equality of survival distributions for the different levels of ckap5_m.

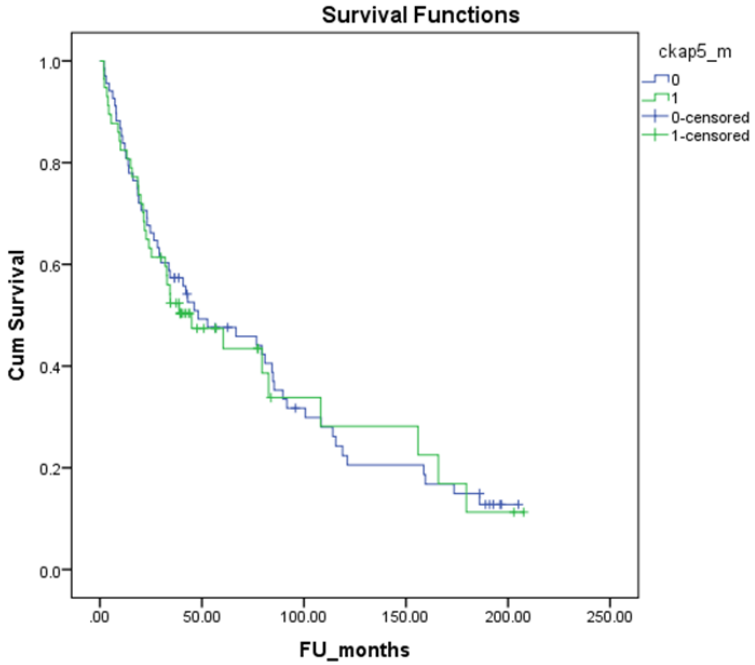

Appendix 8(D): Kaplan-Meier analysis of overall survival (OS) of NSCLC cancer patients dichotomised by median *DLGAP5* mRNA expression. The p value was derived from Log Rank (Mantel-Cox) test.

Means and Medians for Survival Time

	Mean[a]				Median			
			95% Confidence Interval				95% Confidence Interval	
dlgap5_m	Estimate	Std. Error	Lower Bound	Upper Bound	Estimate	Std. Error	Lower Bound	Upper Bound
0	76.820	9.020	59.140	94.499	48.130	19.935	9.057	87.203
1	76.536	10.098	56.744	96.328	45.000	17.274	11.144	78.856
Overall	76.277	6.833	62.885	89.669	46.230	14.175	18.448	74.012

a. Estimation is limited to the largest survival time if it is censored.

Overall Comparisons

	Chi-Square	df	Sig.
Log Rank (Mantel-Cox)	.360	1	.549

Test of equality of survival distributions for the different levels of dlgap5_m.

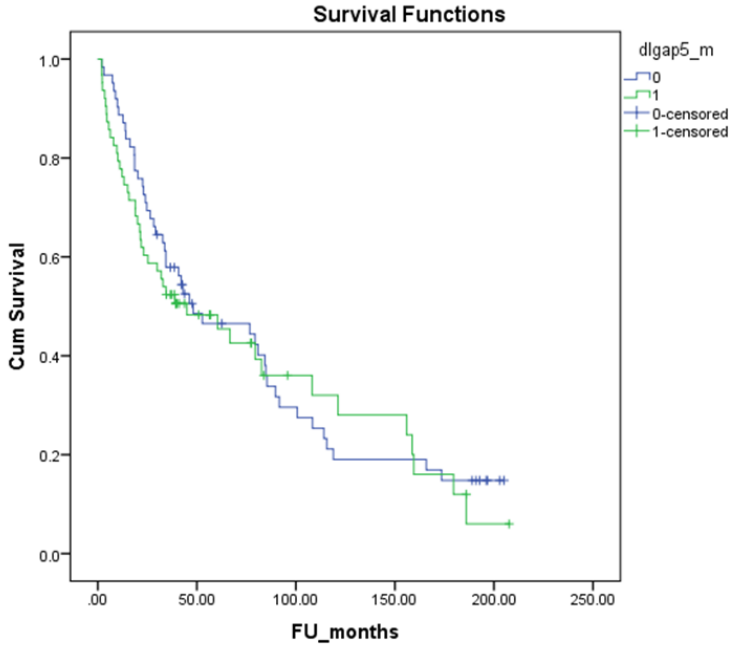

Appendix 8(E): Kaplan-Meier analysis of overall survival (OS) of NSCLC cancer patients dichotomised by median *KIF11* mRNA expression. The p value was derived from Log Rank (Mantel-Cox) test.

Means and Medians for Survival Time

	Mean[a]				Median			
			95% Confidence Interval				95% Confidence Interval	
kif11_m	Estimate	Std. Error	Lower Bound	Upper Bound	Estimate	Std. Error	Lower Bound	Upper Bound
0	75.136	9.635	56.252	94.021	46.230	10.027	26.578	65.882
1	76.676	9.412	58.228	95.123	60.400	23.018	15.285	105.515
Overall	76.277	6.833	62.885	89.669	46.230	14.175	18.448	74.012

a. Estimation is limited to the largest survival time if it is censored.

Overall Comparisons

	Chi-Square	df	Sig.
Log Rank (Mantel-Cox)	.101	1	.751

Test of equality of survival distributions for the different levels of kif11_m.

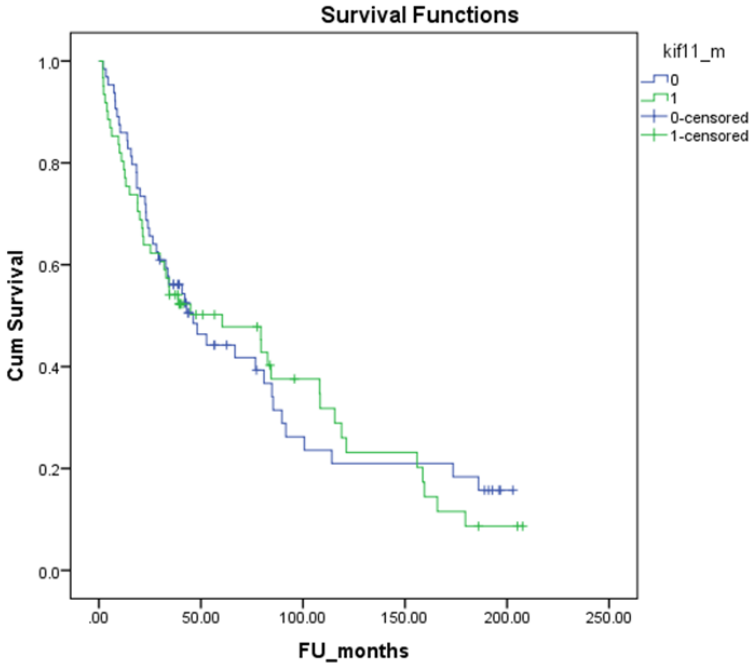

Appendix 8(F): Kaplan-Meier analysis of overall survival (OS) of NSCLC cancer patients dichotomised by median *TTK* mRNA expression. The p value was derived from Log Rank (Mantel-Cox) test.

Means and Medians for Survival Time

ttk_m	Mean[a]				Median			
			95% Confidence Interval				95% Confidence Interval	
	Estimate	Std. Error	Lower Bound	Upper Bound	Estimate	Std. Error	Lower Bound	Upper Bound
0	79.022	10.243	58.945	99.099	48.130	16.094	16.586	79.674
1	73.715	8.950	56.173	91.257	45.000	24.393	.000	92.811
Overall	76.855	6.863	63.403	90.308	46.230	16.556	13.779	78.681

a. Estimation is limited to the largest survival time if it is censored.

Overall Comparisons

	Chi-Square	df	Sig.
Log Rank (Mantel-Cox)	.792	1	.374

Test of equality of survival distributions for the different levels of ttk_m.

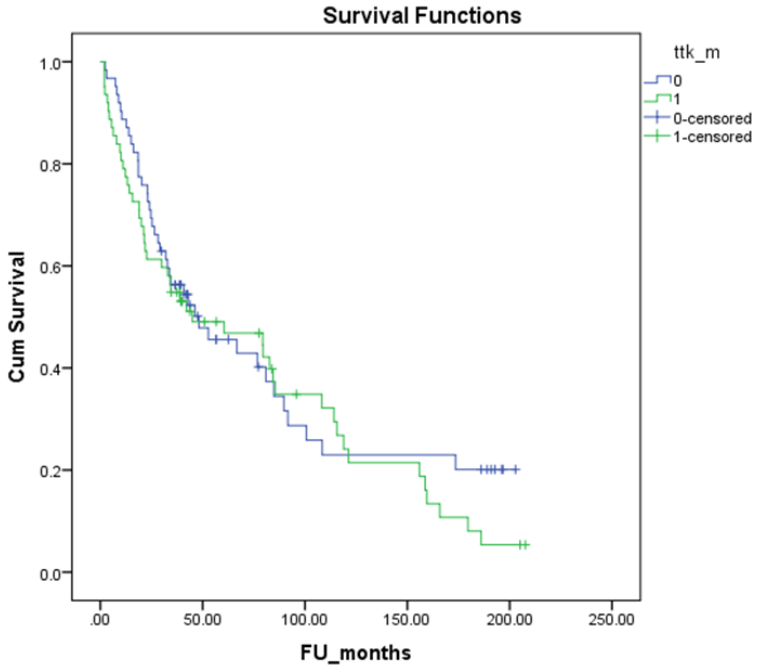

Appendix 8(G): Kaplan-Meier analysis of overall survival (OS) of NSCLC cancer patients dichotomised by median *TUBB* mRNA expression. The p value was derived from Log Rank (Mantel-Cox) test.

Means and Medians for Survival Time

tubb_m	Mean[a]				Median			
			95% Confidence Interval				95% Confidence Interval	
	Estimate	Std. Error	Lower Bound	Upper Bound	Estimate	Std. Error	Lower Bound	Upper Bound
0	78.732	9.045	61.003	96.461	52.770	13.074	27.144	78.396
1	72.039	10.241	51.967	92.110	34.430	29.282	.000	91.822
Overall	76.277	6.833	62.885	89.669	46.230	14.175	18.448	74.012

a. Estimation is limited to the largest survival time if it is censored.

Overall Comparisons

	Chi-Square	df	Sig.
Log Rank (Mantel-Cox)	.949	1	.330

Test of equality of survival distributions for the different levels of tubb_m.

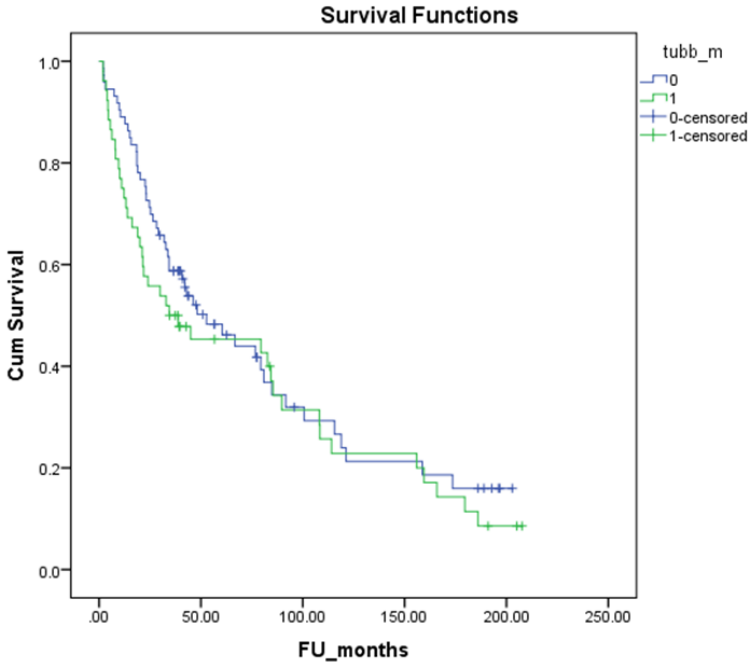

Appendix 8(H): Kaplan-Meier analysis of overall survival (OS) of NSCLC cancer patients dichotomised by median *TUBB3* mRNA expression. The p value was derived from Log Rank (Mantel-Cox) test.

Means and Medians for Survival Time

	Mean[a]				Median			
			95% Confidence Interval				95% Confidence Interval	
tubb3_m	Estimate	Std. Error	Lower Bound	Upper Bound	Estimate	Std. Error	Lower Bound	Upper Bound
0	81.866	9.221	63.793	99.938	48.130	18.888	11.110	85.150
1	69.290	9.956	49.776	88.805	34.430	16.781	1.539	67.321
Overall	76.277	6.833	62.885	89.669	46.230	14.175	18.448	74.012

a. Estimation is limited to the largest survival time if it is censored.

Overall Comparisons

	Chi-Square	df	Sig.
Log Rank (Mantel-Cox)	.926	1	.336

Test of equality of survival distributions for the different levels of tubb3_m.